2017

Tetrabenzo[8]circulene: Synthesis and Structural Properties of Polycyclic Aromatic Hydrocarbons with Negative Curvature

Robert William Miller
University of Vermont

Follow this and additional works at: https://scholarworks.uvm.edu/graddis
Part of the Organic Chemistry Commons

TETRABENZO[8]CIRCULENE: SYNTHESIS AND STRUCTURAL PROPERTIES
OF POLYCYCLIC AROMATIC HYDROCARBONS WITH NEGATIVE
CURVATURE

A Dissertation Presented

by

Robert William Miller

to

The Faculty of the Graduate College

of

The University of Vermont

In Partial Fulfillment of the Requirements
for the Degree of Doctor of Philosophy
Specializing in Chemistry

October, 2017

Defense Date: July 28, 2017
Dissertation Examination Committee:

Adam C. Whalley, Ph.D., Advisor
Adrian Del Maestro, Ph.D., Chairperson
Matthias Brewer, Ph.D.
Rory Waterman, Ph.D.
Cynthia J. Forehand, Ph.D., Dean of the Graduate College

ABSTRACT

Contorted polycyclic aromatic hydrocarbons have found increasing utility in the application of molecular electronics due to the surpamolecular properties that result from these non-planar structures. The [n]circulene series of molecules are particularly attractive members of the contorted aromatic family due to the unique structural implications that result from their changing value of n. For example, when $n \leq 5$, the structures adopt a bowl-like shape; when $n = 6$, a planar structure is observed; and when $7 \leq n \leq 16$, the compounds assume a saddle-like shape. Very few molecules exhibit the structural contortions that these contorted aromatics do – primarily because aromatic molecules desire to adopt highly planar conformations.

Following the model of aromaticity developed by Erich Clar, we set our sights on the synthesis of tetrabenzo[8]circulene, the stabilized form of [8]circulene established through the addition of four fused benzenoid rings around the periphery of the molecule. The initial approach towards this structure employs a Diels-Alder [4 + 2] cycloaddition reaction and a palladium catalyzed arylation reaction as the key transformation steps. The results of these studies were promising, establishing the structural characterization of this new molecule and providing access to functionalized derivatives of the saddle-shaped structure. However, access towards these functionalized derivatives proved limiting, compelling us to investigate alternative synthetic methodologies.

In the course of our studies, we established a new methodology towards 2,5-diarylthiophene-1-oxides, a key precursor to the Diels-Alder cycloaddition reaction. These reactive dienes are prepared from readily available arylacetylene precursors *via* zirconacyclopentadiene intermediates. The isolated yields of the desired thiophene-1-oxides are comparable to those obtained from previously established oxidation strategies while avoiding the formation of over-oxidation products. Of significant importance to scope of our work, this newly established methodology offers broader versatility providing products outfitted with electron-donating or electron-withdrawing groups.

These new methodologies provided access to functionalized derivatives of the saddle-shaped molecule tetrabenzo[8]circulene in improved yield when coupled with a revised Diels-Alder/oxidative cyclodehydrogenation approach. This methodology affords products containing both electron-rich and electron-poor functional groups in a more efficient manner. The optoelectronic effects that result from the introduction of this functionality and investigations into the development of larger contorted aromatic systems are also discussed.

CITATIONS

Material from this dissertation has been published in the following form:

Miller, R. M.; Duncan, A. K.; Schneebeli, S. T.; Gray, D. L.; Whalley, A. C.. (2014). Synthesis and Structural Data of Tetrabenzo[8]circulene. *Chemistry – A European Journal*, *20*, 3705–3711.

Miller, R. M.; Dodge, N. J.; Dyer, A. M.; Fortner-Buczala, E. M.; Whalley, A. C.. (2016). A One-Pot Method for the Preparation of 2,5-Diarylthiophene-1-oxides from Arylacetylenes, *Tetrahedron Letters*, *57*, 1860–1862.

Miller, R. W.; Averill, S. E.; Van Wyck, S. J.; Whalley, A. C.. (2016). General Method for the Synthesis of Functionalized Tetrabenzo[8]circulenes, *The Journal of Organic Chemistry*, *81*, 12001–12005.

DEDICATION

This work is dedicated to my parents. For always encouraging creativity, even if it was

at the expense of so many nice things.   I love you.

ACKNOWLEDGMENTS

I'd like to start by thanking my advisor, Professor Adam Whalley, for his guidance and wisdom during my time here. It was his engaging teaching style that persuaded me to work in his lab and during that time I have undoubtedly learned so much. I will always consider you a close friend even if you would prefer otherwise.

I'd also like to thank the members of my graduate committee, Professors Rory Waterman, Matthias Brewer, and Adrian Del Maestro; I can't thank them enough for their helpful advice, support, and encouragement along the way.

I'm grateful for the research discussions I've been able to have with Jonathan Hollin and Nick Dodge; thank you both for all your help. A special thanks to Drs. Natalie Machamer and Corinne Sadlowski for guiding me through my graduate program, and to Dr. Neil Mucha, whose unsolicited life advice was nevertheless valuable.

My time here wouldn't have been complete without the formation of several new friendships. For their helpful discussions formed over Duff beers and promises to never talk about science at the bar and proceeding to do exactly that, I want to thank Sarah Cleary, Christine Bange, Max & Amanda Graves, Jonathan Hollin, Lane Manning, Dan Sumy, Adam Dyer, and many more. To the members of the exclusive "Team Vortex," for which I do not claim the naming rights and solely pin on Jenna Taft and Morgan Cousins, you were my first friends and my best friends. If I had to do this all over again I can't imagine a better group of friends to have. I wish you all the best in your futures.

My time here was also significantly improved by the members of "the office," the combined assortment of three research groups piled into one room and presumably

TABLE OF CONTENTS

LIST OF TABLES

LIST OF FIGURES

Figure   **Page**

LIST OF SCHEMES

Scheme **Page**

LIST OF ABBREVIATIONS

1,10-phen 1,10-Phenanthroline

6-31G** ....Polarized basis set

^{1}H NMR ....Proton Nuclear Magnetic Resonance

^{13}C NMR ....Carbon Nuclear Magnetic Resonance

AcOH .... Acetic acid

Ar .... Aryl

AWA ....Annulene-within-an-annulene

B(O-i-Pr)$_3$ ....Triisopropyl borate

B3LYP .... Becke, three-parameter, Lee-Yang-Parr

BPO... Benzoyl peroxide

BTEAC ....benzyltriethylammonium chloride

c-axis.. Vertical Crystallographic Axis

c-HBC ....Hexa-$cata$-hexabenzocoronene

CCD .... Charge Coupled Device

CCDC...Cambridge Crystallographic Data Centre

CDIs .... Coronenediimides

CNTs...Carbon Nanotubes

CO$_2$Me .... Acetate

Cp... Cyclopentadienyl

Cp$_2$Zr...Zirconocene

CHAPTER 1: CONTORTED AROMATICS AND THE [*N*]CIRCULENE SERIES OF POLYCYCLIC AROMATIC HYDROCARBONS

1.1 Background

In recent years, non-planar polycyclic aromatic hydrocarbons (PAHs) have found increasing utility in the application of molecular electronics, due to the supramolecular properties that result from their contorted structures.[1] Due to their unique shape, these structures are forced to arrange into energetically favorable linear stacks (**A**, Figure 1.1), thereby mandating the alignment of their electron-rich cores, much like the contorted hexabenzocoronenes (**B**) developed by Nuckolls and coworkers.[1a]
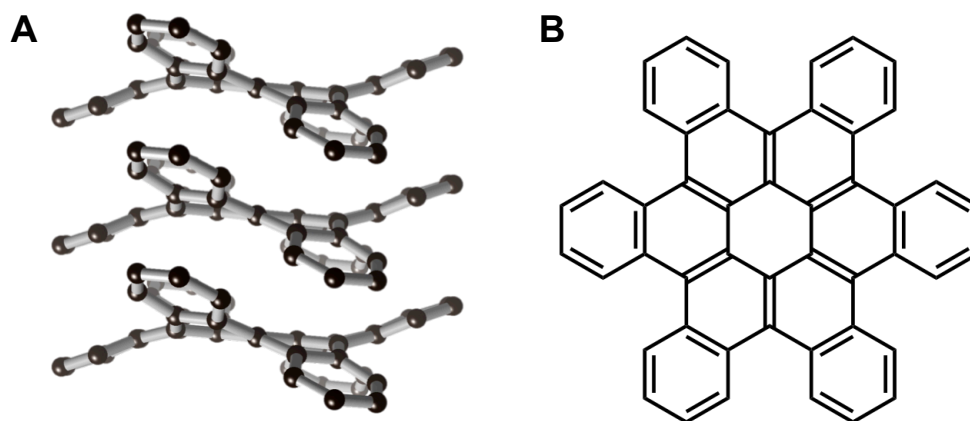
Figure 1.1 A) Energetically favorable linear stacks of **B**) contorted hexabenzocoronene.

---

[1] (a) Xiao, S.; Myers, M.; Miao, Q.; Sanaur, S.; Pang, K.; Steigerwald, M. L.; Nuckolls, C. *Angew. Chem. Int. Ed*. **2005**, *44*, 7390–7394; (b) Tremblay, N. J.; Gorodetsky, A. A.; Cox, M. P.; Schiros, T.; Kim, B.; Steiner, R.; Bullard, Z.; Sattler, A.; So, W. -Y.; Itoh, Y.; Toney, M. F.; Ogasawara, H.; Ramirez, A. P.; Kymissis, I.; Steigerwald, M. L.; Nuckolls, C. *Chem. Phys. Chem.* **2010**, *11*, 799–803; (c) Kang, S. J.; Kim, J. B.; Chiu, C. Y.; Ahn, S.; Schiros, T.; Lee, S. S.; Yager, K. G.; Toney, M. F.; Nuckolls, C. *Angew. Chem., Int. Ed.* **2012**, *51*, 8594–8597; (d) Ball, M.; Zhong, Y.; Wu, Y.; Schenck, C.; Ng, F.; Steigerwald, M.; Xaio, S.; Nuckolls, C. *Acc. Chem. Res.,* **2015**, *48*, 267–276.

Conformational alignment of these structures provides the optimal situation for electron-transfer between molecules, and therefore electron transport through these stacks is highly efficient compared to planar PAHs. While initial studies implementing contorted molecules for this purpose have provided positive results, there are unfortunately very few molecules known to exhibit the necessary structural contortions, primarily because aromatic molecules desire to adopt highly planar conformations.

Non-planarity within these structures is typically a result of the installation of non-hexagonal rings into an otherwise hexagonal framework. These contorted aromatics initially presented themselves in the form of structural disparities within carbon fragments as a result of isomeric changes in connectivity between π-bonded carbon atoms.[2] Such structural inconsistencies were later found to drastically modify the electronic properties of carbon nanosystems.[3] This concept is nicely illustrated by the [n]circulene series, a family of compounds in which a central ring containing *n* atoms is fully saturated with fused benzene rings on all edges.

1.2 The [*n*]Circulene Series

The [*n*]circulene series of structures is particularly relevant because changing the value of n has significant implications on the shape of the molecule. For example, when n ≤ 5 the structures adopt a bowl-like shape, when *n* = 6 a planar structure is observed, and

[2] Stone, A. J.; Wales, D. J. *Chem. Phys. Lett.* **1986**, *128*, 501–503.
[3] Charlier, J. -C. *Acc. Chem. Res.*, **2002**, *35*, 1063–1069.

when $7 \leq n \leq 16$ the compounds assume a saddle-like shape (Figure 1.2).[4] Those with

core structures larger then 16 would theoretically fold in on themselves to form helical

structures.
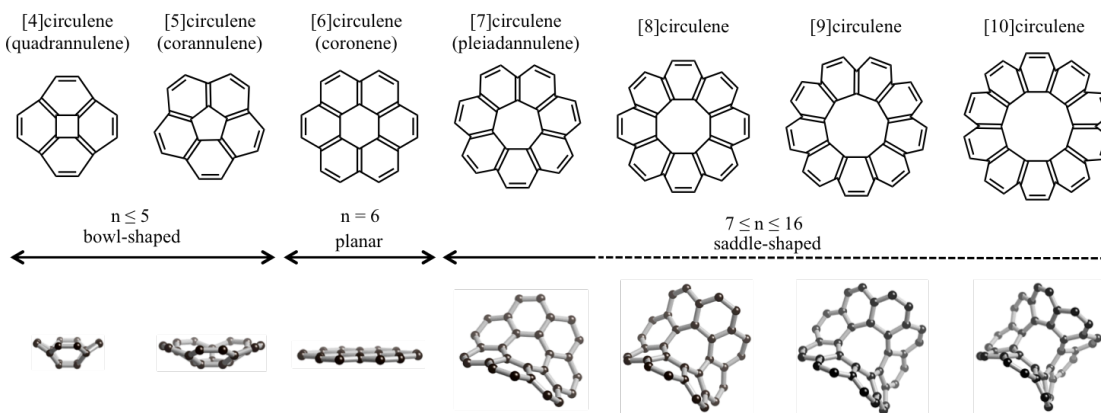
Figure 1.2 Structural conformations of the [*n*]circulene series from n = 4 to n = 10, where n ≤ 5 leads to bowl shaped structures, n = 6 is planar, and 7 ≤ n ≤ 16 leads to saddle-like structures.

These theoretical predictions have been confirmed in the experimental structures

of bowl-shaped quadrannulene [5] (a [4]circulene derivative) and corannulene [6]

([5]circulene), planar coronene[7] ([6]circulene) and the negatively curved pleiadannulene[8]

([7]circulene). Across the series, aromaticity is preserved regardless of the shape and

[4] Christoph, H.; Grunenberg, J.; Hopf, H.; Dix, I.; Jones, P. G.; Scholtissek, M.; Maier, G. *Chem. Eur. J.* **2008**, *14,* 5604–5616.

[5] Bharat, A.; Bhola, R.; Bally, T.; Valente, A.; Cyranski, M. K.; Dobrzycki, Ł.; Spain, S. M.; Rempała, P.; Chin, M. R.; King, B. T. *Angew. Chem. Int. Ed*. **2010**, *49*, 399–402.

[6] (a) Barth, W. E.; Lawton, R. G. *J. Am. Chem. Soc*. **1966**, *88*, 380–381; (b) Barth, W. E.; Lawton, R. G. *J. Am. Chem. Soc*. **1971**, *93*, 1730–1745.

[7] (a) Scholl, R.; Meyer, K. *Ber. Dtsch. Chem. Ges. A* **1932**, *65*, 902–915; (b) Newman, M. S. *J. Am. Chem. Soc*. **1940**, *62*, 1683–1687; (c) Baker, W.; Glockling, F.; McOmie, J. F. W. *J. Chem. Soc*. 1951, 1118–1121; (d) Clar, E.; Zander, M. *J. Chem. Soc*. **1957**, 4616–4619; (e) Craig, J. T.; Halton, B.; Lo, S.-F. *Aust. J. Chem.* **1975**, 28, 913; (f) Jessup, P. J.; Reiss, J. A. *Aust. J. Chem.* **1977**, 30, 843–850.

[8] (a) Yamamoto, K.; Harada, T.; Nakazaki, M.; Nakao, T.; Kai, Y.; Harada, S.; Kasai, N. *J. Am. Chem. Soc*. **1983**, *105*, 7171–7172; (b) Yamamoto, K.; Harada, T.; Okamoto, Y.; Chikamatsu, H.; Nakazaki, M.; Kai, M.; Nakao, T.; Tanaka, M.; Harada, S.; Kasai, N. *J. Am. Chem. Soc*. **1988**, *110*, 3578–3584; (c) Yamamoto, K.; Sonobe, H.; Matsubara, H.; Sato, M.; Okamoto, S.; Kitaura, K. *Angew. Chem. Int. Ed. Engl*. **1996**, *35*, 69–70; (d) Sato, M.; Yamamoto, K.; Sonobre, H.; Yano, K.; Matsubara, H.; Fujita, H.; Sugiomoto, T. *J. Chem. Soc. Perkin Trans. 2* **1998**, 1909–1914.

degree of distortion – making the larger, saddle-shaped compounds ideal candidates for investigation into the relationship between contorted aromatics and intermolecular charge transport.[9]

1.2.1 [4]circulene (quadrannulene)

Quadrannulene, or [4]circulene, is the smallest homologue of the [*n*]circulene family. To date the only example of such structures being synthetically achieved is the reported synthesis of 1,8,9,16-tetrakis(trimethylsilyl)tetra-*cata*-tetrabenzoquadrannulene or TBQ (**1**, Scheme 1.1) by King and co-workers in 2010.[5] However, previous attempts at synthesizing the [4]circulene structure have been reported.[4]
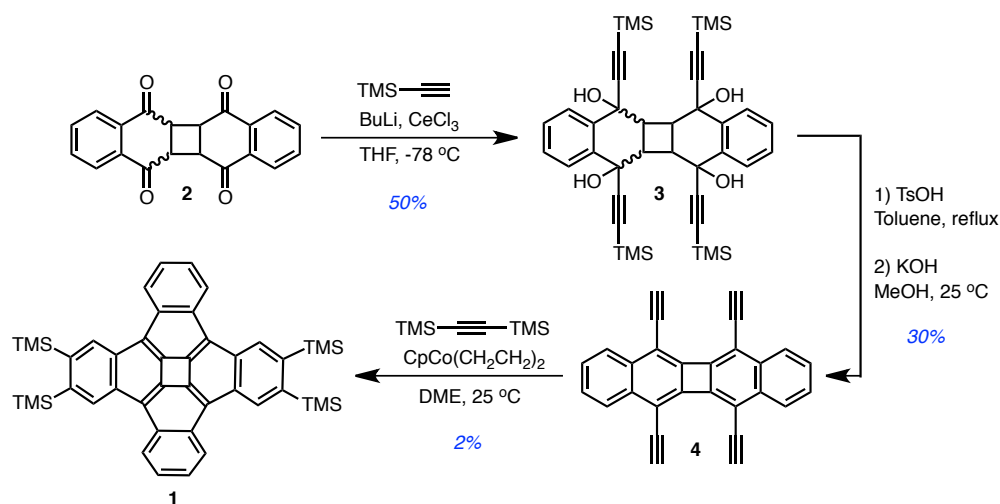
Scheme 1.1 King's reported synthesis of tetrabenzoquadrannulene (TBQ) the smallest member of the [*n*]circulene family; TsOH = p-toluenesulfonic acid, DME = 1,2-dimethoxyethane, Cp = Cyclopentadienyl.

[9]Agranat, I.; Hess, B. A.; Schaad, L. J. *Pure & Appl. Chem.* **1980**, *52*, 1399–1407.

In the reported methodology, alkynylation of the naphthoquinone-dimer (**2**) in the presence of CeCl$_3$ to suppress enolization afforded the desired tetraol (**3**) in 50% yield. Subsequent elimination and desilylation gave **4** in 30% yield. The authors performed the final cyclotrimerization, utilizing bis(trimethylsilyl)acetylene to improve the resulting solubility of the final product and provide a synthetic handle for subsequent functionalization. Jonas' catalyst in the presence of **4** and the acetylene afforded a CoCp complex of **1**, which could be oxidized in the presence of Cp$_2$Fe$^+$ to liberate the desired TBQ (**1**).

Tetrabenzoquadrannulene (**1**) is a radialene, a molecule in which double bonds emanate from all of the vertices of its central ring,[10] an observation that is evident in the reported crystal structure. TBQ takes on a bowl-shape as theoretical calculations would suggest[3] and the resulting pyramidalization (deformation of a trigonal planar molecule into a tetrahedral arrangement) of the four central C atoms of TBQ makes it one of the most highly pyramidalized molecules to be structurally characterized – with a reported hybridization character of sp$^{2.69}$. Despite this successful synthesis, the parent quadrannulene, lacking distal-benzo substituents, has yet to be synthetically achieved.

King notes the importance of elucidating the role that the peripheral benzo-substituents play in promoting the stability of TBQ. It can be surmised that inherent structural instability of the parent molecule has resulted in a lack of synthetic accessability. King's synthetic strategy does suffer from diminishingly low yields, however, this methodology does permit the incorporation of functionalization through

---

[10] Griffin, G. W.; Peterson, L. I. *J. Am. Chem. Soc.* **1962**, *84*, 3398–3400.

relatively simple acetylene precursors or though the late-stage functionalization of its TMS substituents.

1.2.2 [5]circulene (corannulene)

Much like quadrannulene, corannulene also takes on a bowl-shaped conformation. Its name [5]circulene, is derived from its 5-membered center ring surrounded by 5 benzo substituents. It is the only other known bowl-shaped member of the circulene family and its structure makes up 1/3 of the total surface of buckminsterfullerene (C_{60}), (**A**, Figure 1.3). Over the years, these geodesic polyarenes that make up fragments of fullerenes have been the subject of significant interest. Being the minimum repeat subunit structure of C_{60}, corannulene (**B & C**), has recieved increased interest compared toother synthetically viable circulenes.
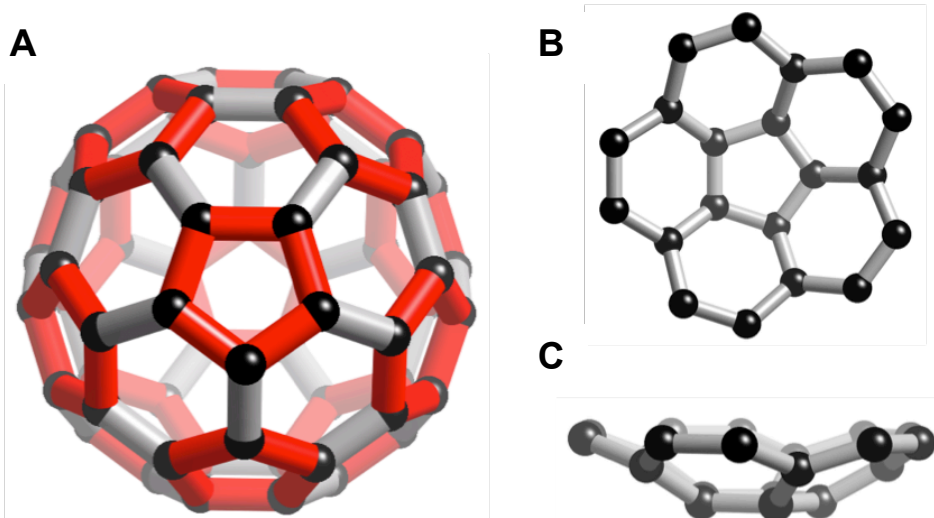
Figure 1.3 A) Top-down view of the spherical C_{60} buckminsterfullerene centered on one of its 5-membered rings, the physical moiety it shares with corannulene. **B**) Top and **C**) side views of the 3-dimensional bowl-shaped fullerene fragment corannulene.

Corannulene's significant synthetic literature presence has led to the structure's wide use and utility among materials chemists. Over a period of two decades between 1990 and 2012, Scott, Siegel and Rabideau independently reported seven different synthetic methodologies towards the synthesis of corannulene.[11] Though Lawton's original synthesis afforded corannulene three decades earlier, the overall synthesis resulted in less than 1% yield in 17 linear steps.[6] The most recent methodology developed by Siegel affords kilogram quantities of corannulene, with a greatly improved yield of 18% in 10 linear steps.[12g] As a result of these efforts corannulene is one of the few commercially available circulenes.

While similar methodologies developed by Scott and Siegel are distinguished by their respective final bond closures summarized in Scheme 1.2. Scott's methodologies rely on the final bond-forming step of **5** occurring at the flanking C–C bond of the peripheral structure from precursor **6a**, which is achieved *via* a one-pot Knoevenagel condensation and Diels-Alder reaction from **7a**. This synthetic strategy utilizes flash vacuum pyrolysis (FVP), a methodology that briefly exposes halocarbon-based precursors to extreme temperatures under dynamic vacuum conditions. Scott has successfully utilized this methodology to develop several geodesic polyarenes, most notably buckminsterfullerene.[12] On the other hand, Siegel's methodologies utilize similar

[11] (a) Scott, L. T.; Hashemi, M. M.; Meyer, D. T.; Warren, H. B. *J. Am. Chem. Soc.* **1991**, *113*, 7082–7084; (b) Borchardt, A.; Fuchicello, A.; Kilway, K. V.; Baldridge, K. K.; Siegel, J. S. *J. Am. Chem. Soc.* **1992**, *114*, 1921–1923; (c) Scott, L. T.; Cheng, P.-C.; Hashemi, M. M.; Bratcherm M. S.; Meyer, D. T.; Warren, H. B. *J. Am. Chem. Soc.* **1997**, *119*, 10963–10968; (d) Aygula, A.; Rabideau, P. W. *J. Am. Chem. Soc.* **2000**, *122*, 6323–6324; (e) Wu, Y. -T.; Siegel, J. S. *Chem. Rev.* **2006**, *106*, 4843–4867; (f) Tsefrikas, V. M.; Scott, L. T. *Chem. Rev.* **2006**, *106*, 4868–4884; (g) Butterfield, A. M.; Gilomen, B.; Siegel, J. S. *Org. Process Res. Dev.* **2012**, *16*, 664–676.
[12] Scott, L. T.; Boorum, M. M.; McMahon, B. J.; Hagen, S.; Mack, J.; Blank, J.; Wegner, H.; De Meijere, A. *Science* **2002**, *295*, 1500–1503.

Knoevenagel and Diels-Alder reactions from more complex quinone precursors **7b**. However, the final bond-forming step from **6b** then proceeds though various benzylic bromination, hydrolysis, and reduction steps to afford the desired corannulene (**5**) *via* the peripheral C–C rim bond. Siegel's strategy, while significantly longer than those developed by Scott, are completely solution based giving it large-scale synthetic advantages.
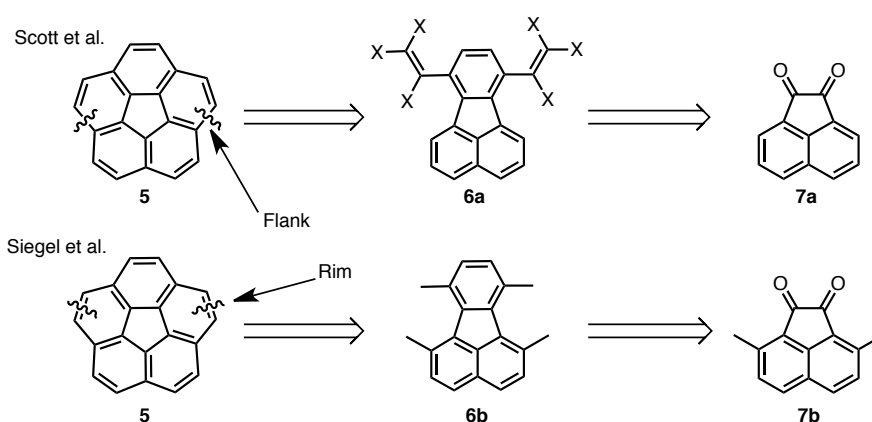
Scheme 1.2 The differing retrosynthetic schemes of both Scott's and Siegel's reported methodologies for corannulene (**5**), where final bond forming steps at both the flank, and the rim result from different fluoranthene precursors **6a** and **6b**.

When Lawton first synthesized [5]circulene in 1966, the name corannulene was proposed based on an annulene-within-an-annulene (AWA) or ring-current model, (Figure 1.4). The AWA model has become one of the more fascinating models of aromaticity within PAHs. Corannulene's aromatic character has been described as a two-ring system, wherein the inner 'core' of the structure is an aromatic 6-electron cyclopentadienyl anion surrounded by a 14-electron annulenyl cation. The two uncoupled annulenes represented together have a doubly-degenerate lowest unoccupied molecular

8

orbital (LUMO) totally localized on the flank and rim of the corannulene and a pair of doubly-degenerate highest occupied molecular orbitals (HOMOs) on the hub. Nevertheless, the AWA model of aromaticity has remained a particular point of contention within the chemical community.[13]

Corannulene   Annulene-within-an-annulene model
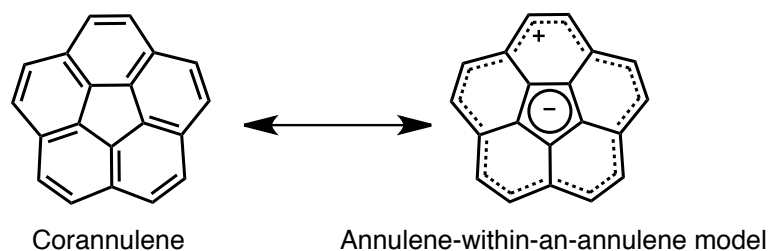
Figure 1.4 Annulene-within-an-annulene model (AWA) of Corannulene, the inner 'core' of the structure is an aromatic 6-electron cyclopentadienyl anion surrounded by a 14-electron annulenyl cation.

The most convincing case for supporting the AWA model was developed by Monaco and Zanasi in an experimental and computational study showing a strong magnetic response of the corannulene dianion characterized by a counter-rotating paratropic rim and diatropic hub observed in the structure's experimental NMR shifts.[13f] The net structure consists of two conrotating paratropic circulations located on the inner and outer rings. However, such observations are made under the notion that these Kekulé structures may only be viewed as uncoupled annulenes. As such, the bond order between the inner and outer rings of the aromatic system must be viewed as single-bond order

[13] (a) Sygula, A.; Rabideau, P. W. *J. Mol. Struc. (Theochem)* **1995**, *333*, 215–226; (b) Zhou, Z. *J. Phys. Org. Chem.* **1995**, *8*, 103–107; (c) Bühl, M. *Chem. Eur. J.* **1998**, *4,* 734–739; (d) Steiner, E.; Fowler, P. W.; Jenneskens, L. W. *Angew. Chem., Int. Ed.* **2001**, *40*, 362–366; (e) Steiner, E.; Fowler, P. W. *J. Phys. Chem. A* **2001**, *105*, 9553–9562; (f) Monaco, G.; Scott, L. T.; Zanasi, R. *J. Phys. Chem. A* **2008**, *112*, 8136–8147; (g) Eisenberg, D.; Shenhar, R. Wires. Comput. Mol. Sci. **2012**, *2*, 525–547; (h) Dickens, T. K.; Mallion, R. B. *Croat. Chem. Acta.* **2014**, *87*, 221–232.

only,[13h] a methodology that does not always hold true in such Kekulé structures. A well-studied aspect of PAHs is their ability to reversibly uptake and delocalize extra electrons. Such permutations on the structure of corannulene have shown its ability to accept both one and two electrons.[14] Surprisingly, generation of the anion was found to have little effect on the contorted structure, whereas, the dianion species observed significant flattening.

Owing to its unique properties, corannulene has attracted significant interest in its utilization as a synthetic precursor to larger aromatic systems. The ever-increasing interest in the development of uniform carbon nanotubes (CNTs) has resulted in synthetic methodologies that take advantage of corannulene's unique bowl-like structure towards the development of hemispherical end-caps in CNTs. These terminal carbon-building blocks have been envisioned as bottom-up templates for the synthesis of uniform CNTs.[15] Unfortunately, attempts at growing CNTs from well-defined templates have, to date, failed to produce structures of uniform shape and size.[16]

Still, the desire to develop well-defined nanocarbon materials has persisted.[17] One such example is Itami and Scott's reported synthesis of a 26-ring $C_{80}H_{30}$ "grossly warped" nanographene (Figure 1.5).[18] $C_{80}H_{30}$ is the first example of a synthetic graphene

[14] Zabula, A. V.; Spisak, S. N.; Filatov, A. S.; Grigoryants, V. M.; Petrukhina, M. A. *Chem. Eur. J.* **2012**, *18*, 6476–6484.

[15] Scott, L. T.; Jackson, E. A.; Zhang, Q.; Steinberg, B. D.; Bancu, M.; Li, B. *J. Am. Chem. Soc.* **2011**, *134*, 107–110.

[16] (a) Omachi, H.; Segawa, Y.; Itami, K. *Acc. Chem. Res.* **2012**, *45*, 1378–1389; (b) Omachi, H.; Nakayama, T.; Takahashi, E.; Segawa, T.; Itami, K. *Nature Chemistry* **2013**, *5*, 572–576.

[17] (a) Sygula, A.; Rabideau, P. W. Carbon-Rich Compounds (eds Haley, M. M.; Tykwinski, R. R.) 529–565 Wiley-VCH, **2006**; (b) Jasti, R.; Bhattacharjee, J.; Neaton, J. B.; Bertozzi, C. R. *J. Am. Chem. Soc.* **2008**, *130*, 17646–17647; (c) Petrukhina, M. A.; Scott, L. T. Fragments of Fullerenes and Carbon Nanotubes: Designed Synthesis, Unusual Reactions, and Coordination Chemistry, Wiley, **2011**; (d) Hirst, E. S.; Jasti, R. *J. Org. Chem.* **2012**, *77*, 10473–10478; (e) Wu, Y, -T; Siegel, J. S. *Chem. Rev.* **2006**, *106*, 4843–4867.

[18] Katsuaki, K.; Zhang, Q.; Segawa, Y.; Scott, L. T.; Itami, K. *Nature Chemistry* **2013**, *5*, 739–744.

sheet containing multiple Stone-Wales defects. This highly-contorted nanographene is a particularly powerful example in initial attempts to develop the controlled construction of large graphene structures from smaller molecular platforms. While planar examples of larger graphene subunits have previously been observed,[19] their significantly reduced solubility has made them nearly impossible to characterize.
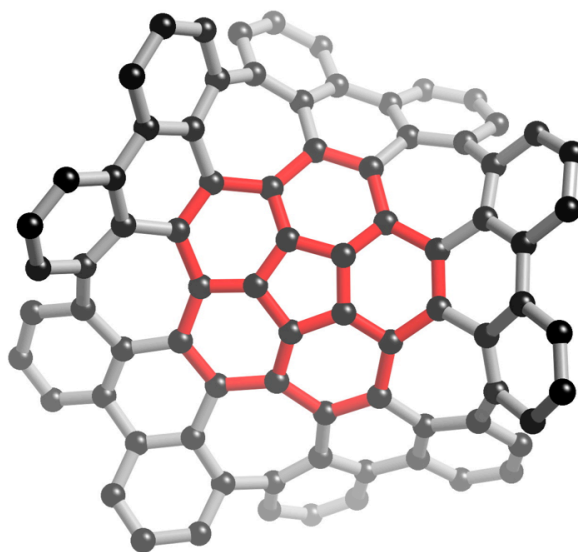
Figure 1.5 3-Dimensional model of $C_{80}H_{30}$, a "grossly warped" nanographene with multiple odd-ring-deficits, corannulene (red) makes up the core structure.

Additionally, the unique bowl-shape of corannulene has led researchers to develop new classes of molecular receptors capable of recognizing the curved surfaces associated with buckybowls and fullerenes. The double-concave corannulene complex synthesized by Rabideau and Olmstead (**A**, Figure 1.6)[20] is the one such example of a

[19] (a) Doetz, F.; Brand, J. D.; Ito, S.; Gherghel, L.; Müllen, K. *J. Am. Chem. Soc.* **2000**, *122*, 7707–7717; (b) Beser, U.; Kastler, M.; Maghsoumi, A.; Wagner, M.; Castiglioni, C.; Tommasini, M.; Narita, A.; Feng, X.; Müllen, K. *J. Am. Chem. Soc.* **2016**, *138*, 4322–4325.
[20] (a) Sygula, A.; Fronczek, F.; Sygula, R.; Rabideau, P.; Olmstead, M. *J. Am. Chem. Soc.* **2007**, *129*, 3842–3843.

buckybowl's unique concave surface forming a complex with the convex surface of a C_{60} fullerene (**B**). The unique-tweezer like shape of the corannulene complex was easily formed through a Diels-Alder reaction between isocorannulenofuran and dibenzocyclooctadiyne. The so-named "buckycatcher" has been proven to be an ideal candidate for investigating host-guest interactions between corannulene and fullerene.
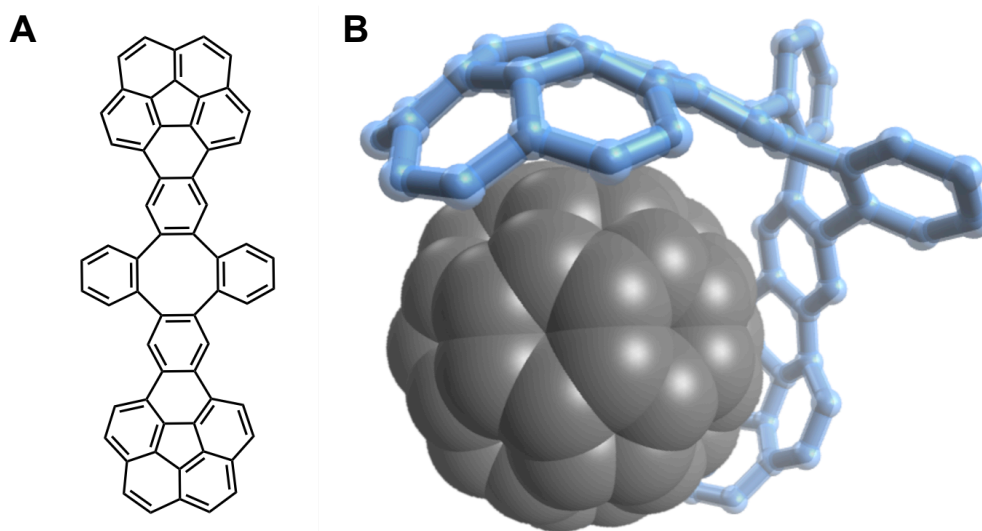
Figure 1.6 A) $C_{60}H_{24}$ molecular tweezers with two corannulene subunits and **B**) 3-dimensional representation of the complex formed between a single C_{60} fullerene and the corannulene buckycatcher.

Corannulene's unique bowl shape and kilogram scale synthesis has made it an exemplary model of the applications that members of the [n]circulene family can have in modern materials chemistry. Its large-scale synthesis, unique contorted shape, and prototypical AWA aromatic structure has made corannulene the most studied non-planar circulene, and a subject of unique interest to both computational and synthetic chemists.

1.2.3 [6]circulene (coronene)

Scholl and Meyer first reported the synthesis of coronene – [6]circulene (**8**, Scheme 1.3) – in 1932 as the decomposition product of *anti-diperi*-dibenzocoronene (**9**), which could be afforded *via* treatment with nitric acid and successive washings with a calcium hydroxide solution.[7a] Sublimation of the crude material afforded coronene (**8**) in 10% yield. The synthesis of coronene would go unreported for another 60 years,[21] and widely ignored until more modern, facile, advances.[22] Interestingly, this is the only member of the circulene family that can be found as a naturally occurring mineral – carpathite, discovered in the Carpathian Mountains of modern-day Slovakia.[23]
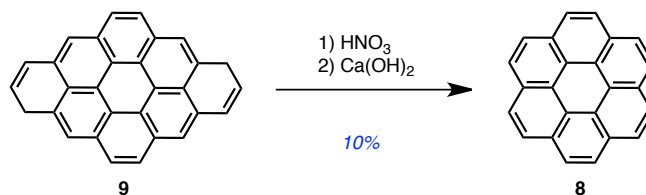
Scheme 1.3 The first reported synthesis of coronene (**8**) by decomposition of *anti-diperi*-dibenzocoronene (**9**) after addition of nitric acid and calcium hydroxide.

Not surprisingly, Scholl and Meyer suggest the structure of coronene (**8**) follows an AWA model of aromaticity in which the so-called 'aromatic Hückel count' is 18 electrons for the outer ring and 6 for the inner ring. In recent years, a new model aptly named the Hückel-London-Pople-McWeeny (HLPM) topological ring-current algorithm

---

[21] Dijk, J. T. M.; Hartwijk, A.; Cleeker, A. C.; Lugtenburg, J.; Cornelisse, J. *J. Org. Chem.* **1996**, *61*, 1136–1139.

[22] (a) Shen, H. -S.; Tang, J. -M.; Chang, H. -K.; Yang, C. -Y.; Liu, R. -S. *J. Org. Chem.* **2005**, *70*, 10113–10116; (b) Zhang, Q.; Peng, H.; Zhang, G.; Lu, Q.; Chang, J.; Dong, Y.; Shi, X.; Wei, J. *J. Am. Chem. Soc.* **2014**, *136*, 5057–5064.

[23] Piotrovsky, G. L. *Lvovskoe geol. Obshch., Mineral. Sbornik* **1955**, *9*, 120–127.

has been utilized to describe the aromaticity within the [*n*]circulene series and larger Kekulene structures.[24] In the case of coronene, it has been shown that the overall structure contains opposing clockwise (hub) and counter-clockwise (rim) ring currents leading to an overall diamagnetic structure that does not conform with the AWA model of aromaticity.[25] It is important to note that the authors report a similar observation for the structure of corannulene.

The crystal structure of coronene first reported in 1944 reports that molecules of coronene take on a herringbone-stacking motif, where a near-complete perpendicular orientation to one another is observed (**A**, Figure 1.7).[26] In some cases, functionalization of the coronene structure has shown to positively alter the herringbone stacking towards a more beneficial slip-stacked structural arrangement (**B**).[27] Such structural motifs exhibit higher-charge transport mobilities due to increased π-orbital overlap.
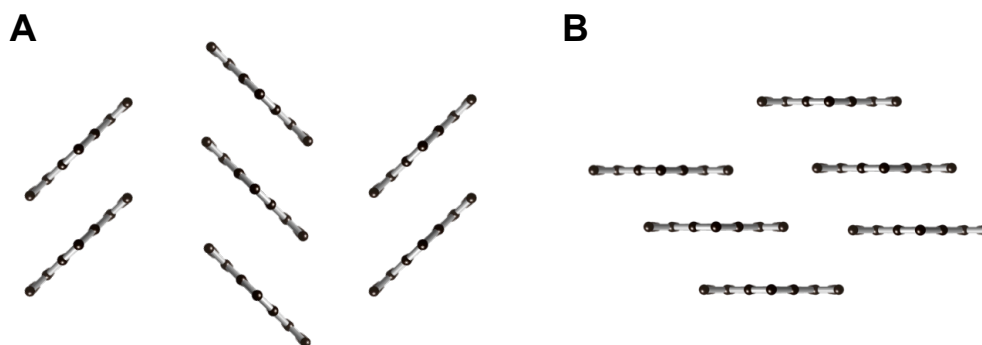
Figure 1.7 Crystal structures of **A**) coronene and **B**) functionalized coronene, viewed along the vertical *c*-axis of the crystal structure; functional groups and hydrogen atoms omitted for clarity.

---

[24] (a) Mallion, R. B. *Croat. Chem. Acta.* **2008**, *81*, 227–246; (b) Balaban, A. T.; Dickens, T. K. Gutman, I.; Mallion, R. B. *Croat. Chem. Acta.* **2010**, *83*, 209–215.

[25] Dickens, T. K.; Mallion, R. B. *Chem. Phys. Lett.* **2011**, *517*, 98–102.

[26] (a) Robertson, J. M.; White, J. G. *Nature* **1944**, *169*, 605–606; (b) Robertson, J. M.; White, J. G. *J. Chem. Soc.* **1945**, 607–617.

[27] Wu, D.; Zhang, H.; Liang, J.; Ge, H.; Chi, C.; Wu, J.; Liu, S. H.; Yin, J *J. Org. Chem.* **2012**, *77*, 11319–11324.

Recently, a new β-herringbone crystal structure (polymorph) has been achieved through the application of a magnetic field during the crystal growing process. These new herringbone structures have unique optical and mechanical properties generating new interest in their application as optoelectronic and potential photovoltaic switches.[28] The coronene structure has itself frequently been the target for molecular electronics. Studies of electronically favorable liquid crystal (LC) perylenediimides (PDIs)[29] have resulted in a new sub-class of materials based off of the coronene structure called coronenediimides (CDIs), which have found near-ubiquitous utility as materials for molecular electronics.[30]

The LC n-type semiconductors that result from these structural modifications, and similar,[31] have drawn ever-increasing interest among synthetic chemists.[32] Modern methodologies towards CDIs have not substantially deviated from early examples of these structures developed by Rohr and Müllen (Scheme 1.4).[30a-b] The 1,7-

[28] Potticary, J.; Terry, L. R.; Bell, C.; Papanikolopoulos, A. N.; Christianen, P. C. M.; Engelkamp, H.; Collins, A. M.; Fontanesi, C.; Kociok-Köhn, G.; Crampin, S.; Da Como, E.; Hall, S. R. *Nat. Commun.* **2016**, *7*, 11555.

[29] For representative examples, please see: (a) Würthner, F. *Chem. Commun.* **2004**, 1564–1579; (b) Iverson, I. K.; Tam-Chang, S.-W. *J. Am. Chem. Soc.* **1999**, *121*, 5801–5802; (c) Gregg, B. A.; Cormier, R. A. *J. Am. Chem. Soc.* **2001**, *123*, 7959–7960; (d) An, Z.; Yu, J.; Jones, S. C.; Barlow, S.; Yoo, S.; Domercq, B.; Prins, P.; Siebbeles, L. D. A.; Kippelen, B.; Marder, S. R. *Adv. Mater.* **2005**, *17*, 2580–2583; (e) Liu, Z., Zhang, G., Cai, Z., Chen, X., Luo, H., Li, Y., Wang, J.; Zhang, D. *Adv. Mater.* **2014,** *26*, 6965–6977; (f) Zhao, D.; Wu, Q.; Cai, Z.; Zheng, T.; Chen, W.; Lu, J.; Yu, L. *Chemistry of Materials* **2016**, *28*, 1139–1146.

[30] (a) Rohr, U.; Schlichting, P.; Böhm, A.; Gross, M.; Meerholz, K.; Bräuchle, C.; and Müllen, K. *Angew. Chem. Int. Ed.* **1998**, *37*, 1434–1437; (b) Rohr, U.; Kohl, C.; Müllen, K.; van de Craats, A.; Warman, J. *J. Mater. Chem.,* **2001**, *11*, 1789–1799; (c) Adachi, M. and Nagao, Y. *Chem. Mater.* **2001**, *13*, 662–669; (d) Samorí, P.; Severin, N.; Simpson, C. D.; Müllen K.; Rabe, J. P. *J. Am. Chem. Soc.* **2002**, *124*, 9454–9457; (e) Müller, S.; Müllen, K. *Chem. Commun.* **2005**, 4045–4046; (f) Nolde, F.; Pisula, W.; Müller, S.; Kohl, C.; Müllen, K. *Chem. Mater.* **2006**, *18*, 3715–3725; (g) Alibert-Fouet, S.; Seguy, I.; Bobo, J.-F.; Destruel P.; Bock, H. *Chem. Eur. J.* **2007**, *13*, 1746–1753; (h) Avlasevich, Y.; Müller, S.; Erk, P.; Müllen, K *Chem. Eur. J.* **2007**, *13*, 6555– 6561; (i) An, Z.; Yu, J.; Domercq, B.; Jones, S. C.; Barlow, S.; Kippelen, B.; Marder, S. R. *J Mater. Chem.* **2009**, *19*, 6688–6698; (j) Yan, Q.; Cai, K. Zhang, C. Zhao, D. *Org. Lett.* **2012**, 4654–4657; (k) Zhang, C.; Shi, K.; Cai, K.; Xie, J.; Lei, T.; Yan, Q.; Wang, J.-Y.; Pei, J.; Zhao, D. *Chem. Commun.* **2015**, *51*, 7144–7147; (l) Endres, A. H.; Schaffroth, M.; Paulus, F.; Reiss, H.; Wadepohl, H.; Rominger, F.; Krämer, R.; Bunz, U. H. F. *J. Am. Chem. Soc.* **2016**, *138,* 1792–1795.

[31] Rao, K. V.; George, S. J. *Org. Lett.* **2010,** *12*, 2656–2659.

[32] Guo, X.; Facchetti, A.; Marks, T. J. *Chem. Rev.* **2014**, *114*, 8943–9021.

dibromoperylene-3,4:9,10-tetracarboxyanhydride (**10**) is a common precursor among the synthetic strategies utilized for these structures and is easily converted to the desired diimide (**11a-g**) using the appropriate amine. Sonogashira coupling of the terminal alkynes affords the functionalized diimides (**12**). The final coronene structure could then be generated through DBU-promoted cyclization of the alkyne, affording the desired CDIs (**13a-g**) in 95-100% yield.
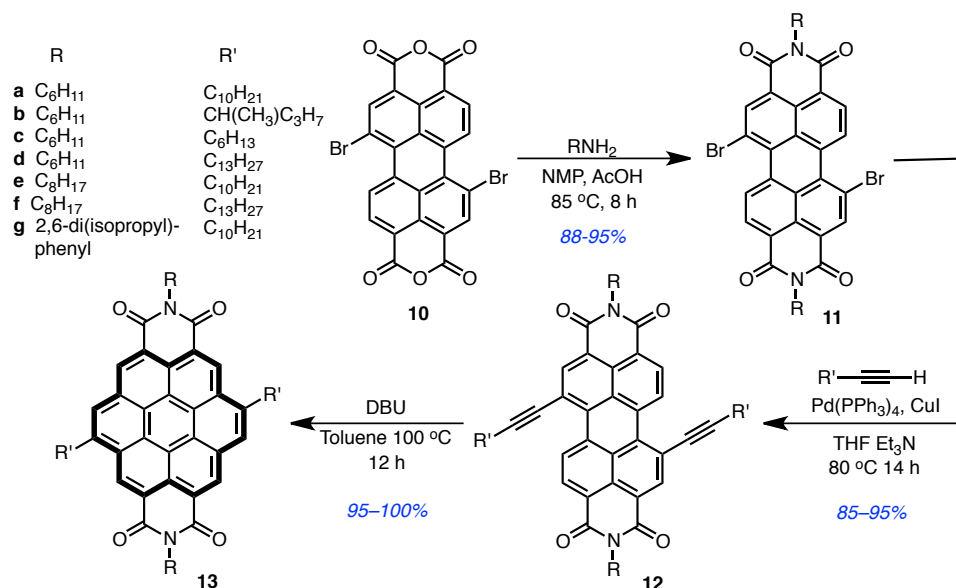
Scheme 1.4 Rohr and Müllen's synthesis of functionalized coronenediimides (**13**), coronene core represented in bold; NMP = N-methyl-2-pyrrolidone; DBU = 1,8-diazabicyclo(5.4.0)undec-7-ene.

This evolving class of coronene-based semiconductors utilizes the n-type functionalization of the diimide and secures additional stability and electron transport capability due to the increased π-orbital overlap. While the charge transport capabilities of these columnar materials are expected to be anisotropic, the precise nature of thin films made from CDIs suggest a mixture of alignments that tends to vary significantly

between samples made under repeat conditions.[29i] This result is in part attributed to the slip-stack nature of functionalized coronenes and begs further investigation.

Decades-long research into the crystal packing nature of functionalized coronenes, their often challenging multi-step synthesis, and the favorable charge transport mobilities of CDIs have led to the emergence of a larger class of π-extended hexabenzocoronenes (HBCs). These extended aromatic systems have been described in both *peri-* (**A**, Figure 1.8) and *cata*-condensed (**B**) structural arrangements.

A   **B**

Hexa-*peri*-hexabenzocoronene   Hexa-*cata*-hexabenzocoronene
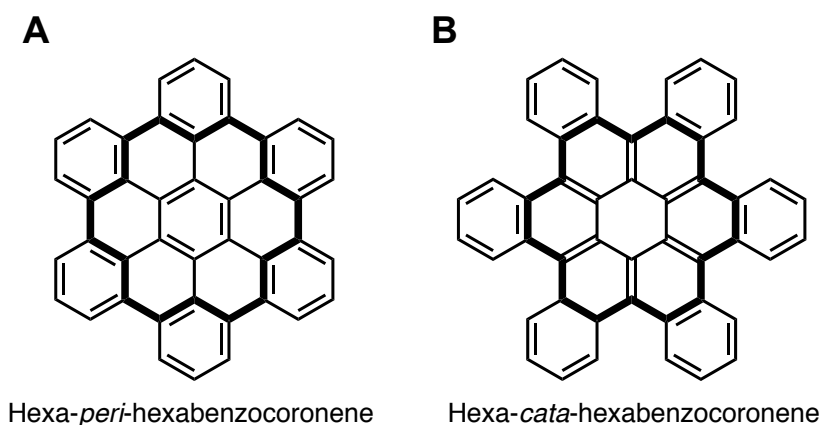
Figure 1.8 Larger π-extended **A**) hexa-*peri*-hexabenzocoronene and **B**) hexa-*cata*-hexabenzocoronene, parent coronene structure highlighted in bold.

Hexa-*peri*-hexabenzocoronene (*p*-HBC) has been synthetically known since 1958 (Scheme 1.5)[33] and not surprisingly shares similar crystal packing behaviors to that of coronene,[34] retaining both herringbone and slip-stacked structural motifs. The synthetic

[33] (a) Clar, E.; Ironside, C. T. *Proc. Chem. Soc.* **1958**, 150; (b) Clar, E.; Ironside, C. T.; Zander, M. *J. Chem. Soc.* **1959**, 142.
[34] (a) Robertson, J. M.; Trotter, J. *J. Chem. Soc.* **1961,** 1280–1284; (b) Men, F. H.; Bellard, S.; Brice, M. D.; Carhwight,B. A.; Doubleday, A.; Higgs, H.; Humpelink, T.; Hummelink-Peters, B. G.; Kennard, O.; Motherwell, W. D. S.; Rodgers, J. R.; Watson, D. G. *Acta Crystallogr.* **1979**, *B35,* 2331–2339; (c) Goddard, R.; Haenel, M. W.; Herndon, W. C.; Krüger, C.; Zander, M. *J. Am. Chem. Soc.* **1995**, *117*, 30–41;

methodology first carried out by Clar and co-workers found that bromination of the 2:3–7:8-dibenzo-*peri*-naphthene (**14**) followed by heating at ca. 150 ºC resulted in the formation of a tetrabenzoperopyrene (**15**) which could subsequently be heated to temperatures > 480 ºC to afford *p*-HBC (**16**) as a bright yellow solid. More recently, the structures of *p*-HBC have been the subject of immense interest, producing materials capable of high charge-carrier mobilities,[35] and aligning into self-assembled helical *p*-HBC nanotubes.[36]
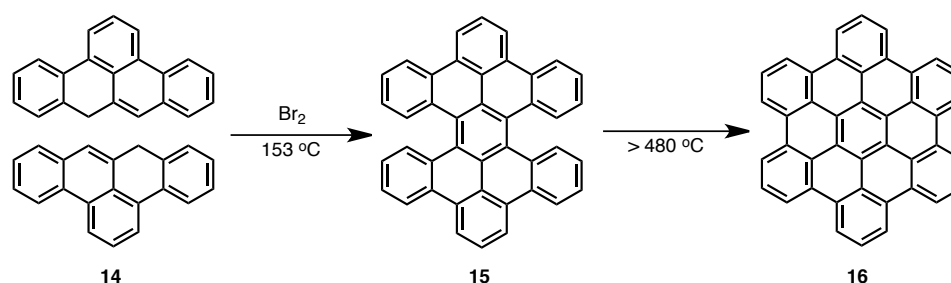
Scheme 1.5 The first reported synthesis of hexa-*peri*-hexabenzocoronene (**16**).

Hexa-*peri*-hexabenzocoronenes maintain simplified synthetic methods over the parent synthesis of the coronene structure, employing powerful reactions such as Diels-Alder,[37] and Vollhardt cyclization,[38] to achieve good yields in fewer steps. Despite these

(d) Breuer, T.; Liues, M.; Liesfeld, P.; Viertel, A.; Conrad, M.; Hecht, S.; Witte, G. *Phys. Chem. Chem. Phys.* **2016***, 18*, 33344–33350.

[35] Wu, J.; Pisula, W.; Müllen, K. *Chem. Rev.* **2007**, *107*, 718–747.

[36] Hill, J. P.' Jin, W.; Kosaka, A.; Fukushima, T.; Ichihara, H.; Shimomura, T.; Ito, K.; Hashizume, T.; Ishii, N.; Aida, T. *Science* **2004**, *304*, 1481–1483.

[37] Iyer, V. S.; Wehmeier, M.; Brand, J. D.; Keegstra, M. A.; Müllen, K. *Angew. Chem. Int. Ed. Engl.* **1997**, *36,* 1604–1607.

[38] (a) Stabel, A.; Herwig, P.; Müllen, K.; Rabe, J. P. *Angew. Chem. Int. Ed. Engl.* **1995**, *34*, 1609–1611; (b) Herwig, P.; Kayser, C. W.; Müllen, K.; Spiess, H. W. *Adv. Mater.* **1996**, *8*, 510-513; (c) Fechtenkötter, A.; Tchebotareva, N.; Watson, M.; Müllen, K. *Tetrahedron* **2001**, *57*, 3769-3783; (d) Pisula, W.; Kastler, M.; Wasserfallen, D.; Tadeusz, P.; Müllen, K. *J. Am. Chem. Soc.* **2004**, *126*, 8074–8075.

significant advances towards larger π-extended coronenes and investigations into the similar, albeit contorted, aromatic systems by Nuckolls and co-workers have delivered some of the most promising results to come from these coronene-containing molecules.[1] Hexa-*cata*-hexabenzocoronene (*c*-HBC), first synthesized by Clar in 1965,[39a] has shown promising results in molecular electronics,[39b-c] netting charge transport mobilities of 0.1 cm^2/V·s compared to 0.016 cm^2/V·s for pure *p*-HBC devices. Contorted aromatics benefit from the ability to align into self-assembling molecular wires, introducing new columnar behaviors. The improved syntheses of *c*-HBCs reported by Nuckolls and co-workers is one of the first examples of Scholl cyclodehydrogenation conditions to be utilized in final bond forming steps of contorted aromatic systems (Scheme 1.6).[40]
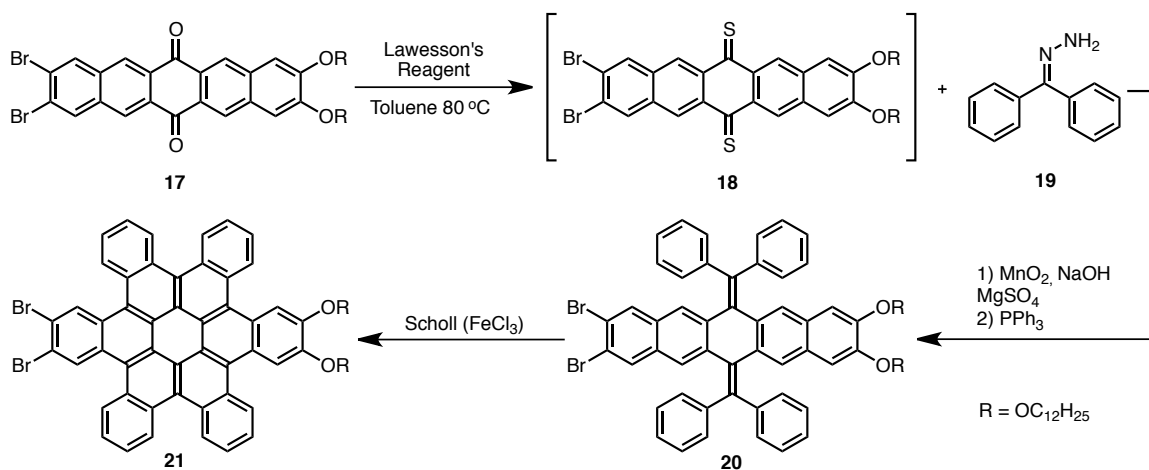
Scheme 1.6 The synthesis of contorted *c*-HBCs (**21**) *via* double Barton-Kellogg olefination to afford (**20**) followed by Scholl cyclodehydrogenation. Reactions progressed favorably with desymmetrized pentacene quinones (**17**).

[39] (a) Clar, E.; Stephen, J. F. *Tetrahedron* **1965**, *21*, 467–470; (b) Xiao, S.; Tang, J.; Beetz, T.; Guo, X.; Tremblay, N.; Siegrist, T.; Zhu, T.; Steigerwald, M.; Nuckolls, C. *J. Am. Chem. Soc.* **2006**, *128*, 10700–10701; (c) Harris, K. D.; Xiao, S.; Lee, C. Y.; Strano, M. S.; Nuckolls, C.; Blanchet, G. B. *J. Phys. Chem. C*, **2007**, *111*, 17947–17951.
[40] Plunkett, K. N.; Godula, K.; Nuckolls, C.; Tremblay, N.; Whalley, A. C.; Xiao, S. *Org. Lett.* **2009**, *11*, 2225–2228.

The synthesis of *c*-HBC can be carried out in as little as four steps from the pentacene quinone precursor **17**. Following treatment with Lawesson's reagent, the dithioquinone (**18**) was subjected to an *in situ* - generated diphenyldiazomethane, which afforded a dithioepoxide that was subsequently reduced in the presence of triphenylphosphine to give (**20**). The resulting double olefin (**20**) was subjected to Scholl conditions, affording desired *c*-HBC (**21**) in good yield. Following the revised synthesis of *c*-HBC, Whalley and Nuckolls reported the synthesis of new bowl-shaped PAHs where the structure of coronene is contained within the contorted aromatic system (**A** & **B**, Figure 1.9).[41]
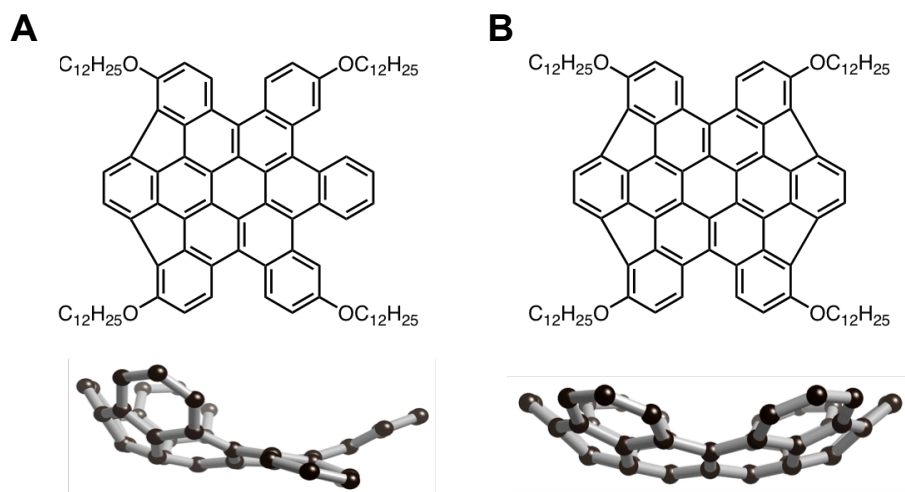
Figure 1.9 Whalley and Nuckoll's bowl-shaped PAHs of **A**) 2-closed and **B**) 4-closed *c*-hexabenzocoronene along with representative *c*-axis DFT calculated structures.

Synthesized from *c*-HBC precursors – using palladium catalyzed Heck-arylation conditions and subsequent and Scholl cyclodehydrogenation reactions closed a maximum

[41] Whalley, A. C.; Plunkett, K. N.; Gorodetsky, A. A.; Schenck, C. L.; Chiu, C. -Y.; Steigerwald, M. L.; Nuckolls, C. *Chem. Sci.* **2011**, *2*, 132–135.

of four C–C bonds between the peripheral benzo-substituents of the parent compound. Bowl-shaped hexabenzocoronenes were found to form strong host-guest interactions with C_{70} with association constants as high as 3.2 x 10^6 M^{-1} – three orders of magnitude higher than those formed between corannulene buckycatcher and C_{60} fullerene.

More recently, Nuckolls and co-workers have developed a new class of contorted aromatics that continue to utilize the coronene core as a common structural theme. These new materials connect a series of CDI (**A**, Figure 1.10) units into helical nanoribbons (**B**).[42] These structures benefit from improved charge transport mobilities[42a] and have been manipulated into large macrocycles as part of a new class of electron transporting materials.[43]
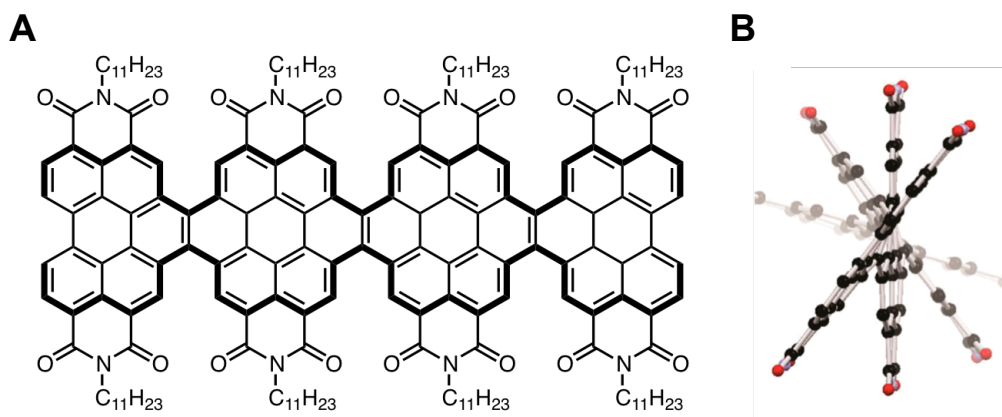
Figure 1.10 A new class of **A**) conjugated oligomers composed of CDIs and the resulting **B**) helical arrangement viewed down the C_2 axis of the nanoribbon structure.

[42] (a) Zhong, Y.; Kumar, B.; Oh, S.; Trinh, M. T.; Wu, Y.; Elbert, K.; Li, P.; Zhu, X.; Xiao, S.; Ng, F.; Steigerwald, M. L.; Nuckolls, C. *J. Am. Chem. Soc.* **2014**, *136*, 8122–8130; (b) Schuster, N. J.; Paley, D. W.; Jockusch, S.; Ng, N.; Steigerwald, M. L.; Nuckolls, C. *Angew. Chem. Int. Ed.* **2016**, *55,* 13519–13523.
[43] (a) Ball, M. Zhong, Y.; Fowler, B.; Zhang, B.; Li, P.; Etkin, G.; Paley, D. W.; Decatur, J.; Dalsania, A. K.; Li, H.; Xiao, S.; Ng, F.; Steigerwald, M. L.; Nuckolls, C. *J. Am. Chem. Soc.* **2016**, *138*, 12861–12867; (b) Zhang, B.; Tuan Trinh, M.; Fowler, B.; Ball, M.; Xu, Q.; Ng, F.; Steigerwald, M. L.; Zhu, X. –Y.; Nuckolls, C.; Zhong, Y. *J. Am. Chem. Soc.* **2016**, *138*, 16426–16431.

Comprised of six *peri*-fused benzene rings, coronene is the only planar member of the circulene family. Its structure has been incorporated into a number of high performing electronic materials.[40-43] While the parent molecules herringbone packing structure is unfavorable for electronics applications, functionalization of these structures has resulted in beneficial slip-stacked packing motifs. CDIs that incorporate the coronene motif into their structural backbone have shown promising charge transport mobilities. Larger π-extended HBCs have shown increased orbital overlap leading to materials with increased charge transport mobilities. Removed from its traditionally planar structure, significant progress has been made utilizing highly contorted coronene in the application of molecular electronics.

1.2.4 [7]circulene (pleiadannulene)

Pleiadannulene is the smallest saddle-shaped member of the highly contorted (negatively curved) circulenes. The synthesis of [7]circulene was first attempted in 1975 by Reiss and Jessup, whose synthetic methodology laid significant groundwork in accessing the final structure.[44] Ultimately, it was the synthetic strategy developed by Yamamoto and co-workers that successfully yielded the saddle-shaped molecule (Scheme 1.7).[8a-b] Reiss and Jessup's methodology could not overcome the strain induced in the final bond forming step due to the rigidity of the naphthalene and phenanthrene backbone. Yamamoto sought a more flexible biphenylnaphthalene cyclophane to achieve the desired structure in a multistep strategy.

---

[44] (a) Jessup, P. J.; Reiss, J. A. *Tetrahedron Lett.* **1975,** *17*, 1453–1454; (b) Jessup, P. J.; Reiss, J. A. *Aust.J. Chem.* **1976**, *29,* 173–178.
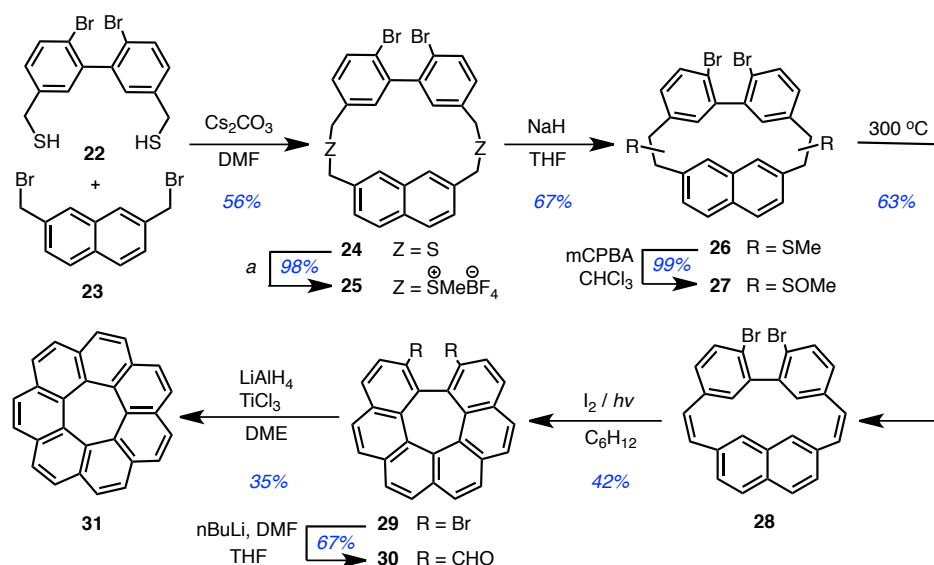
Scheme 1.7 Yamamoto's stepwise synthesis of [7]circulene (**31**) *via* a flexible precursor; biphenylnaphthalene cyclophane (**28**); *a* = dimethoxycarbonium tetrafluoroborate, DME = 1,2-dimethoxyethane.

Following Yamamoto's protocol, the coupling of biphenyl (**22**) and 2,7-bis(bromo-methyl)naphthalene (**23**) was performed in DMF with cesium carbonate to give the dithiocyclophane (**24**). Further reaction of **24** with dimethoxycarbonium fluoroborate [45] in DCM yielded the disulfonium salt, which, following Stevens rearrangement, yielded **26**. Oxidation of the resulting sulfide (**26**) with *meta*-chloroperoxybenzoic acid (*m*CPBA) afforded sulfoxide, **27**, that could easily be converted to **28** by pyrolysis at 300 ºC. A solution of **28** in cyclohexane charged with trace amounts of iodine was irradiated with UV-light, affording 1,16-dehydro-2,15-dibromohexahelicene (**29**). Lithiation of dibromide (**29**) followed by addition of DMF yielded dialdehyde (**30**). Intramolecular McMurry coupling of **30** with LiAlH$_4$ and TiCl$_3$

---

[45] Borch, R. F. *J* . Org. *Chem.* **1969**, *34*, 627–629.

in dimethoxyethane completed the outer diameter of [7]circulene (**31**).

Pleiadannulene (**31**) could be more readily prepared through Yamamoto's revised synthesis, first reported in 1996 (Scheme 1.8).[8c-d]   Wittig olefination of 2,7-naphthalenedicarboxaldehyde (**32**) in NaOMe/DMF afforded **33,** which could be irradiated with uv-light, yielding 2,15-dimethylhexahelicene (**34**) in 59% yield. Subsequent bromination (**35**) and treatment with sodium sulfide nonahydrate afforded hexahelicene sulfide (**36**), which could be oxidized to the sulfone (**37**) in two steps with a 47% yield overall. Flash vacuum pyrolysis afforded the dihydro[7]circulene (**39**) in 24% yield.   Dehydrogenation of **39** with 5% Pd/C in 1-methyl-naphthalene at 280 ºC gave [7]circulene in 85% yield. The authors suggest that the transformation of **37** to **39** goes through an ethano-bridged hexahelicene (**38**), which readily dehydrogenates to **39**. To date, these remain the only known synthetic methodologies to arrive at these contorted saddle-shaped structures.
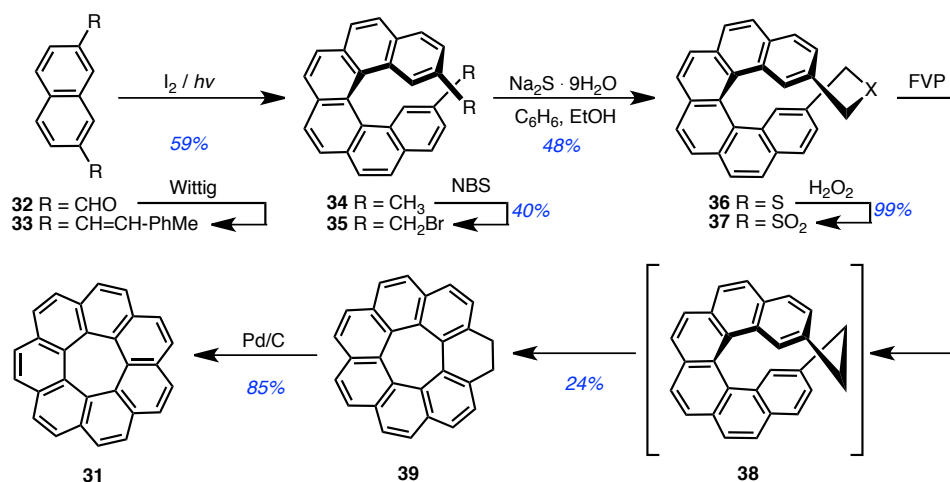
Scheme 1.8 Yamamoto's revised synthesis of [7]circulene (**31**) *via* FVP and hexahelicene precursor **37**.

Despite the presence of these methodologies, investigations into the contorted nature of pleiadannulene have remained relatively stagnant. Recently, Miao and co-workers synthesized a new negatively curved $C_{70}H_{26}$ aromatic structure containing two pleiadannulene subunits (**A**, Figure 1.11).[46] Amorphous films of Miao's saddle-shaped materials displayed low-charge transport mobilities due to the lack of long-range order. Nevertheless, these materials have begun to exploit the saddle-shaped nature of [7]circulene by incorporating their unique physical properties into larger aromatic systems (**B**).

A   **B**

R = n-octyl or n-hexyl
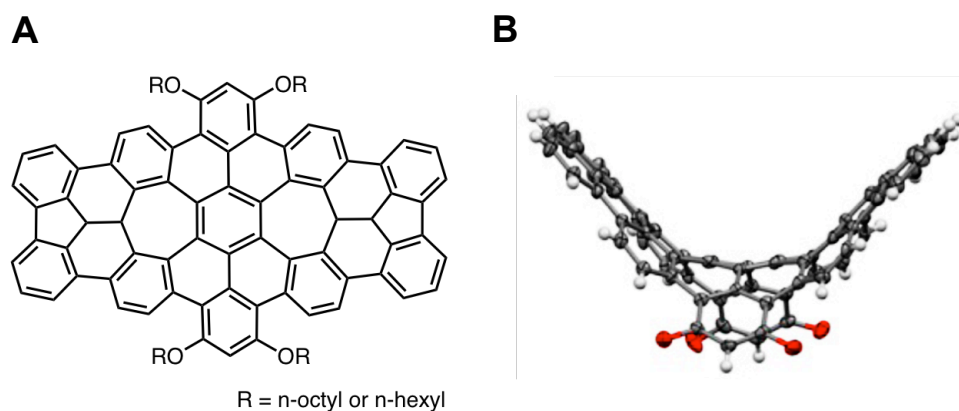
Figure 1.11 A) $C_{70}H_{26}$ aromatic saddle and **B**) its saddle-shaped structural conformation; alkyl groups removed for clarity.

More recently, Miao and co-workers reported a new tetrabenzo[7]circulene (TB[7]C) structure, which, unlike the methodologies reported by Yamamoto relies on the formation of the principle 7-membered ring early on in the reported synthetic procedure

---

[46] Cheung, K. Y.; Xu, X.; Miao, Q. *J. Am. Chem. Soc.* **2015**, *137*, 3910–3914.

(Scheme 1.9).[47] This methodology provides simplified access to the [7]circulene structural motif and these materials act as p-type semiconductors in thin-film transistors.
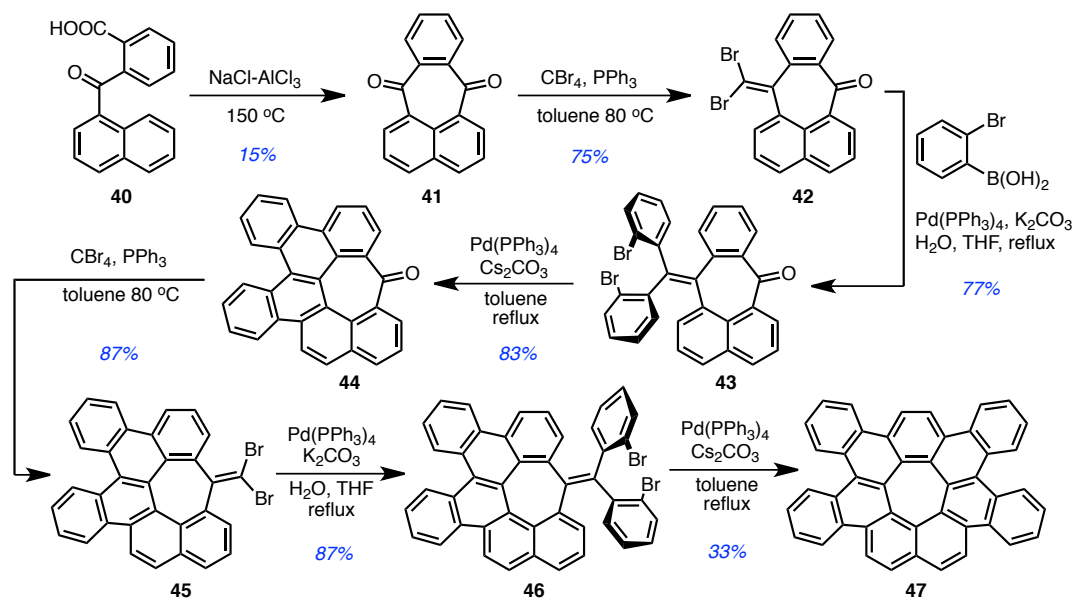
Scheme 1.9 Miao's recently reported synthesis of tetrabenzo[7]circulene (**47**), a new benzo-substituted form of the parent [7]circulene.

Following Miao's reported synthesis, from 2-(1-naphthoyl)-benzoic acid (**40**), an Intramolecular Friedel-Crafts acylation afforded the 5,12-pleiadenedione (**41**), in low yield (15%), which was isolated from the undesired major product benz[*a*]anthraacene-7,12-dione. Corey-Fuchs olefination afforded the desired **42** and subsequent Suzuki coupling afforded the asymmetric arene **43** in 57% yield over two steps. Unfortunately, Miao and co-workers were unable to force the second Corey-Fuchs olefination on the second carbonyl, due to the convex face of **42** being blocked by the newly added bromine atoms. Nevertheless, Pd-catalyzed cyclization of **43** afforded the desired **44**, which could

[47] Gu, X.; Li, H.; Shan, B.; Liu, Z.; Miao, Q. *Org. Lett.* **2017**, *19*, 2246–2249.

subsequently undergo Corey-Fuchs as a result of the reduced steric hindrance, yielding **45**, which underwent Suzuki coupling to yield **46**. Subsequent Pd-catalyzed cyclization afforded the desired TB[7]C (**47**). The authors note that attempts to yield the desired product utilizing the Scholl reaction were unsuccessful.

Miao's newly reported synthesis also provides access to a thiophene-annulated form of [7]circulene. These structures take on an interesting near slip-stacked structural orientation in the crystal form, a surprising result due to their highly contorted nature. This new methodology does provide access to the structural motif of pleiadannulene in higher yields when compared to the original synthetic methodologies presented by Yamamoto. Moreover, Miao and co-workers were able co-crystallize this new TB[7]C with C_{60}.

Pleiadannulene is the smallest saddle-shaped homologue of the [*n*]circulene series, and recent advances in contorted aromatics and their potential charge transport properties have created new interest in the class of saddle-shaped aromatic materials. Miao and co-workers have incorporated these saddle-shaped structures into larger aromatic systems in attempts to further understand their unique structural and electronic properties. While the synthesis of [7]circulenes has been revisited by Yamamoto, its current methodology – relying on scale-limiting FVP – has left further investigations into these materials challenging.

1.2.5 [8]circulene

While molecules containing central rings of four to seven members have been synthesized, the larger members of these series, [8]circulene and above, remain attractive and, until recently, elusive[48] synthetic targets. Calculations predict that instability of these structures is a result of concentric aromatic ring currents.[49] The first attempted synthesis of [8]circulene (**50**, Scheme 1.10) was reported in 1976 by Wennerström and co-workers, but the reversible nature of the photoreaction used in the final step of their synthetic strategy was not conducive to retaining the strain formed in the final bond closures, despite the successful synthesis of the phenanthrene precursor (**49**) from **48**.[50] In order to comprehend why such challenges have been met, a thorough understanding of the electronic structure of **50** has been investigated.
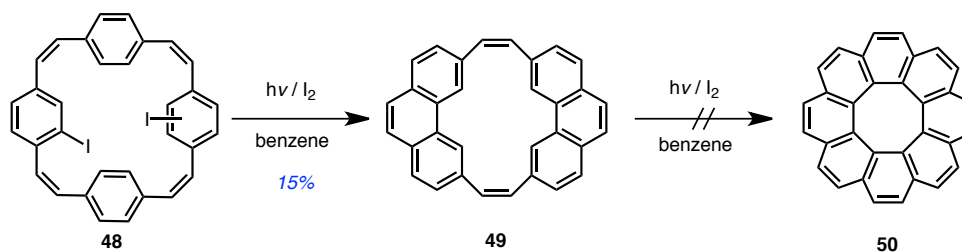
Scheme 1.10 Wennerström's Attempted Synthesis of [8]Circulene in 1976.

The generally accepted model of aromaticity – often referred to as Kekulé structures – proposes that electrons located in the p_z-orbitals of cyclic moieties are free to

[48] Müllen, M.; Iyer, V. S.; Kubel, C.; Enkelmann, V.; Müllen, K. *Angew. Chem. Int. Ed. Engl.* **1997**, *36*, 1607–1610.
[49] Salcedo, R.; Sansores, L. E.; Picazo, A.; Sansón, L. *J. Mol. Struct. (Theochem.)* **2004**, *678*, 211–215.
[50] Thulin, B.; Wennerström, O. *Acta. Chem. Scand. B.* **1976**, *30b*, 369–371.

move throughout the entire π-system of the molecule.[51] However, when applying this concept to larger PAHs, this model falls short of providing an accurate depiction of the aromaticity contained within these systems.[52] A more accurate representation of these structures would be the fully-benzenoid model developed by Erich Clar, wherein all of the double bonds belong to aromatic sextets, resulting in a considerably more stable arrangement than their counterparts containing isolated double bonds.

1.3 Application of Clar's Model of Aromaticity

The Clar model of aromaticity, which depicts π-electrons as localized to individual rings, is a more accurate representation of the aromaticity in PAHs.[53] Simply put, the Clar model says the resonance structure of any PAH that depicts the largest number of aromatic sextets will be the largest contributor to the resonance hybrid and the most important for the characterization and properties of that compound. The molecule kekulene, (Figure 1.12) is a prime example of such localization and a prime example Clar's model applied to these aromatic species. With over 200 possible resonance structures, the Kekulé model would suggest a structure where – if each resonance structure contributed equally to the overall character – individual bonds would average to a single, common length. However, experimental data indicates rings exhibiting aromatic character, as well as quasi-single and -double bonds.

[51] Pauling, L. *J. Chem. Phys.* **1936**, *4*, 673–677.
[52] (a) Krieger, C.; Diederich, F.; Schweitzer, D.; Staab, H. A. *Angew. Chem. Int. Ed. Engl.* **1979**, *18*, 699–701; (b) Kumar, B.; Viboh, R. L.; Bonifacio, M. C.; Thompson, W. B.; Buttrick, J. C.; Westlak, B. C.; Kim, M. -S.; Zoellner, R. W.; Varganov, S. A.; Mȩrschel, P.; Teteruk, J.; Schmidt, M. U.; King, B. T. *Angew. Chem. Int. Ed.* **2012**, *51*, 12795–12800.
[53] Clar, E. *The Aromatic Sextet*, Wiley, New York, **1972**.
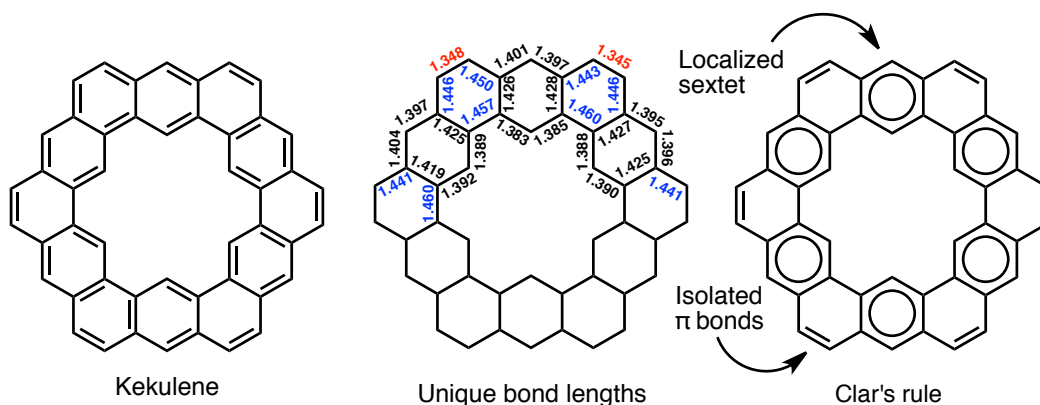
Figure 1.12 Kekulene, a structure with over 200 resonance forms, is a prime example of how localization of aromaticity in larger PAHs results in quasi-type single and double bonds, a source of reactivity in complex aromatic structures.

Clar's model can be applied to PAHs with essentially three results.[54] The most obvious and structurally important for stability considerations is the fully benzenoid model (**A**, Figure 1.13). In such structures, π-electrons are assigned to isolated sextets or are otherwise described as "empty" – containing no localized electrons within a given ring.[55] These structures are described as fully benzenoid, fully aromatic, or Clararomatic. Other structures in which the Clar model can be applied but does not fit the definition of fully-benzenoid carry less strictly defined nomenclature. Nevertheless, the observations that result from the application of these rules can be considerably more important for understanding a given molecule's electronic nature. Applying Clar's model of aromaticity to phenanthrene (**B**, Figure 1.13) nets two structures; the most important for predicting its characteristics carries the largest possible number of aromatic sextets in a given system. Not surprisingly, the olefin-like reactivity of phenanthrene's single

[54] Solá, M. *Front. Chem.* **2013**, *1*, 1–22.
[55] Randic M. *J. Mol. Chem. (Theochem)* **1991**, *229*, 139–153.

localized π-bond is well described and is clearly understood from the Clar structure. Lastly, in examples like anthracene (**C**, Figure 1.13), each aromatic ring contributes equally to the overall structural characteristics. In this case, the aromatic sextet has an equal chance of being localized in any individual ring, and therefore the nature of the aromaticity in these structures is delocalized.
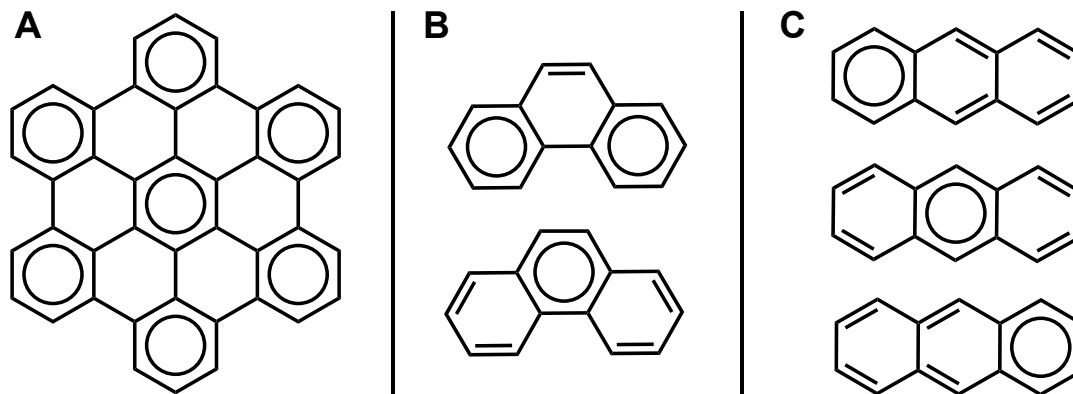
Figure 1.13 A) Fully-benzenoid representation of hexa-*peri*hexabenzocoronene, **B)** localized aromaticity of phenanthrene – top representing two aromatic sextets and one localized π-bond, this representation contributes more to the overall character. **C)** anthracene whose migrating sextet contributes equally to each ring.

When we analyze the electronic structure of [8]circulene (**A**, Figure 1.14), it is clear that four of the double bonds are not part of aromatic sextets. Although such bonds also exist in smaller circulene analogues, the greater strain inherent to [8]circulene has the potential to make these bonds more reactive and is therefore a source of instability. The installation of four fused benzene rings, however, incorporates these isolated double bonds into the additional sextets provided by the fused rings (**B**, Figure 1.14). With the stability of PAHs being directly related to the incorporation of π-bonds into aromatic sextets and any external double bonds being a source of instability, using Clar's rule, we set our sights on the synthesis of a stable tetrabenzo[8]circulene (TB[8]C).

31
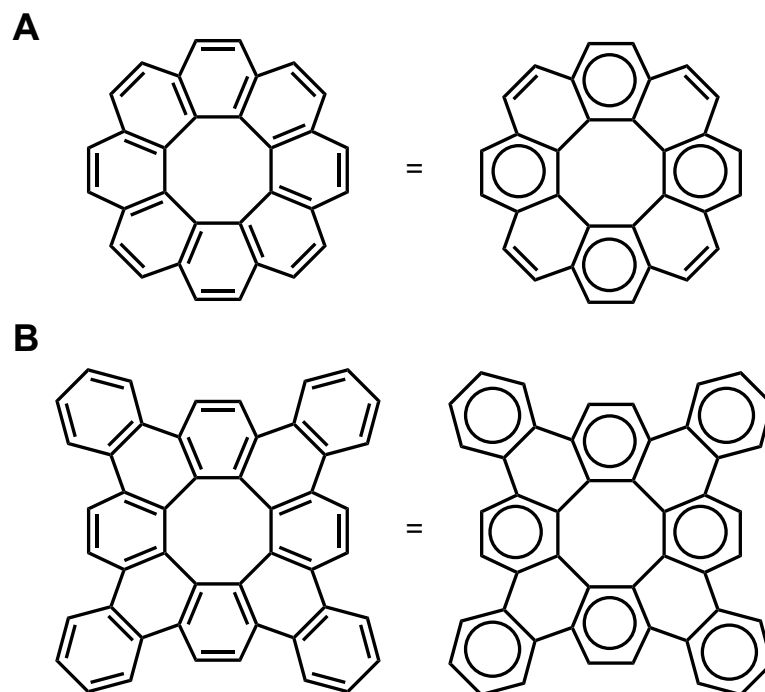
Figure 1.14 Kekulé and Clar structures of localized aromatic sextets in **A)** [8]circulene and **B)** tetrabenzo[8]circulene. By introducing four fused benzene rings the isolated double bonds apparent in the top structure are incorporated into aromatic sextets in the bottom structure, imparting additional stability on the system.

1.4 Modern Advances Towards [8]Circulene

During the preparation of our original manuscript related to this work, two remarkably different strategies towards the synthesis of [8]circulene derivatives were achieved. The first of these strategies was developed by Wu and co-workers who reported a number of highly substituted [8]circulene derivatives.[56] The following sections will

---

[56] Feng, C. -N.; Kuo, M. Y.; Wu, Y, -T. *Angew. Chem. Int. Ed.* **2013**, *52*, 7791–7794.

introduce these recent synthetic strategies, followed by a detailed account of the work performed in our laboratory towards the successful synthesis of tetrabenzo[8]circulene.

1.4.1 Wu's Synthesis of [8]Circulene

Wu and co-workers were the first to report the synthesis of a highly functionalized version of the parent molecule [8]circulene. Wu's synthesis relies foremost on the construction of the eight-membered core, followed by palladium-catalyzed annulation of iodo-substituted tetraphenylenes (**51a-b**, Scheme 1.11) with substituted aryl alkynes. The synthetic pathway developed by Wu and co-workers resulted in a regioisomeric mixture where the final annulation procedure results in notably good yields (60–75%), albeit lacking the stability of its benzo-substituted successor.

and regioisomers
51a R = OMe
51b R = Me

50a R = Me, Ar = 4-(CH$_3$)C$_6$H$_4$, 60%
50b R = Me, Ar = 3,5-(CH$_3$)$_2$C$_6$H$_3$, 68%
50c R = OMe, Ar = 4-(CH$_3$)C$_6$H$_4$, 75%
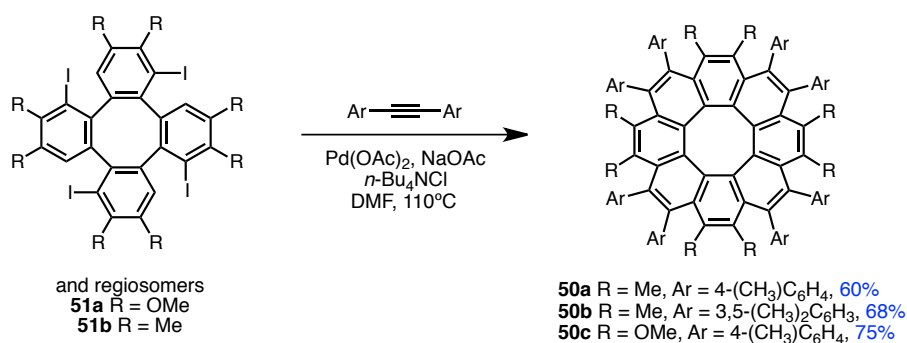
Scheme 1.11 Preparation of the highly functionalized [8]circulenes (**50a-c**) by Wu and co-workers in one step from tetraphenylene (**51a-b**).

As calculations predicted, these highly-strained derivatives (**50a-c**) undergo

complete decomposition in as little as 24 hours. The authors cite the calculated instability of these structures based on the theoretical work by Sansón and co-workers, referenced earlier, highlighting the particular difficulties in developing such materials.[49]

Nevertheless, this methodology provided significant understanding to the contorted nature and stability of these structures and Wu's [8]circulene provided new precedence for our targeted tetrabenzo[8]circuene structure. HOMA values calculated on both the experimental and DFT calculated structures further supported the concept of localized aromaticity within these PAHs as alternating rings within the molecule observed higher aromatic character, suggesting that the structure contained four aromatic sextets as described above in Figure 1.13.

Since saddle shaped aromatics are particularly uncommon, Wu and co-workers were able to determine the inversion barrier of these structures to be ca. 20 kcal mol^{-1}. When compared to the theoretically calculated inversion barrier for [7]circulene (8.5 kcal mol^{-1}),[57] it is clear that structures based on the [8]circulene motif are significantly more rigid then their smaller saddle-shaped counterparts. Ultimately, Wu's synthetic strategy necessitates the utilization of methyl and methoxy groups for both their directing abilities and to block the formation of undesired oligomers that would result under such conditions. Furthermore, these structures would not be easily accessible without the use of diphenylacetylenes utilizing palladium-catalyzed annulation conditions imparting additional functionalization on the targeted parent structure. While the scope of materials is partially limited by these synthetic methodologies, Wu and co-workers present three new [8]circulene structures that were inaccessible prior to their report.

---

[57] Shen, M.; Ignatyev, I. S.; Xie, Y.; Schaefer III, H. F. *J. Phys. Chem.* **1993**, *97*, 3212–3216.

1.4.2 Suzuki's Synthesis of Tetrabenzo[8]circulene

Following Wu's report, Suzuki and Sakamoto described a route towards stabilized structures. The synthetic pathway provided by Suzuki resulted in the construction of the core eight-membered ring as the final step of their unique synthesis (Scheme 1.12).[58] This methodology takes on a vastly different approach from the methods developed concurrently in our laboratory.
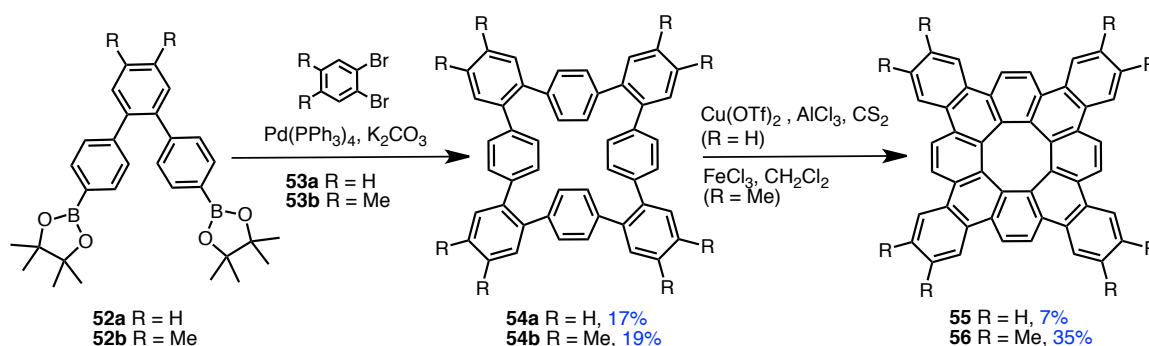
Scheme 1.12 Preparation of substituted tetrabenzo[8]circulenes (**55** & **56**) by Suzuki.

Suzuki and Sakamoto utilize the oxidative cyclodehydrogenation, introduced earlier in this text as the Scholl reaction, to carry out the final bond-forming reaction between precursors **54a-b** towards tetrabenzo[8]circulene (**55a-b**). Despite this advancement, it is the preceding Suzuki coupling reaction that limits the overall productivity of this synthetic strategy. The lack of regiocontrol inherent to this methodology leads to oligomerization of boronic acid (**52a-b**) with dibromobenzene (**53a-b**) in the initial steps of their synthetic strategy. Additional dimerization as a result

---

[58] Sakamoto, Y.; Suzuki, T. *J. Am. Chem. Soc*. **2013**, *135*, 14074–14077.

of the final transformation further diminishes the overall productivity of this synthetic strategy.

Although the Scholl reaction has the benefit of not requiring the installation of halides to accomplish bond formation, it suffers from the fact that the reaction can be extremely temperamental. The success of the transformation is typically highly dependent on the substrate, and electron-donating groups are often required to promote the oxidative coupling as demonstrated in the improved yields of Suzuki's methyl substituted variant.[59] Furthermore, Scholl reactions are typically used for ring closures on planar species,[37, 60] most notably in the final bond formation of hexa-peri-hexabenzocoronene,[38] and aside from the synthesis of **55 & 56** by Suzuki, few examples of strained non-planar PAHs formed through such conditions existed prior to these methods and those to be discussed in chapter 4.[40,61] In their procedure, octaphenylenes were prepared by Suzuki-coupling methods, followed by Scholl reaction conditions to form the final eight-membered core.

Surprisingly, Suzuki and Sakamoto provided little discussion of the remarkable stability of these compound despite the low stability of the parent compound predicted by calculations,[4] and observed in the rapid degradation of Wu's structures.[55] Like the methodology developed by Wu and co-workers, Suzuki's methodology is limited by the necessity to utilize methyl-directing groups to inhibit the formation of oligomers in the

[59] (a) Rempala, P.; Kroulík, J.; King, B. T. *J. Am. Chem. Soc.* **2004**, *126*, 15002–15003; (b) King, B. T.; Kroulík, J.; Robertson, C. R.; Rempala, P.; Hilton, C. L.; Korinek, J. D.; Gortari, L. M. *J. Org. Chem.* **2007**, *72*, 2279–2288.
[60] (a) Takase, M.; Enkelmann, V.; Sebastiani, D.; Baumgarten, M.; Müllen, K. *Angew. Chem. Int. Ed.* **2007**, *46*, 5524–5527; (b) Takase, M.; Narita, T.; Fujita, W.; Asano, M. S.; Nishinaga, T.; Benten, H.; Yoza, K.; Müllen, K. *J. Am. Chem. Soc.* **2013**, *135*, 8031–8040.
[61] (a) Wang, Z.; Dçtz, F.; Enkelmann, V.; Müllen, K. Angew. Chem. Int. Ed. **2005**, *44*, 1247–1250; (b) Luo, J.; Xu, X.; Mao, R.; Miao, Q. *J. Am. Chem. Soc.* **2012**, *134*, 13796–13803.

final bond-forming step of the reported synthesis. This result is evident in the reported 7% yield, vs. the 35% yield for those structures with the reported methyl directing groups.

The theoretical work reported by Suzuki and Sakamoto determined that the structure of tetrabenzo[8]circulene is substantially more rigid than that of the parent circulene. The reported inversion barrier for TB[8]C is 125 kcal mol^{-1}, indicating that the planar transition state is inaccessible. However, pseudo-rotation of the structure leads to a tub-to-tub inversion through a non-planar transition state with a substantially more accessible barrier of 7.3 kcal mol^{-1}. In the following sections, the synthetic strategies employed to arrive at our stabilized version of TB[8]C *via* an inside-out approach as well the inherent structural features that led to the molecules' increased stability are described.

1.5 Conclusions and Introductory Remarks

In recent years, contorted aromatics and in particular [*n*]circulenes, have found increasing application in the fields of molecular electronics as electron charge transport devices, optoelectronics, molecular semiconductors, and photovoltaic materials. Further elaboration of these structures towards the controlled growth of all-carbon nanomaterials, CNTs, and graphene sheets has yielded promising results in the field of materials synthesis. Contorted aromatics have shown strong complex forming abilities with fullerenes for size-selective materials, and the ability to coordinate metal ions for applications in molecular electronics.

Despite these advances, only a small number of the [*n*]circulene series of PAHs have been synthetically achieved. In the following chapters, the work performed in our laboratory towards the synthesis of tetrabenzo[8]circulene, a structural isomer of *c*-HBC, will be described. Furthermore, a detailed account of the work that has been done to advance the versatility of these structures through functionalization, as well as a number of yield-improving steps, are reported. Synthetic challenges, breakthroughs, characterization, as well optoelectronic and electronic properties will be discussed along with the future direction of the work presented herein.

CHAPTER 2: SYNTHESIS, STRUCTURAL DATA, AND FUNCTIONALIZATION OF TETRABENZO[8[CIRCULENE

2.1 Background and Introduction

Since 1825, Faraday's discovery and isolation of benzene has driven the concept of aromaticity to become a prevalent aspect of scientific discourse.[62] For nearly two centuries, significant efforts have been made to understand the unique stability and reactivity that are inherent to cyclic species possessing conjugation and, in particular, PAHs. The [*n*]circulene series represents a large group of these PAHs that are of significant interest due to their contorted nature and applications in materials research. Work presented herein describes the synthesis of several derivatives of the saddle-shaped molecule [8]circulene. Through the application of Clar's model of aromaticity on the parent molecule, we have developed the fully-aromatic tetrabenzo[8]circulene structure.

Wennerström and coworkers' first attempted synthesis of [8]circulene in 1976[50] has been met with highly-competitive progress towards the construction of this complicated structure.[56,58] Our approach employs Diels-Alder [4 + 2] cycloaddition and palladium-catalyzed arylation reactions as the key transformative steps. The synthesized compounds exhibit remarkable stability under ambient conditions – even at elevated temperatures – with no signs of decomposition over several months. To date, these contorted [8]circulene structures remain the largest member of the [*n*]circulene series to be synthetically achieved.

---

[62] Faraday, M. *Phil. Trans. R. Soc. Lond.* **1825**, *115*, 440–466.

2.2 Retrosynthetic Plan and Synthetic Precursors

As an early synthetic target towards our desired structure, we set our sights on the synthesis of a halogen-substituted dibenzocyclooctadiyne (**57**, Scheme 2.1). This molecule was of interest due to the incorporation of the core eight-membered ring, a key challenge to the synthesis of tetrabenzo[8]circulene (**55**). Additionally, the presence of two strained alkynes would allow access to the Diels-Alder [4 + 2] cycloaddition product (**59**) while the fused halides provide a synthetic handle for a subsequent C–C bond forming Heck arylation.
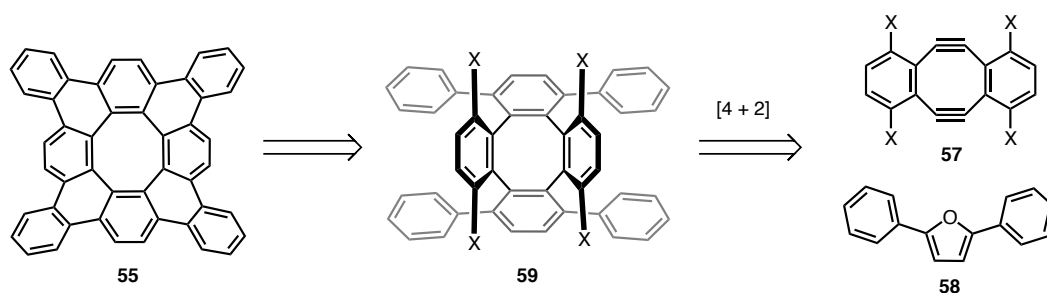
Scheme 2.1 Original retrosynthetic plan towards the synthesis of the stabilized contorted aromatic tetrabenzo[8]circulene (**55**).

We envisioned 2,5-diphenylfuran (**58**) as an efficient diene for Diels-Alder cycloadditions with **57**. Aromatic heterocycles such as furan have been used efficiently in Diels-Alder reactions since the early days of the named reaction.[63] Unlike Suzuki's synthesis of tetrabenzo[8]circulene involving the formation of the central eight-membered ring at a late stage, our synthesis of **55** started with the central ring intact.

---

[63] (a) Diels, O.; Alder, K.; Naujoks, E. *Der. Dtsch. Chem. Ges.* **1929**, *62*, 554; (b) Diels, O.; Alder, K.; *Justus Liebigs Ann. Chem.* **1931**, 490, 243–257.

2.2.1 Towards the Synthesis of Tetrachloro-dibenzocyclooctadiyne

This general sequence towards the desired core structure begins with chlorination of commercially available 2,3-dimethylaniline (**60**, Scheme 2.2) using N-chlorosuccinimide affording 4-chloro-2,3-dimethylaniline (**61**), which was achieved via electrophilic aromatic substitution with yields in accordance with literature values.[40] Subsequently, 1,4-dichloro-2,3-dimethylbenzene (**62**) was obtained in 90% yield *via* Sandmeyer reaction conditions as reported in the synthesis of *c*-HBC.[40] Following Wohl-Ziegler bromination of the benzylic carbons, the desired 1,4-dichloro-2,3-bis(dibromomethyl)benzene (**63**) was afforded in 80% yield, corresponding to reported values.[64]
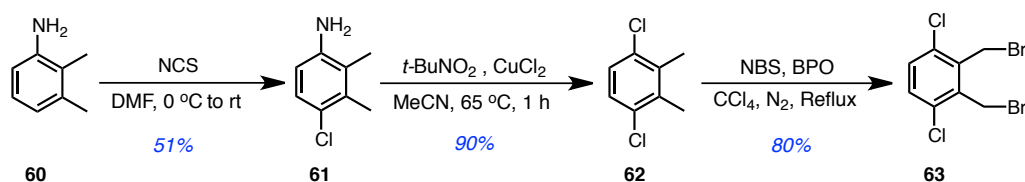
Scheme 2.2 Synthesis of 1,4-dichloro-2,3-bis(dibromomethyl)benzene (**63**), the synthetic parent to halogen-substituted dibenzocyclooctadiene; NCS = N-chlorosuccinimide, NBS = N-bromosuccinimide, BPO = dibenzoyl peroxide.

This parent material was envisioned as the synthetic precursor for two converging pathways towards the desired core structure. Dibromide (**63**, Scheme 2.3) could be used to form both phosphonium salt (**64**) and dialdehyde (**66**). Transformation of **63** to afford diol **65** and formation of the phosphonium salt (**64**) was carried out successfully in

[64] Thibault, M. E.; Closson, T. L. L.; Manning, S. C.; Dibble, P. W. *J. Org. Chem*. **2003,** *68*, 8373–8378.

accordance with reported literature.[65] Unfortunately, all attempts at the subsequent Swern oxidation proved to be unsuccessful and **66** was not observed as a reaction product.[66] It is important to note that in most cases the mono-oxidation product was obtained. Attempts to re-introduce this material to a similar set of reaction conditions did not afford the desired dialdehyde.
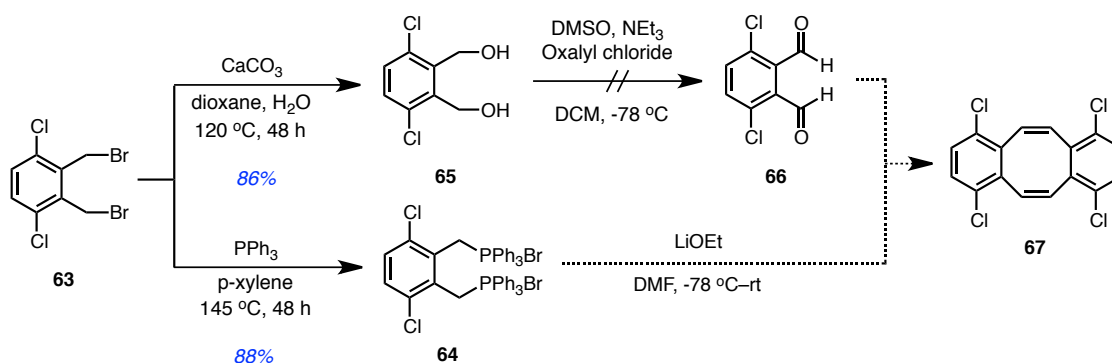
Scheme 2.3 Attempted synthesis of dibenzocyclooctadiene (**67**) precursor.

In all, 7 total steps would be required using our proposed methodology towards chloro-fused (**67**, Scheme 2.4). While a series of model studies on non-halogenated species provided precedence for the bromination of **67** affording vicinal dibromide (**68**) and subsequent E2 dehydrohalogenation towards **57**, ultimately, the failure of the Swern oxidation forced us to consider an alternative methodology towards our desired core structure.
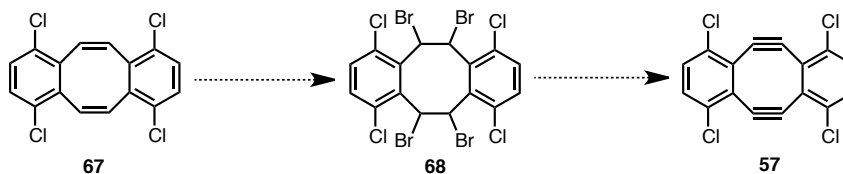
Scheme 2.4 Final steps of the proposed methodology towards dibenzocyclooctadiyne (**57**) precursor.

[65] Bieber, T. I.; Eisman, E. H. *J. Org. Chem.* **1962**, *27*, 678–679.
[66] Shu, Y.; Lim, Y.; Li, Z. *Chem. Sci.* **2011**, *2*, 363–368.

Moving away from the chloro-substituted dibenzocyclooctadiyne (**57**), we ultimately constructed a new synthetic plan wherein fused chloro-substituents could be placed as reactive sites on the diene rather than the dienophile. This method would result in a similar end-game strategy as proposed in our original retrosynthetic scheme. Furthermore, precedence for the expeditious and simplified synthesis of 1,2,5,6-dibenzocyclooctadiyne already existed,[67] and we were confident that this new route would lead to more promising results.

2.2.2 Dibenzocyclooctadiyne (The Sondheimer–Wong Diyne)

Initally we had steered away from this particular strategy (Scheme 2.5), as free-rotation along the C–C bond of the phenyl substituents of **71** could potentially inhibit the forward progress of our transformation. Additionally, oligomerization between tetraphenylenes could result more readily due to the sterically-hindered nature of the structure. In the former plan, the C–X bond of the dienophile is forced into a favorable position for reactivity with the phenyl substituents of the substituted precursor.
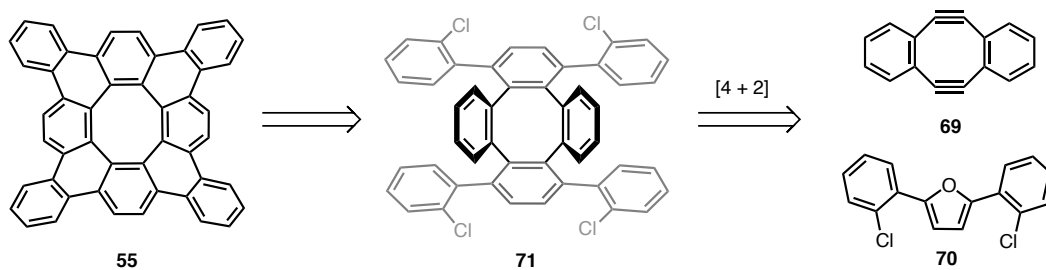
Scheme 2.5 Revised retrosynthetic plan starting from **69** towards TB[8]C (**55**).

[67] (a) Wong, H. N. C.; Garratt, P. J.; Sondheimer, F. J. Am. Chem. Soc. **1974**, *96*, 5604−5605; (b) Man, Y. -M.; Mak, T. C. W.; Wong, H. N. C. *J. Org. Chem.* **1990**, *55*, 3214−3221.

Sondheimer and Wong first reported the synthesis of dibenzocyclooctadiyne in 1974 *via* a 5-step linear methodology (Scheme 2.6).[67] Starting from a modified form of their original procedure, α,α′-Dibromo-*o*-xylene (**72**) was treated with lithium granules in THF under refluxing conditions, affording the desired [8]annulene (**73**) in 82% yield. It is important to note that this synthetic transformation was surprisingly temperamental and could frequently result in formation of the larger [12]annulene, which was challenging to isolate from the crude mixture and in most cases was brought forward without any purification. Subsequent bromination of **73** could be carried out in 95% yield affording dibromide (**74**). The following elimination (**75**) and bromination steps furnished the desired tetrabromide (**76**) in good yield. Subsequent reintroduction to elimination conditions with **76** in the presence of potassium *tert*-butoxide gave the desired dibenzocyclooctadiyne in 23% yield overall. Subsequent attempts to utilize chloroform in place of carbon tetrachloride during the substitution steps resulted in drastic yield reductions.
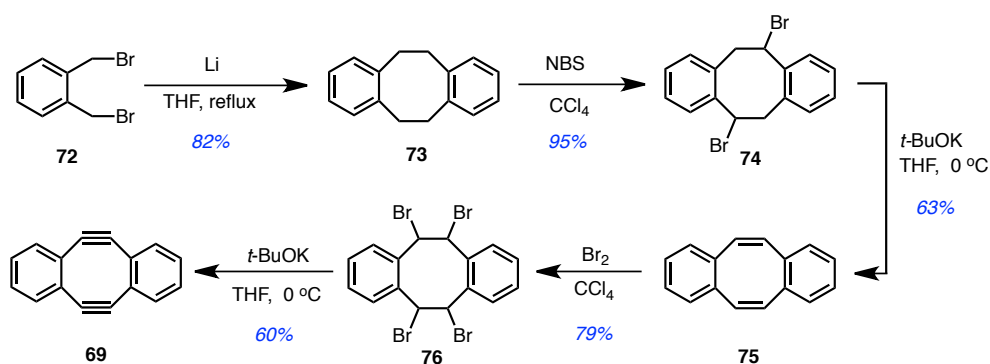
Scheme 2.6 Synthesis of Sondheimer-Wong diyne (**69**) in a reported 23% overall yield from α,α′-Dibromo-*o*-xylene (**72**).

In the course of our studies we came across a methodology developed by Otera and co-workers accessing the desired diyne (**69**) in fewer synthetic steps. This new route (Scheme 2.7)[68] avoids formation of the undesired [12]annulene that could often predominate mixtures in the previous synthesis. Following the methodology as reported, a 9% yield of the desired Sondheimner-Wong diyne could be obtained in four steps, which is in agreement with the reported literature values.
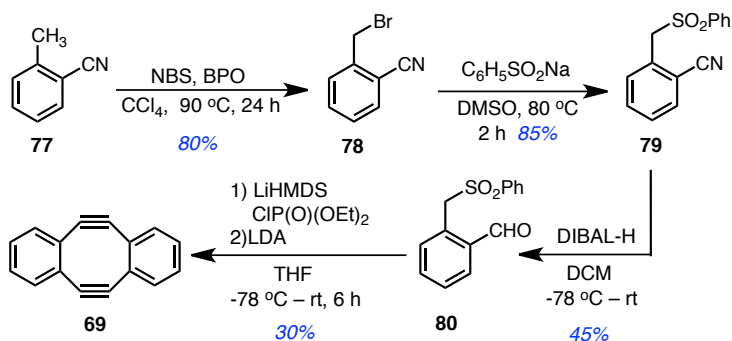
Scheme 2.7 Otera's reported synsthesis of the Sondheimer-Wong diyne (**69**) in four steps from o-tolunitrile (**77**); DIBAL-H = Diisobutylaluminium hydride, LiHMDS = Lithium bis(trimethylsilyl)amide, ClP(O)(OEt)$_2$ = Diethyl chlorophosphate.

From o-tolunitrile (**77**), bromination afforded the desired benzylic bromide (**78**) in 80% yield, benzenesulfinic acid sodium salt was used to produce the *ortho*-(phenylsulfonylmethyl)benzonitrile (**79**) in 85% yield. Reduction of the nitrile to the imine with DIBAL-H, followed by a modified acid workup, resulted in the formation of aldehyde (**80**). The original DIBAL-H reduction – washing the reaction products with a 2 M solution of HCl prior to extraction – provided some initial difficulty, however through a more proven procedure where the reaction products were quenched in a 6 M solution of

[68] (a) Orita, A.; Hasegawa, D.; Nakano, T.; Otera, J. *Chem. Eur. J.* **2002**, 8, 2000−2004; (b) Chaffins, S.; Brettreich, M.; Wudl, F. *Synthesis* **2002**, 1191−1194; (c) Xu, F.; Peng, L.; Shinohara, K.; Morita, T.; Yoshida, S.; Hosoya, T.; Orita, A.; Otera, J. *J. Org. Chem.* **2014**, *79*, 11592−11608.

HCl overnight, we were able to gain access to yields upwards of 45%. The final bond forming steps occur through a single-pot Horner-Wadsworth-Emmons reaction and a subsequent E2 elimination to afford the 1,2,5,6-dibenzocyclooctadiyne (**69**) in 30% yield. In total, a 9% yield over four steps was obtained, in agreement with the reported literature. While this yield is reportedly lower than the original procedure to arrive at the identical diyne, we discovered that a simple modification to the synthetic procedure would allow us to access the diyne in significantly improved yield.

In subsequent attempts to synthesize the desired dialkyne, we discovered that simply changing the order of reactions – performing the DIBAL-H reduction on benzylic bromide (**78**, Scheme 2.8) and substitution on aldehyde **81** – afforded yields of 90% on both synthetic transformations. This revised strategy afforded the desired 1,2,5,6-dibenzocyclooctadiyne in 20% yield overall.
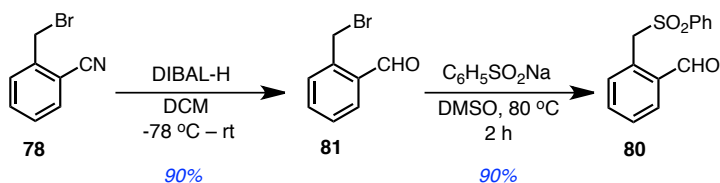
Scheme 2.8 Revised synthesis of 2-((phenylsulfonyl)methyl)benzaldehyde (**80**).

The strategies developed by Sondheimer, Wong, and Otera have been synthetically useful in obtaining the desired 1,2,5,6-dibenzocyclooctadiyne structure. The methodology first developed in 1974 utilizes commercially cheaper starting materials and reagents, but ultimately suffers in part due to temperamental conditions that can lead to undesired formation of oligomers and the larger [12]annulene. The methodology

developed by Otera and co-workers accesses the desired final product in similar yield, albeit utilizing more costly reagents. This methodology has lead to more notably consistent results and is significantly more reliable on larger scales.

2.2.3 Screening of Dienes

With the Sondheimer–Wong diyne in hand we focused our work on the synthesis of the requisite diene capable of carrying out the desired Diels-Alder [4 + 2] cycloaddition reaction. In developing our second substrate, it was initially envisioned that a furan with 2,5-diphenyl substituents would be ideal for the formation of the fused benzene rings through Diels-Alder reaction conditions with the tetrachloro-dibenzocyclooctadiyne. To this end, 2,5-diphenylfuran was synthesized as a model candidate for these studies (Scheme 2.9).
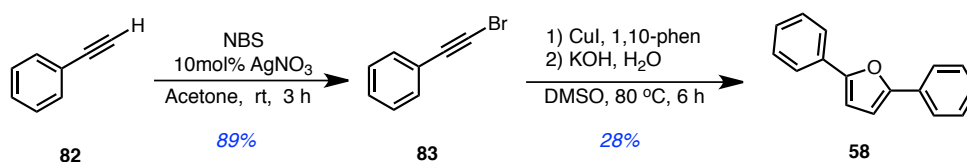
Scheme 2.9 Reported Synthesis of 2,5-diphenylfuran (**58**), synthetic precursor to proposed Diels-Alder [4 + 2] cycloadditions; 1,10-phen = 1,10-phenanthroline.

Bromoalkyne, **83**, was prepared from **82** using N-bromosuccinimide and a 10 mol% solution of silver nitrate in 89% yield. Copper-catalyzed arylation of **83** formed

2,5-diphenylfuran (**58**) in 28% yield – this corresponds to previously reported literature values.[69]

Although the Diels-Alder reaction of 3,4-disubstituted furan derivatives had previously been reported on large PAH structures,[20, 70] extension of this method for use with 2,5-diphenylfurans (**58**) on our newly envisioned alkyne proved unsuccessful. This failure is likely a result of the higher temperature required to overcome the increased steric bulk introduced by the incorporation of the phenyl substituents at the reactive carbons of the diene. This steric bulk proved to be a factor that could not easily be overcome due to the relatively low decomposition temperature of dienophile **69** (Scheme 2.10).[67] Attempts to accelerate the reaction by microwave irradiation were also unsuccessful.
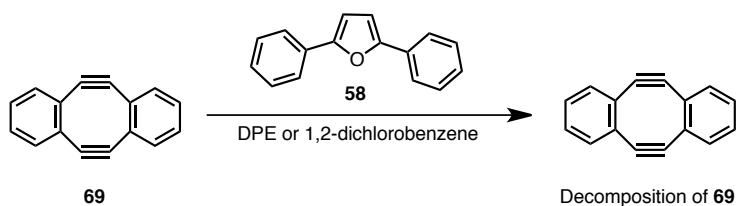
Scheme 2.10 Attempted [4 + 2] Diels-Alder cycloaddition *via* 2,5-diphenylfuran (**58**) and observed decomposition of dialkyne (**69**). DPE = Diphenyl ether.

Upon further studies we came across a methodology using thiophene oxides as powerful Diels-Alder adducts.[71] Shifting our focus from the substituted dibenzocyclooctadiyne to the un-substituted variant allowed us to move towards directly synthesizing the chloro-substituted diphenylthiophene as the diene for Diels-Alder

[69] Jiang, H.; Zeng, W.; Li, Y.; Wanqing, W.; Liangbing, H.; Fu, W. *J. Org. Chem.* **2012**, *77*, 5179–5183.
[70] Wong, H. N. C.; Man, Y. -M.; Mak, T. C. W. *Tetrahedron Lett.* **1987**, *28,* 6359–6362.
[71] P. Pouzet, I. Erdelmeier, D. Ginderow, J.-P. Mornon, P. Dansette, D. Mansuy, *J. Chem. Soc. Chem. Commun.* **1995**, 473–474.

cycloadditions, allowing us to carry out the intramolecular Heck arylation as the final

step of our synthetic strategy.

Starting from 2-chlorobenzaldehyde (**84**, Scheme 2.11), Corey-Fuchs[72] reaction

conditions afforded dibromoalkene (**85**). A 95% yield was obtained through formation of

the active ylide generated in the presence of 2-chlorobenzaldehyde. Further treatment of

the product with one equivalent of base in the presence of a phase-transfer catalyst

resulted in a beta-elimination[69] and formation of **86**.
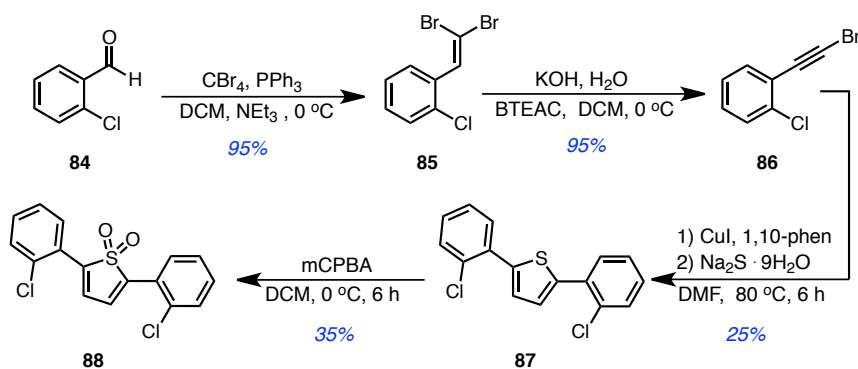
Scheme 2.11 Synthesis of 1,1-dioxide (**88**), synthetic precursor to proposed Diels-Alder [4 + 2] cycloadditions; BTEAC = benzyltriethylammonium chloride, mCPBA = 3-chloroperbenzoic acid.

Subsequent generation of 2,5-bis(2-chlorophenyl)thiophene, **87** went in 25%

yield, and formation of the 1,1-dioxide, **88** using mCPBA in 35%.[73] Unfortunately, 2,5-

diphenylthiophene dioxides, such as (**88**, Scheme 2.12) also proved to be an inefficient

diene in subsequent Diels-Alder cycloaddition reactions. This result is, again, due to the

high temperatures required for their use as we observed only decomposition of the

---

[72] Yao, P.; Zhang, Y.; Hsung, R.; Zhao, K. *Org. Lett.* **2008**, *10*, 4275–4278.
[73] (a) Kellog, R. M. in *Comprehensive Heterocyclic Chemistry,* ed. Katrizky, A. R. and Rees, C. W. Pergamon Press; Oxford, **1984**, *4*, 713–934; (b) Raasch, M. S. in *Chemistry of Heterocyclic Compounds, Thiophene and its Derivatives*, ed. Gronwitz, S. John Wiley & Sons; New Jersey, **1985**, *44*, 571–628.

dialkyne (**69**). Attempts to accelerate the reaction by microwave irradiation were also unsuccessful.
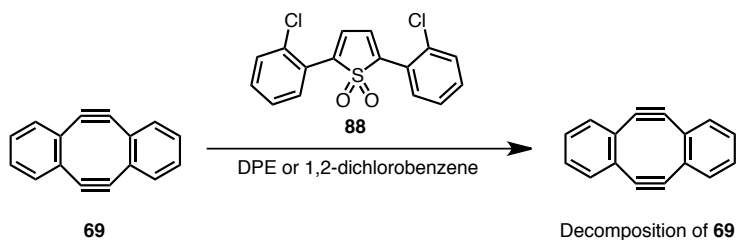
Scheme 2.12 Attempted [4 + 2] Diels-Alder cycloaddition *via* 2,5-diphenylthiophene dioxides (**88**) and observed decomposition of dialkyne (**69**); DPE = Diphenyl ether.

Next, we turned our focus to 2,5-disubstituted sulfoxide **91**. Sulfoxides derived from thiophenes have been identified as intermediates in the formation of thiophene dioxides, as a result of the self-dimerization products of the sulfoxide being present following oxidation reactions. Surprisingly, despite the fact that methods to synthesize these compounds[74] have been known for nearly five decades, these molecules have been significantly underutilized as dienes in Diels-Alder reactions. In the course of our studies we found that sulfoxides are much more reactive dienes than their dioxide counterparts and typically require lower reaction temperatures. This makes them an ideal candidate for reactions incorporating temperature sensitive dienophiles. While the copper-catalyzed pathway towards substituted thiophenes proved successful, we envisioned a faster and higher yielding route towards these molecules through a simplified Suzuki coupling procedure. Our target diene could be readily synthesized from the coupling of 2,5-dibromothiophene (**89**) and *o*-chlorophenylboronic acid (**90**) to produce 2,5-diarylthiophene (**87**) as shown in Scheme 2.13.

---

[74] Mock, W. L. *J. Am. Chem. Soc.* **1970**, *92*, 7610–7612.
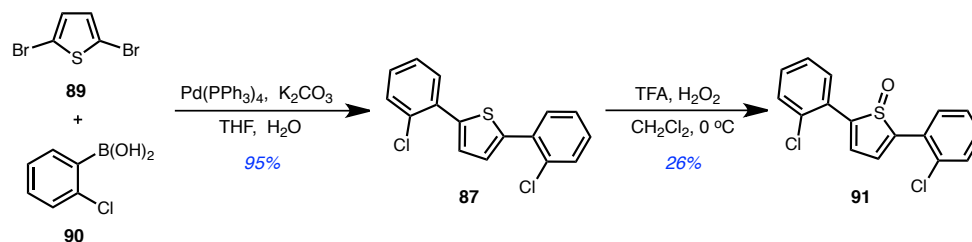
Scheme 2.13 Synthesis of sulfoxide (**91**), synthetic precursor to proposed Diels-Alder [4 + 2] cycloadditions; TFA = trifluoroacetic acid.

The oxidation of **87** was carried out through the dropwise addition of 30% H_2O_2 (aq.) into a TFA/CH_2Cl_2 (1:2) mixture at 0 °C to produce **91** in 26% yield. It is important to note that this reaction is highly time-dependent and extended reaction times led to increased production of the undesired dioxide. To avoid over-oxidation, shorter reaction times – typically 3 h – were utilized. Although this resulted in low yields of the desired product, a near-quantitative recovery of unreacted starting material was possible. Compound **91** can be stored for extended periods of time at 0 °C but decomposes quickly at ~120 °C to thiophene precursor **87**. We were excited to discover that sulfoxides were sufficiently capable of reacting with dibenzocyclooctadiyne (**69**).

2.3 End Game Synthesis of Tetrabenzo[8]circulene

The double Diels-Alder reaction between diyne **69** and sulfoxide **91** proceeded smoothly in PhMe at 100 °C (Scheme 2.14). The ^{1}H NMR spectrum of product **71** (Appendix 1, Figure AI.12), however, exhibits an unexpectedly large number of broad peaks in the aromatic region indicating hindered rotation of the chlorinated phenyl rings.

As a result, this compound likely exists as a mixture of atropisomers. Variable-temperature ^{1}H NMR of **71** in [D$_6$]DMSO at 100 °C provided no resolution of these broad peaks, indicating a significantly high barrier of rotation within the molecule. The high steric congestion responsible for this rotational barrier also provides some insight into the low yields of the Diels-Alder reaction.
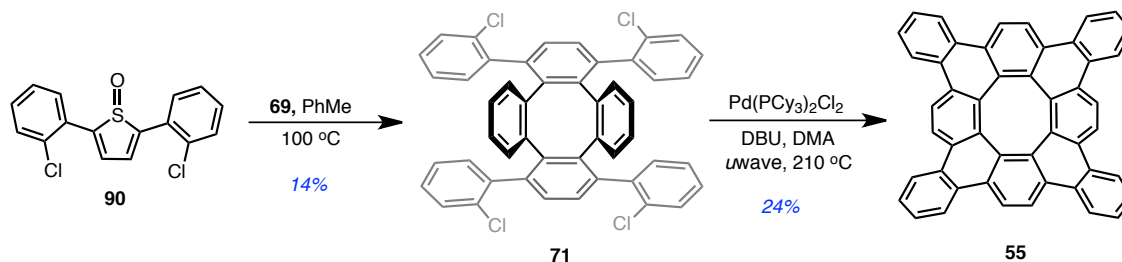
Scheme 2.14 Preparation of tetrabenzo[8]circulene (**55**) from sulfoxide (**91**) ; DBU = 1,8-diaza-bicycloundec-7-ene ; DMA = N,N-dimethylacetamide ; and Cy = cyclohexyl.

Compound **71** was exposed to microwave-assisted arylation conditions using Pd(PCy$_3$)$_2$Cl$_2$ as the catalyst and DBU as the base. These coupling conditions have been used to produce a number of contorted PAHs and this method has proven to be extremely powerful at generating strained molecules.[41, 75] Surprisingly, using standard reaction times and temperatures (80-100 °C) under microwave irradiation we observed only starting material with no formation of the desired compound. This result can also be attributed to the high rotational barrier of the pendant aryl rings and the fact that these rings must be provided with enough energy to allow them to overcome this barrier and

[75] (a) Reisch, H. A.; Bratcher, M. S.; Scott, L. T. *Org. Lett.* **2000**, *2*, 1427–1430; (b) Wang, L.; Shevlin, P. B. *Org. Lett.* **2000**, *2*, 3703–3705; (c) Wang, L.; Shevlin, P. B. *Tetrahedron Lett.* **2000**, *41*, 285–288; (d) Jackson, E. A.; Steinberg, B. D.; Bancu, M.; Wakamiya, A.; Scott, L. T. *J. Am. Chem. Soc.* **2007**, *129*, 484–485; (e) Wu, T. -C.; Chen, M. -K.; Lee, Y. -W.; Kuo, M. -Y.; Wu, Y. -T. *Angew. Chem. Int. Ed.* **2013**, *52*, 1289–1293.

rotate into a reactive position. As a result, it was required that we heat our reaction to 210 °C to provide the necessary energy to perform the transformation; **55** was isolated in an impressive 24% (70% per coupling) yield.

Despite the significant differences between our synthetic strategy and the one employed by Suzuki,[58] the overall yields of our sequences from known materials are quite similar. We believe, however, that our method provides a significant advantage. For the final strain-inducing bond formation, we employed the reliable palladium-catalyzed arylation reaction, whereas the method developed by Suzuki utilizes an oxidative coupling commonly referred to as the Scholl reaction.

While the Scholl reaction has the benefit of not requiring the installation of halides in order to accomplish bond formation, it suffers from the fact that the reaction can be extremely temperamental. The success of the transformation is typically highly dependent on the substrate, and electron-donating groups are often required to promote the oxidative coupling.[59] Additionally, Scholl reactions are historically used for ring closures on planar species,[37, 60] most notably in the final bond formation of hexa-*peri*-hexabenzocoronene,[38] and aside from the synthesis of **55** by Suzuki, there are few examples of strained non-planar PAHs that are formed through such conditions.[40, 61] While this fact makes the methodology developed by Suzuki even more impressive, we believe that the implementation of the Scholl reaction, as applied by Suzuki, has present limitations on the functionality that can be introduced onto the periphery of compound **55**. As a result of this limitation – and as our later work will show – we believe that the method reported herein, based on an "outward extension of the octagon" from dibenzocyclooctadiyne, provides greater potential to incorporate a range of functional

groups and thereby allows greater control over this new structure's optoelectronic properties. The methodology – as presented by Suzuki – requires the installation of methyl-directing groups to promote the "inward formation of the octagon" in their final structure. This methodology inherently lowers the available functionalization of these contorted aromatic structures.

2.4 Structural Characterization of Tetrabenzo[8]circulene

Compound **55** has limited solubility in common organic solvents, although it will readily dissolve in 1,2-dichlorobenzene (ca. 10 mg / mL) upon heating. Unlike the [8]circulene derivatives synthesized by Wu,[56] the compound is highly stable and no decomposition was observed after five months of storage under ambient conditions. Furthermore, heating **55** in an aerobic solution of [D$_6$]DMSO at 100 °C for 24 h revealed no observable decomposition products.

The ^{1}H NMR spectrum of **55** matches the previously reported spectrum[58] and is composed of three peaks of equal integration at δ 8.09, 7.69, and 7.56 ppm. Similarly, the ^{13}C NMR spectrum displays only six different chemical environments for the 48 carbon atoms in the structure. This indicates that **55** is highly symmetric, and the experimental data agrees with the saddle-shaped structure (**A** & **B** Figure 2.1) of D$_{2d}$ symmetry derived from gas-phase DFT calculations (B3LYP/6-31G** and M06-2X/6-31G** produced nearly identical structures).
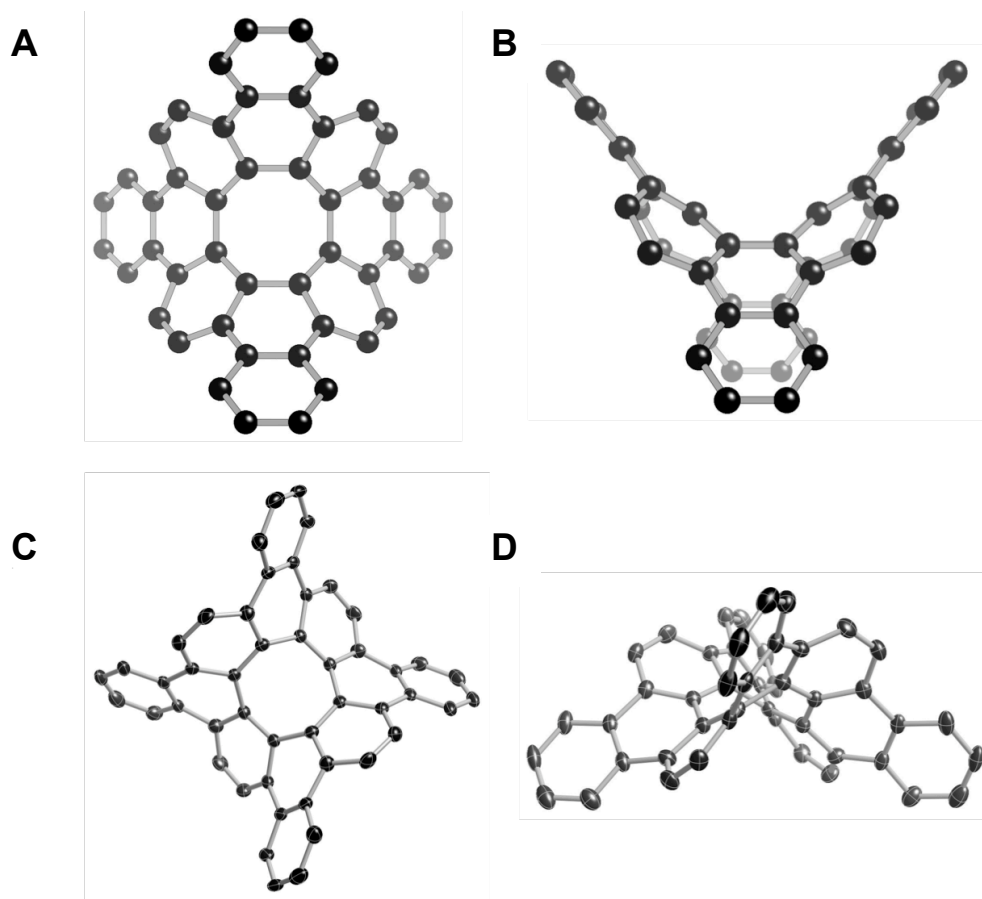
Figure 2.1 A) Top and **B)** side views of the DFT-minimized structure (B3LYP/6- 31G**) of **55. C)** Top and **D)** side views of residue I of the X-ray structure of **55**; thermal ellipsoids are displayed at 50% probability and the hydrogen atoms have been removed for clarity. Disordered solvent was SQUEEZED during refinement.

Yellow, block-like crystals of **55** were grown from the slow evaporation of 1,2-dichlorobenzene, and the structure confirmed by x-ray crystallography[76] is identical to the reported structure obtained from crystals grown from toluene.[58] As has been observed

---

[76] Single-crystal X-ray diffraction analysis was performed on a Bruker Apex II [Mo_{Ka} (l = 0.71073)] at 125(2) K. Data was collected and processed by using a Bruker Kappa/Apex II CCD detector. Crystal data for **55**: $C_{48}H_{24}$; tetragonal; space group I4; unit-cell dimensions: a = 17.1355(2), b = 17.1355(2), c = 10.7485(1) Å; α = 90, β = 90, γ = 90°; V = 3156.0(6) Å^3; Z = 2; $R1$ = 0.0409; $wR2$ = 0.0924. CCDC-960537 contains the supplementary crystallographic data for this compound. These data can be obtained free of charge from The Cambridge Crystallographic Data Centre via www.ccdc.cam.a- c.uk/data_request/cif.

previously, the solid-state structure deviates significantly from the DFT predictions. Two symmetry-independent molecules of **55** (residue I is displayed in Figure 2.1 **C & D**) that belong to an S_4 point group are present in the crystal. These residues are not significantly different from each other (Figure 2.2) – the mean comparable bond distance between the two residues is 0.01 Å with a maximum deviation of 0.04 Å and a root-mean squared deviation (RMSD) in atomic positions of 0.196 Å. The residues contain a single repeating asymmetric unit (**A**) – an image overlaying these two residues is displayed (**B**) and for our purposes the structure of only one of these residues will be discussed.
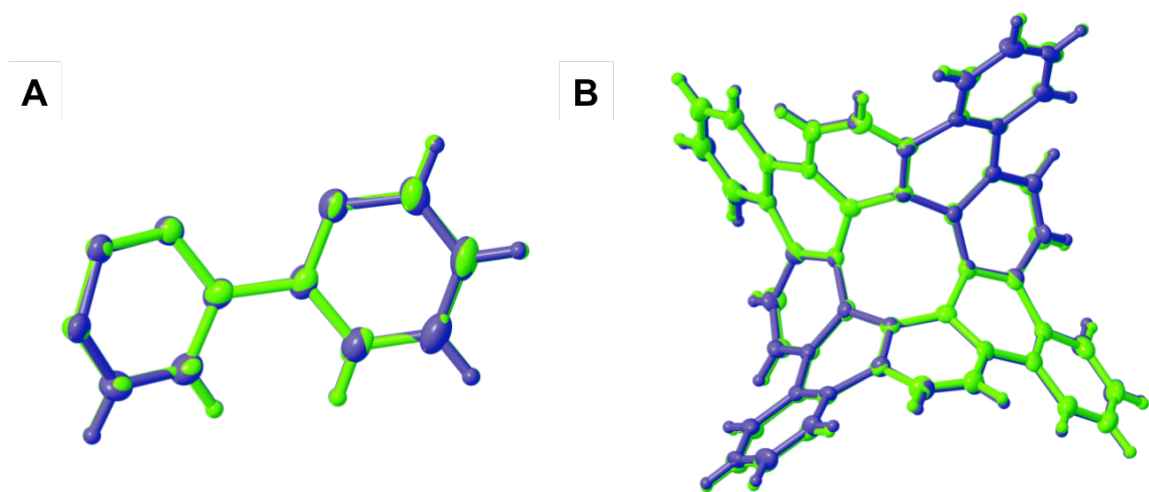
Figure 2.2 Overlaying structures of the **A**) asymmetric unit and the **B**) whole structure of the symmetrically-independent residues in the crystal structure. The RMSD of the asymmetric unit is 0.034 Å and the RMSD of the entire structure is 0.196 Å.

DFT calculations are typically accurate at predicting the structure of contorted PAHs. As a result of the high symmetry indicated by ^{1}H NMR and ^{13}C NMR spectroscopy, we believe the DFT structure is an accurate representation of the molecule as it exists in solution (the solid-state structures with S_4 symmetry would display six unique proton signals in the ^{1}H NMR spectrum) and that crystal packing forces in the

solid state are responsible for the distortion in the x-ray structure. To identify which arrangement is more stable, single point calculations (M06-2X/6-311G**++//M06-2X/6-31G**) were performed and demonstrating that the DFT structure is lower in energy by ~1.8 kcal / mol when compared to the x-ray structures.[77]

The two pinwheel-like residues present in the crystal structure of **55** and a representation of the crystal packing of these residues are displayed in **A**, Figure 2.3. As a result of the highly-contorted nature of **55**, we initially predicted that these structures would form self-complementary linear stacks much like the contorted derivatives of hexa-*cata*-hexabenzocoronene developed by Nuckolls.[1, 40] We were therefore surprised to observe the unique packing structure inherent to these molecules. Rather than a herringbone or slip-stacked packing typical of PAHs, we find that the structure instead forms a complex 3-dimensional arrangement in which each of the four peripheral benzenoid rings on each molecule of residue I forms a π-stacking interaction with the analogous rings on a molecule of residue II. These rings are offset with a minimum intermolecular C–C distance of 3.25 Å (**B & C**). Likewise, each molecule of residue II forms equivalent interactions, with four molecules of residue I providing an uninterrupted 3-dimensional π-stacking network.

---

[77] The relative energies were obtained with density functional theory (DFT) calculations at the M06-2X/6-311G**++//M06-2X/6-31G** level, performed using the Jaguar (see: Jaguar, Version 7.9; Schrödinger, LLC, New York, USA, 2012) software package. The pseudospectral methodology (see: Friesner, R. A. *J. Phys. Chem.* **1988**, *92*, 3091–3096.), which significantly speeds up the SCF iterations, was employed in all calculations. Default grids and SCF convergence criteria, as implemented in Jaguar, were used.
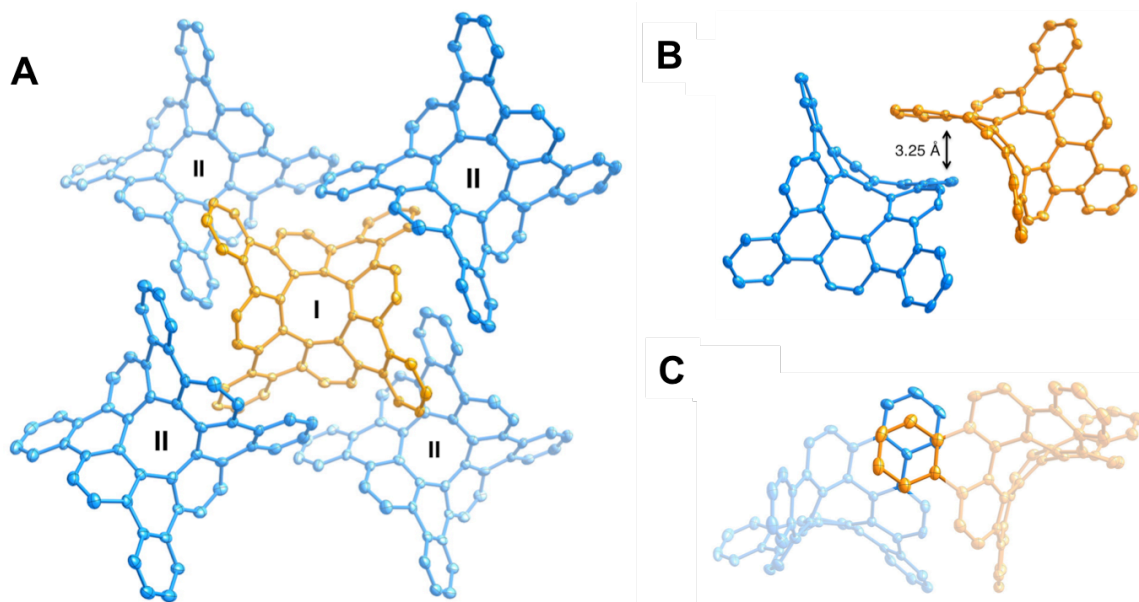
Figure 2.3 A) Illustration of the crystal packing between residue I (orange) and residue II (blue) in the crystal structure of **55**; the peripheral benzenoid rings of each residue form π–stacking interactions with the analogous rings of four molecules of the opposite residue (two on each face) create a 3-dimensional π–stacking network. **B**) Side view of the π-stacking between residue I and II displaying the minimum intermolecular C–C distance of 3.25 Å. **C**) Top view of the π-stacking interaction indicating that the rings involved in the interaction are slipped rather than in direct alignment. The thermal ellipsoids are displayed at 50% probability and the hydrogen atoms have been removed for clarity. Disordered solvent was SQUEEZED during refinement.

The experimental structure is higher in energy than the DFT structure and the manner in which this tension is distributed throughout the molecule is particularly interesting. To analyze the strain, π-orbital axis vector (POAV)[78] pyramidalization angles (defined as $\theta_{\sigma\pi}$–90°) were calculated for the relevant carbon atoms in the x-ray and DFT structures (**A & B**, Figure 2.4). The most noteworthy angles arise from the 8-membered ring. In the DFT structure, strain is evenly distributed throughout the ring, with each carbon atom displaying a POAV angle of 3.53° (**A**). In the x-ray structure however, the

---

[78] (a) Haddon, R. C.; Scott, L. T. *Pure Appl. Chem.* **1986**, *58*, 137–142. (b) Haddon, R. C. *J. Am. Chem. Soc.* **1990**, *112*, 3385–3389.

strain is distributed on alternating carbon atoms. For example, half of the carbon atoms

(**B**) have POAV angles of 6.08° and the remaining carbon atoms are completely planar –

i.e., exhibit POAV angles of 0°. Moving away from the central ring, the DFT structure

exhibits symmetrical strain with decreasing POAV angles as we approach the peripheral

benzenoid rings. The corresponding POAV angles in the experimental structure are larger

and continue to lack the symmetrical distribution of strain observed in the DFT structure.
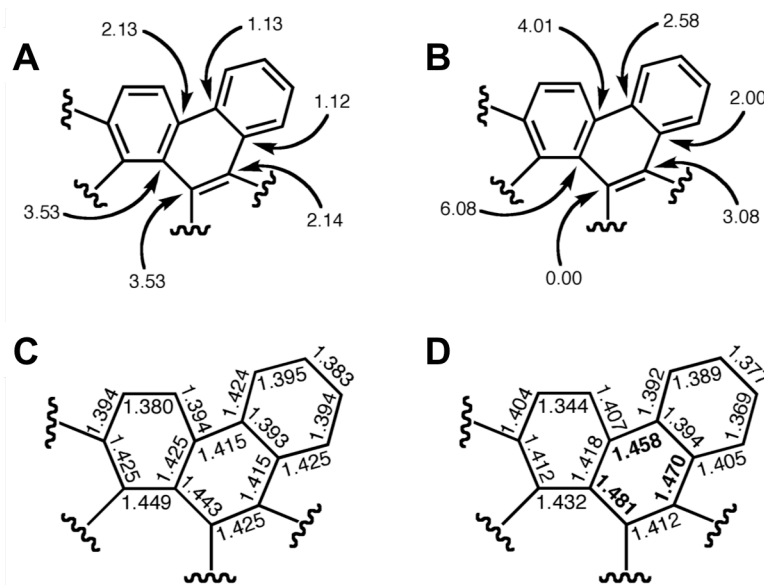
Figure 2.4 POAV angles [°] of **A**) the DFT minimized structure and **B**) the solid-state structure of TB[8]C (**55**). Selected bond lengths [Å] of **C**) the DFT minimized structure and **D**) the solid-state structure. Quasi-single bonds identified in the solid-state structure are indicated by bold values. A complete list of bond lengths and their associated errors can be found in Table AII.1 from Appendix II.

Despite the relatively large POAV angles and the twisted nature of the solid-state

structure, the hexagonal rings of **55** remain quite planar. For our purposes, we define non-

planarity (NP) as the average distance of the carbon atoms in a ring from a generated

best-fit plane. Using this method, a ring that has an average carbon–plane distance of 0 Å

is considered to be completely planar, and an increase in this value is indicative of an increase in the distortion from planarity. The relatively planar nature of these rings indicates that a majority of the strain is built up at the sites of ring fusion rather than within the rings themselves. Notably, the carbon atoms in the ring that is "empty" in the Clar structure (Table 2.1, ring B) are displaced from the plane significantly more than those in the rings containing aromatic sextets (rings A and C), i.e., the rings that are expected to exhibit localized aromaticity display less deviation from a planar structure than those that are not.

Table 2.1 Structural data of the calculated and solid-state conformations.[a]
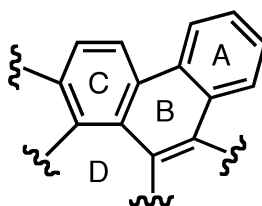
	Ring	DFT Structure	X-ray Structure
Non-Planarity [Å][b]	A	0.002	0.011
	B	0.116	0.130
	C	0.096	0.080
	D	0.397	0.375
Average Bond Length [Å]	A	1.402	1.402
	B	1.420	1.438
	C	1.411	1.403
	D	1.446	1.457
HOMA Index[c]	A	0.880	0.965
	B	0.689	0.064
	C	0.716	0.744
	D	0.131	−0.364

[a] The structural data is presented as symmetrical averages. [b] Planarity values were calculated by constructing a best-fit plane through the individual rings of **55** and measuring the average distance of the carbon atoms from this plane. [c] HOMA indices were calculated using a normalization constant, α, of 257.7 and the optimal C–C bond length, $R_{opt,}$ of 1.338 Å.

This is strong evidence that the Clar representation is an accurate depiction of the aromaticity in this molecule. As expected, the central 8-membered ring (Table 2.1, ring D) distorts significantly to avoid the anti-aromaticity that would potentially result from it adopting a planar conformation. Further evidence supporting the Clar structure can be observed in the bond lengths of the calculated and experimental structures. Similar to the POAV angles, the bond lengths of the DFT structure are highly symmetrical whereas those of the solid-state structure are not. Despite this dissymmetry, the bond lengths of the experimental structure correlate strongly with those expected from the Clar structure. Most notable is that three quasi-single bonds – i.e., bonds that are significantly longer than all of the other bonds in the molecule (represented as bold, **C & D**, Figure 2.4) – are present in the "empty" ring of the Clar structure. This is expected as these bonds are not members of aromatic rings and serve only to connect the areas of localized aromaticity. As a direct consequence of these longer bonds, we observe that the rings containing aromatic sextets have a significantly shorter average bond length (1.402 Å and 1.403 Å) compared to the "empty" ring (1.438 Å).

The harmonic oscillator model of aromaticity (HOMA) was used to determine the aromaticity of the individual rings in the calculated and x-ray structure (Table 2.1).[79] HOMA values of -1, 0, and 1 indicate anti-aromaticity, non-aromaticy, and aromaticity, respectively. While the calculated structure exhibits moderate to high levels of aromaticity for each of the hexagonal rings, the values calculated for the solid-state structure correlate strongly with the Clar structure. We observe values approaching 1 for the two rings represented as sextets in the Clar structure (Table 2.1) with values of 0.965

[79] Krygowski, T. M.; Ejsmont, K.; Stepień, B. T.; Cyrański, M. K.; Poater, J.; Solà, M. *J. Org. Chem.* **2004**, *69*, 6634–6640.

and 0.744 for rings A and C, respectively. Similarly, it is interesting to note that the ring

that is represented as "empty" in the Clar structure (Table 2.1, ring B) exhibits a HOMA

value of 0.064, indicating that this ring can be regarded as non-aromatic. These results

are in agreement with the nucleus-independent chemical shift (NICS)[80] data calculated by

Suzuki, in which the two sextet containing rings exhibited aromatic character and the

"empty" ring was only moderately aromatic (Table 2.2).[58]

Table 2.2 NICS and HOMA analysis for Suzuki's[58] and Wu's[56] reported structures.
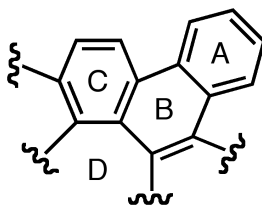
	Ring	DFT Structure	X-Ray Structure
NICS(0) ppm from Suzuki[a]	A	-9.2	NR
	B	-3.6	NR
	C	-3.8	NR
	D	NR	NR
NICS(0) ppm and [HOMA Index] from Wu[b]	B	-4.1 [0.650]	-3.9 [0.629]
	C	-4.0 [0.418]	-3.4 [0.369]
	D	12.2 [0.007]	12.9 [0.056]

[a] Nucleus-independent chemical shifts (NICS) calculated at the B3LYP/6-31G(d) level for [8]circulene. NICS values were computed at ring centers. [b] The geometric calculations were performed with density functional theory using Gaussian 09 at the ωB97X-D/6-31G** level. The NICS(0) values were calculated using the GIAO/HF/6-31+G* level. NR = Not reported.

Interestingly, the central 8-membered ring exhibits slight anti-aromaticity in the

experimental structure. This is in contrast to the values calculated from the crystal

---

[80] Chen, Z.; Wannere, C. S.; Corminboeuf, C.; Puchta, R.; Schleyer, P. v. R.; *Chem. Rev.* **2005**, *105*, 3842–3888.

structure of the [8]circulene derivatives synthesized by Wu,[56] in which this ring exhibited non-aromatic character. Overall, this data provides further evidence that the Clar representation of the structure is accurate. With the synthesis and structural properties of TB[8]C established, we set our sights on the synthesis of a series of functionalized derivatives. The following section will highlight the functional group tolerance of our [4+2] Diels-Alder cycloaddition and arylation reactions, as well as progress towards a general route towards these functionalized aromatics.

2.5 Early Developments in the Functionalization of Tetrabenzo[8]circulene

Following the successful synthesis of TB[8]C, we sought to produce a number of newly contorted structures that, through functionalization, could result in new electronic properties and structural arrangements in both solution and solid-state structural conformations. Through functionalization, we aimed to improve charge transport mobilities of the tetrabenzo[8]circulene motif. To this end, we envisioned that a linear stacking arrangement or a more tightly packed complex 3-dimensional packing arrangement would afford the necessary structural variation for such studies. Through modification of our reported methodology into these molecules, we were able to access new TB[8]C structures containing electron donating and withdrawing functional groups, in addition to structures that would allow us to access broad-spectrum functionalization at a late stage.

2.5.1 Synthesis of Tetraoctyloxy-tetrabenzo[8]circulene

The first of our synthetic targets was a tetraoctyloxytetrabenzo[8]circulene as substitution of long alkyl chains onto PAHs is a well-known synthetic instrument of applying solvent-based conformational change.[81] As such, we envisioned that increased bulk on the four peripheral benzo-substituents would be the simplest route in disturbing crystal-packing forces achieved in the parent molecule. With the groundwork set out from our previous work, we envisioned a new route towards tetraoctyloxytetrabenzo[8]circulene (**98**) *via* simple modification of the 2,5-thiophene precursor (Scheme 2.15).
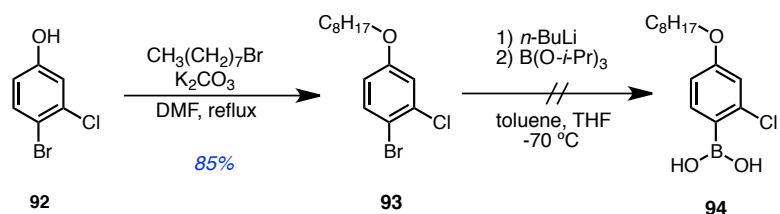
Scheme 2.15 Proposed synthesis of substituted boronic acid **94** *via* Williamson ether synthesis and subsequent borylation; B(O-*i*-Pr)$_3$ = triisopropyl borate.

From 4-chloro-3-bromophenol (**92**) clean Williamson ether synthesis of 1-bromooctane gave **93** in 85% yield. Borylation of the C–Br halide was envisioned; however, attempted synthesis and isolation of **94** failed after a number of modified

[81] For Representative examples, please see: (a) Palermo, V.; Samori, P. *Angew. Chem. Int. Ed.* **2007**, *46*, 4428–4432; (b) Grimsdale, C.; Müllen, K. *Angew. Chem. Int. Ed.* **2005**, *44*, 5592–5629; (c) van der Auweraer, M.; De Schryver, F. C. *Nat. Mater.* **2004**, *3*, 507–508; (d) Elemans, J. A. A. W.; van Hameren, R.; Nolte, R. J. M.; Rowan, A. E. *Adv. Mater.* **2006**, *18*, 1251–1266; (e) Adam, D.; Schuhmacher, P.; Simmerer, J.; Haussling, L.; Siemensmeyer, K.; Etzbach, K. H.; Ringsdorf, H.; Haarer, D. *Nature* **1994**, *371*, 141–143.

attempts. Alternatively, adaptation of the procedure towards a direct one-pot generation of functionalized thiophenes *via in-situ* generation of the borylated species and subsequent Suzuki coupling of 2,5-dibromothiophene (Scheme 2.16) resulted directly in the formation of substituted 2,5-arylthiophenes (**95**) in 80% yield. This one-pot modification of our initial approach allowed us to bypass isolation of the borylated species.
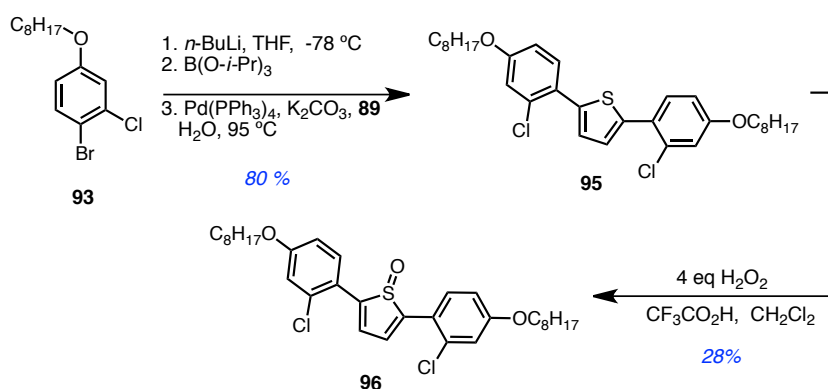
Scheme 2.16 Direct one-pot synthesis of **95** *via* in-situ generation of the borylated species followed by oxidation **47**.

As previously reported, oxidation of **46** was carried out through the dropwise addition of 30% H_2O_2 (aq) into a TFA/CH_2Cl_2 (1:2) mixture at 0 °C to produce **96** in 28% yield. Subsequent double Diels-Alder reaction (Scheme 2.17) between **69** and sulfoxide **96** proceeded cleanly in 1,2-dichlorobenzene at 210 °C. The switch from PhMe to 1,2-dichlorobeneze resulted in no observable increase in decomposition products, while the ability to produce a comparable material in significantly shorter reaction times was achieved. Compound **97** was exposed to microwave-assisted arylation conditions using $Pd(PCy_3)_2Cl_2$ as the catalyst and DBU as the base, leading to **98**, in 10% yield.
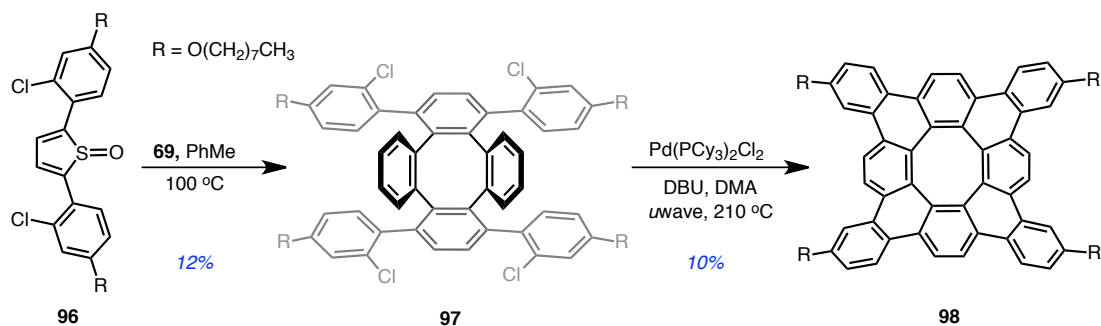
Scheme 2.17 Subsequent Diels-Alder [4+2] cycloaddition affording **97** in low yield, followed by microwave-assisted arylation affording the desired functionalized TB[8]C **98** in low yield.

The successful synthesis of **98** exploits the versatility of the methods employed in the synthesis of TB[8]C. The ^{1}H NMR spectrum (Appendix I, Figure AI.26**)** shows that **98** forms aggregates in solution – an early indicator of liquid crystalline type properties.[82] Unfortunately, the low yields and quantity of materials made through these synthetic methodologies limited our ability to utilize these materials in further molecular electronics studies. To date, we have been unable to develop transistors with uniform films of high enough quality to be utilized as electronic devices from these materials but have continued attempts at developing thin films of high enough quality for molecular electronics studies.

Nevertheless, a number of substituted TB[8]C structures have also been developed by our group through these synthetic methodologies. Through the synthetic methodologies laid out in the development of **98** we envisioned a modified strategy that would allow us to access a TB[8]C precursor capable of acting as a synthetic handle for

---

[82] Bushey, M. L.; Nquyen, T. -Q.; Nuckolls, C. *J. Am. Chem. Soc.* **2003**, *125,* 8264–8269.

broad spectrum synthesis of a number of functionalized species. In doing so, we also developed a more facile and functionally tolerant route towards our 2,5-arylthiophene precursors.

2.5.2 Synthesis of Tetra(trimethylsilyl)-tetrabenzo[8]circulene

Given the difficulties previously demonstrated with borylation of aryl bromides, borylation of aryl iodides (**99**) was significantly more powerful, accessing boronic acid, **100** in 85% yield (Scheme 2.18). Subsequent Suzuki coupling led to the substituted 2,5,-diarylthiophene (**101**). In this case the lower yield, 42%, can be attributed to competition between the 2,5-dibromothiophene and activation of the C–Br bond present in the boronic acid, resulting in a mixture of self-reaction products as well as tri- and tetra-coupled thiophenes, which became difficult to separate upon workup. These products were afforded even upon lowering the stoichiometric ratio of boronic acid to 2,5-dibromothiophene (**89**).
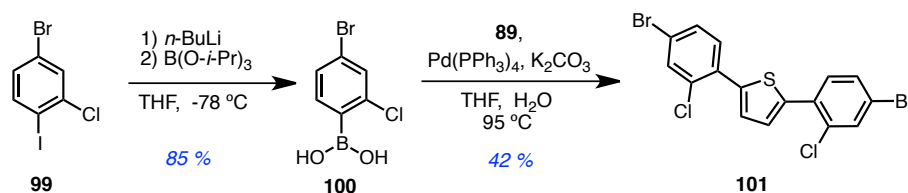
Scheme 2.18 Successful borylation of **99** affording **100**, while subsequent Suzuki coupling afforded **101** in less-than-desired yields.

Ultimately, the 25% overall yield for 2 steps was less than optimal, and we sought new means of accessing **101**. We came across a simple procedure for the synthesis of 2,5-

distannylthiophenes (**102**), which would alleviate the synthetic challenges of acquiring the substituted boronic acid.[83] Halogenated thiophenes could now be achieved in a simple one-step un-optimized Stille coupling, affording (**101**, Scheme 2.19) in yields in excess of 99%. Furthermore, this process could also be used in the synthesis of the previously obtained **95** through a relatively simpler synthetic procedure over the *in-situ* Suzuki coupling, albeit with slightly longer reaction times – 4 h for aryl bromides – as compared to the aryl iodides of the present synthesis. TMS protection of the peripheral bromines followed by oxidation of **103** led to desired sulfoxide (**104**). Surprisingly, the oxidation process is less facile then that of previously observed 2,5-diarylthiopenes and yields varied between 22% to 26%.
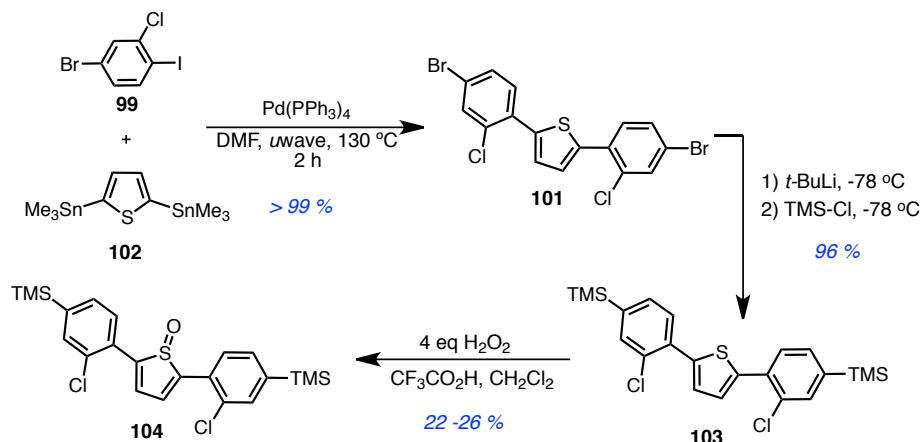
Scheme 2.19 Stille coupling of **99** and **102** to afford 2,5-diarylthiopene (**101**) in near quantitative yield, followed by TMS protection and oxidation to afford **104**.

Diels-Alder reactions between **69** and **104** were carried out in toluene at 210 °C (Scheme 2.20). Compound **105** was exposed to microwave-assisted arylation conditions,

[83] Heinrich, A. C. J.; Thiedemann, D.; Gates, P. J.; Staubitz, A. *Org. Lett.* **2013**, *15*, 4666–4669.

again, using Pd(PCy$_3$)$_2$Cl$_2$ as the catalyst and DBU affording **106** in 10% yield. The tetra(trimethylsilyl)tetrabenzo[8]circulene (**106**) has been easily converted to iodo-precursor (**107**) in near-quantitative yield using excess iodinemonochloride at 0 °C. From tetraiodotetrabenzo[8]circulene, a number of functionalized products could be envisioned using available coupling methods to obtain these substituted structures.
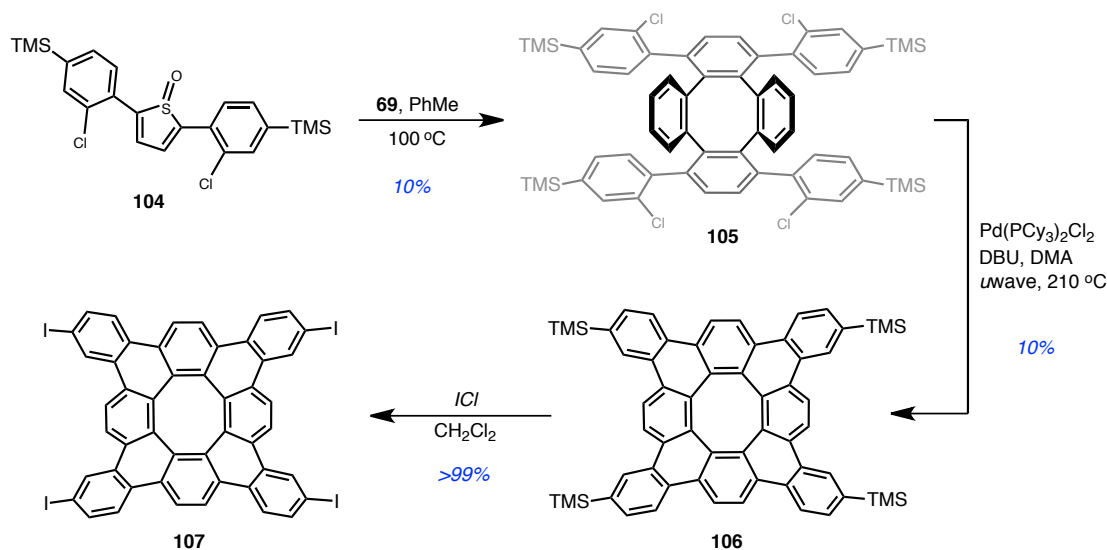
Scheme 2.20 Diels-Alder of **69** and **104** to afford the TMS-tetraphenylene (**105**) and subsequent arylation to afford desired **106** and formation of tetraiodo-tetrabenzo[8]circulene, **107**.

While the low yields that resulted from these synthetic methodologies ultimately proved too restricting to carry these materials further, we were able to grow crystals of **106** sufficient for X-ray analysis. Dark red, block-like crystals of **106** were grown from the slow evaporation of toluene and the structure confirmed by x-ray crystallography.[84]

---

[84] Single-crystal X-ray diffraction analysis was performed on a Bruker Apex II [Mo$_{Ka}$ (l = 0.71073)] at 125(2) K. Data was collected and processed by using a Bruker Kappa/Apex II CCD detector. Crystal data for **106**: C$_{48}$H$_{24}$; triclinic; space group P1; unit-cell dimensions: a = 11.4308(0), b = 14.9774(0), c = 15.9220(0) Å; α = 75.5, β = 68.9, γ = 84.8.

Structures of **106** are significantly contorted compared to molecules of **55** and do not possess the S_4 symmetry of the previously described solid-state structure. Molecules of **106** belong to a P1 point group and are present in the crystal structure as illustrated in **A** & **B** (Figure 2.5).
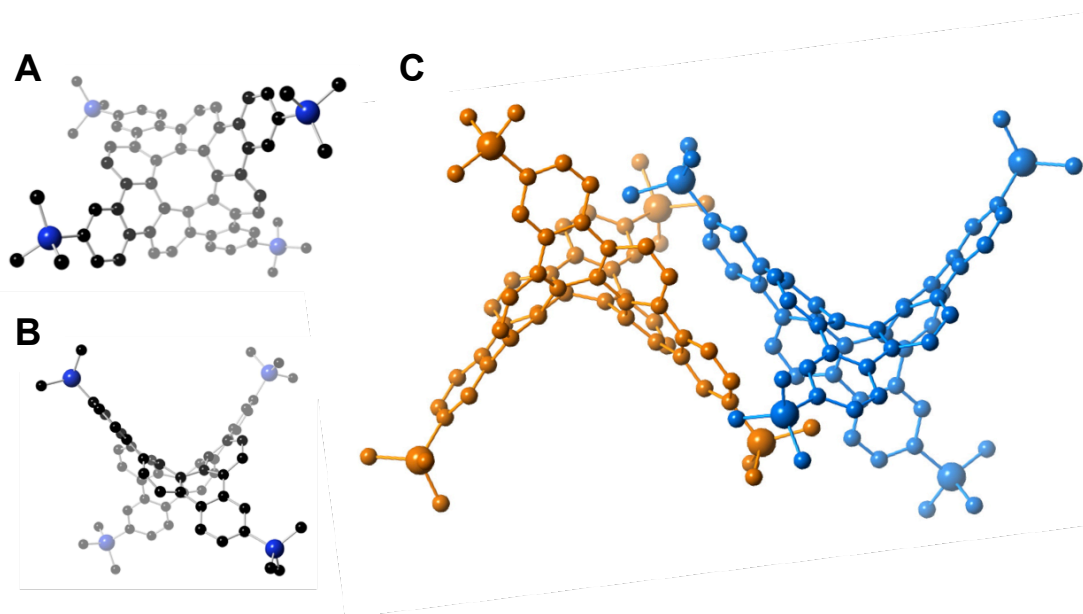
Figure 2.5 Illustration of top **A**) and **B**) side views of the X-ray structure of **106** and **C**) illustration of the crystal packing between two molecules of **106**, the peripheral and internal benzenoid rings of each structure form π–stacking interactions with the analogous rings of four molecules (two on each face), creating a 3-dimensional π–stacking network. Hydrogen atoms have been removed for clarity. A complete list of bond lengths and their associated errors can be found in Table AII.2 from Appendix II

Molecules of **106** form a complex 3-dimensional packing arrangement (**C**) much like molecules of TB[8]C, however, the intermolecular π-stacking interaction between these structures occur through the peripheral benzo rings and internal benzenoid substituents of the core structure. These rings are offset with an intermolecular C–C distance of 4.18 Å, a distance of 0.93 Å greater than that of the parent TB[8]C structure.

Trimethylsilyl-protected **106** is less twisted than our parent structure, with a deeper saddle-shape than TB[8]C. We were surprised to find that these structures had increased structural overlap, given the excess bulk of the TMS-protecting groups. The results of functionalization with bulky TMS groups prompted us to investigate structures with smaller functional groups, with the hopes of uncovering a linear stacking arrangement as originally proposed or more tightly-packed 3-dimensional packing arrangement.

2.5.3 Synthesis of Tetrafluoro-tetrabenzo[8]circulene

As a final route towards more functionalized structures of **55,** we decided to investigate the functional group tolerance of our central Diels-Alder and arylation reactions. We came across a number of publications highlighting the interesting effects that fluorinated aromatics had on both solid-state and electronic properties over their un-substituted predecessors. [85] Given the positive results that we found with the functionalized TMS-TB[8]C, we envisioned that a tetrafluoro-tetrabenzo[8]circulene would provide promising contorted and electronic behaviors.

Our studies led us to fluoro-functionalized *c*-HBCs that were observed to have significantly increased out of plane contortion and a 'metastable' conformation that was able to be observed after the final cyclization reaction, but reverted back to its original state after heating at 100 ºC.[84a] The following work highlights our progress in developing a tetrafluorotetrabenzo[8]circulene structure. Substituting **108** for **99**, we were able to

[85] (a) Loo, Y. -L. Hiszpanski, A.; Kim, B.; Wei, S.; Chiu, C. -Y.; Steigerwald, M.; Nuckolls, C. *Org. Lett.* **2010**, *12*, 4840–4843; (b) Chase, D.; Fix, A.; Kang, S. J.; Rose, B.; Weber, C.; Zhong, Y.; Zakharov, L.; Lonergan, M.; Nuckolls, C.; Haley, M. *J. Am. Chem. Soc.* **2012**, *124*, 10349–10352.

modify our existing protocol to access the desired 2,5-diarylthiophene-1-oxide precursor

in excellent yield, (**110**, Scheme 2.21).
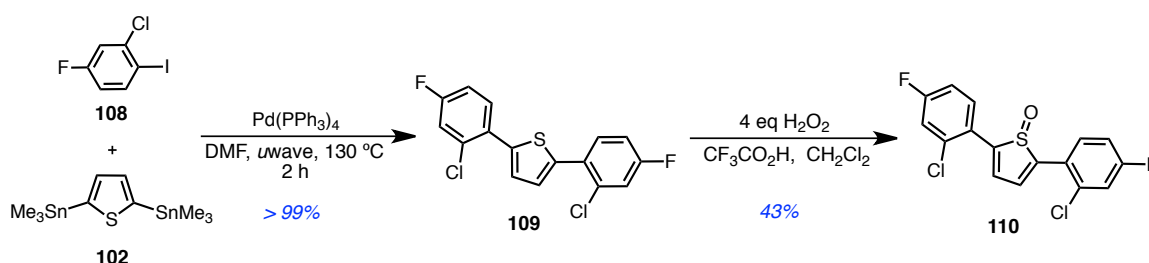
Scheme 2.21 Stille coupling of **102** and **108** to afford 2,5-diarylthiophene (**109**) and subsequent oxidation, affording **110** in remarkable 43% yield.

Surprisingly, oxidation of **109** using similar reaction times and molar ratios

afforded oxidized **110** in 43% yield; a significant improvement over non-functionalized

and electron-rich thiophenes. We were able to carry out our Diels-Alder and arylations

reactions to afford the desired tetrafluorotetrabenzo[8]circulene (**112**) from **111** in similar

yields (Scheme 2.22). The solubility of **112** is significantly increased over the parent

structure **55**, and is a fluorescent red solid, similar to that of **106** and **107**. The ^{1}H NMR

(Figure AI.43 from Appendix I) of **112** is substantially more spilt as a result of

heteronuclear spin-spin coupling.
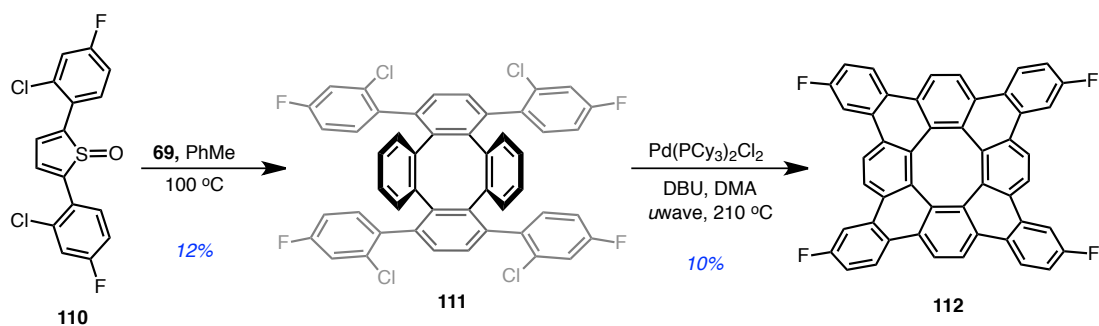
Scheme 2.22 Diels-Alder of **110** with **69** affording the desired tetraphenylene (**111**) followed by subsequent arylation to afford desired tetrafluorotetrabenzo[8]circulene (**112**) in low yield.

Unfortunately, the low yields obtained in the final steps of our synthetic methodology described herein made utilization of our new functionalized derivatives challenging. As a result of these challenges, our group began to investigate alternative routes towards our desired structures. The work detailed in the following chapters will highlight the results of these studies.

2.6 Conclusions

Through application of Clar's theory *via* the simple installation of four benzene rings around the periphery of [8]circulene, we were able to access the completely stable TB[8]C structure. In contrast to the previous report by Suzuki in which the requisite 8-membered ring was formed in the final step of the synthetic sequence,[58] we chose to initiate our synthesis with this ring already assembled. Exhibiting a deep saddle-shaped structure, TB[8]C is quite malleable and distorts significantly in the solid state to form a complex 3-dimensional π-stacking network. Despite the twisted nature of the solid-state

structure, measurements of ring planarity, bond lengths, and HOMA values all confirm the Clar representation of a fully-benzenoid species, thereby offering an explanation for the structure's high stability. Elaboration of our TB[8]C methodology has provided synthetic access to a number of functionalized derivatives. Unfortunately, the low yields that have resulted from these methodologies have suppressed the adaptation of these structures towards increased functionality and further investigation into the unique electronic properties of these molecules.

In the course of our studies, we found that the synthesis of TB[8]Cs could be achieved in a expedited methodology utilizing Scholl cyclodehydrogenation conditions from simplified 2,5-diphenylthiophene-1-oxides. In doing so, we also developed a more facile and functional group tolerant route towards our 2,5-arylthiophene-1-oxides precursors in one synthetic transformation. Surprisingly, we found that the oxidation strategies utilized in our early methodology detailed herein were intolerant of a variety of functional groups installed on the aryl rings of 2,5-diarylthiophenes. The work presented in the following chapters will detail the work performed by our group that resulted in a new route towards 2,5-diarylthiophene-1-oxides and a more facile synthesis of functionalized TB[8]Cs by the Scholl cyclodehydrogenation reaction.

CHAPTER 3: A ONE-POT METHOD FOR THE PREPARATION OF 2,5-DIARYLTHIOPHENE-1-OXIDES FROM ARYLACETYLENES

3.1 Introduction

The work presented herein will address our revised methodology towards 2,5-diarylthiophene-1-oxides, which can be made *via* readily available arylacetylene precursors. This new methodology relies on a zirconacyclopentadiene intermediate that provides access to our desired 2,5-diarylthiophene-1-oxides in a one-pot transformation. The isolated yields of the desired thiophene-1-oxides are comparable to those obtained from our previously utilized oxidation strategy from thiophene derivatives, while avoiding the formation of over-oxidation products. Furthermore, this route offers broader versatility than commonly used methods by providing products outfitted with electron-donating or electron-withdrawing groups with very little variation in isolated product yields. Finally, this strategy provides access to products containing functional groups that are not compatible with oxidation conditions. These methods developed in our laboratory have provided simplified access to functionalized TB[8]C structures, which will be discussed in the following chapter.

The [4 + 2] Diels-Alder cycloaddition reaction – the key transformation step of our methodology – has had a profound effect on synthetic organic chemistry due to its ability to generate 6-membered rings with high regio- and stereochemical control.[86] As a

---

[86] Diels, O.; Alder, K. *J. Liebigs Ann. Der Chem.* **1928**, *460,* 98–122.

result, the reaction has found utility in areas ranging from natural product synthesis[87] to the preparation of organic materials.[88] Of particular interest to the field of polycyclic aromatic hydrocarbons (PAHs) are cyclic dienes that undergo Diels-Alder reactions with alkynes, then subsequently fragment to produce substituted benzene rings in a single synthetic step. Although there is potential for dienes outfitted with aryl groups at the 1- and 4-positions to act as synthons for the fabrication of PAHs, such compounds are surprisingly uncommon. While 2,5-diarylated thiophene, thiophene dioxides, and furans are synthetically accessible, these compounds typically require the use of strongly-activated dienophiles or forcing conditions (high temperatures and/or pressures) to react by cycloaddition.[63,89] Cyclopentadienone and isobenzofuran derivatives are inherently more reactive, but synthesizing the 2,5-diarylated analogs of these compounds without additional substituents is exceedingly difficult.[37,48, 90] Thiophene-1-oxides originally identified as intermediates in the oxidation of thiophenes to thiophene dioxides,[91] on the other hand, have recently shown the potential to behave as highly-reactive dienes in both

[87] For a comprehensive review, please see: Nicolaou, K. C.; Snyder, S. A.; Montagnon, T.; Vassilikogiannakis, G. *Angew. Chem. Int. Ed.* **2002**, *41*, 1668–1698.

[88] For a comprehensive review, please see Zydziak, N.; Yameen, B.; Barner-Kowollik, C.; *Polym. Chem.* **2013**, *4*, 4072–4086.

[89] (a) Rheinhoudt, D. N.; Kouwenhoven, C. G. *Tetrahedron* **1974**, *30*, 2093–2098; (b) Rheinhoudt, D. N.; Trompenaars, W. P.; Geevers, J. *Tetrahedron Lett.* **1976**, *17*, 4777–4780; (c) Nakayama, J.; Kuroda, M.; Hoshino, M. *Heterocycles*, **1986**, *24*, 1233–1236; (d) Jursic, B. S. *J. Heterocyclic Chem.* **1995**, *32*, 1445–1455.

[90] (a) Sivasakthikumaran, R.; Nandakumar, M.; Mohanakrishnan, A. K. *J. Org. Chem.* **2012**, *77*, 9053–9071; (b) Nandakumar, M.; Sivasakthikumaran, R.; Mohanakrishnan, A. K. *Eur J. Org. Chem.* **2012**, 3647–3657.

[91] (a) Hashmall, J. A.; Horak, V.; Khoo, L. E.; Quicksall, C. O.; Sun, M. K. *J. Am. Chem. Soc.* **1981**, *103*, 289–295; (b) Naperstkow, A. M.; Macaulay, J. B.; Newlands, M. J.; Fallis, A. G. *Tetrahedron Lett.* **1989**, *30*, 5077–5080; (c) Li, Y; Thiemann, T; Sawada, T; Masashi, T. *J. Chem. Soc., Perkin Trans. 1.* **1994**, 2323–2329; (d) Thiemann, C.; Thiemann, T.; Li, Y.; Sawada, T.; Nagano, Y.; Tashiro, M. *Bull. Chem. Soc. Jpn.* **1994**, *67*, 1886–1893; (e) Li, Y.; Thiemann, T.; Mimura, K.; Sawada, T.; Mataka, S.; Tashiro, M. *Eur. J. Org. Chem.* **1998**, 1841–1850; (f) Thiemann, T,; Ohira, D.; Li, Y.; Sawada, T.; Mataka, S.; Rauch, K.; Noltemeyer, M.; de Meijere, A. *J. Chem. Soc., Perkin Trans. 1.* **2000**, 2968–2976; (g) Thiemann, T.; Sá e Melo, M. L.; Campos Neves, A. S.; Li, Y.; Mataka, S.; Tashiro, M.; Geißler, U.; Walton, D. *J. Chem. Research (S)* **1998**, 346–347.

our synthesis of TB[8]C and in the highly-visible reported synthesis of hexaarylbenzenes (HABs, **114**) from tetraarylthiophene-1-oxides (**113**) by Yamaguchi, (Scheme 3.1).[92]
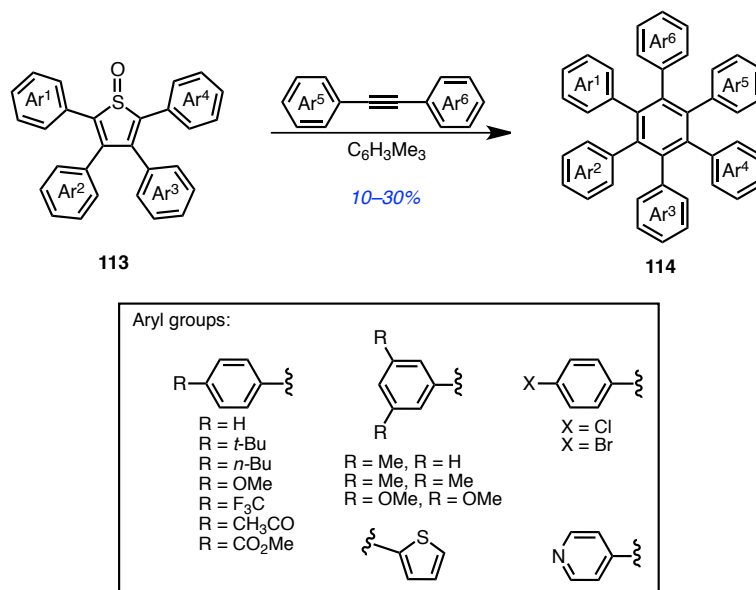
Scheme 3.1 Synthesis of HABs from thiophene-1-oxide precursors and diarylacetylene. Note: thiophenes could not be placed as substituents to the 1-oxide precursor.

Despite these recent advances, these dienes have yet to find widespread utility, likely as a result of the absence of methodology capable of consistently providing functionalized derivatives. To remedy this situation, we have developed a one-pot strategy that converts easily accessible arylacetylenes into 2,5-diarylthiophene-1-oxides. Importantly, the yields achieved through this process are comparable to those achieved through the most commonly used oxidation strategies, but with a much higher functional group tolerance.

---

[92] Suzuki, S.; Segawa, Y.; Itami, K.; Yamaguchi, J. *Nature Chemistry.* **2015**, *7*, 227–233.

3.2 Background

Thiophene-1-oxides are commonly synthesized through the oxidation of the corresponding thiophene derivative. The earliest example of this strategy employed *m*-chloroperoxybenzoic acid (*m*CPBA) as the oxidizing agent, though, this could only provide thiophene-1-oxides bearing bulky substituents (in order to prevent self-dimerization) in very low yields (~5%); the majority of the material recovered from these reactions was the sulfone – the product of over-oxidation (**A**, Figure 3.1). It was later realized that the introduction of either a strong Brönsted-Lowry (**B**)[71, 73] or Lewis acid (**C**)[93] to the oxidative conditions hinders the over-oxidation process, resulting in an improvement in reaction yields. In our studies, we were surprised to find that these oxidation strategies were intolerant of a variety of functional groups installed on the aryl rings of 2,5-diarylthiophenes, most notably alkoxy and alkyl moieties. Furthermore, for the compounds that could be successfully oxidized, the reactions had to be monitored closely to limit the formation of the sulfone and as a result, the yields of these reactions varied significantly.

---

[93] (a) Li, Y.; Matsuda, M.; Thiemann, T.; Sawada, T.; Mataka, S.; Tashiro, M. *Synlett* **1996**, 461–464; (b) Nakayama, J.; Yu, T.; Sugihara, Y.; Ishii, A. *Chem. Lett.* **1997**, *26*, 499–500; (c) Li, Y.; Thiemann, T.; Sawada, T.; Mataka, S.; Tashrio, M. *J. Am. Chem Soc.* **1997**, *62*, 7926–7936; (d) Furukawa, N.; Zhang, S.; Sato, S.; Higaki, M. *Hetercycles* **1997**, *44*, 61–66.

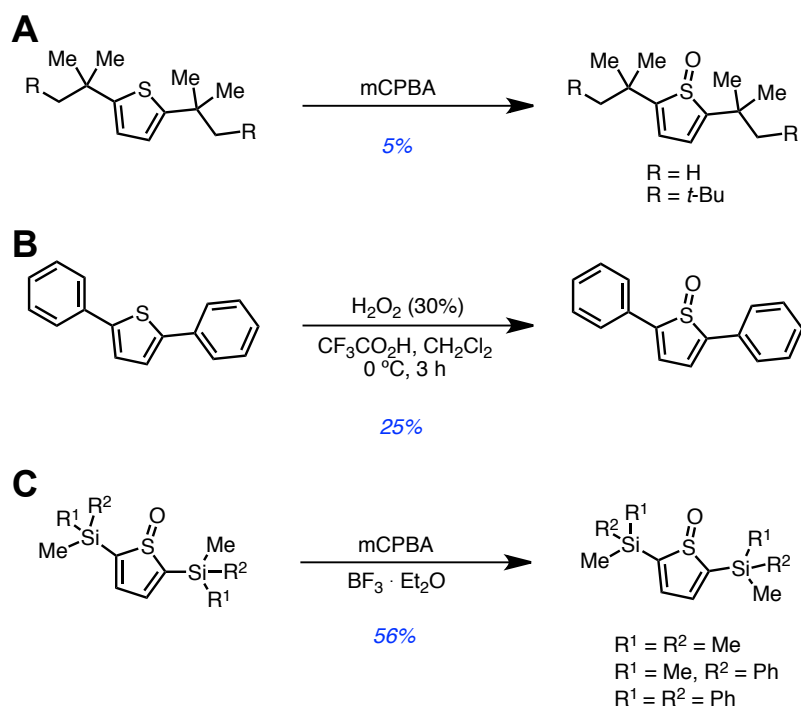**Figure 3.1 A**) The earliest example of the oxidation of thiophenes from *meta*-chloroperoxybenzoic acid (mCPBA), **B**) oxidation of thiophenes from hydrogen peroxide in the presence of a Brönsted-Lowry acid, and **C**) oxidation of thiophenes from mCPBA in the presence of a Lewis acid.

An alternate strategy for the synthesis of thiophene-1-oxides relies on the reaction of zirconacyclopentadiene precursors with either thionyl chloride (**A**, Figure 3.2)[94] or sulfur dioxide (**B**).[95] This method is particularly attractive as it avoids the undesired over-oxidation discussed above and exhibits a greater functional group tolerance. Although a vast array of metallole-heterocycles have been derived from zirconacyclopentadiene

[94] (a) Fagen, P. J.; Nugent, W. A. *J. Am. Chem. Soc.* **1988**, *110*, 2310–2312; (b) Meier-Brocks, F.; Weiss, E. *J. Organometal. Chem.* **1993**, *453*, 33–45. (c) Fagen, P. J.; Nugent, W. A.; Calabrese, J. C. *J. Am. Chem. Soc.* **1994**, *116*, 1880–1889.
[95] (a) Jaing, B.; Tilley, T. D. *J. Am. Chem. Soc.* **1999**, *121*, 9744–9745; (b) Suh, M. C.; Jiang, B.; Tilley, T. D. *Angew. Chem. Int. Ed.* **2000**, *39*, 2870–2837.

intermediates,[94,96] these reactions almost exclusively employ disubstituted acetylenes for the generation of tetrasubstituted species.
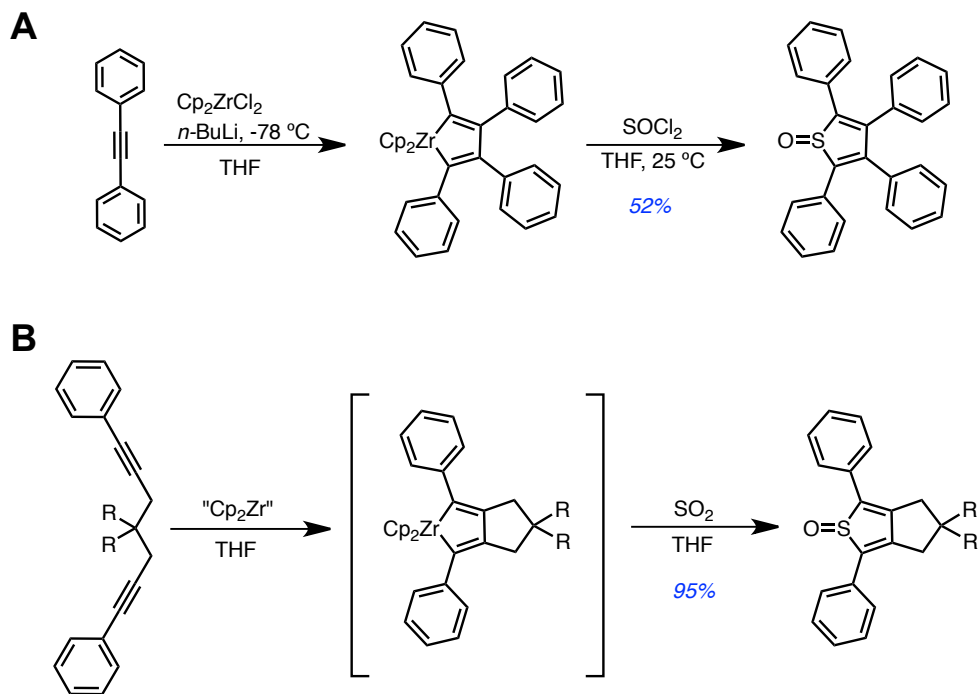

Figure 3.2 Thiophene-1-oxides bearing substituents on all four carbons as synthesized from zirconacyclopentadiene by **A**) Fagan and Nugent, and **B**) Jiang and Tilley.

Terminal acetylenes, on the other hand, have only been employed on a handful of occasions[97] likely due to the fact that such systems have been observed to lead to mixtures of the regioisomeric 2,4- and 2,5-disubstituted products.[98] Surprisingly, the

---

[96] (a) Fagan, P.J.; Burns, E. G.; Calabrese, J. C. *J. Am. Chem. Soc.* **1988**, *110*, 2979–2981; (b) Yan, X; Xi, C. *Acc. Chem. Res.* **2015**, *48*, 935–946.

[97] (a) Zirngast, M; Marschner, C.; Baumgertner, J. *Organometallics* **2008**, *27*, 2570–2583; (b) Bousrez, G.; Jaroschik, F.; Martinez, A.; Harakat, D.; Nicolas, E.; Le Goff, X. F.; Szymoniak, J. *Dalton Trans.* **2013**, *42*, 10997–11004.

[98] (a) Skibbe, V.; Erker, G. *J. Organomet. Chem.* **1983**, *241*, 15–26; (b) Ren, S.; Seki, T.; Necas, D.; Shimizu, H.; Nakajima, K.; Kanno, K.; Song, Z.; Takahashi, T. *Chem. Lett.* **2011**, *40*, 1443–1444.

conditions presented herein produce only the 2,5-diarylated product, and we did not observe any of the undesired isomers from our reaction mixtures.[99]

3.3 Synthesis

A simple example of the one-pot synthesis of 2,5-diarylthiophene-1-oxides is displayed in Scheme 3.2. Initially, "Cp$_2$Zr" was generated by the slow addition of *n*-BuLi to Cp$_2$ZrCl$_2$ at −78 ºC under a nitrogen atmosphere. The reaction mixture was allowed to warm to room temperature until a dark red solution developed.
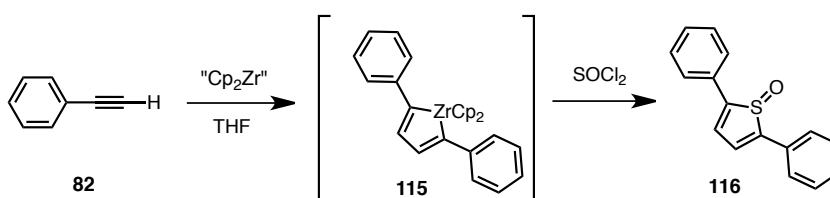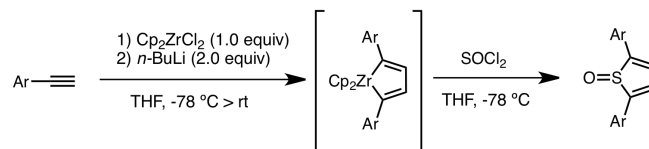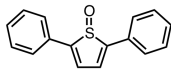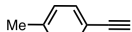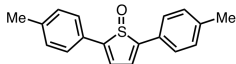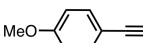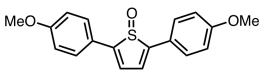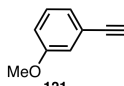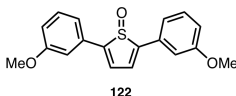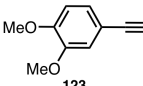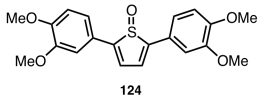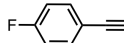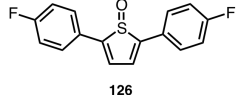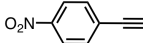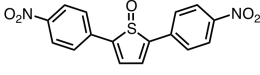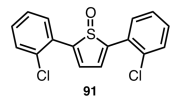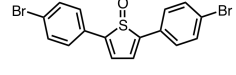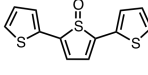

Scheme 3.2 Synthesis of 2,5-diphenylthiophene-1-oxide through zirconacyclopentadiene intermediate.

Phenylacetylene (**82**) was then added at 0 ºC to generate the diphenylzirconacyclopentadiene intermediate (**115**). The reaction mixture was then cooled back down to −78 ºC and thionyl chloride was added drop-wise to the reaction mixture, affording a bright yellow solution. The cold reaction mixture was directly added to a plug of silica and the product (**116**) was eluted in 30% yield (Table 3.1, Entry 1).

---

[99] The position of the aryl substituents on each of the thiophene-1-oxide products was confirmed using Heteronuclear Single Quantum Coherence (HSQC) spectroscopy. The carbon alpha to the sulfoxide on the thiophene-1-oxide ring has a characteristic downfield shift of ca. 150 ppm and for each substrate it was confirmed that this carbon atom was not directly attached to a proton. HSQC are provided in Appendix I.

Table 3.1 Reaction substrate scope.

Entry	Substrate	Product	Yield (%)[a]
1	82	116	30
2	117	118	30
3	119	120	29
4	121	122	28
5	123	124	32
6	125	126	23
7	127	128	0
8	129	91	27
9	130	131	29
10	132	133	10[b]

[a]Isolated yield obtained by quenching with thionyl chloride.
[b]Isolated yield obtained by quenching with SO_2.

It is important to note that our initial attempts to perform these reactions using standard Negishi workup conditions resulted in surprisingly low (ca. 5%) yields of the desired thiophene-1-oxides.[100] Additionally, crude reaction mixtures that were left in a -20 °C freezer overnight were devoid of the desired product upon subsequent analysis. We suspect that byproducts resulting from the thermal decomposition[101] of the "Cp$_2$Zr" – namely 1-butene (**A**) and cyclopentadiene (**B**), and either 3,5- or 3,4-diarylthiophenes (**C**) – are capable of reacting in a Diels-Alder fashion with our desired product (Figure 3.3).
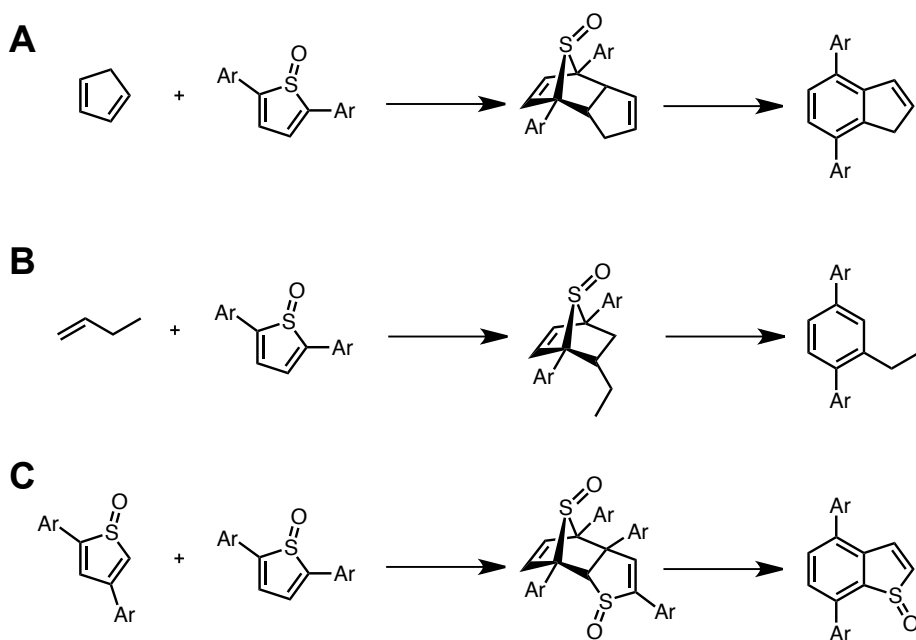
Figure 3.3 Formation of undesired byproducts from **A**) 1-butene and **B**) cyclopentadiene as a result of the thermal decomposition of zirconocene. **C**) Rapid reaction of 3,5-diarylthiophenes.

---

[100] (a) Negishi, E.; Cederbaum; F. E.; Takahashi; T. *Tetrahedron Lett.* **1986**, *27*, 2829–2832; (b) Negishi, E.; Takahashi, T. *Acc. Chem. Res.* **1994**, *27*, 124–130.
[101] Dioumaev, V. K.; Harrod, J. F. *Organometallics* **1997**, *16*, 1452–1464.

Considerably better yields can be achieved by filtering the cold reaction mixture through a plug of silica and eluting any potentially reactive intermediates with hexanes prior to isolating the desired compound using more polar eluents. The isolated products undergo slight decomposition when left in organic solvents for extended periods of time, but they can be stored as solids at 0 ºC for months with little to no decomposition. Having established that the desired reactivity could be achieved, we were excited to find that the reaction is tolerant of a range of electronically diverse functional groups, as observed in Table 3.1.

3.3.1 Electron-Donating Substituents

When electron-donating functionality was introduced to the *para* position of the aryl ring of the arylacetylene – such as the methyl (**117**) and methoxy (**119**) substituted derivatives – we observed the formation of products **118** and **120** in yields that were nearly identical to that of the unsubstituted precursor (**116**). When the methoxy group is shifted *meta* to the alkyne (**121**), where it is theoretically less able to donate electron-density into the triple-bond, **122** is afforded with no decrease in yield. Even the veritrole-based system, (**123**) equipped with two electron-donating methoxy groups, displays only a minor increase in the yield of **124**, compared to the less electron-rich systems.

3.3.2 Electron-Withdrawing Substituents

At the opposite end of the spectrum, we observe a slight but noteworthy decrease in the yield when mildly electron-withdrawing fluorine groups are installed on the aryl ring (**125**), and a complete loss of reactivity when nitro groups are incorporated (**127**). To investigate this observation, we used density functional theory (DFT) calculations to generate electrostatic potential maps (Figure 3.4) of each of the arylacetylenes listed in Table 3.1.[102] These maps indicate the presence of a distinctly negative environment surrounding the alkyne for each of the compounds except for **127**, which has a noticeably positive electrostatic potential surrounding the triple bond. Based on this evidence, it is reasonable to conclude that the strongly electron-withdrawing nature of the nitro group renders the alkyne sufficiently electron-poor such that it is unable to react with the generated "Cp$_2$Zr" species.

---

[102] Electrostatic potential maps were generated using DFT calculations (B3LYP functional, LACVP** basis set for bromine and 6–31G** basis set for all other atoms) performed using Jaguar (see Jaguar: Version 8.3, Maestro: Version 9.8, Schrödinger, LLC, New York, USA, **2014**) software package.

phenylacetylene (**82**)

4-fluorophenylacetylene (**125**)

4-ethynyltoluene (**117**)

4-nitrophenylacetylene (**127**)

4-ethynylanisole (**119**)

2-chlorophenylacetylene (**129**)

3-ethynylanisole (**121**)

4-bromophenylacetylene (**130**)

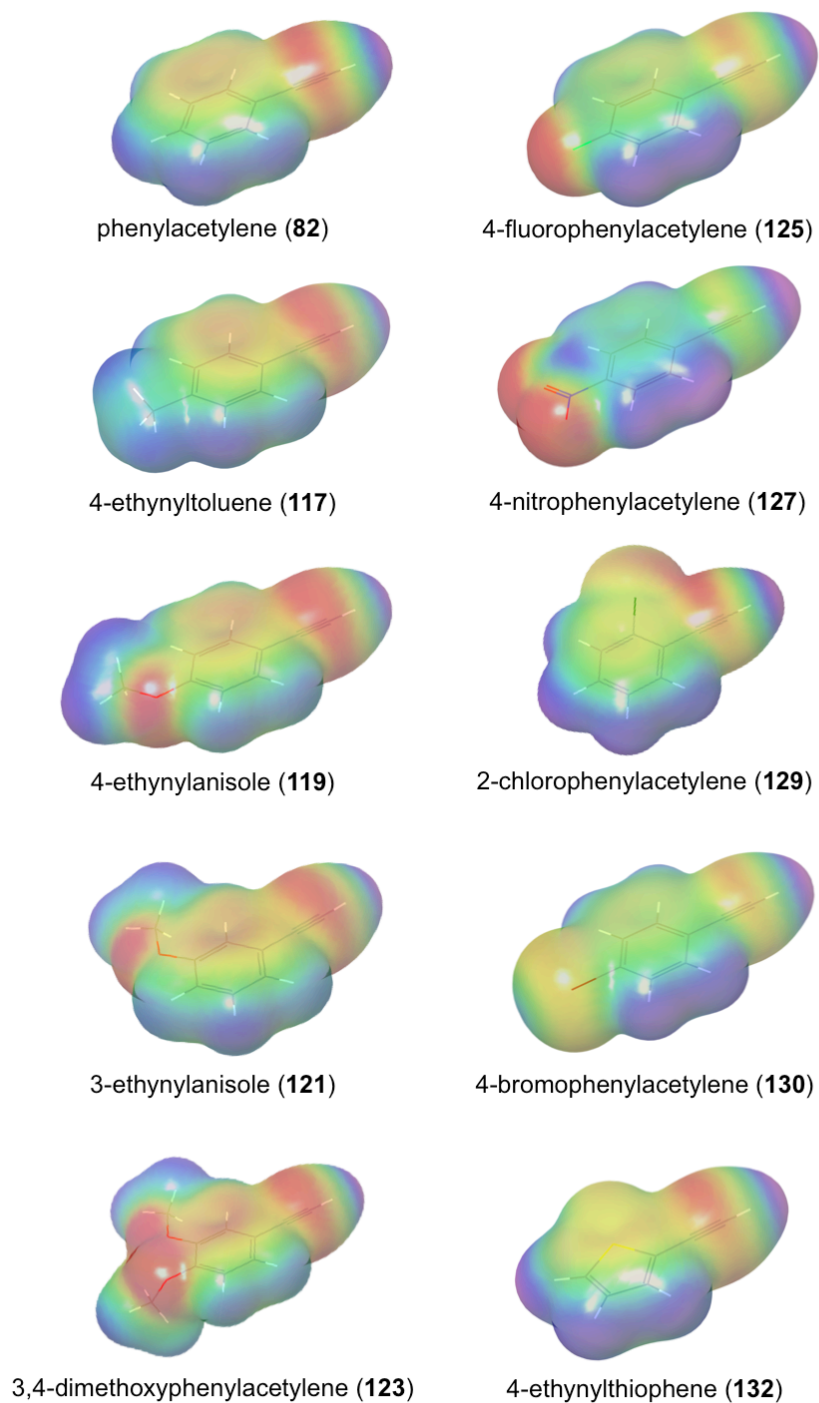3,4-dimethoxyphenylacetylene (**123**)

4-ethynylthiophene (**132**)

Figure 3.4 Relative electrostatic potential maps of phenyl acetylenes with electron-donating and electron-withdrawing substituents.

3.3.3 Reactive Halides

Substrates **129** and **130** further demonstrate the utility of this methodology. The *o*-chloro derivative **129** illustrates that substituents *ortho* to the alkyne have little impact on the reaction yield due to steric effects. Furthermore, due to the position of the chlorine atom on this substrate **129** has the potential to find significant utility in generating fused ring systems through sequential Diels-Alder / palladium-catalyzed arylation reactions as we demonstrated in the synthesis of tetrabenzo[8]circulene. In a similar vein, the brominated derivative, **130**, illustrates that more reactive halides survive the reaction conditions with no observable decrease in yield. Such functional groups have the potential to provide a synthetic handle for further transformations through metal-catalyzed cross-coupling reactions.

3.3.4 Mixed Thiophene

Finally, in addition to phenyl-substituted thiophene-1-oxides, mixed thiophene/thiophene-1-oxides are an attractive synthetic target, as such structures cannot be obtained though the traditional oxidation procedures. Surprisingly, while we were able to observe the conversion of 2-ethynylthiophene (**132**) into the desired compound (**133**), the formation of a complex mixture of products made it particularly challenging to isolate the desired product. The replacement of thionyl chloride with SO_2 produced a much cleaner reaction and allowed us to isolate the desired product in 10% yield (Entry

9).[103] To our knowledge this is the first report of a thiophene/thiophene-1-oxide oligomer that is free of substituents at the 3- and 4-positions of each on the thiophene rings.

3.4 Conclusions

In summary, we have presented a convenient one-pot method for the synthesis of 2,5-diarylthiophene-1-oxides. This transformation avoids the problematic formation of 1,1-dioxides that result from oxidation strategies while providing the desired products in comparable yields. The methodology is tolerant of an array of electron-donating and electron-withdrawing functionalities, halogens, substituents positioned in sterically demanding positions, and functional groups that we found to be completely intolerant towards the oxidation conditions presented in our initial synthesis of TB[8]C. We have found that this method for the synthesis of 2,5-diarylthiophene-1-oxides allows us to access functionalized versions of our target compound. Lastly, these materials have advanced our ability to incorporate functionality in TB[8]C and these methods will be discussed in the following chapter.

---

[103] Despite reports that the yields of similar systems were increased by replacing thionyl chloride with sulfur dioxide (Jaing, B.; Tilley, T. D. *J. Am. Chem. Soc.* **1999**, *121*, 9744–9745.) this was not observed for our substrates. However, reactions carried out under these conditions tended to afford notably cleaner crude reaction mixtures.

CHAPTER 4: I. GENERAL METHODS FOR THE SYNTHESIS OF FUNCTIONALIZED TETRABENZO[8]CIRCULENES AND II. STUDIES TOWARDS EXPANDED [8]CIRCULENE STRUCTURES

4.1 Background

With the functionalized 2,5-diarylthiophene-1-oxides in hand we set our sights on the synthesis of functionalized tetrabenzo[8]circulenes containing both electron-rich and electron-poor functional groups. Functionalized derivatives of the saddle-shaped molecule tetrabenzo[8]circulene were successfully synthesized from our readily available starting materials in a more efficient manner than those introduced in chapter 2. These advances allowed us to investigate the optoelectronic properties that result from the introduction of functionality on these highly contorted aromatic structures.

Despite their unique structures, [8]circulenes and the stable TB[8]C have yet to receive significant attention, likely owing to the lack of methodology to generate functionalized derivatives and a consistent, high-yielding, synthetic approach. This is particularly relevant considering the extensive literature detailing the synthesis and electronic properties of the analogous hetero[8]circulenes (Figure 4.1),[104] and the vast theoretical investigations of such structures.[105] Such structures have been observed to be

[104] (a) Baryshnikov, G. V.; Minaev, B. F.; Minaeva, V. A. *Russ. Chem. Rev.* **2015**, *84*, 455−484; (b) Hensel, T.; Andersen, N. N.; Plesner, M.; Pittelkow, M. *Synlett* **2016**, *27*, 498−525.
[105] (a) Baryshnikov, G. V.; Minaev, B. F.; Pittelkow, M.; Nielsen, C. B.; Salcedo, R. *J. Mol. Model.* **2013**, *19*, 847−850; (b) Baryshnikov, G. V.; Valiev, R. R.; Karaush, N. N.; Minaev, B. F. *Phys. Chem. Chem. Phys.* **2014**, *16*, 15367−15374; (c) Dong, H.; Gilmore, K.; Lin, B.; Hou, T.; Lee, S.-T.; Guo, Z.; Li, Y. *Carbon* **2015**, *89*, 249−259; (d) Obayes, H. R.; Al Obaidy, A. H.; Alwan, G. H.; Al-Amiery, A. A. *Cogent Chemistry* **2015**, *1*, 1026638; (e) Baryshnikov, G. V.; Karaush, N. N.; Valiev, R. R.; Minaev, B. F. J. Mol. Model. **2015**, *21*, 136; (f) Obayes, H. R.; Al-Gebori, A. M.; Khazaal, S. H.; Jarad, A. J.; Alwan, G. H.; Al-

completely planar as a result of the incorporation of 5-membered rings and heteroatom ring junctions.
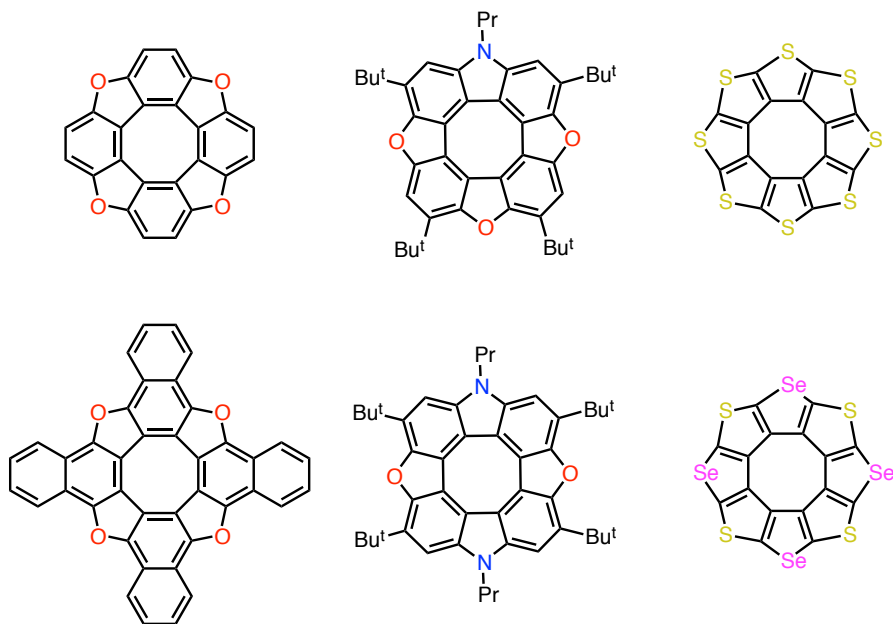

Figure 4.1 Examples of heteroatom six- and five-membered rings whose structures include oxygen, nitrogen, sulfur, and selenium. Incorporation of five-membered rings and their associated heteroatom junctions have resulted in complete planarization of the traditionally non-planar 8-membered core.

Herein we describe a new and general method for the synthesis of a number of functionalized tetrabenzo[8]circulene derivatives in yields significantly improved from our earlier methodology. Through this work we aimed to improve charge transport mobilities of the TB[8]C structural motif. To this end, we envisioned that access to functionalized forms of the TB[8]C structure would allow us to design a new class of tunable molecular electronics. Through modification of our reported methodology into these molecules, we were able to access new TB[8]C structures containing electron

Amiery, A. A. J. *Nanoelectron. Optoelectron.* **2015**, *10*, 711−716; (g) Baryshnikov, G. V.; Valiev, R. R.; Karaush, N. N.; Sundholm, D.; Minaev, B. F. *Phys. Chem. Chem. Phys.* **2016**, *18*, 8980−8992.

donating and withdrawing functional groups, in addition to structures that would allow us to access broad-spectrum functionalization at a late stage.

4.2 Revised Synthesis of Functionalized Tetrabenzo[8]circulenes

In our initial synthesis of the parent structure (**55**), we chose to utilize a palladium-catalyzed arylation reaction for the final step of our synthetic procedure as seen in Figure 4.2, **A**.[41, 75] The reaction methodology was expected to provide high functional group tolerance, however, the substrate scope was limited, with decomposition observed for a range of substrates. Furthermore, overly-complex synthetic precursors were required to install the appropriately placed chlorine atoms required for the final bond closure, limiting the quantity of material that could be produced.
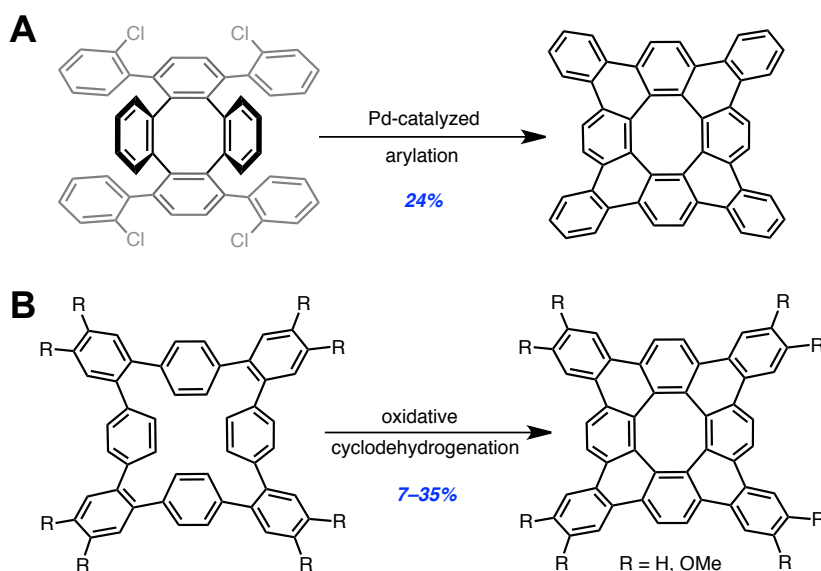

Figure 4.2 Comparison of the originally reported synthetic methods towards tetrabenzo[8]circulene by **A**) outward extension of the octagon *via* the Pd-catalyzed arylation reaction and **B**) inward formation of the octagon by Suzuki et al. through oxidative cyclodehydrogenation.

91

Oxidative cyclodehydrogenation reactions (that would circumvent the need for chlorine atoms) were originally avoided due to a similar substrate producing rearrangement products rather than the desired bond closures.[48] Nevertheless, the development of new oxidative cyclodehydrogenation conditions – and an increase in the number of non-planar aromatics generated through such methods[106] – including the concomitant report by Suzuki and co-workers (Figure 4.2, **B**)[58] compelled us to evaluate the potential of these reactions.

While common methods employing FeCl$_3$ in CH$_2$Cl$_2$, CuCl$_2$ and AlCl$_3$ in CS$_2$ or Cu(OTf)$_2$ and AlCl$_3$ in CS$_2$ displayed some promise, these conditions ultimately proved insufficient, as partially-closed products dominated crude reaction mixtures and the desired product was isolated in low yields. To our surprise, however, the use of CF$_3$SO$_3$H and DDQ in CH$_2$Cl$_2$ for the conversion of tetraphenylene (**134**) into **55** (Table 4.1) produced the desired product in a much higher yield and in a more energy efficient manner than our previous reported method. It is important to note that while completion of the reaction was observed by TLC in as little as 15 minutes, our best yields were obtained by allowing reactions to continue for 16 hours. With the oxidative coupling reaction proving successful for the synthesis of the parent compound, we then directed our attention to determining the substrate scope of this methodology.

---

[106] Zhai, L.; Shukla, R.; Wadumethrige, S. H.; Rathore, R. *J. Org. Chem.* **2010**, *75*, 4748−4760.

**Table 4.1** Screening of various oxidative cyclodehydrogenation conditions.
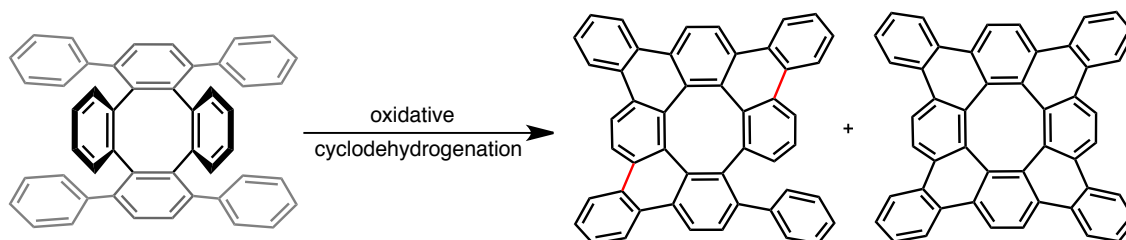
Entry	Conditions	Solvent	Time (h)	Isolated yield (%)[a]	Isolated yield (%)[b]
1	FeCl$_3$ (10 equiv)	CH$_2$Cl$_2$	12	12	1
2	AlCl$_3$ (30 equiv) CuCl$_2$ (30 equiv)	CS$_2$	5	15	2
3	AlCl$_3$ (30 equiv) CuCl$_2$ (30 equiv)	CS$_2$	12	20	5
4	AlCl$_3$ (30 equiv) Cu(OTf)$_2$ (30 equiv)	CS$_2$	12	26	3
5	TfOH (20 equiv) DDQ (5 equiv)	CH$_2$Cl$_2$	0.5	5	21
6	TfOH (20 equiv) DDQ (5 equiv)	CH$_2$Cl$_2$	16	0	47

[a] Isolated yield of partially-closed products and mixtures of partially-closed products that could not be separated. [b] Isolated yield of the desired TB[8]C.

4.2.1 Diels-Alder [4 + 2] Cycloaddition

As illustrated in Scheme 4.1, functional groups are most easily introduced through the use of substituted 2,5-diarylthiophene-1-oxides (**116**, **118**, **120**, **126**, and **131**), which we were able to synthesize through the zirconium-mediated cyclization reaction discussed in the previous chapter. These thiophene oxides were reacted *via* the [4 + 2] Diels-Alder cycloaddition reaction with the Sondheimer-Wong diyne (**69**)[67] in toluene at 80 °C to produce a range of substituted tetraphenylene derivatives (**134–138**). In the

course of our studies, we found that minor yield improvements were obtained when these reactions were carried out at slightly lower temperatures from our earlier methodology. While we expected the removal of the chlorine atoms from the dienophile to positively impact the yield of the Diels-Alder reaction due to decreased steric effects and planarization of the substrate, this was not the case. However, we do observe a correlation between reaction yield and the electronic nature of the diene consistent with an inverse demand Diels-Alder reaction; for example, yields of the electron-rich tetramethoxylated species (**136**) and electron-poor tetrafluorinated species (**137**) are 10% and 25% respectively.
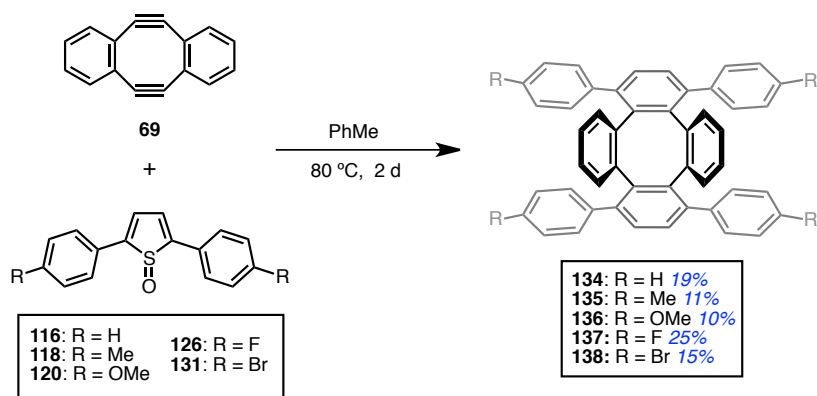
Scheme 4.1 Diels-Alder cycloaddition of thiophenes (**116**, **118**, **120**, **126**, and **131**) with dibenzocyclooctadiyne (**69**) affording the desired tetraphenylenes (**134–138**).

While attempts were made to utilize the 2,5-bis(3,4-dimethoxyphenyl)-thiophene-1-oxide (**124**) as a diene in our double Diels-Alder cycloaddition reaction, we were unfortunately unable to isolate material in high enough yield for accurate characterization. We were able to carry out the desired transformation with 2,5- bis(3-methoxyphenyl)thiophene-1-oxide (**122**) to afford the desired Diels-Alder adduct

94

1,4,9,12-tetrakis(3-methoxyphenyl)tetraphenylene (**136'**) in similar yield to that of reported **136**.

4.2.2 Oxidative Cyclodehydrogenation

Subsequent oxidative cyclodehydrogenation reactions of **134–138** were successfully accomplished using CF_3SO_3H and DDQ in CH_2Cl_2 at room temperature with isolated yields ranging from 47-72% (Scheme 4.2). Although electron-donating groups typically facilitate these reactions,[59] no significant correlation was observed between the electronic nature of the functional group and the reaction yield. We initially rationalized this to be a result of the positioning of the functional groups *meta* to the site of bond closure rather than *para*, which was done to guarantee the formation of only a single regioisomer from the oxidative cyclodehydrogenation reaction. When the methoxy group was moved *para* to the site of bond formation (**136'**) we observed no change in reaction yield. Interestingly, we only observe the single desired regioisomer, indicating that the functional groups retain their directing effects.

134: R = H	**55**: R = H *47%*
135: R = Me	**139**: R = Me *72%*
136: R = OMe	**140**: R = OMe *68%*
137: R = F	**112**: R = F *65%*
138: R = Br	**141**: R = Br *70%*

TfOH, DDQ
CH_2Cl_2, rt
16 h
47–72%
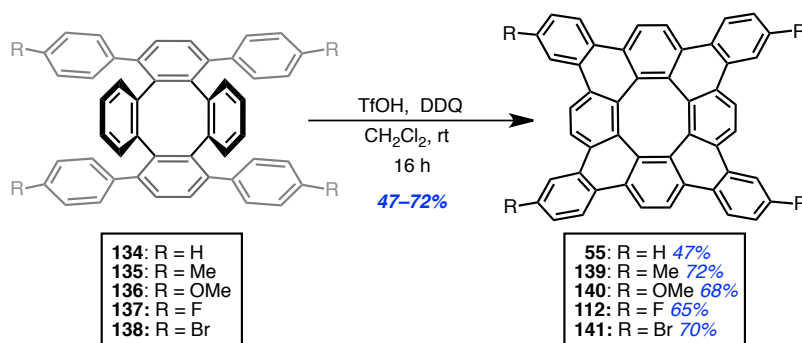
Scheme 4.2 Oxidative cyclodehydrogenation of **134–138** successfully accomplished using TfOH and DDQ with isolated yields ranging from 47-72%.

While the absence of a correlation between the electronic nature of a substituent and reactivity is surprising, it also indicates an increase in the functional group tolerance of the reaction. For example, compounds outfitted with electron-withdrawing fluorine (**137**) and bromine (**138**) atoms were successfully converted to the corresponding tetrabenzo[8]circulene derivatives, **112** and **141** respectively, in yields comparable to those achieved with electron-donating substituents. The main factor in this reaction appears to be the presence of a functional group (no matter its electronic nature), as we only observe a significant decrease in yield for the formation of the parent compound, **55**. While this is likely a result of the functional groups sterically inhibiting intermolecular bond formation during the coupling reaction, we were unable to confirm the presence of any dimers / oligomers in the mass spectral analysis of the crude reaction mixture that produced **55**. It is important to note that attempts to furnish the desired **122** *via* the earlier reported oxidative cyclodehydrogenation conditions by Suzuki afforded only unreacted starting material.

4.2.3 Late Stage Diversification

The synthesis of the tetrabrominated compound, **141**, is particularly relevant as it provides a means for late-stage diversification through metal-catalyzed cross-coupling reactions. The effectiveness of these potential modifications are illustrated by the conversion of **141** to **142** through the use of standard, unoptimized Suzuki-Miyaura

cross-coupling conditions, which provided the tetraphenylated derivative in near quantitative yield (Scheme 4.3).
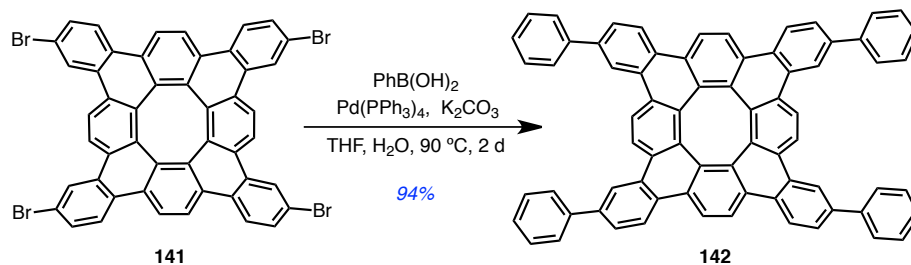
Scheme 4.3 Suzuki-Miyaura cross-coupling of phenylboronic acid and **141** to afford **142**, a prime example of the utility and late stage diversification of these new materials.

The methods reported herein provided higher yielding access to TB[8]C structures. Of particular importance is the ability to access **141**, whose structure can be functionalized at a late stage in the synthetic methodology. While our previous methodology did provide access to such structures, tetraiodo-tetrabenzo[8]circulene (**107**), the necessary protection steps and overall low yielding process made this material challenging to carry forward.

4.3 Optoelectronic Properties

The effect of functionalization on the optoelectronic properties of the substrate has been investigated through UV-Vis and cyclic voltammetry (CV). In the UV-Vis spectra of **55**, **112**, & **139–142** (Figure 4.3), we see little change in the molar absorptivity as functionalization is introduced (with the exception of **142**, which is the only species

where the π-system has been extended). However, an increase in the fine structure for the halogenated and phenylated substrates is observed. This observation is likely an electronic effect, resulting in the clearly visible vibronic progression in the UV-Vis spectrum. Such observations have been made both computationally [107] and experimentally,[108] in regards to similar contorted aromatic ring systems. Interestingly, the band edge of the low energy transitions for each of the substrates consistently appears at ca. 550 nm.
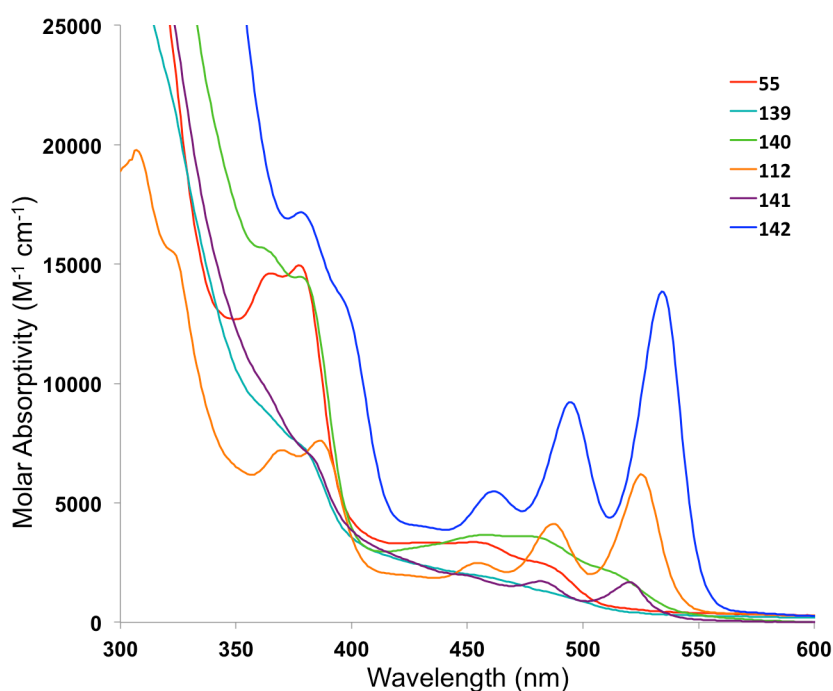
Figure 4.3. UV−vis absorption spectra of tetrabenzo[8]circulenes **55**, **112**, and **139−142** in CH_2Cl_2 (~50 μM).

These optical gaps are in agreement with the electrochemical data obtained from CV (Table 4.2), which consistently provide HOMO-LUMO gaps of 2.22 ± 0.01 eV (with

[107] Karaush, N. N.; Valiev, R. R.; Baryshnikov, G. V.; Minaev, B. F.; Ågren, H. *Chem. Phys.* **2015**, *459*, 65−71.
[108] Tokoro, Y.; Oishi, A.; Fukuzawa, S. *Chem. Eur. J.* **2016**, *22*, 13908−13915.

the exception of the fluorinated derivative, **112**, which has a gap of 2.29 eV). The energy

levels of these orbitals also appear to change very little (ca. 0.06 eV), again with the

exception of fluorinated derivative **112**.

Table 4.2 Electrochemical data of tetrabenzo[8]circulenes.[a]

	E_{ox} (V)	E_{red} (V)	HOMO (eV)	LUMO (eV)	E-Chem Gap, (eV)
55	0.44	-1.79	-5.24	-3.01	2.23
139	0.39	-1.83	-5.19	-2.97	2.22
140	0.38	-1.83	-5.18	-2.97	2.21
112	0.54	-1.75	-5.34	-3.05	2.29
141	0.39	-1.83	-5.19	-2.97	2.22
142	0.45	-1.77	-5.25	-3.03	2.22

[a]All potentials were measured in CH_2Cl_2, containing 0.05 M tetrabutylammonium tetrakis(pentafluorophenyl)borate as the supporting electrolyte. Values are referenced versus a ferrocene/ferrocenium redox couple. E_{ox} and E_{red} are the average of the anionic and cationic current peak maxima for the reversible first oxidation and reduction couple, respectively. HOMO and LUMO values were calculated on the basis of the oxidation of a ferrocene reference in vacuum (4.8 V). Additional oxidation and reduction potentials are provided in Appendix II.

In order to more thoroughly understand the electronic character of our

tetrabenzo[8]circulene structure, we decided to investigate the chemically-induced

reduction of **55** into its radical anion and dianionic state. When **55** is exposed to excess

metallic potassium in THF under an inert atmosphere, the immediate formation of a green

solution – indicative of the one-electron radical anion (**143**) – is observed (a ^{1}H NMR is

included in Appendix I, Figure AI.88 for reference). Continued exposure to metallic

potassium further reduces the radical anion into its dianion (**144**), a dark red solution,

which can easily be observed by ^{1}H and ^{13}C NMR. Similar observations have been made

in our lab for the reported structure of tridecacyclene.[109] The addition of negative charge induces magnetic shielding on the nuclei, so NMR spectroscopy can be used to analyze the charge distribution within these structures. The ^{13}C NMR Spectrum (Table 4.3) exhibits strong upfield shifts; $\delta = 24.8$ ppm for **C6**, 14.6 ppm for **C3**, and 11.2 ppm for **C1**, indicating localization of electron density around the inner 8-membered ring of **144**, while electrostatic repulsion is primarily responsible for the electron density at the outer-periphery of the structure observed at **C1 & C3**. In addition, the remaining carbons of the dianion species are shifted downfield with the exception of **C2,** which remains relatively constant in both neutral and dianionic species. Proton-coupled HSQC and HMBC experiments made it possible to determine the precise structural assignments of the TB[8]C neutral and dianion species.

Table 4.3 ^{13}C NMR and ^{1}H NMR chemical shifts, in ppm, of the TB[8]C structure.
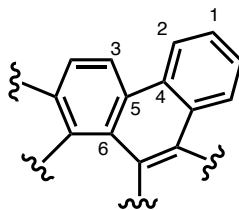
	C1 (H1)	C2 (H2)	C3 (H3)	C4	C5	C6
55	134.90 (7.55)	123.95 (8.16)	124.55 (7.76)	130.60	130.88	134.91
144	123.71 (7.00)	123.04 (7.58)	109.91 (7.11)	135.79	132.98	110.09

Structural assignments were confirmed by HSQC and HMBC 2D NMR experiments. All chemical shifts reported in ppm and were observed in THF-d_8.

It is evident from the observed ^{1}H and ^{13}C NMR that the reduction process is

[109] (a) Sumy, D. P.; Dodge, N. J.; Harrison C. M.; Finke, A. D.; Whalley, A. C. *Chem. Eur. J.* **2016**, *22*, 4709–4712; (b) Sumy, D. P.; Finke, A. D.; Whalley, A. C. *Chem. Commun.* **2016**, *52*, 12368–12371.

accompanied by direct symmetry changes in the structure of the TB[8]C dianion (**144**).

The charge density on the carbon π-framework is calculated using the differences in the

^{13}C NMR spectra of the neutral species and the dianion by employing Equation 4.1.[110]

$$\rho_\pi = \Delta\delta_c / K_c \tag{4.1}$$

K_c is a calculated proportionality constant (with a normal value of ca. 160.0

ppm/electron), and ρ_π is the change in the π-charge on the carbon, and $\Delta\delta_c$ is the chemical

shift change of the associated carbon from the anionic to the neutral state. The results of

these calculations are reported in Table AII.4 of Appendix II and are clearly illustrated in

Figure 4.4. As evident from the observed NMR shifts, the electronic charge is centered

on the core of 8-membered ring of **144.**
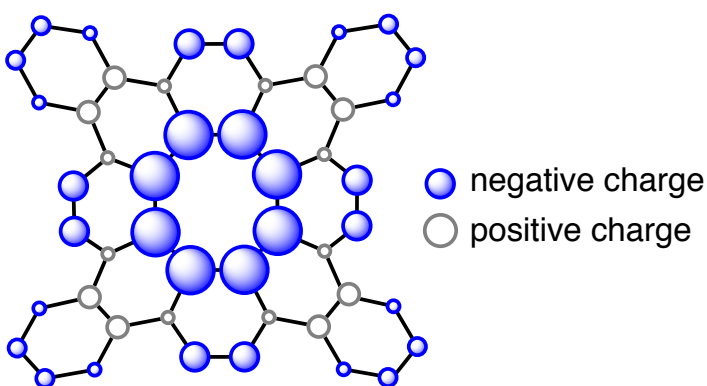
Figure 4.4 The charge distribution of TB[8]C dianion (**144**) according to the ^{13}C NMR spectrum.

---

[110] (a) Fraenkel, G.; Carter, R. E.; McLachlan A.; Richards, J. H. *J. Am. Chem. Soc.* **1960**, *82*, 5846–5850; (b) Spiesecke H.; Schneider, W. G. *Tetrahedron Lett.* **1961**, 468–472; (c) Lauterbur, P. C. *Tetrahedron Lett.* **1961**, 274–279; (d) Schaefer T.; Schneider, W. G. *Can. J. Chem.* **1963**, *41*, 966–982; (e) Olah G. A.; Mateescu, G. D. *J. Am. Chem. Soc.* **1970**, *92*, 1430–1432; (f) O'Brien, D. H.; Hart, A. J.; Russell, C. R. *J. Am. Chem. Soc.* **1975**, *97*, 4410–4412.

Reduction of **55** to **144** with potassium metal shows that the electronic character of this reduced structure is localized on the core 8-membered ring of the circulene structure. To date, we have been unable to grow crystals of **144** of sufficient quality for X-ray analysis; the reduction of **55** can be exceedingly temperamental, and prolonged exposure of the dianion with metallic potassium causes a black solid to precipitate from solution. We suspect the dianion **144** requires a special stabilizing effect that occurs through the formation of a supramolecular dimer; such observations have previously been reported in similarly contorted PAHs.[111] Nevertheless, we have been unable to confirm the existence of such species or resolve the solid black precipitate formed in these reactions.

4.4 Expansion of the [8]circulene Structural Motif

As evident herein and in the proceeding chapters, the major limiting aspect of this work remains the low yielding Diels-Alder [4 + 2] cycloaddition reaction. While the use of various thiophene-1-oxides has proven quite powerful in achieving the desired transformation, we have investigated several other cyclic dienes for their potential to greatly improve on this synthetic transformation. Attempts based on the furan and sulfone cyclopentadiene to afford the TB[8]C structure were introduced in the beginning of Chapter 2, however in the course of our studies we investigated the use of

[111] (a) Aprahamian, I.; Bodwell, G. J.; Fleming, J. J.; Manning, G. P.; Mannion M. R.; Sheradsky, T.; Vermeij, R. J.; Rabinovitz, M. *J. Am. Chem. Soc.* **2003**, *125*, 1720–1721; (b) Aprahamian, I.; Preda, D. V.; Bancu, M.; Belanger, A. P.; Sheradsky, T.; Scott, L. T.; Rabinovitz, M. *J. Org. Chem.* **2006**, *71*, 290–298; (c) Aprahamian, I.; Wegner, H. A.; Sternfeld, T.; Rauch. K.; de Meijere, A.; Sheradsky, T.; Scott, L. T.; Rabinovitz, M. *Chem. Asian J.* **2006**, *1,* 678–685.

cyclopentadienones and 1,3-diphenylisobenzofuran substrates for the synthesis of larger contorted aromatic structures. To this end, two routes towards expanded contorted aromatic frameworks of [8]circulene have been envisioned and investigated by our group. These routes can be summarized by two means; the outward expansion of the octagon, and the outward expansion of the TB[8]C structural motif.

4.4.1 Outward Expansion of the Octagon

It has been well documented that cyclopentadienones are an incredibly reactive species of compounds, often requiring a slew of trapping agents in order to slow their reactivity.[112] The utility of tetraphenylcyclopentadienones (**145**) with substituted alkynes has been extensively researched by Müllen and coworkers for the formation of larger planar PAH systems[113] first appearing in literature as early as the mid 1960s. To date, these structures have remained powerful dienes in the synthesis of larger PAHs with Müllen and coworkers first attempting to extend this methodology towards the 8-membered contorted motif of [8]circulene in 1997. Ultimately, they were unable to close the four inner-most carbon bonds of their targeted structure, affording only **147** from **146** (Scheme 4.4).[37] There is little precedence for extending this methodology to less substituted 2,5-diphenylcyclopentadienones and, coupled with their highly reactive nature, this becomes a synthetically-challenging task. Nevertheless, with the results of

[112] (a) Gaviña, F.; Costero, A. M.; Gil, P.; Luis, S. V. *J. Am. Chem. Soc*. **1984,** *106,* 2077–2080; (b) Gaviña, F.; Costero, A. M.; Gil, P.; Palazon, B.; Luis, S. V. *J. Am. Chem. Soc*. **1981,** *103***,** 1797–1798.
[113] (a) Simpson, S. D.; Brand, J. D.; Berresheim, A. J.; Przybilla, L.; Rader, H. J.; Müllen, K. *Chem. Eur. J.* **2002**, *8*, 1424–1429; (b) Wu, J.; Tomovic, Z.; Enkelmann, V.; Müllen, K. *J. Am. Chem. Soc.* **2004**, *69*, 5179–5186.

Müllen's work in mind, we envisioned two routes towards this desired contorted structure.
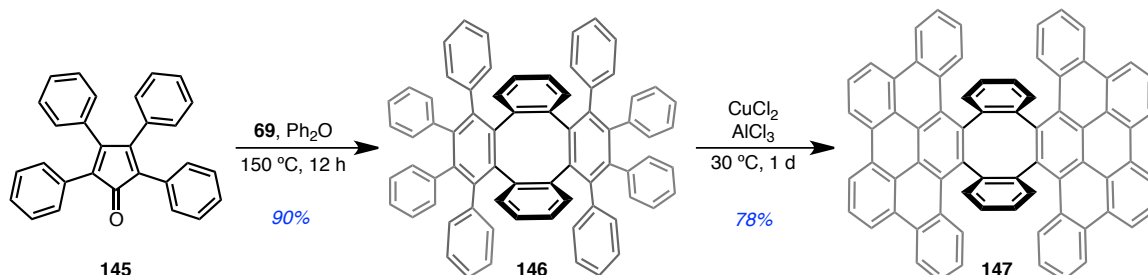
Scheme 4.4 Müllen's attempted synthesis of the 8-membered contorted motif of [8]circulene stopping short at **147** from tetraphenylcyclopentadienone (**145**).

We first sought to exploit the palladium-catalyzed arylation reaction originally established for the synthesis of TB[8]C to carry out the final bond forming steps towards the expanded [8]circulene structure. Alternatively, we envisioned that the oxidative cyclodehydrogenation reaction successfully utilized in our revised synthesis of TB[8]C would be capable of establishing the desired bond formation. To our knowledge, functionalization of tetraphenylcyclopentadienones following formation of the cyclopentadienone ring has not been reported in literature, however, a variant of 2,5-bis(chlorophenyl)-cyclopentadienone (**151**) was successfully synthesized by Shapiro and Becker (Scheme 4.5).[114] Reacting benzil (**148**) and dibenzyl ketone **149** in EtOH, followed by the addition of catalytic base, afforded the desired cyclopentadienone in 85% yield.

---

[114] Shapiro, E. L.; Becker, E. I. *J. Am. Chem. Soc.* **1953**, *75*, 4769–4775.
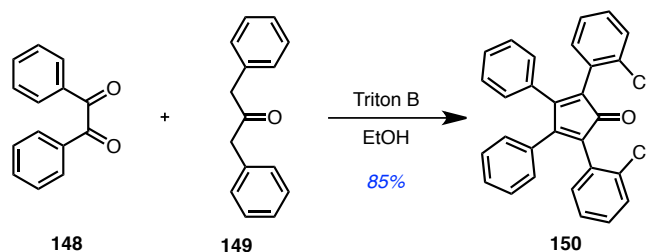
Scheme 4.5 The synthesis of 2,5-bis(chlorophenyl)-cyclopentadienone (**148**) developed by Sapiro and Becker in 1953. Triton B = benzyltrimethylammonium hydroxide.

Much to our surprise, we found that **148** was almost completely unreactive with **69** and we were unable to afford isolatable quantities of the desired Diels-Alder adduct **151** – even under forcing conditions (ca. 210 ºC) – and predominantly decomposition of the cyclic diyne **69** was observed (Scheme 4.6).
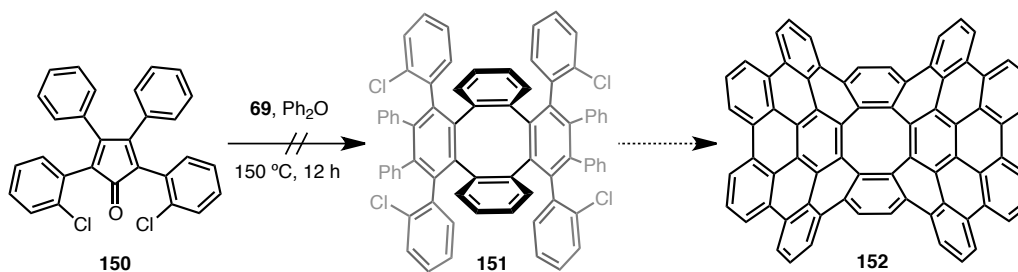
Scheme 4.6 Attempted Diels-Alder cycloaddition of **151** from 2,5-bis(chlorophenyl)-cyclopentadienone (**150**) and subsequent bond forming steps towards **152**.

While we were able to reproduce the unsubstituted [4 + 2] cycloaddition between **145** and **69** reported by Müllen and co-workers, we found that the DDQ and CF_3SO_3H conditions utilized in our revised synthesis were also incapable of affording the desired expanded [8]circulene structure **152**, affording **147** in yields comparable to those reported

by Müllen and co-workers. We suspect that the resulting strain induced by the planarization of the tribenzopentaphene substituents of the tetraphenylene structure is too great to overcome in the subsequent bond formation step.

Given the synthetic challenges presented by these final bond closures on synthetic precursors bearing π-expanded substituents, we were interested in investigating the effect that similarly contorted and smaller π-systems would have on the overall performance of the oxidative cyclodehydrogenation reaction. Accordingly, we determined that 1,3-diphenylisobenzofurans, highly reactive Diels-Alder dienes,[115] would be ideal candidates for continued studies into the nature of the oxidative cyclodehydrogenation reaction on more forcibly-planarized structures. These structures would introduce only two new benzo-substituents to our already established TB[8]C structure, forming a new hexabenzo[8]circulene molecule (**153**, Scheme 4.7).
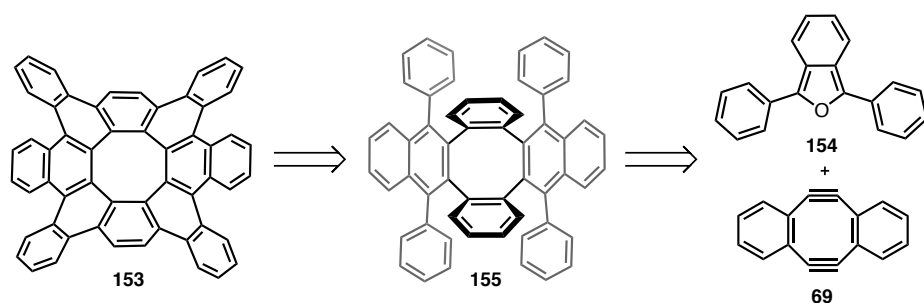
Scheme 4.7 Retrosynthetic plan for the synthesis of hexabenzo[8]circulene (**153**) from 1,3-diphenylisobenzofuran (**154**).

---

[115] (a) Geibel, K.; Heindl, J. *Tetrahedron. Lett.* **1970**, *11*, 2133–2136; (b) Battiste, M. A.; Sprouse, C. T. *Tetrahedron Lett.* **1970**, *11*, 4661–4664; (c) Cava, M. P.; Narasimhan, K. *J. Org. Chem.* **1970**, *36*, 1419–1423; (d) Binger, P.; Wedemann, P.; Goddard, R.; Brinker, U. H. *J. Org. Chem.* **1996**, *61*, 6462–6464.

Following the retrosynthetic plan, the reaction between isobenzofuran **154** and our diyne **69** proceeded smoothly, affording the desired oxirane (**156,** Scheme 4.6) as two isomers, which were easily separated by column chromatography in a combined 90% yield. Subsequent reduction and aromatization of **156** with titanium tetrachloride[116] afforded the desired dibenzo-tetraphenylene (**155**, Scheme 4.8) in excellent 85% yield without the need for purification.
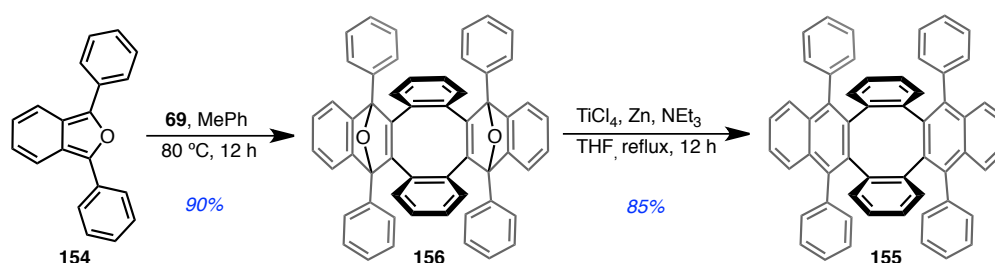
Scheme 4.8 Diels-Alder reaction between **69** and 1,3-diphenylisobenzofuran (**154**) followed by subsequent aromatization of oxirane **156**, affording the desired dibenzotetraphenylene **155**.

The final bond-forming oxidative cyclodehydrogenation of **155** utilizing the DDQ/ CF$_3$SO$_3$H conditions failed to yield the desired hexabenzo[8]circulene (**153**), although, we were able to isolate the product of two C–C bond formations (**157**) in 56% yield (Scheme 4.9). The ^{1}H NMR spectrum of **157** (Figure AI.97), exhibits two broad peaks in the aromatic region centered at δ = 7.15 and 7.01 ppm, indicating hindered rotation between the unbound phenyl rings and the tetraphenylene core.

---

[116] Wong, H. N. C. *Acc. Chem. Res.* **1989**, *22,* 145–152.
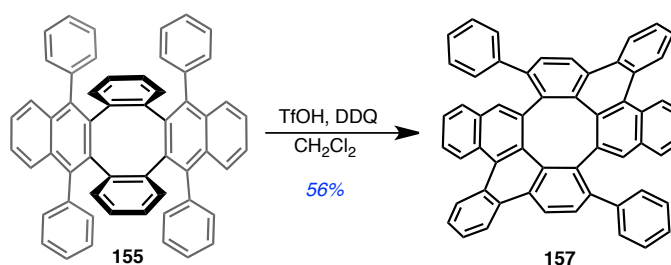
Scheme 4.9 Oxidative cyclodehydrogenation of **155** affording the product of two C–C bond formations (**157**).

Attempts to subject **157** to the DDQ/CF$_3$SO$_3$H reaction conditions, or any of the previously discussed oxidative cyclodehydrogenation conditions, failed to afford **153,** and no further bond formations were observed. Additional attempts to carry out the desired bond formation on **156** prior to aromatization of the tetraphenylene ring also failed to afford the desired product. With these results in mind, it became clear that planarization of the [8]circulene motif had a significant impact on the formation of the internal C–C bonds of the desired structure. Following the report of a C$_{80}$H$_{30}$ warped nanographene sheet from corannulene by Itami and co-workers, we envisioned that expansion of the [8]circulene π-system could be more readily achieved with the core structure intact, starting from our tetrabenzo[8]circulene molecule.

4.4.2 Outward Expansion of the TB[8]C Structural Motif

In accordance with the work detailed by Itami and co-workers, we set our sights on the synthesis of a similarly warped graphene sheet based on the core structure of

TB[8]C (Figure 4.5). Using our established synthesis for **55** and Itami's reported direct arylation reaction[117] as a means of fusing biphenyl substituents to the inner four benzo-rings of our molecules, we envisioned a $C_{96}H_{32}$ contorted nanographene sheet.
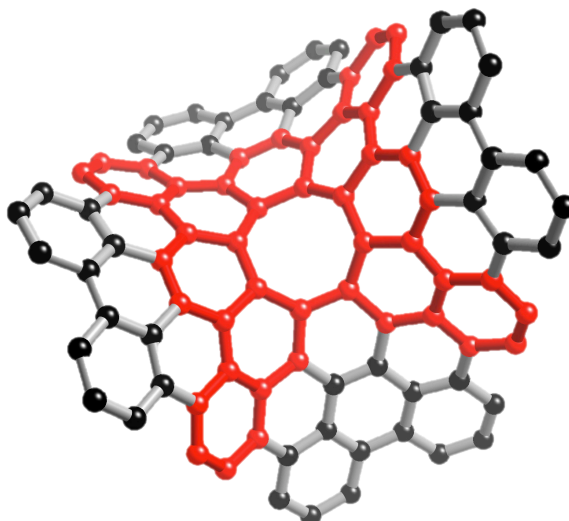
Figure 4.5 Proposed 3-dimensional representation of the $C_{96}H_{32}$ contorted graphene sheet based on the structure of TB[8]C (highlighted in red).

Itami's palladium catalyzed direct arylation importantly relies on the inclusion of K-region character,[118] conveniently displayed in our structure within the inner tetraphenylene benzo-substituents of the molecule. While these rings are predominately aromatic as reported, they are favorably lower in aromatic character than the outermost benzo-substituents, with reported HOMA values of 0.716 and 0.744 for the interior benzo-groups, and 0.880 and 0.965 for the fused benzo-groups in the DFT and experimental structure, respectively. It should be noted that the C–C bond lengths of interest in the DFT structure more closely represent that of traditional benzene at 1.380

---

[117] Mochida, K.; Kawasumi, K.; Segawa, Y.; Itami, K. *J. Am. Chem. Soc.* **2011**, *133*, 10716–10719.
[118] Ozaki, K.; Kawasumi, K.; Shibata, M.; Ito, H.; Itami, K. *Nat. Commun.* **2015**, *6*, 6251.

Å, while this same C–C bond more closely represents the desired K-region double bond character at 1.344 Å in the experimental structure, giving TB[8]C the necessary structural requirements. As such, we subjected **55** to the necessary Pd-catalyzed direct arylation and oxidative cyclodehydrogenation reaction (Scheme 4.10).
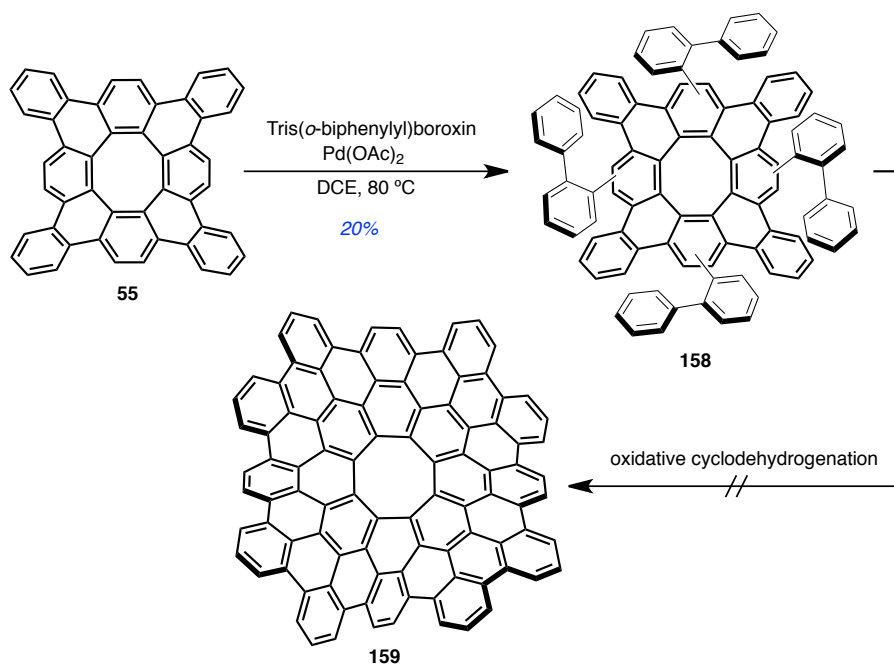
Scheme 4.10 Pd-catalyzed direct arylation of **55** affording regioisomers of **158**, followed by the subsequent oxidative cyclodehydrogenation reaction.

The C–H activation of **55** was carried out in the presence of freshly prepared tris(*o*-biphenylyl)boroxin and Pd(OAc)$_2$, affording a mixture of the desired regioisomers of **158** in 20% yield. Employing the less-aggressive oxidative cyclodehydrogenation reactions (FeCl$_3$ in CH$_2$Cl$_2$, CuCl$_2$ and AlCl$_3$ in CS$_2$ or Cu(OTF)$_2$ and AlCl$_3$ in CS$_2$) failed to afford **159**. In subsequent attempts utilizing, DDQ and CF$_3$SO$_3$H and following the disappearance of the starting material, we were unable to identify the product of 12 C–C

bond closures in our crude reaction mixture. Given the failure of this transformation and the challenging characterization of **158**, we ultimately decided to forgo this methodology.

4.4.3 Concurrent Formation of the Octagon

During the course of our work on these contorted structures, Miao and co-workers reported the elegant synthesis of a C_{96} twisted nanographene sheet based on the core structure of TB[8]C (Figure 4.6).[119] Their methodology takes advantage of an inside-out approach to construct the framework of the contorted structure. Their report describes the methodology as an "inward formation of the octagon," however, a seemingly more complex series of bond formations and structural requirements were necessary to arrive at the desired structure.
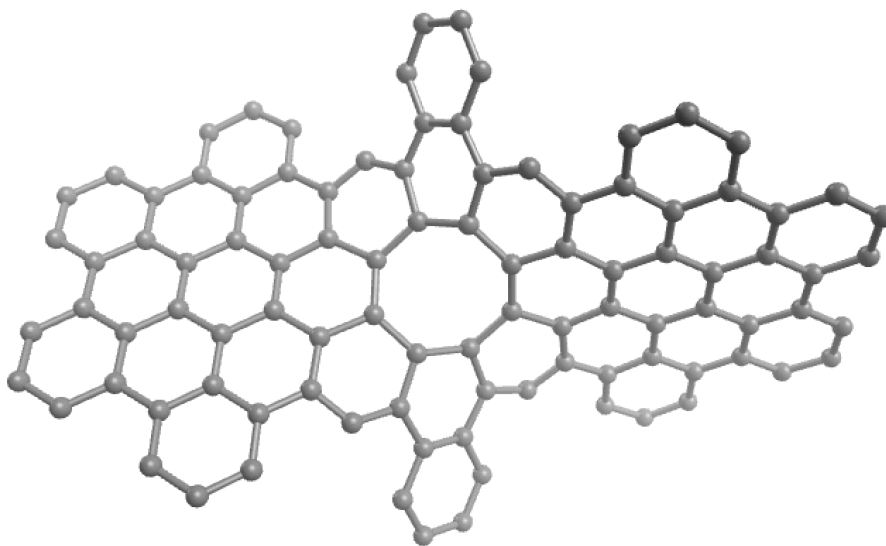
Figure 4.6 Three-Dimensional rendering of the C_{96} twisted graphene sheet developed by Miao and co-workers.

---

[119] Cheung, K. Y.; Chan, C. K.; Liu, Z.; Miao, Q *Angew. Chem.* **2017**, *31*, 9131–9135.

Following their reported synthesis from **160**, Miao and co-workers utilize the oxidative cyclodehydrogenation conditions employed in the synthesis of TB[8]C (Scheme 4.11). From **160**, exposure to DDQ and CF$_3$SO$_3$H affords a mixture of products, namely the desired **161** and major byproducts **162** and **163**. Further subjection of **162** to the oxidative cyclodehydrogenation conditions afforded the desired **161** in 1% yield.
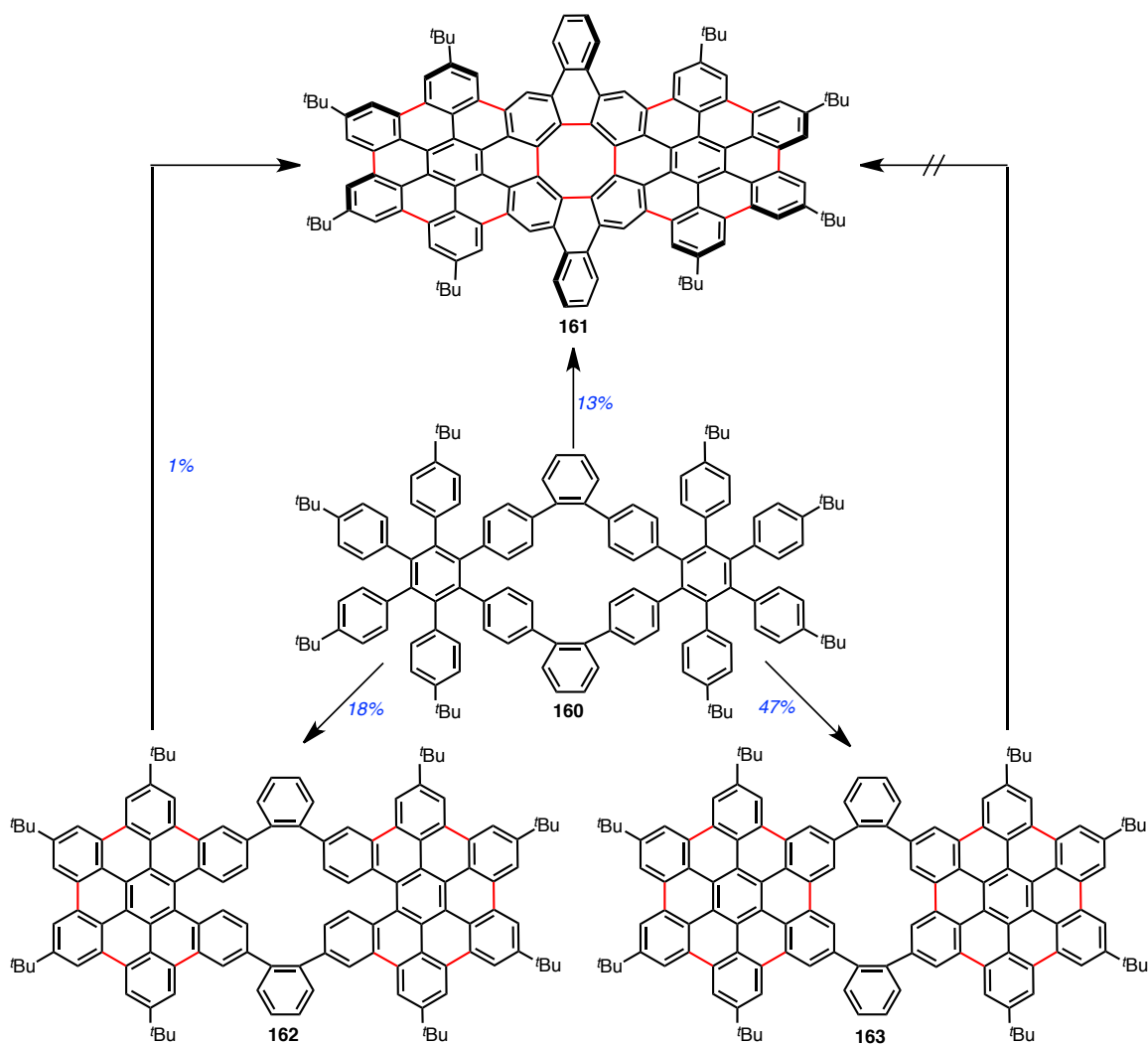
Scheme 4.11 Miao's reported synthesis of **161** from **160** in 13% yield with undesired formation of **163** and intermediate **162**, which can be further subjected to oxidative cyclodehydrogenation to afford the desired twisted nanographene.

The work by Miao and co-workers helped to reaffirm the observations made in our lab following the attempted synthesis of these π-expanded [8]circulenes. While Miao was able to afford the desired C_{96} structure (**161**), it is clear that formation of the internal C–C bonds is, in general, required to occur before or concurrently with the formation of the planar substructure of these targeted molecules. The specific order of these bond-forming reactions is paramount in the success of the desired transformation.

4.5 Future Work

While the synthesis of larger contorted aromatic systems based the on the TB[8]C structure have proven challenging, the results of these investigations in our lab have helped understand the structural requirements for accessing these expanded π-systems. As such, investigations into these structures may be substantially improved though the inclusion of solubility-promoting alkoxy groups. Access to such structures could theoretically be achieved through the synthetic methods outlined in this chapter. Additionally, while the work performed in our lab has established a contextual understanding of the limitations of the oxidative cyclodehydrogenation reaction in regards to the [8]circulene structural motif, a more complete investigation into limitations of similarly contorted PAHs would prove beneficial in establishing a more thorough understanding of these powerful C–C bond-forming reactions.

4.6 Conclusions

In conclusion, we have demonstrated a route to functionalized tetrabenzo[8]circulene derivatives that provides access to substrates containing both electron-rich and electron-poor functional groups. While these functional groups have little effect on the energetics of the frontier molecular orbitals, we envision that the methodology demonstrated herein will provide a foundation for further investigation of the electronic and supramolecular properties inherent to these topologically-unique structures. Furthermore, the investigations into larger structures based on the [8]circulene motif have established new insight into the limitations of the oxidative cyclodehydrogenation reaction, which has proven to be a powerful tool in the synthesis of PAHs.

CHAPTER 5: EXPERIMENTAL PROCEDURES

5.1 Methods and Materials

Anhydrous and anaerobic solvents were obtained from purification columns (Pure Process Technology, Nashua, NH). Commercially available starting materials were purchased from Sigma-Aldrich, Fischer Scientific, Acros Organics, Matrix Chemical or TCI Chemical and used as received. All reactions were run under a nitrogen atmosphere and monitored by thin layer chromatography (TLC) by using silica-gel 60 F_{254} pre-coated plates (Silicycle Inc., Québec, Canada). Air sensitive reactions were run in an inert atmosphere Argon glove box (Vacuum Atmospheres Company, Hawthorne CA). Column chromatography was performed on a CombiFlash® Rf 200 system using RediSep[TM] normal phase silica columns (ISCO, Inc., Lincoln, NE).

^{1}H (500 MHz), ^{13}C (125 MHz), HSQC, and HMBC NMR spectra were recorded on a Bruker Ascend 500 MHz spectrometer at rt; peaks were calibrated against an internal TMS standard. Data is reported as follows: chemical shift, multiplicity (s = singlet, d = doublet, t = triplet, q = quartet, m = multiplet), coupling constants (Hz), and number of protons. High-resolution mass spectra were recorded on a Waters corp. Xevo G2-XS LCMS QTOF mass spectrometer with a Waters corp. NanoAcquity UPLC (Waters Corp., Milford, MA). Low-resolution mass spectra were recorded on a Bruker Daltonics UltrafleXtreme MALDI-TOF-MS or Waters Micromass 70-VSE EI/CI/FD/FI mass spectrometer.

Electrochemical potentials were obtained on a PAR model 273 potentiostat (Princeton Applied Research, Oak Ridge, TN) interfaced to a computer using in-house software. UV-Vis spectra were obtained on a Shimadzu UV-2450 spectrophotometer (Shimadzu, Kyoto, Japan). Melting points were obtained on a Mel-Temp apparatus and are uncorrected.

5.2 Experimental procedures for SYNTHESIS, STRUCTURAL DATA, AND FUNCTIONALIZATION OF TETRABENZO[8[CIRCULENE
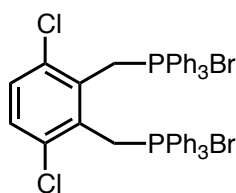
64

1,2-Bis(methyltriphenylphosphonium)-3,6-dichlorophenyl dibromide (64): A 50 mL round bottom flask equipped with a stir bar, reflux condenser, and *p*-xylene (20 mL) charged with **63** (1.00 g, 3.01 mmol, 1 eq) and triphenylphosphine (1.73 g, 6.61 mmol, 2.2 eq) was refluxed at 145 ºC for 2 d. The resulting white solid was filtered from the reaction mixture and dried under reduced pressure affording pure **64** (2.58 g, 80 %). TLC (ethyl acetate, 2:3 v/v) R_f = 0.15. ^{1}H NMR (500 Mhz, CDCl$_3$) δ = 8.02 (m, 12H), 7.71 (m, 6H), 7.64 (m, 12H), 6.86 (s, 2H), 5.29 (s, 2H), 5.26 ppm (s, 2H); ^{13}C NMR (125 MHz, CDCl$_3$) δ = 134.9, 134.4, 134.3, 130.54, 130.49, 130.42, 118.1, 117.4, 31.6, 31.2 ppm.
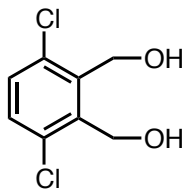
65

(3,6-Dichloro-1,2-phenylene)dimethanol (65): A 250 mL round bottom flask equipped with a stir bar and a reflux condenser was charged with a mixture of Dioxane (200 mL), DI H_2O (100 mL), 2,3-bis(bromomethyl)-1,4-dichlorobenzene (5.00 g, 14.93 mmol, 1 eq), and $CaCO_3$ (7.53 g, 74.65 mmol, 5 eq). The reaction mixture was stirred and refluxed at 120 ºC for 2 d. Solvent was removed under reduced pressure and the remaining aqueous slurry was quenched with 6 M HCl yielding a white solid that was easily separated and dried under reduced pressure to afford pure **65** (2.24 g, 85%). TLC (ethyl acetate) R_f = 0.30. ^{1}H NMR (500 Mhz, CDCl$_3$) δ = 7.32 (s, 2H), 4.97 (s, 4H), 2.76 ppm (s, 2H); ^{13}C NMR (125 MHz, CDCl$_3$) δ = 139.1, 133.5, 130.4, 60.2 ppm.

87
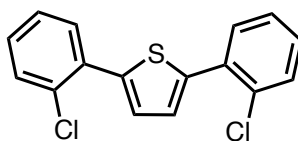
2,5-Bis(2-chlorophenyl)thiophene (87) via 86: A 50 mL round bottom flask equipped with a stir bar and reflux condenser was charged with **86** (1.00 g, 4.64 mmol, 1 eq), CuI (0.13 g, 0.69 mmol, 15 mol %), 1,10-phenanthroline (0.17 g, 0.93 mmol, 20 mol %), and $Na_2S \cdot 9H_2O$ (5.57 g, 23.20 mmol, 5 eq) in DMF (20 mL). The reaction mixture was stirred vigorously at 80 ºC for 12 h. The resulting suspension was filtered and dried under reduced pressure affording pure **87** (0.18 g, 25 %). TLC (SiO$_2$, hexanes) R_f = 0.51. ^{1}H

NMR (500 MHz, CDCl$_3$) δ = 7.60 (dd, J = 7.5, 1.5 Hz, 2H), 7.50 (dd, J = 8.0, 1.5 Hz, 2H), 7.39 (s, 2H), 7.32 (td, J = 6.0, 1.5 Hz, 2H), 7.27 ppm (m, 2H); ^{13}C NMR (125 MHz, CDCl$_3$) δ = 140.9, 132.9, 132.2, 131.3, 130.6, 128.7, 127.7, 127.0 ppm; HRMS ESI [M + 1]: calcd. for C$_{16}$H$_{11}$Cl$_2$S$_1$: 304.9953, found: 304.9953.

88
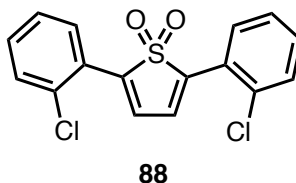
2,5-Bis(2-chlorophenyl)thiophene-dioxide (88): A 10 mL round bottom flask charged with **31** (0.11 g, 0.36 mmol, 1 eq) in CH$_2$Cl$_2$ (5 mL) was cooled to 0 ºC to which meta-chloroperoxybenzoic acid (0.21 g, 1.24 mmol, 3.5 eq) dissolved in CH$_2$Cl$_2$ (5 mL) was added dropwise. The reaction mixture was kept at this temperature for 6 h and quenched with NaHCO$_3$ (20 mL) extracted with CH$_2$Cl$_2$ (3 x 20mL). The combined extracts were dried with MgSO$_4$ and solvent was removed under reduced pressure. The crude product was purified by column chromatography (SiO$_2$, hexanes:CH$_2$Cl$_2$, 1:1 v/v, R_f = 0.20) affording pure **88** (0.04 g, 35%). ^{1}H NMR (500 MHz, CDCl$_3$) δ = 8.06 (d, J = 5 Hz, 2H), 7.54 (d, J = 10Hz, 2H), 7.46 (s, 2H), 7.38 ppm (t, J = 5, 4H); ^{13}C NMR (125 MHz, CDCl$_3$) δ = 137.5, 134.0, 131.2, 131.0, 129.6, 127.3, 126.7, 125.6 ppm. HRMS ESI [M + 1]: calcd. for C$_{16}$H$_{11}$Cl$_2$O$_2$S$_1$: 336.9857, found: 336.9858.

87
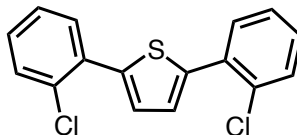
2,5-Bis(2-chlorophenyl)thiophene (87) via 89: In a 250 mL two-necked round bottom flask equipped with a stir bar and reflux condenser a mixture of deionized H_2O (62.5 mL) and THF (125 mL) was degassed by bubbling nitrogen for 15 minutes. 2,5-dibromothiophene **89** (5.00 g, 20.7 mmol, 1eq), 2-chlorophenylboronic acid **90** (6.93 g, 45.5 mmol, 2.2 eq), K_2CO_3 (17.13 g, 124.0 mmol, 6 eq), and $Pd(PPh_3)_4$ (1.19 g, 1.03 mmol, 5 mol %) were added and the reaction mixture was vigorously stirred at reflux over a period of 12 h. The reaction mixture was cooled to room temperature and quenched by the addition of saturated NH_4Cl (aq) (50 mL). The crude reaction mixture was extracted with EtOAc (3 x 30 mL). The combined extracts were dried ($MgSO_4$) and the solvent was removed under reduced pressure. Purification by column chromatography (SiO_2, hexanes, $R_f = 0.51$) afforded pure 2,5-bis(2-chlorophenyl)thiophene **87** (6.27 g, 95%) as a white solid. Spectral characterization is in agreement with our previously reported result.

91
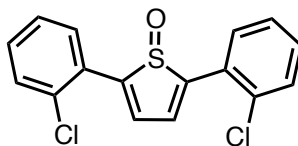
**2,5-Bis(2-chlorophenyl)thiophene-1-oxide (91):** In a 25 mL round bottom flask equipped with a stir bar, **87** (5.31 g, 17.39 mmol) was added to a solution of CF_3CO_2H (20 mL) and CH_2Cl_2 (40 mL). The mixture was cooled to 0 ºC in an ice/water bath and a

30% H$_2$O$_2$ (7.89 g, 69.6 mmol) solution was added dropwise over a period of 5 minutes. The temperature was maintained at 0 ºC for 3 h before the reaction was quenched by the addition of sat. NaHCO$_3$ (aq) (100 mL). The crude reaction mixture was extracted with CH$_2$Cl$_2$ (4 x 25 mL), the combined extracts were dried (MgSO$_4$) and solvent was removed under reduced pressure. Purification of the crude material by column chromatography (SiO$_2$, hexanes:CH$_2$Cl$_2$, 1:1 v/v, R_f = 0.22) afforded pure **91** (1.43 g, 26%) as a yellow solid. ^{1}H NMR (500 MHz, CDCl3) δ = 7.78 (dd, J = 7.0, 1.5 Hz, 2H), 7.53 (dd, J = 6.5, 0.5 Hz, 2H), 7.37 (m, 4H), 7.19 ppm (s, 2H); ^{13}C NMR (125 MHz, CDCl$_3$) δ = 150.5, 132.8, 131.5, 130.9, 130.2, 129.2, 128.8, 127.4 ppm; HRMS ESI [M + 1]: calcd. for C$_{16}$H$_{11}$Cl$_2$O$_1$S$_1$: 320.9902, found: 320.9905.


71
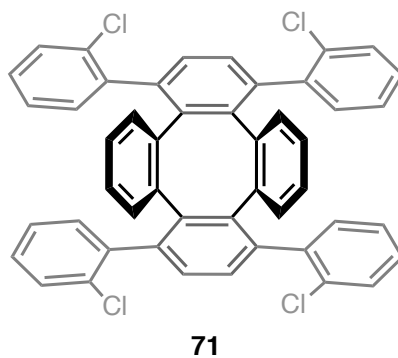
1,4,9,12-Tetrakis(2-chlorophenyl)tetraphenylene (71): In an oven dried two neck 25 mL round bottom flask equipped with a reflux condenser and a stir bar, **91** (1.06 g, 3.29 mmol, 2.2 eq) and dibenzocyclooctyne **69** (300 mg, 1.50 mmol, 1 eq) were dissolved in anhydrous toluene (12 mL) and the reaction mixture was heated at 100 ºC for 16 h. The crude reaction mixture was cooled to room temperature and solvent was removed under reduced pressure. Column chromatography (SiO$_2$, hexanes:CH$_2$Cl$_2$, 4:1 v/v, R_f = 0.26)

afforded pure **71** (161.10 mg, 14%) as an orange-red solid. ^{1}H NMR (500 MHz CD$_2$Cl$_2$) was very complex due to the presence of atropisomers and therefore values are not reported. A ^{1}H spectrum is included as Figure AI.12; HRMS ESI [M + NH$_4$$^+$]: calcd. for C$_{48}H_{32}Cl_4N_1$: 764.1254, found: 764.1254.


55
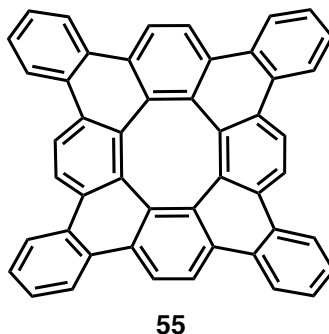
Tetrabenzo[8]circulene (55): In a 10 mL oven-dried microwave tube equipped with a stir bar, **71** (29.64 mg, 0.040 mmol) was dissolved in dimethylacetamide (1.4 mL) and the reaction mixture was degassed by with bubbling nitrogen for 15 min. Subsequently, DBU (304.48 mg, 2.00 mmol 50 eq) and Pd(PCy$_3$)$_2$Cl$_2$ (61.12 mg, 0.083 mmol, 40 mol%) were added and the reaction mixture was heated in a microwave reactor (max 200W) at 210 ºC for 1 h in a sealed microwave vial. After cooling, the reaction mixture was poured into H$_2$O (20 mL), extracted with CH$_2$Cl$_2$ (5 x 10 mL), dried (MgSO$_4$) and the solvent was removed under reduced pressure. Purification of the product by column chromatography (SiO$_2$, hexanes:CH$_2$Cl$_2$, 4:1 v/v, R_f = 0.20) afforded the desired product and a small amount of the remaining palladium catalyst. Careful washing of this material with cold toluene afforded pure **55** (5.76 mg, 24%) as a crystalline yellow solid. ^{1}H NMR (500 MHz, CDCl$_3$) δ = 8.11 (dd, J = 6.0, 3.0 Hz, 8H), 7.68 (s, 8H), 7.57 ppm (dd, J = 6.0 Hz, 3.0 Hz, 8H); ^{1}H NMR (500 Mhz, THF-d_8) δ = 8.16 (dd, J = 6.0, 3.0 Hz, 8H), 7.76 (s,

8H), 7.55 (dd, J = 6.0, 3.0 Hz, 8H). ^{13}C NMR (125 MHz, CDCl$_3$) δ = 134.0, 129.7, 129.4, 127.3, 123.5, 122.9 ppm; ^{13}C NMR (125 MHz, THF-d_8) δ = 134.9, 130.9, 130.6, 128.2, 124.5, 123.9 ppm; HRMS ESI [M+1]: calcd. for C$_{48}$H$_{25}$: 601.1956, found: 601.1907.

93
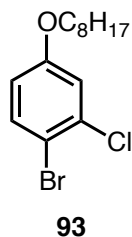
1-Bromo-2-chloro-4-octyloxybenzene (93): In a 25 mL round bottom flask equipped with a stir bar and a reflux condenser and DMF (12 mL) was degassed by bubbling nitrogen for 15 minutes. 4-bromo-3-chlorophenol **92** (1.65 g, 7.95 mmol, 1 eq), 1-bromooctane (1.52 g, 7.87 mmol, 99 mol%), K$_2$CO$_3$ (2.20 g, 15.91 mmol, 2 eq) were added and the reaction mixture was vigorously stirred at 120 ºC for 16 h. The reaction mixture was cooled to room temperature and quenched by the addition of sat. NH$_4$Cl (40 mL) and H$_2$O (60 mL). The crude product was extracted from with EtOAc (3 x 30 mL). The combined extracts were dried (MgSO$_4$) and the solvent was removed under reduced pressure. Purification by column chromatography (SiO$_2$, hexanes, R_f = 0.45) afforded pure 1-bromo-2-chloro-4-octyloxybenzene **93** (2.16 g, 85%) as a clear oil. ^{1}H NMR (500 Mhz, CDCl$_3$) δ = 7.44 (d, J = 9 Hz, 1H), 6.99 (d, J = 3 Hz, 1H), 6.67 (dd, J = 9, 3 Hz, 1H), 3.90 (t, 2H), 1.76 (m, 2H), 1.43 (t, 2H), 1.33- 1.30 (m, 8H), 0.88 ppm (t, 3H); ^{13}C NMR (125 MHz, CDCl$_3$) δ = 158.9, 133.8, 116.4, 114.9, 112.5, 68.6, 31.8, 29.3, 29.2,

29.1, 25.9, 22.7, 14.1 ppm; HRMS ESI [M + 1]: calcd. for $C_{14}H_{21}BrClO$: 319.0464, found: 319.0461.

95
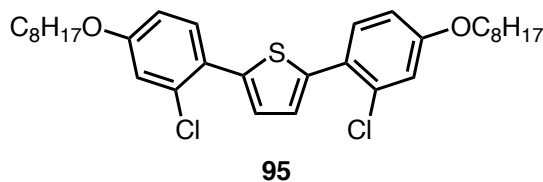
2,5-Bis(2-chloro-4-(octyloxy)phenyl)thiophene (95) via 93: In a flame dried 50 mL round bottom flask THF (25 mL) was charged with **93** (2.00 g, 6.26 mmol, 1 eq) and triisopropyl borate (1.41 g, 7.50 mmol, 1.2 eq). The reaction mixture was cooled to -78 ºC using a dry ice/acetone bath and *n*-BuLi (2.76 mL, 6.88 mmol, 2.5 M, 1.1 eq) was added dropwise to the reaction mixture. The reaction mixture was allowed to warm to rt and was cannula transferred to a 100 mL round bottom flask charged with DI H_2O (10 mL), **89** (0.72 g, 2.98 mmol, 48 mol%), K_2CO_3 (2.60 g, 18.76 mmol, 3 eq), $Pd(PPh_3)_4$ (0.12 g, 0.63 mmol, 2 mol%). The reaction mixture was heated to 95 ºC for 4 h and quenched with NH_4Cl. The crude material was extracted with EtOAc (3 x 80 mL) and dried ($MgSO_4$). Solvent was removed under reduced pressure and the crude product was purified by column chromatography (SiO_4, hexanes, R_f = 0.16) afforded pure **95** (1.33 g, 80%). ^{1}H NMR (500 Mhz, $CDCl_3$) δ = 7.46 (d, J = 8.5 Hz, 2H), 7.25 (s, 2H), 7.00 (d, J = 2.5 Hz, 2H), 6.82 (dd, J = 9, 2.5 Hz, 2H), 3.96 (t, J = 6.5, 4H), 1.78 (t, J = 7.5, 4H), 1.45 (t, J = 7.5, 4H), 1.34-1.29 (m, 16H), 0.89 ppm (t, J = 6.5, 6H); ^{13}C NMR (125 MHz, $CDCl_3$) δ = 159.0, 140.3, 132.8, 131.9, 126.9, 125.3, 116.2, 113.7, 68.5, 31.8, 29.3, 29.2,

29.1, 26.0, 22.7, 14.1 ppm; HRMS ESI [M + 1]: calcd. for $C_{32}H_{43}Cl_2O_2S$: 561.2335, found: 561.2355.

95
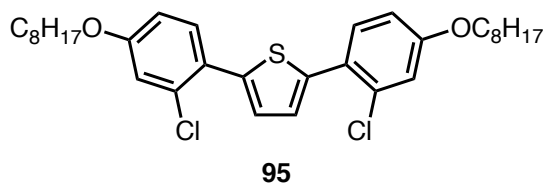
**2,5-Bis(2-chloro-4-(octyloxy)phenyl)thiophene (95) via 102:** A flame-dried 30 mL microwave tube equipped with a stir bar and anhydrous DMF (20 mL) was charged with 2,5- bis(trimethylstannyl)thiophene **53** (1.0 g, 2.44 mmol, 1 eq), 1-bromo-2-chloro-4-(octyloxy)benzene, **44** (1.55 g, 4.88 mmol, 2 eq), and $Pd(PPh_3)_3$ (84.60 mg, 0.07 mmol, 3 mol%). The reaction mixture was heated in a microwave reactor (max 200W) 130 ºC for 2 h in a sealed microwave vial. After cooling, the reaction mixture was washed with H_2O (200 mL) and the resulting suspension was extracted with Et_2O (3 x 80 mL). The combined extracts were dried ($MgSO_4$) and the solvent was removed under reduced pressure. Purification of the crude material by column chromatography (SiO_4, hexanes, R_f = 0.16) afforded the desired 2,5-bis(2-chloro-4-octyloxy)phenyl)thiophene, **95** (0.90 g, 66%) as a white solid. Spectral characterization is in agreement with our previously reported result.

96
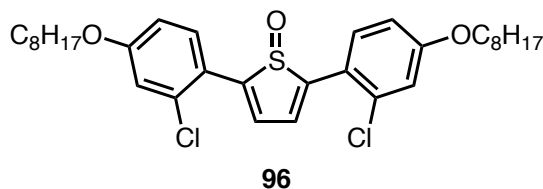
2,5-Bis(2-chloro-4-(octyloxy)phenyl)thiophene-1-oxide (96): In a 100 mL round bottom flask equipped with a stir bar, **95** (1.06g, 1.89 mmol, 1 eq.) was added to a solution of CF_3CO_2H (20 mL) and CH_2Cl_2 (40 mL). The mixture was cooled to 0 ºC in an ice/water bath. A 30 % H_2O_2 (7.59 g, 0.86 mmol) solution was added dropwise over a period of 5 minutes and the temperature was maintained at 0 ºC for 3 h and was quenched by the addition of sat. $NaHCO_3$ (aq) (100 mL). The crude reaction mixture was extracted with CH_2Cl_2 (4 x 30 mL), the combined extracts were dried ($MgSO_4$) and the solvent was removed under reduced pressure. Purification of the crude material by column chromatography (SiO_2, hexanes:CH_2Cl_2, 1:1 v/v, R_f = 0.18) afforded pure **96** (298.0 mg, 28%) as a bright yellow solid. ^{1}H NMR (500 Mhz, CDCl$_3$) δ = 7.69 (d, J = 9 Hz, 2H), 7.07 (s, 2H), 7.02 (d, J = 2.5 Hz, 2H), 6.87 (dd, J = 8.5, 2.5 Hz, 2H), 3.97 (s, 4H), 1.78 (m, 4H), 1.45 (t, 4H), 1.34-1.29 (m, 16H), 0.89 ppm (t, 6H); ^{13}C NMR (125 MHz, CDCl$_3$) δ = 160.1, 149.2, 133.5, 132.0, 127.6, 121.5, 116.9, 113.8, 68.5, 31.8, 29.3, 29.2, 29.1, 26.0, 22.7, 14.1 ppm; HRMS ESI [M + 1]: calcd. for $C_{32}H_{43}Cl_2O_3S$: 577.2304, found: 577.2316.
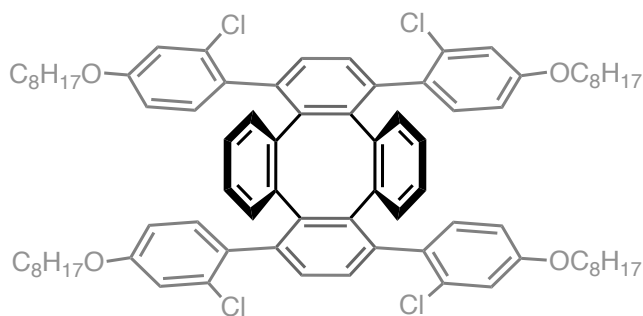
97

1,4,9,12-tetrakis(2-chlorophenyl)tetraphenylene (97): In an oven dried two neck 25 mL round bottom flask equipped with a reflux condenser and a stir bar, **47** (0.60 g, 1.04 mmol, 2.2 eq) and dibenzocyclooctyne **33** (0.09 g, 0.47 mmol, 1 eq) were dissolved in anhydrous 1,2-dichlorobenzene (10 mL) and the reaction mixture was heated at 180 °C for 12 hours. The crude reaction mixture was cooled to room temperature and the solvent was removed by vacuum distillation. Column chromatography (SiO$_2$, hexanes:CH$_2$Cl$_2$, 4:1 v/v, R_f = 0.26) afforded pure **97** (0.08 g, 15 %) as a red solid. ^{1}H NMR (500 MHz CD$_2$Cl$_2$) was very complex due to the presence of atropisomers and therefore values are not reported. HRMS ESI [M + Na$^+$]: calcd. for C$_{80}$H$_{92}$Cl$_4$O$_4$Na: 1281.5640, found: 1281.5643.

98
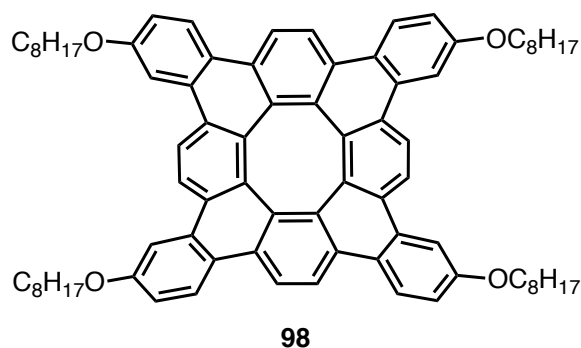
Tetraoctyloxy-tetrabenzo[8]circulene (98): In a 10 mL oven-dried microwave tube equipped with a stir bar, **97** (0.07 g, 0.06 mmol, 1eq) was dissolved in dimethylacetamide (2 mL) and the reaction mixture was degassed by with bubbling nitrogen for 15 min. Subsequently, DBU (0.46 g, 3.01 mmol, 50 eq) and Pd(PCy$_3$)$_2$Cl$_2$ (0.02 g, 0.02mmol, 40 mol%) were added and the reaction mixture was heated in a microwave reactor (max 200W) at 210 °C for 4 h in a sealed microwave vial. After cooling, the reaction mixture was poured into H$_2$O (20 mL), extracted with CH$_2$Cl$_2$ (5x 10 mL), dried (MgSO$_4$) and the solvent was removed under reduced pressure. Purification of the product by column chromatography (SiO$_2$, hexanes: CH$_2$Cl$_2$, 4:1 v/v, R_f = 0.40) afforded the desired product **98** as a red solid (1.0 mg, 10%). ^{1}H NMR (500 Mhz, CDCl$_3$) δ = 7.98 (d, J = 8.5, 4H), 7.56 (s, 4H), 7.55 (s, 4H), 7.45 (d, J = 2 Hz, 4H), 7.15 (dd, J = 9, 2.5 Hz), 4.06 (s, 8H), 1.81 (m, 8H), 1.55–1.45 (m, 9H), 1.36–1.23 (m, 45H), 0.87 ppm (m, 15H); ^{13}C NMR (125 MHz, CDCl$_3$) δ = 158.5, 134.5, 133.2, 130.6, 129.4, 129.3, 124.4, 123.3, 123.0, 117.0, 68.3, 31.8, 29.7, 29.4, 29.3, 29.2, 26.1, 22.7, 14.1 ppm; HRMS ESI [M + 1]: calcd. for C$_{80}$H$_{89}$O$_4$: 1113.6755, found: 1113.6736.
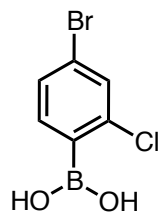
100

(4-Bromo-2-chlorophenyl)boronic acid (100): In a flame dried 100 mL round bottom flask equipped with a stir bar THF (50 mL) and **99** (5.00 g, 15.75 mmol, 1 eq). The reaction mixture was cooled to -78 °C and *n*-BuLi (7.56 mL, 18.90 mmol, 2.5 M, 1.2 eq) was added dropwise to the reaction mixture followed by the dropwise addition of triisopropyl borate (3.55 g, 18.9 mmol, 1.2 eq) after 1 h. The reaction mixture was maintained at -78 °C for an additional 1 h. The desired product was purified via acid/base extraction affording pure **100** (2.87 g, 85%) as a white solid. ^{1}H NMR (500 Mhz, CDCl$_3$) δ = 7.81 (d, *J* = 10, 1H), 7.54 (s, H1), 7.46 (d, *J* = 10, 1H), 5.24 ppm (s, 2H); ^{13}C NMR (125 MHz, CDCl$_3$) δ = 139.5, 138.5, 132.1, 130.2, 126.1, 106.0 ppm.

101
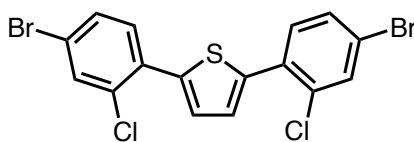
2,5-Bis(4-bromo-2-chlorophenyl)thiophene (101) via 100: In a 100 mL round bottom flask equipped with a stir bar and a reflux condenser a mixture of THF (40 mL) and DI H$_2$O (20 mL) was charged with **100** (1.47 g, 6.10 mmol, 1 eq), **89** (2.87 g, 12.20 mmol, 2 eq), K$_2$CO$_3$ (5.05 g, 36.6 mmol, 6 eq) and Pd(PPh$_3$)$_4$ (352.5 mg, 0.31 mmol, 5 mol%) and

heat to 40 °C for 2 d. The reaction mixture was quenched with NH$_4$Cl and extracted with EtOAc (3 x 60 mL). The combined extracts were dried (MgSO$_4$) and solvent was removed under reduced pressure. Purification of the crude material by column chromatography (SiO$_2$, hexanes, R_f = 0.40) afforded the desired 2,5-bis(4-bromo-2-chlorophenyl)thiophene, **101** (2.23 g, 42%) as a white solid. ^{1}H NMR (500 Mhz, CDCl$_3$) δ = 7.66 (t, J = 1.1 Hz, 2H), 7.44 (d, J = 1.1 Hz, 4H), 7.37 (s, 2H), 7.26 ppm (s, 2H); ^{13}C NMR (125 MHz, CDCl$_3$) δ = 140.1, 133.2, 133.1, 132.1, 131.8, 130.3, 128.0, 121.8 ppm; HRMS ESI [M + 1]: calcd. for C$_{16}$H$_9$Br$_2$Cl$_2$S: 462.8149, found: 462.8166.

101
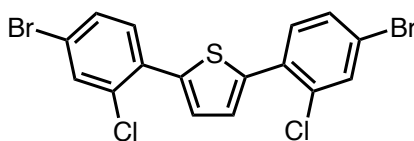
2,5-Bis(4-bromo-2-chlorophenyl)thiophene (101) via 102: A flame-dried 30 mL microwave tube equipped with a stir bar and anhydrous DMF (12 mL) was charged with 2,5-bis(trimethylstannyl)thiophene **102** (1.99 g, 4.84 mmol, 1 eq), 4-bromo-2-chloro-1-iodobenzene (3.07 g, 9.68 mmol, 2 eq), and Pd(PPh$_3$)$_4$ (168.33 mg, 0.15 mmol, 3 mol%). The reaction mixture was heated in a microwave reactor (max 200W) 130 °C for 2 h in a sealed microwave vial. After cooling, the reaction mixture was washed with H$_2$O (200 mL) and the resulting suspension was extracted with Et$_2$O (3 x 60 mL). The combined extracts were dried (MgSO$_4$) and the solvent was removed under reduced pressure. Purification of the crude material by column chromatography (SiO$_2$, hexanes, R_f = 0.42) afforded the desired 2,5-bis(4-bromo-2-chlorophenyl)thiophene, **101** (2.23 g, > 99 %) as

a white solid. Spectral characterization is in agreement with our previously reported result.
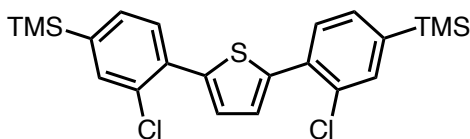
103

2,5-Bis(2-chloro-4-(trimethylsilyl)phenyl)thiophene (103): A flame dried 250 mL round bottom flask equipped with a stir bar and anhydrous THF (120 mL) was charged with **101** (4.49 g, 9.69 mmol, 1 eq.) and cooled to -78 ºC in a dry ice/acetone bath. A solution of *t*-BuLi in pentane (20.40 mL, 1.9 M, 4 eq.) was added dropwise to the reaction mixture over a period of 15 min. The reaction mixture was stirred vigorously and maintained at -78 ºC. At 1 h chlorotrimethylsilane (2.70 mL, 21.32 mmol, 2.2 eq.) was added dropwise and the reaction mixture and maintained for an additional 1 h at -78 ºC before allowing the reaction mixture warm to rt. The reaction was quenched by addition of sat. NH$_4$Cl (aq) (100 mL) and extracted with EtOAc (3 x 100 mL), the combined extracts were dried (MgSO$_4$) and volatiles were removed under reduced pressure affording pure **103** (4.00 g, 92%) as a white solid. ^{1}H NMR (500 Mhz, CDCl$_3$) δ = 7.59 (d, J = 1 Hz, 2H), 7.57 (d, 7.57, J = 7.5 Hz, 2H), 7.42–7.40 (m, 4H) 7.41 ppm (s, 2H); ^{13}C NMR (125 MHz, CDCl$_3$) δ = 142.2, 141.0, 135.3, 133.0, 131.9, 131.7, 130.5, 127.8, -1.3 ppm; HRMS ESI [M + 1]: calcd. for C$_{22}$H$_{27}$Cl$_2$SSi$_2$: 449.0744, found: 449.0722.

104
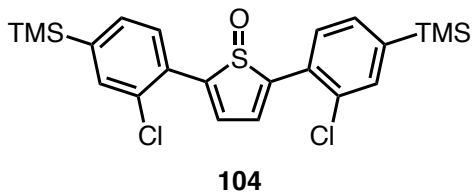
2,5-Bis(2-chloro-4-(trimethylsilyl)phenyl)thiophene-1-oxide (104): In a 100 mL round bottom flask equipped with a stir bar, **103** (1.06 g, 1.89 mmol, 1 eq.) was added to a solution of CF_3CO_2H (20 mL) and CH_2Cl_2 (40 mL). The mixture was cooled to 0 ºC in an ice/water bath and a 30 % H_2O_2 (7.59 g, 0.86 mmol) solution was added dropwise over a period of 5 minutes. The temperature was maintained at 0 ºC for 3 h before the reaction was quenched by the addition of sat. $NaHCO_3$ (aq) (100 mL). The crude reaction mixture was extracted with CH_2Cl_2 (4 x 30 mL), the combined extracts were dried ($MgSO_4$) and the solvent was removed under reduced pressure. Purification of the crude material by column chromatography (SiO_2, hexanes:CH_2Cl_2, 1:4 v/v, R_f = 0.37) afforded pure **104** (298.0 mg, 28%) as a bright yellow solid. ^{1}H NMR (500 Mhz, $CDCl_3$) δ = 7.69 (d, J = 9 Hz, 2H), 7.07 (s, 2H), 7.02 (d, J = 2.5 Hz, 2H), 6.87 (dd, J = 8.5, 2.5 Hz, 2H), 3.97 (s, 4H), 1.78 (m, 4H), 1.45 (t, 4H), 1.34-1.29 (m, 16H), 0.89 ppm (t, 6H); ^{13}C NMR (125 MHz, $CDCl_3$) δ = 160.1, 149.2, 133.5, 132.0, 127.6, 121.5, 116.9, 113.8, 68.5, 31.8, 29.3, 29.2, 29.1, 26.0, 22.7, 14.1 ppm; HRMS ESI [M + 1]: calcd. for $C_{22}H_{27}Cl_2SSi_2O$: 465.0698, found: 465.0703.

105
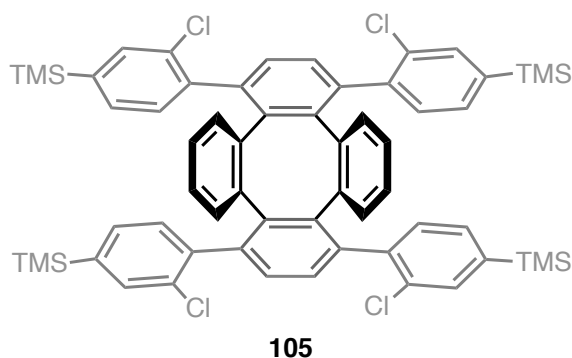
1,4,9,12-Tetrakis(2-chloro-4-(trimethylsilyl)phenyl)tetraphenylene (105): In an flame

dried two neck 10 mL round bottom flask equipped with a reflux condenser and a stir bar,

104 (724.6 mg, 1.56 mmol, 2.2 eq) and dibenzocyclooctyne **69** (141.5 mg, 0.71 mmol, 1

eq.) were dissolved in anhydrous 1,2- dichlorobenzene (5 mL) and the reaction mixture

was heated at 180 ºC for 2 h. The crude reaction mixture was cooled to room temperature

and the solvent was removed under reduced pressure. Column chromatography (SiO$_2$,

hexanes:CHCl, 4:1 v/v, R_f = 0.28) afforded pure **105** (113.0 mg, 15%) as a dark red solid.

^{1}H NMR (500 MHz CD$_2$Cl$_2$) was very complex due to the presence of atropisomers and

therefore values are not reported; HRMS ESI [M + 1]: calcd. for C$_{60}$H$_{60}$Cl$_4$Si$_4$Na:

1057.2410, found: 1057.2434.

106
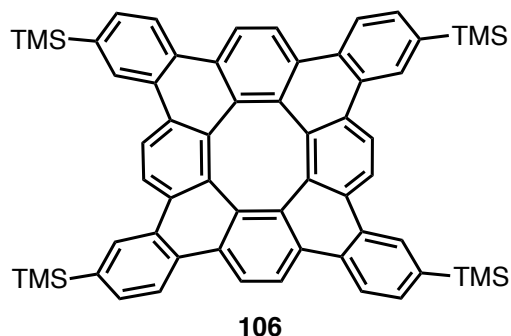
Tetra(trimethylsilyl)-tetrabenzo[8]circulene (106): In a 10 mL oven-dried microwave tube equipped with a stir bar, **105** (113.0 mg, 0.11 mmol, 1 eq) was dissolved in dimethylacetamide (3 mL) and the reaction mixture was degassed by with bubbling nitrogen for 15 min. Subsequently, DBU (830.8 mg, 5.45 mmol, 50 eq) and $Pd(PCy_3)_2Cl_2$ (32.2 mg, 0.04 mmol, 40 mol%) were added and the reaction mixture was heated in a microwave reactor (max 200W) at 210 ºC for 4 h and in a sealed microwave vial. After cooling, the reaction mixture was poured into H_2O (20 mL), extracted with CH_2Cl_2 (5x 10 mL), dried ($MgSO_4$) and the solvent was removed under reduced pressure. Purification of the product by column chromatography (SiO_2, 4:1 hexanes: CH_2Cl_2, R_f = 0.30) afforded the desired product **106** (10.03 mg, 10%) as a crystalline red solid. ^1H NMR (500 Mhz, $CDCl_3$) δ = 8.23 (s, 4H), 8.06 (d, J = 8 Hz, 4H), 7.71 (s, 4H), 7.70 (m, 12H), 0.33 ppm (s, 36H); ^{13}C NMR (125 MHz, $CDCl_3$) δ = 139.4, 134.2, 134.0, 131.8, 129.8, 129.6, 129.6, 128.6, 128.0, 123.4, 123.3, 121.9, -1.02 ppm; HRMS ESI [M + 1]: calcd. for $C_{60}H_{57}Si_4$: 889.3532, found: 889.3544.

107
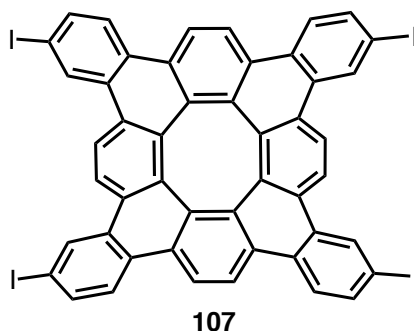
Tetraiodo-tetrabenzo[8]circulene (107): In a flame dried 10 mL round bottom flask equipped with a stir bar was charged with **106** (5.0 mg, 0.005 mmol, 1 eq) in CH_2Cl_2 (5 mL) ICl (4.28 mg, 0.026 mmol, 5 eq) was added. The reaction mixture was stirred for 2 h and quenched with a solution of sodium thiosulfate (10 mL). The crude product was extracted with CH_2Cl_2 (3 x 10 mL) and the combined extracts were dried ($MgSO_4$). Solvent was removed under reduced pressure affording **107** as a red solid that could be used without further purification (6.1 mg, 99%). ^{1}H NMR (500 Mhz, $CDCl_3$) δ = 8.49 (d, J = 1 Hz, 4H), 7.88 (m, 12H), 5.99 ppm (d, J = 2 Hz, 4H).

109
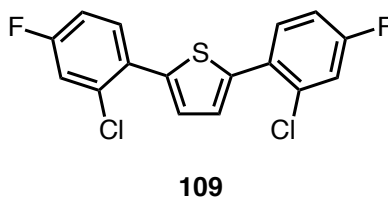
2,5-Bis(2-chloro-4-fluorophenyl)thiophene (109): A flame-dried 30 mL microwave tube equipped with a stir bar and anhydrous DMF (20 mL) was charged with 2,5-bis(trimethylstannyl)thiophene **102** (3.0 g, 7.32 mmol, 1 eq), 2-chloro-4-fluoro-1-iodobenzene **108** (3.75 g, 14.65 mmol, 2 eq), and Pd(PPh$_3$)$_4$ (254.22 mg, 0.22 mmol, 3 mol %). The reaction mixture was heated in a microwave reactor (max 200W) 130 ºC for

2 h in a sealed microwave vial. After cooling, the reaction mixture was washed with H_2O (200 mL) and the resulting suspension was extracted with Et_2O (3 x 80 mL). The combined extracts were dried ($MgSO_4$) and the solvent was removed under reduced pressure. Purification of the crude material by column chromatography (SiO_2, hexanes, R_f = 0.49) afforded the desired 2,5-bis(2-chloro-4-florophenyl)thiophene, **109** (2.49 g, 98%) as a white solid. ^{1}H NMR (500 Mhz, CD_2Cl_2) δ = 7.57 (dd, J = 8.5, 6 Hz, 2H), 7.32 (s, 2H), 7.27 (dd, J = 8.5, 2.5 Hz, 2H), 7.08 ppm (td, J = 8.5, 2.5 Hz, 2H); ^{13}C NMR (125 MHz, CD_2Cl_2) δ = 163.5, 161.5 140.5, 133.7, 133.6, 133.13, 133.06, 129.8, 128.4, 118.4, 118.2, 115.1, 114.9 ppm; HRMS ESI [M + 1]: calcd. for $C_{16}H_9Cl_2F_2S$: 339.9692, found: 339.9710.
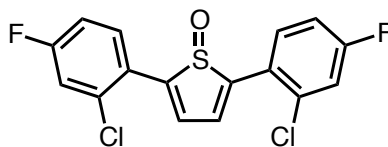
110

2,5-Bis(2-chloro-4-fluorophenyl)thiophene-1-oxide (110): In a 25 mL round bottom flask equipped with a stir bar, **109** (304.9 mg , 0.90 mmol) was added to a solution of CF_3CO_2H (5 mL) and CH_2Cl_2 (10 mL). The mixture was cooled to 0 ºC in an ice/water bath and a 30 % H_2O_2 (0.41 g, 3.58 mmol) solution was added dropwise over a period of 5 minutes. The temperature was maintained at 0 ºC for 3 h 30 minutes before the reaction was quenched by the addition of sat. $NaHCO_3$ (aq) (100 mL). The crude reaction mixture was extracted with CH_2Cl_2 (4 x 15 mL), the combined extracts were dried ($MgSO_4$) and the solvent was removed under reduced pressure. Purification of the crude material by

column chromatography (SiO$_2$, hexanes:CH$_2$Cl$_2$, 1:4 v/v, R_f = 0.30) afforded pure **110** (89.0 mg, 28%) as a bright yellow solid. ^{1}H NMR (500 Mhz, CDCl$_3$) δ = 7.77 (dd, J = 8.5, 6 Hz, 2H), 7.28 (dd, J = 8.5, 2.5 Hz, 2H), 7.13 (s, 2H), 7.11 ppm (m, 2H); ^{13}C NMR (125 MHz, CDCl$_3$) δ = 163.6, 161.6, 149.3, 134.0, 133.9, 132.64, 132.56, 128.73, 128.71, 125.44, 125.41, 118.5, 118.3, 115.0, 114.8 ppm; HRMS ESI [M + 1]: calcd. for C$_{16}$H$_9$Cl$_2$F$_2$OS: 356.9713, found: 356.9730.

111
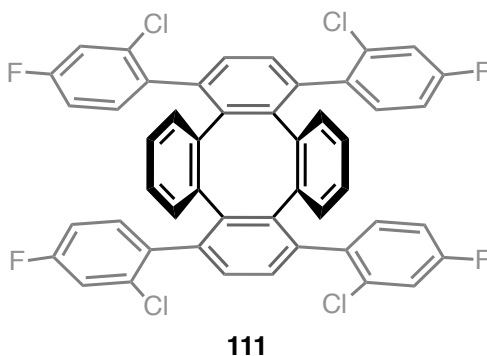
1,4,9,12-Tetrakis(2-chloro-4-fluorophenyl)tetraphenylene (111): In an oven dried two neck 25 mL round bottom flask equipped with a reflux condenser and a stir bar, **110** (304.0 mg, 0.85 mmol, 2.2 eq) and dibenzocyclooctyne **69** (77.7, 0.39 mmol) were dissolved in anhydrous toluene (5 mL) and the reaction mixture was heated at 100 ºC for 2 h. The crude reaction mixture was cooled to room temperature and the solvent was removed under reduced pressure. Column chromatography (SiO$_2$, hexanes:CH$_2$Cl$_2$, 4:1 v/v, R_f = 0.38) afforded pure **111** (30.0 mg, 10%) as a red solid. H NMR (500 MHz CD$_2$Cl$_2$) was very complex due to the presence of atropisomers and therefore values are not reported.

112
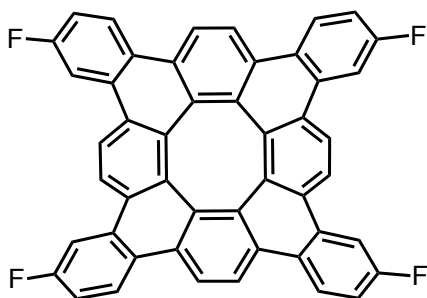
Tetra(fluoro)-tetrabenzo[8]circulene (112): In a 10 mL oven-dried microwave tube equipped with a stir bar, **111** (29.6 mg, 0.036 mmol, 1 eq) was dissolved in dimethylacetamide (2.0 mL) and the reaction mixture was degassed by with bubbling nitrogen for 15 min. Subsequently, DBU (275.3 mg, 1.81 mmol, 50 eq) and $Pd(PCy_3)_2Cl_2$ (10.70 mg, 0.014 mmol, 40 mol%) were added and the reaction mixture was heated in a microwave reactor (max 200W) at 210 ºC for 4 h in a sealed microwave vial. After cooling, the reaction mixture was poured into H_2O (20 mL), extracted with CH_2Cl_2 (5x 10 mL), dried ($MgSO_4$) and the solvent was removed under reduced pressure. Purification of the product by column chromatography (SiO_2, hexanes:CH_2Cl_2, 4:1 v/v, R_f = 0.40) afforded the desired product **112** (3.10 mg, 12%) as a crystalline yellow solid. ^{1}H NMR (500 MHz, $CDCl_3$) δ = 8.11 (m, 4H), 7.77 (dd, J = 10.0, 2.5 Hz, 4H), 7.65 (s, 4H), 7.63 (s, 4H), 7.33 ppm (td, J = 9.0, 2.5 Hz, 4H); ^{13}C NMR (125 MHz, $CDCl_3$) δ = 162.3 (d, J = 245.0), 134.5, 133.6, 130.6, 129.5, 129.4, 125.9, 125.3 (d, J = 7.5 Hz), 123.7, 123.6, 116.0 (d, J = 22.5 Hz), 108.5 ppm (d, J = 22.5 Hz); HRMS and accurate CHN analysis were attempted, however, the molecular ion was not observed and accurate CHN was unable to be obtained.

5.3 Experimental procedures for A ONE-POT METHOD FOR THE

PREPERATION OF 2,5-DIARYLTHIOPHENE-1-OXIDES FROM

ARYLACETYLENES

General procedure for the preparation of 2,5-diarylthiophene-1-oxides: A flame-dried 25 mL round-bottom flask equipped with a stir bar was charged with Cp_2ZrCl_2 (584 mg, 2.0 mmol) in anhydrous THF (10 mL) and cooled to -78 ºC in a dry-ice/acetone bath. *n*-BuLi (2.5 M in hexanes, 4.0 mmol, 1.58 mL) was added dropwise and the mixture was allowed to stir for 20 min after which the cold bath was removed and the reaction was allowed to warm to rt. After 1 h the solution developed a dark red color. The reaction mixture was then cooled to 0 ºC, arylacetylene (4.0 mmol) was added dropwise, and the reaction was allowed to warm to rt over the course of 3 h. The crude mixture was then cooled back down to -78 ºC and thionyl chloride (237.9 mg, 2.0 mmol, 0.15 mL) was added dropwise. After 30 min the cold reaction mixture was poured onto a plug of silica (80 g) pre-packed with hexanes. 100 mL of hexanes was passed over the crude material and the resulting clear eluent was discarded. Addition of a more polar solvent (CH_2Cl_2 or EtOAc; subject to the polarity of the desired substrate) eluted the desired product, which was detected by the presence of a characteristic bright yellow band. Solvent was removed under reduced pressure affording the desired product as a yellow solid. Analytically pure material could be achieved through further column chromatography. Thionyl chloride was purified from elemental sulfur by distillation as previously reported.[120] Acetylenes

---

[120] Cottle; D. L. *J. Am. Chem. Soc.* **1946**, *68*, 1380–1381.

4-ethynyltoluene (**1b**), [121] 4-ethynylanisole (**1c**),[121] 3-ethynylanisole (**1d**), [122] 3,4-dimethoxyphenylacetylene (**1e**), [123] 4-fluorophenylacetylene (**1f**),[121] 4-nitrophenylacetylene (**1g**),[122] 2-chlorophenylacetylene (**1h**),[124] 4-bromophenylacetylene (**1i**),[122] 2-ethynylthiophene (**1j**)[125] were synthesized in accordance with the reported literature.

[2,2':5',2''-terthiophene]-1'-oxide (133) was prepared by bubbling a steady stream of SO_2 through the reaction mixture at -78 ºC in place of thionyl chloride.
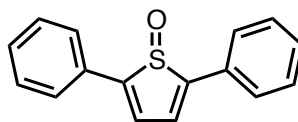
116

2,5-diphenylthiophene-1-oxide (116): Yellow solid (151.3 mg, 30%). TLC (CH_2Cl_2) R_f = 0.20; elute solution (CH_2Cl_2). ^1H NMR (500 MHz, $CDCl_3$) δ = 7.78 (d, J = 8.5 Hz, 4H), 7.48 (t, J = 8.5 Hz, 4H), 7.42 (t, J = 8.5 Hz, 2H), 6.97 ppm (s, 2H); ^{13}C NMR (125 MHz, $CDCl_3$) δ = 152.2, 130.8, 129.3, 129.2, 126.6, 123.6 ppm; HRMS ESI [M + 1] calcd for $C_{16}H_{13}O_1S_1$: 253.0687; found: 253.0694.

[121] Sugimoto, K.; Hayashi, R.; Nemoto, H.; Toyooka, N.; Matsuya, Y. *Org. Lett.* **2012**, *14*, 3510–3213.
[122] Ueda, H.; Yamaguchi, M.; Kameya, H.; Sugimoto, K.; Tokuyama, H. *Org Lett.* **2014**, *16*, 4948–4951.
[123] Abrams, M. L.; Foarta, F.; Landis, C. R. *J. Am. Chem. Soc.* **2014**, *136*, 14583–14588.
[124] Nepveu, F.; Kim, S.; Boyer, J.; Chatrian, O.; Ibrahim, H.; Reybier, K.; Monje, M.,-C.; Chevalley, S.; Perio, P.; Lajoie, B. H.; Bouajila, J.; Deharo, E.; Sauvain, M.; Tahari, R.; Basoci, L.; Pantaleo, A.; Turini, F.; Arese, P.; Valentin, A.; Thompson, E.; Vivas, L.; Petit, S.; Nallet, J.-P. *J. Med. Chem.* **2010**, *53* 699–714.
[125] Carpita, A.; Rossi, R.; Veracint, C. A. *Tetrahedron* **1985**, *41*, 1919–1929.
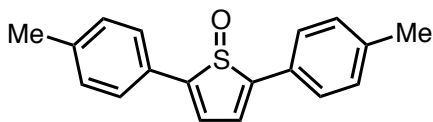
118

2,5-di-*p*-tolylthiophene-1-oxide (118): Yellow solid (168.0 mg, 30%). TLC (CH$_2$Cl$_2$) R_f = 0.18; elute solution (CH$_2$Cl$_2$). ^{1}H NMR (400 MHz, CDCl$_3$) δ = 7.63 (d, J = 10 Hz, 4H), 7.25 (m, 4H), 6.88 (s, 2H), 2.39 ppm (s, 6H); ^{13}C NMR (125 MHz, CDCl$_3$) δ = 151.7, 139.4, 129.9, 128.2, 126.5, 122.9, 21.4 ppm; HRMS ESI [M + 1] calcd for C$_{18}$H$_{17}$O$_1$S$_1$: 281.1000; found: 281.1006.
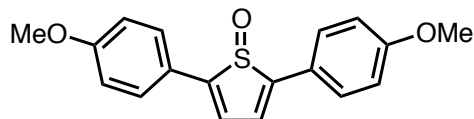
120

2,5-bis(4-methoxyphenyl)thiophene-1-oxide (120): Yellow solid (184.5 mg, 29%). TLC (hexanes:ethyl acetate, 2:3 v/v) R_f = 0.30; elute solution (hexanes:ethyl acetate, 1:1 v/v). ^{1}H NMR (500 MHz, CDCl$_3$) δ = 7.68 (d, J = 9 Hz, 4H), 6.98 (d, J = 9 Hz 4H), 6.79 (s, 2H), 3.85 ppm (s 6H); ^{13}C NMR (125 MHz, CDCl$_3$) δ = 160.4, 150.6, 127.9, 123.8, 122.0, 114.7, 55.4 ppm; HRMS ESI [M + 1] calcd for C$_{18}$H$_{17}$O$_3$S$_1$: 313.0898; found: 313.0908.
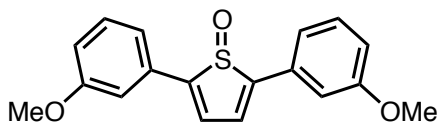
122

2,5-bis(3-methoxyphenyl)thiophene-1-oxide (122): Yellow solid (173.2 mg, 28%). TLC (hexanes:ethyl acetate, 2:3 v/v) R_f = 0.37; elute solution (hexanes:ethyl acetate, 1:1 v/v). ^{1}H NMR (500 MHz, CDCl$_3$) δ = 7.38–7.32 (m, 4H), 7.26 (m, 2H), 6.94 (m, 4H), 3.86 ppm (s, 6H); ^{13}C NMR (125 MHz, CDCl$_3$) δ = 160.1, 152.1, 132.0, 130.2, 123.9, 119.3, 115.3, 111.8, 55.4 ppm; HRMS ESI [M + 1] calcd for C$_{18}$H$_{17}$O$_3$S$_1$: 313.0898; found: 313.0904.
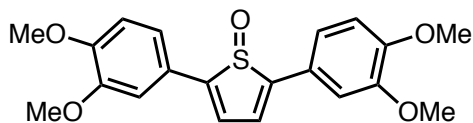
124

2,5-bis(3,4-dimethoxyphenyl)thiophene-1-oxide (124): Yellow solid (238.3 mg, 32%). TLC (hexanes:ethyl acetate, 1:3 v/v) R_f = 0.20; elute solution (hexanes:ethyl acetate, 1:9 v/v). ^{1}H NMR (500 MHz, CDCl$_3$) δ = 7.35 (dd, J = 8.5, 2 Hz, 2H), 7.25 (m, 2H), 6.93 (d, 8.5 Hz, 2H), 6.84 (s, 2H), 3.97 (s, 6H), 3.95 ppm (s, 6H); ^{13}C NMR (125 MHz, CDCl$_3$) δ = 150.8, 150.2, 149.4, 124.0, 122.2, 119.8, 111.6, 109.2, 56.03, 56.02 ppm; HRMS ESI [M + 1] calcd for C$_{20}$H$_{21}$O$_5$S$_1$: 373.1110; found: 373.1117.
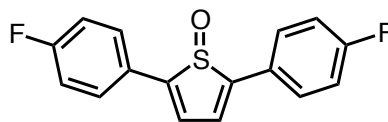
126

2,5-bis(4-fluorophenyl)thiophene-1-oxide (126): Yellow solid (132.2 mg, 23%). TLC (CH$_2$Cl$_2$) R_f = 0.28; elute solution (CH$_2$Cl$_2$). ^{1}H NMR (500 MHz, CDCl$_3$) δ = 7.72 (m. 4H), 7.15 (m, 4H), 6.88 ppm (s, 2H); ^{13}C NMR (125.77 MHz, CDCl$_3$) δ = 163.3 (d, J = 250.3 Hz), 150.9, 128.7 (d, J = 8.8 Hz), 127.0 (d, 3.8 Hz), 123.4, 116.4 ppm (d, 22.6 Hz); HRMS ESI [M + 1] calcd for C$_{16}$H$_{11}$O$_1$S$_1$: 289.0499; found: 289.0508.

91
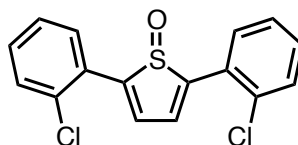
2,5-bis(2-chlorophenyl)thiophene-1-oxide (91): Yellow solid (170.1 mg, 27%). TLC (CH$_2$Cl$_2$) R_f = 0.31; elute solution (CH$_2$Cl$_2$). Spectral characterization is in agreement with our previously reported result.
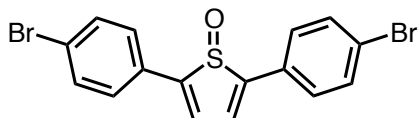
131

2,5-bis(4-bromophenyl)thiophene-1-oxide (131): Yellow solid (235.1 mg, 29%). TLC
(CH$_2$Cl$_2$) R_f = 0.27; elute solution (CH$_2$Cl$_2$). ^{1}H NMR (500 MHz, CDCl$_3$) δ = 7.60 (m,
8H), 6.95 ppm (s, 2H); ^{13}C NMR (125 MHz, CDCl$_3$) δ = 151.2, 132.5, 129.5, 127.9,
124.0, 123.8 ppm; HRMS ESI [M + 1] calcd for C$_{16}$H$_{11}$Br$_2$O$_1$S$_1$: 410.8871; found:
410.8878.
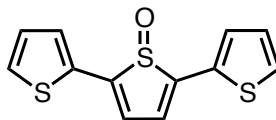
133

[2,2':5',2''-terthiophene]-1'-oxide (133): From bubbling SO$_2$, Yellow/orange solid
(51.2 mg, 10%). TLC (CH$_2$Cl$_2$) R_f = 0.21; elute solution (CH$_2$Cl$_2$). ^{1}H NMR (500 MHz,
CDCl$_3$) δ = 7.60 (dd, J = 3.0, 0.5 Hz, 2H), 7.37 (dd, J = 4.5, 0.5 Hz, 2H), 7.11 (m, 2H),
6.73 ppm (s, 2H); ^{13}C NMR (125 MHz, CDCl$_3$) δ = 145.2, 133.8, 128.5, 127.1, 127.0,
122.8 ppm; HRMS ESI [M + 1] calcd for C$_{12}$H$_9$O$_1$S$_3$: 264.9816; found: 264.9821.

143

5.4 Experimental procedures for I. GENERAL METHODS FOR THE SYNTHESIS OF FUNCTIONALIZED TETRABENZO[8]CIRCULENES AND II. STUDIES TOWARDS EXPANDED [8]CIRCULENE STRUCTURES

General Procedure for the Diels-Alder Reaction. A flame dried 25 mL round-bottom flask equipped with a reflux condenser and a stir bar was charged with 2,5-diarylthiophene-1-oxide (2.1 equiv.) and dibenzocyclooctadiyne (1 equiv.) in anhydrous toluene. The reaction mixture was heated at 80 ºC for 48 h. The crude reaction mixture was cooled to rt, and the solvent was removed under reduced pressure. Column chromatography afforded pure product as a red-yellow solid.
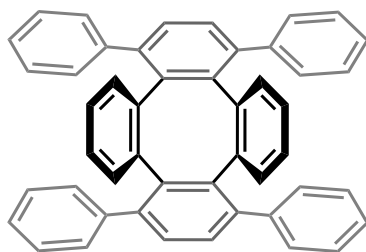
134

1,4,9,12-Tetraphenyltetraphenylene (134): Following the general Diels–Alder procedure, **69** (472 mg, 2.36 mmol) and **116** (1.22 g, 4.83 mmol) in toluene (20 mL) afforded **134** as a yellow solid (271 mg, 19%): mp 310 – 316 ºC. Purified by column chromatography (SiO$_2$, CH$_2$Cl$_2$:hexanes, 1:4 v/v) R_f = 0.20. ^{1}H NMR (500 MHz, CDCl$_3$) δ = 7.38 (s, 4H), 7.15 (t, J = 7 Hz, 4H), 7.06–7.01 (m, 16H), 6.76 ppm (s, 8H); ^{13}C NMR

(125 MHz, CDCl$_3$) δ = 141.0, 140.5, 140.1, 139.1, 130.9, 130.8, 129.7, 127.5, 126.4, 125.4 ppm; HRMS ESI [M + 1] calcd for C$_{48}$H$_{33}$: 609.2582; found: 609.2588.

135
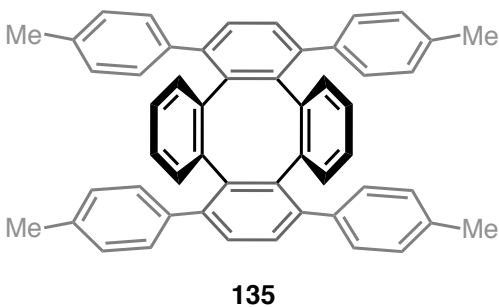
1,4,9,12-Tetra-p-tolyltetraphenylene (135): Following the general Diels–Alder procedure, **69** (52.7 mg, 0.263 mmol) and (155 mg, 0.553 mmol) in toluene (5 mL) afforded **135** as a yellow solid (19.2 mg, 11%): mp 370 – 377 ºC. Purified by column chromatography (SiO$_2$, CH$_2$Cl$_2$:hexanes, 3:7 v/v) R_f = 0.49. ^{1}H NMR (500 MHz, CDCl$_3$) δ = 7.34 (s, 4H), 6.85 (m, 16H), 6.77 (m, 8H), 2.30 ppm (s, 12H); ^{13}C NMR (125 MHz, CDCl$_3$) δ = 140.4, 140.3, 138.7, 138.1, 135.7, 130.8, 130.6, 129.6, 128.2, 125.3, 21.1 ppm; HRMS ESI [M + 1] calcd for C$_{52}$H$_{41}$: 665.3208; found: 665.3227.

136
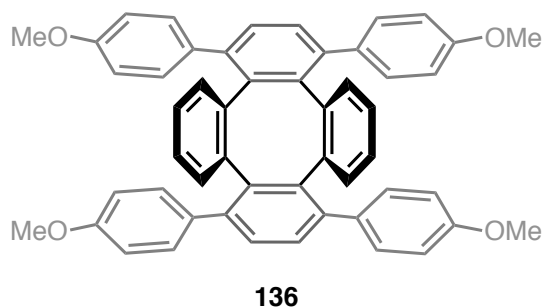
1,4,9,12-Tetrakis(4-methoxyphenyl)tetraphenylene (136): Following the general Diels–Alder procedure, **69** (88.2 mg, 0.441 mmol) and **120** (289 mg, 0.925 mmol) in toluene (7 mL) afforded **136** as a orange solid (31.0 mg, 10%): mp 380 – 385 ℃. Purified by column chromatography (SiO$_2$, CH$_2$Cl$_2$;hexanes, 3:2 v/v) R_f = 0.23. ^{1}H NMR (500 MHz, CDCl$_3$) δ = 7.32 (s, 4H), 6.90 (d, J = 8.5 Hz, 8H), 6.77 (m, 8H), 6.58 (d, J = 8.5 Hz 8H), 3.75 ppm (s, 12H); ^{13}C NMR (125 MHz, CDCl$_3$) δ = 158.3, 140.7, 140.6, 138.4, 133.7, 132.0, 131.1, 129.8, 125.6, 113.1, 55.2 ppm; HRMS ESI [M + 1] calcd for C$_{52}$H$_{41}$O$_4$: 729.3005; found: 729.3004.
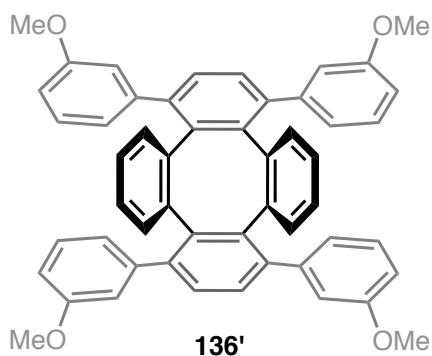
136'

1,4,9,12-Tetrakis(3-methoxyphenyl)tetraphenylene (136'): Following the general Diels–Alder procedure, **69** (122 mg, 0.611 mmol) and **122** (400 mg, 1.28 mmol) in toluene (10 mL) afforded **136'** as a yellow solid (40.0 mg, 10%): mp 380 – 385 ℃.

Purified by column chromatography (SiO$_2$, CH$_2$Cl$_2$:hexanes, 3:2 v/v) R_f = 0.24. ^{1}H NMR (500 MHz, CDCl$_3$) δ = 7.38 (s, 4H), 6.82 (m, 8H), 6.79 (s, 8H), 6.97 (dd, J = 8.5, 3 Hz, 4H), 6.35 (d, J = 8.5 Hz, 4H), 3.64 (s, 12H); ^{13}C NMR (125 MHz, CDCl$_3$) δ = 158.8, 142.2, 140.4, 140.2, 138.9, 130.8, 129.5, 128.4, 125.5, 123.7, 115.9, 112.5, 55.2 ppm; HRMS ESI [M + 1] calcd for C$_{52}$H$_{41}$O$_4$: 729.3005; found: 729.3010.
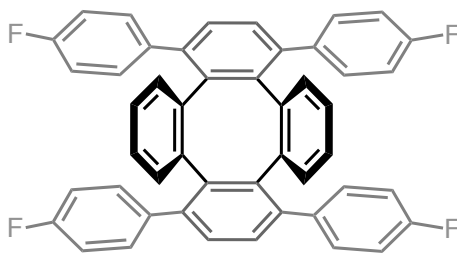
137

1,4,9,12-Tetrakis(4-fluorophenyl)tetraphenylene (137): Following the general Diels–Alder procedure, **69** (30.0 mg, 0.148 mmol) and **126** (90.1 mg, 0.312 mmol) in toluene (5 mL) afforded **137** as a bright yellow solid (25.5 mg, 25%): mp 380 – 385 ºC. Purified by column chromatography (SiO$_2$, CH$_2$Cl$_2$:hexanes, 1:4 v/v) R_f = 0.25. ^{1}H NMR (500 MHz, CDCl$_3$) δ = 7.33 (s, 4H), 6.91 (m, 8H), 6.81 (m, 4H), 6.77–6.72 ppm (m, 12H); ^{13}C NMR (125 MHz, CDCl$_3$) δ = 161.9 (d, J = 245.0 Hz), 140.7, 140.1, 138.2, 136.9 (d, J = 3.8 Hz) 132.4 (d, J = 7.5 hz), 131.0, 129.9, 126.0, 114.6 ppm (d, J = 20 Hz); LRMS [M] calcd for C$_{48}$H$_{28}$F$_4$: 680.2; found: 680.2; HRMS and accurate CHN analysis were attempted, however, the molecular ion was not observed and accurate CHN was unable to be obtained.
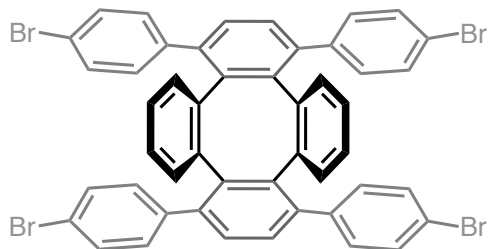
138

1,4,9,12-Tetrakis(4-bromophenyl)tetraphenylene (138): Following the general Diels–Alder procedure, **69** (23.1 mg, 0.115 mmol) and **131** (100 mg, 0.242 mmol) in toluene (8 mL) afforded **138** as a bright red solid (15.4 mg, 15%): mp 380 – 385 ºC. Purified by column chromatography (SiO$_2$, CH$_2$Cl$_2$:hexanes, 1:4 v/v) R_f = 0.35. ^{1}H NMR (500 MHz, CDCl$_3$) δ = 7.32 (s, 4H), 7.20 (d, J = 8.5 Hz, 8H), 6.83 (m, 4H), 6.76 (d, J = 8.5 Hz, 8H) 6.73 ppm (m, 4H); ^{13}C NMR (125 MHz, CDCl$_3$) δ = 140.4, 139.6, 139.5, 138.0, 132.2, 130.80, 130.76, 129.6, 126.0, 121.1 ppm; HRMS and accurate CHN analysis were attempted, however, the molecular ion was not observed and accurate CHN was unable to be obtained.

General Procedure for the Oxidative Cyclodehydrogenation. A flame dried 10 mL round-bottom flask equipped with a stir bar was charged with tetraphenylene (1 equiv.) and DDQ (5 equiv.) in anhydrous CH$_2$Cl$_2$. Under vigorous stirring triflic acid (20 equiv.) was added dropwise to the reaction mixture. After stirring at rt for 16 h, the reaction mixture was quenched with a solution of sat. NaHCO$_3$ (aq). The organic layer was separated and extracted with CH$_2$Cl$_2$. The combined extract was dried (MgSO$_4$) and concentrated under reduced pressure. Column chromatography afforded pure product as a red-yellow solid.

55
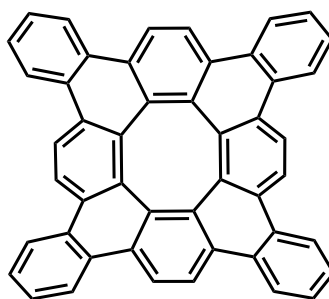
Tetrabenzo[8]circulene (55): Following the general oxidative cyclodehydrogenation procedure, **134** (30.0 mg, 0.049 mmol), DDQ (55.9 mg, 0.246 mmol) and triflic acid (148 mg, 0.087 mL, 0.985 mmol) in CH_2Cl_2 (10 mL) afforded **55** as a yellow solid (14 mg, 47%): mp > 420 ºC. Purified by column chromatography (SiO$_2$, CH_2Cl_2:hexanes, 1:4 v/v) R_f = 0.20. Spectral characterization was in agreement with our previously reported results.
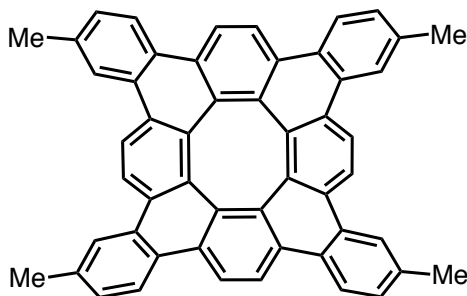
139

Tetramethyl-tetrabenzo[8]circulene (139): Following the general oxidative cyclodehydrogenation procedure, **135** (8.0 mg, 0.01 mmol), DDQ (466 mg, 2.05 mmol) and triflic acid (36.1 mg, 21.3 µL, 0.241 mmol) in CH_2Cl_2 (2 mL) afforded **139** as an orange solid (5.6 mg, 72%): mp > 420 ºC. Purified by column chromatography (SiO$_2$, CH_2Cl_2:hexanes, 3:7 v/v) R_f = 0.51. ^{1}H NMR (500 MHz, CDCl$_3$) δ = 7.98 (d, J = 8.0 Hz,

4H), 7.87 (s, 4H), 7.64 (s, 4H), 7.62 (s, 4H), 7.37 (d, J = 8.0 Hz, 4H), 2.53 ppm (s, 12H);

^{13}C NMR (125 MHz, CDCl$_3$) δ = 136.9, 134.1, 133.7, 129.5, 129.43, 129.41, 128.7,

127.2, 123.3, 123.2, 122.80, 122.78 ppm; HRMS ESI [M + 1] calcd for C$_{52}$H$_{33}$: 657.2582;

found: 657.2575.

140
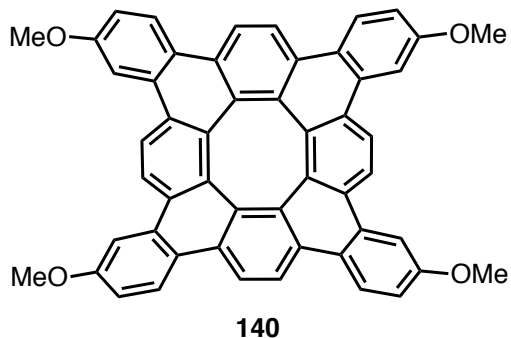
Tetramethoxy-tetrabenzo[8]circulene (140): From **136**: Following the general

oxidative cyclodehydrogenation procedure, **136** (24.0 mg, 0.033 mmol), DDQ (37.4 mg,

0.164 mmol) and triflic acid (98.8 mg, 58.3 μL, 0.658 mmol) in CH$_2$Cl$_2$ (6 mL) afforded

a dark red solid (15.9 mg, 67%): mp > 420 °C. From **136'**: Following the general

oxidative cyclodehydrogenation procedure, **136'** (33.9 mg, 0.047 mmol), DDQ (58 mg,

0.26 mmol) and triflic acid (153 mg, 90.2 μL, 1.02 mmol) in CH$_2$Cl$_2$ (6 mL) afforded **140**

as a dark red solid (22.8 mg, 68%): mp > 420 ºC. Purified by column chromatography

(SiO$_2$, CH$_2$Cl$_2$:hexanes, 3:2 v/v) R_f = 0.25. ^{1}H NMR (500 MHz, CD$_2$Cl$_2$) δ = 8.04 (d, J =

8.5 Hz, 4H), 7.66 (s, 4H), 7.62 (s, 4H), 7.53 (d, J = 2 Hz, 4H) 7.21 (dd, J = 8.5, 2 Hz, 4H)

3.93 ppm (s, 12H); This product proved to be too insoluble for ^{13}C NMR

characterization; HRMS ESI [M + 1] calcd for C$_{52}$H$_{33}$O$_4$: 721.2379; found: 721.2386.

112
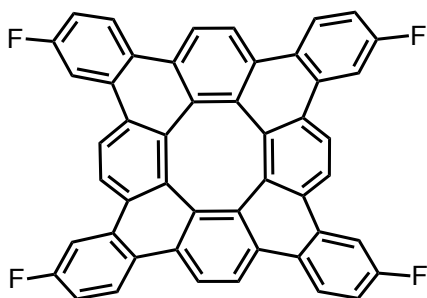
Tetrafluoro-tetrabenzo[8]circulene (112): Following the general oxidative cyclodehydrogenation procedure, **137** (22.0 mg, 0.032 mmol), DDQ (36.7 mg, 0.162 mmol) and triflic acid (97.0 mg, 57.2 µL, 0.646 mmol) in CH_2Cl_2 (6 mL) afforded **112** as a fluorescent orange solid (14.0 mg, 65%): mp > 420 ºC. Purified by column chromatography (SiO_2, CH_2Cl_2;hexanes, 1:4 v/v) R_f = 0.19. The spectroscopic data matches that of material produced through our original palladium-catalyzed arylation methodology.
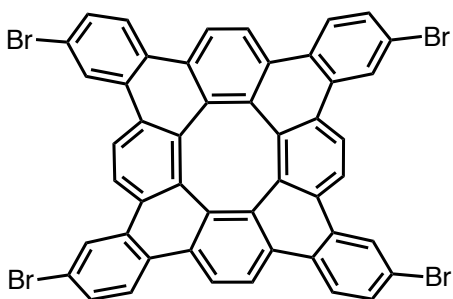
141

Tetrabromo-tetrabenzo[8]circulene (141): Following the general oxidative cyclodehydrogenation procedure, **138** (13.0 mg, 0.014 mmol), DDQ (16.0 mg, 0.070 mmol) and triflic acid (42.6 mg, 25.1 µL, 0.284 mmol) in CH_2Cl_2 (5 mL) afforded **141** as a bright orange solid (9.0 mg, 70%): mp > 420 ºC. Purified by column chromatography

(SiO$_2$, CH$_2$Cl$_2$:hexanes, 1:4 v/v) R_f = 0.27. ^{1}H NMR (500 MHz, CDCl$_3$) δ = 8.22 (d, J = 2.0 Hz, 4H), 7.95 (d, J = 8.5 Hz, 4H), 7.67 (dd, J = 8.5, 2 Hz, 4H), 7.62 (s, 4H), 7.61 ppm (s, 4H); ^{13}C NMR (125 MHz, CDCl$_3$) δ = 134.2, 133.9, 130.9, 130.6, 129.4, 129.0, 128.1, 125.7, 124.8, 123.7, 123.6, 121.6 ppm; HRMS and accurate CHN analysis were attempted, however, the molecular ion was not observed and accurate CHN was unable to be obtained.

142
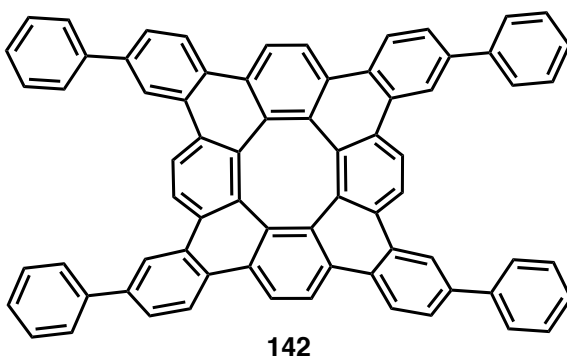
Tetraphenyl-tetrabenzo[8]circulene (142): In a 2-necked roundbottom flask equipped with a stir bar and reflux condenser, 6 mL of THF and 3 mL of water was degassed by bubbling with nitrogen for 15 minutes. **141** (5.0 mg, 5.5 μmol, 1 equiv.) and phenylboronic acid (3.0 mg, 24.6 μmol, 4.5 equiv.), Pd(PPh$_3$)$_4$ (1.1 mg, 1.1 μmol, 20 mol %), and K$_2$CO$_3$ (9.0 mg, 65.5 μmol, 12 equiv.) were added and the reaction stirred at 90 °C for 48 h. The reaction mixture was cooled to RT and a solution of sat. NH$_4$Cl(aq) (5 mL) was added. The organic layer was separated and the aqueous layer was extracted with EtOAc (3 x 10 mL). The organic fractions were combined, dried over MgSO$_4$, and solvent was removed under reduced pressure. Purified by column chromatography (SiO$_2$, CH$_2$Cl$_2$:hexanes, 1:4 v/v) R_f = 0.24; afforded pure **142** as a bright fluorescent orange solid (4.6 mg, 94%): mp > 420 ºC. ^{1}H NMR (500 MHz, CDCl$_3$) δ = 8.31 (d, J = 0.5 Hz, 4H),

8.20 (d, J = 8.5 Hz, 4H), 7.82 (dd, J = 8.5, 0.5 Hz, 4H), 7.78 (s, 4H), 7.76 (s, 4H), 7.71 (d, J = 8 Hz, 8H), 7.48 (t, J = 7.5 Hz, 8H), 7.38 ppm (t, 7.5 Hz, 4H); ^{13}C NMR (125 MHz, CDCl$_3$) δ = 141.1, 140.3, 134.3, 134.2, 130.1, 129.8, 129.6, 128.9, 128.6, 127.7, 127.5, 127.4, 126.7, 123.6, 123.5, 121.4 ppm; MALDI MS [M] calcd for C$_{72}$H$_{40}$: 904.31; found: 904.23. HRMS and accurate CHN analysis were attempted, however, the molecular ion was not observed and accurate CHN was unable to be obtained.

143
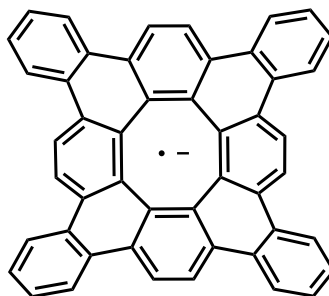
Tetrabenzo[8]circulene radical anion (143): In a glove box under a nitrogen atmosphere freshly cut potassium metal (excess) was added to tetrabenzo[8]circulene (10 mg, 0.015 mmol) dissolved in 1.0 mL THF in a scintillation vial with vigorous stirring. Reduction to the radical anion was observed as the soloution adopted a dark green color, followed by reduction to the dianion indicated by a dark red solution. Excess potassium was removed throught filtration and tetrabenzo[8]circulene (**55**) was again added to the reaction mixture (10 mg 0.015 mmol) in 1.0 mL THF producting a dark green solution as the radial anion (**143**). ^{1}H NMR (Figure AI.88) showed no identifiable peaks, consistent of a species with an unpaired electron.

144
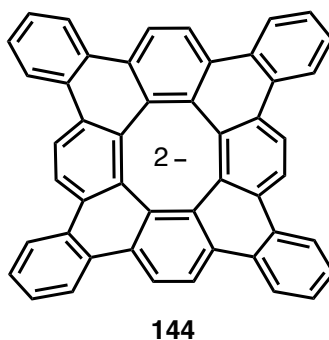
Tetrabenzo[8]circulene dianion (144): In a glove box under nitrogen atmosphere freshly cut potassium metal (excess) was added to tetrabenzo[8]circulene (20 mg, 0.033 mmol) dissolved in 1.0 mL THF in a scintillation vial with vigorous stirring. Reduction to the dianion was observed as the reaction mixture adopted a dark red color. Excess potassium metal was removed through filtration to yield the dianion **144**. ^{1}H NMR (500 Mhz, THF-d_8) δ = 7.58 (dd, J = 6.0, 3.0 Hz, 8H), 7.11 (s, 8H), 7.00 ppm (dd, J = 6.0, 3.0 Hz, 8H); ^{13}C NMR (125 MHz, CDCl$_3$) δ = 135.8, 132.0, 123.7, 123.0, 110.1, 109.9 ppm.

156
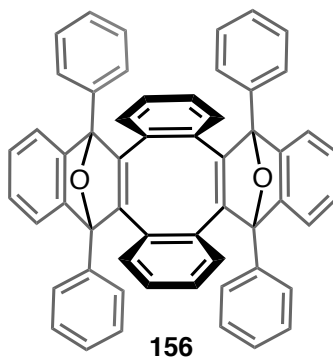
5,10,15,20-tetraphenyl-5,10,15,20-tetrahydro-5,10:15,20-diepoxydibenzo[*b*,*n*]tetraphenylene (156): A flame dried 25 mL round-bottom flask equipped with a reflux condenser and a stir bar was charged with 1,3-diphenylisobenzofuran (2 eq, 1.0 g, 3.70 mmol) and dibenzocyclooctadiyne (1 eq, 370.36 mg, 1.85 mmol) in anhydrous toluene.

The reaction mixture was heated at 80 ºC for 16 h. The crude reaction mixture was cooled to rt, and the solvent was removed under reduced pressure. Purified by column chromatography (SiO$_2$, CH$_2$Cl$_2$:hexanes, 3:1 v/v) R_f = 0.54 & R_f = 0.13; afforded as two isomers of pure **156** as a yellow solids (1.2 g combined, 90%). ^{1}H NMR (500 MHz, CDCl$_3$) δ = 7.69 (m, 2H), 7.64 (d, J = 10 Hz, 4H), 7.51 (d, J = 10 Hz, 4H), 7.42, (m, 12H), 7.27 (m, 2H), 7.20 (m, 2H), 6.90 (t, J = 10 Hz, 2H), 6.82 (m, 4H), 6.73 (t, J = 10 Hz, 2H), 6.28 ppm (d, J = 5 Hz, 2H); ^{13}C NMR (125 MHz, CDCl$_3$) δ = 154.7, 153.9, 151.8, 151.3, 136.3, 134.7, 134.2, 132.2, 131.7, 130.6, 128.7, 127.9, 127.8, 127.6, 127.5, 127.4, 126.6, 126.1, 125.3, 125.2, 124.2, 121.6, 119.5, 94.9, 93.7, 31.6, 22.6, 20.7 ppm; LRMS [M + 1] calcd for C$_{56}$H$_{37}$O$_2$: 741.88; found: 741.5.

155
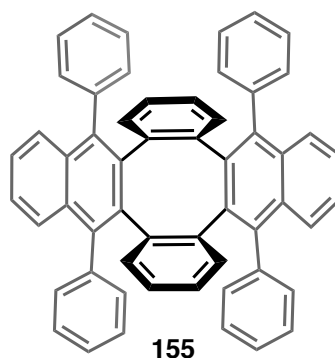
5,10,15,20-tetraphenyldibenzo[*b,n*]tetraphenylene (155): A flame dried 50 mL multi-neck round bottom flask charged with 20 mL THF was cooled to -78 ºC and TiCl$_4$ (12 eq, 13.5 mmol, 1.4 mL) was added dropwise over a period of 15 min. To the resulting yellow solution was added metallic Zn (16 eq, 17.9 mmol, 1.2 g) followed by the dropwise addition of NEt$_3$ (3 eq, 3.4 mmol, 0.5 mL). The resulting mixture was then

removed from the -78 ºC bath and heated at reflux for 30 min. After a period of cooling

156 (1 eq, 1.12 mmol, 800 mg) dissolved in 10 mL of THF was added dropwise to the

reaction mixture and refluxed for a period of 12 h. The crude reaction mixture was

cooled to rt, and quenched with a sat. K_2CO_3 (50 mL) and extracted with EtOAc. The

combined extracts were dried ($MgSO_4$) and solvent was removed under reduced pressure.

Purified by column chromatography (SiO_2, CH_2Cl_2:hexanes, 1:1 v/v) R_f = 0.60; afforded

pure **155** as a yellow solid (640 mg, 85%). ^{1}H NMR (500 MHz, CDCl$_3$) δ = 7.49 (q, J =

10, 5 Hz 4H), 7.43 (d, 10 Hz, 4H), 7.35 (td, J = 5, 0.5 Hz, 4H), 7.28 (q, J = 10, 5 Hz,

4H), 7.26 (m, 4H), 7.03 (td, J = 5, 0.5 Hz, 4H), 6.86 (d, J = 10 Hz, 4H), 6.67 ppm (m,

8H); ^{13}C NMR (125 MHz, CDCl$_3$) δ = 140.5, 138.7, 138.6, 136.8, 132.7, 132.4, 132.1,

131.4, 132.2, 131.4, 127.5, 127.12, 127.05, 126.6, 125.5, 125.1 ppm; LRMS [M + 1]

calcd for $C_{56}H_{37}$: 709.3; found: 709.5.

157
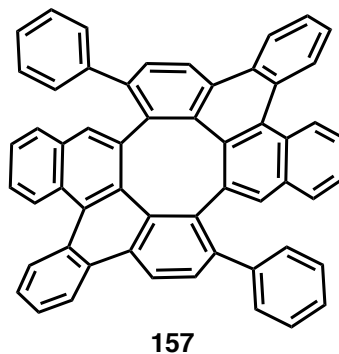
11,23-diphenyldibenzo[*b,n*]dinaphtho[1,2,3,4-*def*:4',3',2',1'-*pqr*]tetraphenylene (157):

A flame dried 10 mL round-bottom flask equipped with a stir bar was charged **155** (1 eq,

150 mg, 0.21 mmol) and DDQ (5 eq, 240.8 mg, 1.05 mmol) in anhydrous CH_2Cl_2. Under

vigorous stirring triflic acid (1 mL) was added dropwise to the reaction mixture. After

stirring at rt for 16 h, the reaction mixture was quenched with a solution of sat. $NaHCO_3$ (aq). The organic layer was separated and extracted with CH_2Cl_2. The combined extract was dried ($MgSO_4$) and concentrated under reduced pressure. Purified by column chromatography (SiO_2, EtOAc:hexanes, 1:9 v/v) $R_f = 0.42$; afforded pure **157** as a yellow solid (83 mg, 56%). ^{1}H NMR (500 MHz, $CDCl_3$) $\delta = 8.64$ (td, $J = 5$, 0.5 Hz, 4H), 8.52 (d, $J = 10$ Hz, 2H), 7.98 (d, $J = 10$ Hz, 2H), 7.60 (m, 6H), 7.49 (d, $J = 10$ Hz, 2H), 7.35 (m, 4H) 7.24 (m, 4H), 7.15 (*br* s, 2H), 7.01 (*br* s, 2H), 6.90 ppm (m, 4H); ^{13}C NMR (125 MHz, $CDCl_3$) $\delta = 151.7$, 139.1, 138.1, 137.8, 136.3, 133.0, 131.9, 131.4, 130.7, 130.2, 129.5, 129.3, 128.3, 128.2, 127.8, 127.5, 127.4, 127.2, 126.9, 126.7, 126.2, 126.1, 124.6, 124.22, 124.20, 121.7 ppm; LRMS [M + 1] calcd for $C_{56}H_{33}$: 705.2; found: 705.5.
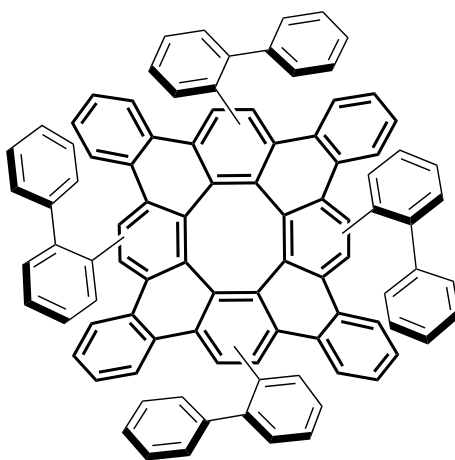
158

Tetrakis(*o*-biphenylyl)tetrabenzo[8]circulene (158): A solution of $Pd(OAc)_2$ (3.0 mg, 0.01 mmol, 20 mol%), o-chloranil (81.9 mg, 0.33 mmol, 5.0 equiv.), tetrabenzo[8]circulene **55** (40 mg, 0.07 mmol, 1.0 equiv.) and tris(o-biphenylyl)boroxin (72.0 mg, 0.13 mmol, 2.0 equiv.) in dry 1,2-dichloroethane (10 ml) was stirred at 80 ºC

for 16 hours under nitrogen. The reaction mixture was then passed through a pad of silica gel with copious washings of CH_2Cl_2 (50 ml). The filtrate was concentrated and subjected to silica-gel column chromatography (SiO$_2$, CH_2Cl_2:hexanes, 1:3 v/v) $R_f = 0.20$ to give pentakis(o-biphenylyl)corannulene **158** (16 mg, 20% yield) as a mixture of regioisomers. LRMS [M + 1] calcd for $C_{56}H_{33}$: 1210.5; found: 1210.7.

COMPREHENSIVE LIST OF REFRENCES

Abrams, M. L.; Foarta, F.; Landis, C. R. *J. Am. Chem. Soc.* **2014**, *136*, 14583–14588.

Adachi, M. and Nagao, Y. *Chem. Mater.* **2001**, *13*, 662–669.

Adam, D.; Schuhmacher, P.; Simmerer, J.; Haussling, L.; Siemensmeyer, K.; Etzbach, K. H.; Ringsdorf, H.; Haarer, D. *Nature* **1994**, *371*, 141–143.

Agranat, I.; Hess, B. A.; Schaad, L. J. *Pure & Appl. Chem.* **1980**, *52*, 1399–1407.

Alibert-Fouet, S.; Seguy, I.; Bobo, J.-F.; Destruel P.; Bock, H. *Chem. Eur. J.* **2007**, *13*, 1746–1753.

An, Z.; Yu, J.; Domercq, B.; Jones, S. C.; Barlow, S.; Kippelen, B.; Marder, S. R. *J Mater. Chem.* **2009**, *19*, 6688–6698.

An, Z.; Yu, J.; Jones, S. C.; Barlow, S.; Yoo, S.; Domercq, B.; Prins, P.; Siebbeles, L. D. A.; Kippelen, B.; Marder, S. R. *Adv. Mater.* **2005**, *17*, 2580–2583.

Aprahamian, I.; Bodwell, G. J.; Fleming, J. J.; Manning, G. P.; Mannion M. R.; Sheradsky, T.; Vermeij, R. J.; Rabinovitz, M. *J. Am. Chem. Soc.* **2003**, *125*, 1720–1721.

Aprahamian, I.; Preda, D. V.; Bancu, M.; Belanger, A. P.; Sheradsky, T.; Scott, L. T.; Rabinovitz, M. *J Org. Chem.* **2006**, *71*, 290–298.

Aprahamian, I.; Wegner, H. A.; Sternfeld, T.; Rauch. K.; de Meijere, A.; Sheradsky, T.; Scott, L. T.; Rabinovitz, M. *Chem. Asian J.* **2006**, *1,* 678–685.

Avlasevich, Y.; Müller, S.; Erk, P.; Müllen, K *Chem. Eur. J.* **2007**, *13*, 6555– 6561.
Aygula, A.; Rabideau, P. W. *J. Am. Chem. Soc.* **2000**, *122*, 6323–6324.

Baker, W.; Glockling, F.; McOmie, J. F. W. *J. Chem. Soc.* 1951, 1118–1121.

Balaban, A. T.; Dickens, T. K. Gutman, I.; Mallion, R. B. *Croat. Chem. Acta.* **2010**, *83*, 209–215.

Ball, M. Zhong, Y.; Fowler, B.; Zhang, B.; Li, P.; Etkin, G.; Paley, D. W.; Decatur, J.; Dalsania, A. K.; Li, H.; Xiao, S.; Ng, F.; Steigerwald, M. L.; Nuckolls, C. *J. Am. Chem. Soc.* **2016**, *138*, 12861–12867.

Ball, M.; Zhong, Y.; Wu, Y.; Schenck, C.; Ng, F.; Steigerwald, M.; Xaio, S.; Nuckolls, C. *Acc. Chem. Res.,* **2015**, *48*, 267–276.

Barth, W. E.; Lawton, R. G. *J. Am. Chem. Soc.* **1966**, *88*, 380–381.

Barth, W. E.; Lawton, R. G. *J. Am. Chem. Soc.* **1971**, *93*, 1730–1745.

Baryshnikov, G. V.; Karaush, N. N.; Valiev, R. R.; Minaev, B. F. J. Mol. Model. **2015**, *21*, 136.

Baryshnikov, G. V.; Minaev, B. F.; Minaeva, V. A. *Russ. Chem. Rev.* **2015**, *84*, 455−484.

Baryshnikov, G. V.; Minaev, B. F.; Pittelkow, M.; Nielsen, C. B.; Salcedo, R. *J. Mol. Model.* **2013**, *19*, 847−850.

Baryshnikov, G. V.; Valiev, R. R.; Karaush, N. N.; Minaev, B. F. *Phys. Chem. Chem. Phys.* **2014**, *16*, 15367−15374.

Baryshnikov, G. V.; Valiev, R. R.; Karaush, N. N.; Sundholm, D.; Minaev, B. F. *Phys. Chem. Chem. Phys.* **2016**, *18*, 8980−8992.

Battiste, M. A.; Sprouse, C. T. *Tetrahedron Lett.* **1970**, *11*, 4661–4664.

Beser, U.; Kastler, M.; Maghsoumi, A.; Wagner, M.; Castiglioni, C.; Tommasini, M.; Narita, A.; Feng, X.; Müllen, K. *J. Am. Chem. Soc.* **2016**, *138*, 4322–4325.

Bharat, A.; Bhola, R.; Bally, T.; Valente, A.; Cyranski, M. K.; Dobrzycki, Ł.; Spain, S. M.; Rempała, P.; Chin, M. R.; King, B. T. *Angew. Chem. Int. Ed.* **2010**, *49*, 399–402.

Bieber, T. I.; Eisman, E. H. *J. Org. Chem.* **1962**, *27*, 678–679.

Binger, P.; Wedemann, P.; Goddard, R.; Brinker, U. H. *J. Org. Chem.* **1996**, *61*, 6462–6464.

Borch, R. F. *J* . Org. *Chem.* **1969**, *34*, 627–629.

Borchardt, A.; Fuchicello, A.; Kilway, K. V.; Baldridge, K. K.; Siegel, J. S. *J. Am. Chem. Soc.* **1992**, *114*, 1921–1923.

Bousrez, G.; Jaroschik, F.; Martinez, A.; Harakat, D.; Nicolas, E.; Le Goff, X. F.; Szymoniak, J. *Dalton Trans.* **2013**, *42*, 10997–11004.

Breuer, T.; Liues, M.; Liesfeld, P.; Viertel, A.; Conrad, M.; Hecht, S.; Witte, G. *Phys. Chem. Chem. Phys.* **2016***, 18*, 33344–33350.

Bühl, M. *Chem. Eur. J.* **1998**, *4, * 734–739.

Bushey, M. L.; Nquyen, T. -Q.; Nuckolls, C. *J. Am. Chem. Soc.* **2003**, *125,* 8264–8269.

Butterfield, A. M.; Gilomen, B.; Siegel, J. S. *Org. Process Res. Dev.* **2012**, *16*, 664–676.

Carpita, A.; Rossi, R.; Veracint, C. A. *Tetrahedron* **1985**, *41*, 1919–1929.

Cava, M. P.; Narasimhan, K. *J. Org. Chem.* **1970**, *36*, 1419–1423.

Chaffins, S.; Brettreich, M.; Wudl, F. *Synthesis* **2002**, 1191−1194. (c) Xu, F.; Peng, L.; Shinohara, K.; Morita, T.; Yoshida, S.; Hosoya, T.; Orita, A.; Otera, J. *J. Org. Chem.* **2014**, *79*, 11592−11608.

Charlier, J. -C. *Acc. Chem. Res.*, **2002**, *35*, 1063–1069.

Chase, D.; Fix, A.; Kang, S. J.; Rose, B.; Weber, C.; Zhong, Y.; Zakharov, L.; Lonergan, M.; Nuckolls, C.; Haley, M. *J. Am. Chem. Soc.* **2012**, *124*, 10349–10352.

Chen, Z.; Wannere, C. S.; Corminboeuf, C.; Puchta, R.; Schleyer, P. v. R.; *Chem. Rev.* **2005**, *105*, 3842–3888.

Cheung, K. Y.; Chan, C. K.; Liu, Z.; Miao, Q *Angew. Chem.* **2017**, *31*, 9131–9135.

Cheung, K. Y.; Xu, X.; Miao, Q. *J. Am. Chem. Soc.* **2015**, *137*, 3910–3914.

Christoph, H.; Grunenberg, J.; Hopf, H.; Dix, I.; Jones, P. G.; Scholtissek, M.; Maier, G. *Chem. Eur. J.* **2008**, *14,* 5604–5616.

Clar, E. *The Aromatic Sextet*, Wiley, New York, **1972**.

Clar, E.; Ironside, C. T. *Proc. Chem. Soc.* **1958**, 150;.

Clar, E.; Ironside, C. T.; Zander, M. *J. Chem. Soc.* **1959**, 142.

Clar, E.; Stephen, J. F. *Tetrahedron* **1965**, *21*, 467–470

Clar, E.; Zander, M. *J. Chem. Soc.* **1957**, 4616–4619.

Cottle; D. L. *J. Am. Chem. Soc.* **1946**, *68*, 1380–1381.

Craig, J. T.; Halton, B.; Lo, S.-F. *Aust. J. Chem.* **1975**, 28, 913.

Dickens, T. K.; Mallion, R. B. *Chem. Phys. Lett.* **2011**, *517*, 98–102.

Dickens, T. K.; Mallion, R. B. *Croat. Chem. Acta.* **2014**, *87*, 221–232.

Diels, O.; Alder, K. *J. Liebigs Ann. Der Chem.* **1928**, *460,* 98–122.

Diels, O.; Alder, K.; *Justus Liebigs Ann. Chem.* **1931**, 490, 243–257.

Diels, O.; Alder, K.; Naujoks, E. *Der. Dtsch. Chem. Ges.* **1929**, *62*, 554.

Dijk, J. T. M.; Hartwijk, A.; Cleeker, A. C.; Lugtenburg, J.; Cornelisse, J. *J. Org. Chem.* **1996**, *61*, 1136–1139.

Dioumaev, V. K.; Harrod, J. F. *Organometallics* **1997**, *16*, 1452–1464.

Doetz, F.; Brand, J. D.; Ito, S.; Gherghel, L.; Müllen, K. *J. Am. Chem. Soc.* **2000**, *122*, 7707–7717.

Dong, H.; Gilmore, K.; Lin, B.; Hou, T.; Lee, S.-T.; Guo, Z.; Li, Y. *Carbon* **2015**, *89*, 249−259.

Eisenberg, D.; Shenhar, R. Wires. Comput. Mol. Sci. **2012**, *2*, 525–547.

Elemans, J. A. A. W.; van Hameren, R.; Nolte, R. J. M.; Rowan, A. E. *Adv. Mater*. **2006**, *18*, 1251–1266.

Endres, A. H,; Schaffroth, M.; Paulus, F.; Reiss, H.; Wadepohl, H.; Rominger, F.; Krämer, R.; Bunz, U. H. F. *J. Am. Chem. Soc.* **2016**, *138,* 1792–1795.

Fagan, P.J.; Burns, E. G.; Calabrese, J. C. *J. Am. Chem. Soc.* **1988**, *110*, 2979–2981.

Fagen, P. J.; Nugent, W. A. *J. Am. Chem. Soc.* **1988**, *110*, 2310–2312.

Fagen, P. J.; Nugent, W. A.; Calabrese, J. C. *J. Am. Chem. Soc.* **1994**, *116*, 1880–1889.

Faraday, M. *Phil. Trans. R. Soc. Lond.* **1825**, *115*, 440–466.

Fechtenkötter, A.; Tchebotareva, N.; Watson, M.; Müllen, K. *Tetrahedron* **2001**, *57*, 3769-3783.

Feng, C. -N.; Kuo, M. Y.; Wu, W. T. *Angew. Chem. Int. Ed.* **2013**, *52*, 7791–7794.

Fraenkel, G.; Carter, R. E.; McLachlan A.; Richards, J. H. *J. Am. Chem. Soc.* **1960**, *82*, 5846–5850.

Furukawa, N.; Zhang, S.; Sato, S.; Higaki, M. *Hetercycles* **1997**, *44*, 61–66.

Gaviña, F.; Costero, A. M.; Gil, P.; Luis, S. V. *J. Am. Chem. Soc.* **1984,** *106,* 2077–2080.

Gaviña, F.; Costero, A. M.; Gil, P.; Palazon, B.; Luis, S. V. *J. Am. Chem. Soc.* **1981,** *103,* 1797–1798.

Geibel, K.; Heindl, J. *Tetrahedron. Lett.* **1970**, *11*, 2133–2136.

Goddard, R.; Haenel, M. W.; Herndon, W. C.; Krüger, C.; Zander, M. *J. Am. Chem. Soc.* **1995**, *117*, 30–41.

Gregg, B. A.; Cormier, R. A. *J. Am. Chem. Soc.* **2001**, *123*, 7959–7960.

Griffin, G. W.; Peterson, L. I. *J. Am. Chem. Soc.* **1962**, *84*, 3398–3400.

Grimsdale, C.; Müllen, K. *Angew. Chem. Int. Ed.* **2005**, *44*, 5592–5629.

Gu, X.; Li, H.; Shan, B.; Liu, Z.; Miao, Q. *Org. Lett.* **2017**, *19*, 2246–2249.

Guo, X.; Facchetti, A.; Marks, T. J. *Chem. Rev.* **2014**, *114*, 8943–9021.

Haddon, R. C. *J. Am. Chem. Soc.* **1990**, *112*, 3385–3389.

Haddon, R. C.; Scott, L. T. *Pure Appl. Chem.* **1986**, *58*, 137–142.

Harris, K. D.; Xiao, S.; Lee, C. Y.; Strano, M. S.; Nuckolls, C.; Blanchet, G. B. *J. Phys. Chem. C*, **2007**, *111*, 17947–17951.

Hashmall, J. A.; Horak, V.; Khoo, L. E.; Quicksall, C. O.; Sun, M. K. *J. Am. Chem. Soc.* **1981**, *103*, 289–295.

Heinrich, A. C. J.; Thiedemann, D.; Gates, P. J.; Staubitz, A. *Org. Lett.* **2013**, *15*, 4666–4669.

Hensel, T.; Andersen, N. N.; Plesner, M.; Pittelkow, M. *Synlett* **2016**, *27*, 498−525.

Herwig, P.; Kayser, C. W.; Müllen, K.; Spiess, H. W. *Adv. Mater.* **1996**, *8*, 510-513.

Hill, J. P.' Jin, W.; Kosaka, A.; Fukushima, T.; Ichihara, H.; Shimomura, T.; Ito, K.; Hashizume, T.; Ishii, N.; Aida, T. *Science* **2004**, *304*, 1481–1483.

Hirst, E. S.; Jasti, R. *J. Org. Chem.* **2012**, *77*, 10473–10478.

Iverson, I. K.; Tam-Chang, S.-W. *J. Am. Chem. Soc.* **1999**, *121*, 5801–5802.

Iyer, V. S.; Wehmeier, M.; Brand, J. D.; Keegstra, M. A.; Müllen, K. *Angew. Chem. Int. Ed. Engl.* **1997**, *36,* 1604–1607.

Jackson, E. A.; Steinberg, B. D.; Bancu, M.; Wakamiya, A.; Scott, L. T. *J. Am. Chem. Soc.* **2007**, *129*, 484–485.

Jaing, B.; Tilley, T. D. *J. Am. Chem. Soc.* **1999**, *121*, 9744–9745.

Jasti, R.; Bhattacharjee, J.; Neaton, J. B.; Bertozzi, C. R. *J. Am. Chem. Soc.* **2008**, *130*, 17646–17647.

Jessup, P. J.; Reiss, J. A. *Aust.J. Chem.* **1976**, *29,* 173–178.

Jessup, P. J.; Reiss, J. A. *Aust. J. Chem*. **1977**, 30, 843–850.

Jessup, P. J.; Reiss, J. A. *Tetrahedron Lett.* **1975,** *17*, 1453–1454.

Jiang, H.; Zeng, W.; Li, Y.; Wanqing, W.; Liangbing, H.; Fu, W. *J. Org. Chem*. **2012**, *77*, 5179–5183.

Jursic, B. S. *J. Heterocyclic Chem.* **1995**, *32*, 1445–1455.

Kang, S. J.; Kim, J. B.; Chiu, C. Y.; Ahn, S.; Schiros, T.; Lee, S. S.; Yager, K. G.; Toney, M. F.; Nuckolls, C. *Angew. Chem., Int. Ed.* **2012**, *51*, 8594–8597.

Karaush, N. N.; Valiev, R. R.; Baryshnikov, G. V.; Minaev, B. F.; Ågren, H. *Chem. Phys*. **2015**, *459*, 65−71.

Katsuaki, K.; Zhang, Q.; Segawa, Y.; Scott, L. T.; Itami, K. *Nature Chemistry* **2013**, *5*, 739–744.

Kellog, R. M. in *Comprehensive Heterocyclic Chemistry,* ed. Katrizky, A. R. and Rees, C. W. Pergamon Press; Oxford, **1984**, *4*, 713–934.

King, B. T.; Kroulík, J.; Robertson, C. R.; Rempala, P.; Hilton, C. L.; Korinek, J. D.; Gortari, L. M. *J. Org. Chem*. **2007**, *72*, 2279–2288.

Krieger, C.; Diederich, F.; Schweitzer, D.; Staab, H. A. *Angew. Chem. Int. Ed. Engl*. **1979**, *18*, 699–701.

Krygowski, T. M.; Ejsmont, K.; Stepień, B. T.; Cyrański, M. K.; Poater, J.; Solà, M. *J. Org. Chem.* **2004**, *69*, 6634–6640.

Kumar, B.; Viboh, R. L.; Bonifacio, M. C.; Thompson, W. B.; Buttrick, J. C.; Westlak, B. C.; Kim, M. -S.; Zoellner, R. W.; Varganov, S. A.; Mçrschel, P.; Teteruk, J.; Schmidt, M. U.; King, B. T. *Angew. Chem. Int. Ed.* **2012**, *51*, 12795–12800.

Lauterbur, P. C. *Tetrahedron Lett.* **1961**, 274–279.

Li, Y; Thiemann, T; Sawada, T; Masashi, T. *J. Chem. Soc., Perkin Trans. 1.* **1994**, 2323–2329.

Li, Y.; Matsuda, M.; Thiemann, T.; Sawada, T.; Mataka, S.; Tashiro, M. *Synlett* **1996**, 461–464.

Li, Y.; Thiemann, T.; Mimura, K.; Sawada, T.; Mataka, S.; Tashiro, M. *Eur. J. Org. Chem.* **1998**, 1841–1850.

Li, Y.; Thiemann, T.; Sawada, T.; Mataka, S.; Tashrio, M. *J. Am. Chem Soc.* **1997**, *62*, 7926–7936.

Liu, Z., Zhang, G., Cai, Z., Chen, X., Luo, H., Li, Y., Wang, J.; Zhang, D. *Adv. Mater.* **2014,** *26*, 6965–6977.

Loo, Y. -L. Hiszpanski, A.; Kim, B.; Wei, S.; Chiu, C. -Y.; Steigerwald, M.; Nuckolls, C. *Org. Lett.* **2010**, *12*, 4840–4843.

Luo, J.; Xu, X.; Mao, R.; Miao, Q. *J. Am. Chem. Soc.* **2012**, *134*, 13796–13803.

Mallion, R. B. *Croat. Chem. Acta.* **2008**, *81*, 227–246.

Man, Y. -M.; Mak, T. C. W.; Wong, H. N. C. *J. Org. Chem.* **1990**, *55*, 3214−3221.

Meier-Brocks, F.; Weiss, E. *J. Organometal. Chem.* **1993**, *453*, 33–45.

Men, F. H.; Bellard, S.; Brice, M. D.; Carhwight,B. A.; Doubleday, A.; Higgs, H.; Humpelink, T.; Hummelink-Peters, B. G.; Kennard, O.; Motherwell, W. D. S.; Rodgers, J. R.; Watson, D. G. *Acta Crystallogr.* **1979**, *B35,* 2331–2339.

Mochida, K.; Kawasumi, K.; Segawa, Y.; Itami, K. *J. Am. Chem. Soc.* **2011**,*133*, 10716–10719.

Mock, W. L. *J. Am. Chem. Soc.* **1970**, *92*, 7610–7612.

Monaco, G.; Scott, L. T.; Zanasi, R. *J. Phys. Chem. A* **2008**, *112*, 8136–8147.

Müllen, M.; Iyer, V. S.; Kubel, C.; Enkelmann, V.; Müllen, K. *Angew. Chem. Int. Ed. Engl.* **1997**, *36*, 1607–1610.

Müller, S.; Müllen, K. *Chem. Commun.* **2005**, 4045–4046.

Nakayama, J.; Kuroda, M.; Hoshino, M. *Heterocycles*, **1986**, *24*, 1233–1236.

Nakayama, J.; Yu, T.; Sugihara, Y.; Ishii, A. *Chem. Lett.* **1997**, *26*, 499–500.

Nandakumar, M.; Sivasakthikumaran, R.; Mohanakrishnan, A. K. *Eur J. Org. Chem.* **2012**, 3647–3657.

Naperstkow, A. M.; Macaulay, J. B.; Newlands, M. J.; Fallis, A. G. *Tetrahedron Lett.* **1989**, *30*, 5077–5080.

Negishi, E.; Cederbaum; F. E.; Takahashi; T. *Tetrahedron Lett.* **1986**, *27*, 2829–2832.

Negishi, E.; Takahashi, T. *Acc. Chem. Res.* **1994**, *27*, 124–130.

Nepveu, F.; Kim, S.; Boyer, J.; Chatrian, O.; Ibrahim, H.; Reybier, K.; Monje, M.,-C.; Chevalley, S.; Perio, P.; Lajoie, B. H.; Bouajila, J.; Deharo, E.; Sauvain, M.; Tahari, R.; Basoci, L.; Pantaleo, A.; Turini, F.; Arese, P.; Valentin, A.; Thompson, E.; Vivas, L.; Petit, S.; Nallet, J.-P. *J. Med. Chem.* **2010**, *53* 699–714.

Newman, M. S. *J. Am. Chem. Soc.* **1940**, *62*, 1683–1687.

Nicolaou, K. C.; Snyder, S. A.; Montagnon, T.; Vassilikogiannakis, G. *Angew. Chem. Int. Ed.* **2002**, *41*, 1668–1698.

Nolde, F.; Pisula, W.; Müller, S.; Kohl, C.; Müllen, K. *Chem. Mater.* **2006**, *18*, 3715–3725.

O'Brien, D. H.; Hart, A. J.; Russell, C. R. *J. Am. Chem. Soc.* **1975**, *97*, 4410–4412.

Obayes, H. R.; Al Obaidy, A. H.; Alwan, G. H.; Al-Amiery, A. A. *Cogent Chemistry* **2015**, *1*, 1026638.

Obayes, H. R.; Al-Gebori, A. M.; Khazaal, S. H.; Jarad, A. J.; Alwan, G. H.; Al-Amiery, A. A. J. *Nanoelectron. Optoelectron.* **2015**, *10*, 711−716.

Olah G. A.; Mateescu, G. D. *J. Am. Chem. Soc.* **1970**, *92*, 1430–1432.

Omachi, H.; Nakayama, T.; Takahashi, E.; Segawa, T.; Itami, K. *Nature Chemistry* **2013**, *5*, 572–576.

Omachi, H.; Segawa, Y.; Itami, K. *Acc. Chem. Res.* **2012**, *45*, 1378–1389.

Orita, A.; Hasegawa, D.; Nakano, T.; Otera, J. *Chem. Eur. J.* **2002**, 8, 2000−2004.

Ozaki, K.; Kawasumi, K.; Shibata, M.; Ito, H.; Itami, K. *Nat. Commun.* **2015**, *6*, 6251.

P. Pouzet, I. Erdelmeier, D. Ginderow, J.-P. Mornon, P. Dansette, D. Mansuy, *J. Chem. Soc. Chem.* Commun. **1995**, 473–474.

Palermo, V.; Samori, P. *Angew. Chem. Int. Ed*. **2007**, *46*, 4428–4432.
Pauling, L. *J. Chem. Phys*. **1936**, *4*, 673–677.

Petrukhina, M. A.; Scott, L. T. Fragments of Fullerenes and Carbon Nanotubes: Designed Synthesis, Unusual Reactions, and Coordination Chemistry, Wiley, **2011**.

Piotrovsky, G. L. *Lvovskoe geol. Obshch., Mineral. Sbornik* **1955**, *9*, 120–127.

Pisula, W.; Kastler, M.; Wasserfallen, D.; Tadeusz, P.; Müllen, K. *J. Am. Chem. Soc.* **2004**, *126*, 8074–8075.

Plunkett, K. N.; Godula, K.; Nuckolls, C.; Tremblay, N.; Whalley, A. C.; Xiao, S. *Org. Lett.* **2009**, *11*, 2225–2228.

Potticary, J.; Terry, L. R.; Bell, C.; Papanikolopoulos, A. N.; Christianen, P. C. M.; Engelkamp, H.; Collins, A. M.; Fontanesi, C.; Kociok-Köhn, G.; Crampin, S.; Da Como, E.; Hall, S. R. *Nat. Commun.* **2016**, *7*, 11555.

Raasch, M. S. in *Chemistry of Heterocyclic Compounds, Thiophene and its Derivatives*, ed. Gronwitz, S. John Wiley & Sons; New Jersey, **1985**, *44*, 571–628.

Randic M. *J. Mol. Chem. (Theochem)* **1991**, *229*, 139–153.

Rao, K. V.; George, S. J. *Org. Lett.* **2010,** *12*, 2656–2659.

Reisch, H. A.; Bratcher, M. S.; Scott, L. T. *Org. Lett.* **2000**, *2*, 1427–1430.

Rempala, P.; Kroulík, J.; King, B. T. *J. Am. Chem. Soc.* **2004**, *126*, 15002–15003.

Ren, S.; Seki, T.; Necas, D.; Shimizu, H.; Nakajima, K.; Kanno, K.; Song, Z.; Takahashi, T. *Chem. Lett.* **2011**, *40*, 1443–1444.

Rheinhoudt, D. N.; Kouwenhoven, C. G. *Tetrahedron* **1974**, *30*, 2093–2098.

Rheinhoudt, D. N.; Trompenaars, W. P.; Geevers, J. *Tetrahedron Lett.* **1976**, *17*, 4777–4780.

Robertson, J. M.; Trotter, J. *J. Chem. Soc.* **1961,** 1280–1284.

Robertson, J. M.; White, J. G. *J. Chem. Soc.* **1945**, 607–617.

Robertson, J. M.; White, J. G. *Nature* **1944**, *169*, 605–606.

Rohr, U.; Kohl, C.; Müllen, K.; van de Craats, A.; Warman, J. *J. Mater. Chem.,* **2001**, *11*, 1789–1799.

Rohr, U.; Schlichting, P.; Böhm, A.; Gross, M.; Meerholz, K.; Bräuchle, C.; and Müllen, K. *Angew. Chem. Int. Ed.* **1998**, *37*, 1434–1437.

Sakamoto, Y.; Suzuki, T. *J. Am. Chem. Soc.* **2013**, *135*, 14074–14077.

Salcedo, R.; Sansores, L. E.; Picazo, A.; Sansón, L. *J. Mol. Struct. (Theochem.)* **2004**, *678*, 211–215.

Samorí, P.; Severin, N.; Simpson, C. D.; Müllen K.; Rabe, J. P. *J. Am. Chem. Soc.* **2002**, *124*, 9454–9457.

Sato, M.; Yamamoto, K.; Sonobre, H.; Yano, K.; Matsubara, H.; Fujita, H.; Sugiomoto, T. *J. Chem. Soc. Perkin Trans. 2* **1998**, 1909–1914.

Schaefer T.; Schneider, W. G. *Can. J. Chem.* **1963**, *41*, 966–982.

Scholl, R.; Meyer, K. *Ber. Dtsch. Chem. Ges. A* **1932**, *65*, 902–915.

Schuster, N. J.; Paley, D. W.; Jockusch, S.; Ng, N.; Steigerwald, M. L.; Nuckolls, C. *Angew. Chem. Int. Ed.* **2016**, *55,* 13519–13523.

Scott, L. T.; Boorum, M. M.; McMahon, B. J.; Hagen, S.; Mack, J.; Blank, J.; Wegner, H.; De Meijere, A. *Science* **2002**, *295*, 1500–1503.

Scott, L. T.; Cheng, P.-C.; Hashemi, M. M.; Bratcherm M. S.; Meyer, D. T.; Warren, H. B. *J. Am. Chem. Soc.* **1997**, *119*, 10963–10968.

Scott, L. T.; Hashemi, M. M.; Meyer, D. T.; Warren, H. B. *J. Am. Chem. Soc.* **1991**, *113*, 7082–7084.

Scott, L. T.; Jackson, E. A.; Zhang, Q.; Steinberg, B. D.; Bancu, M.; Li, B. *J. Am. Chem. Soc.* **2011**, *134*, 107–110.

Shapiro, E. L.; Becker, E. I. *J. Am. Chem. Soc.* **1953**, *75,* 4769–4775.

Shen, H. -S.; Tang, J. -M.; Chang, H. -K.; Yang, C. -Y.; Liu, R. -S. *J. Org. Chem.* **2005**, *70*, 10113–10116.

Shen, M.; Ignatyev, I. S.; Xie, Y.; Schaefer III, H. F. *J. Phys. Chem.* **1993**, *97*, 3212–3216.

Shu, Y.; Lim, Y.; Li, Z. *Chem. Sci.* **2011**, *2*, 363–368.
Simpson, S. D.; Brand, J. D.; Berresheim, A. J.; Przybilla, L.; Rader, H. J.; Müllen, K. *Chem. Eur. J.* **2002**, *8*, 1424–1429.

Sivasakthikumaran, R.; Nandakumar, M.; Mohanakrishnan, A. K. *J. Org. Chem.* **2012**, *77*, 9053–9071.

Skibbe, V.; Erker, G. *J. Organomet. Chem.* **1983**, *241*, 15–26.

Solá, M. *Front. Chem.* **2013**, *1*, 1–22.

Spiesecke H.; Schneider, W. G. *Tetrahedron Lett.* **1961**, 468–472.

Stabel, A.; Herwig, P.; Müllen, K.; Rabe, J. P. *Angew. Chem. Int. Ed. Engl*. **1995**, *34*, 1609–1611.

Steiner, E.; Fowler, P. W. *J. Phys. Chem. A* **2001**, *105*, 9553–9562.

Steiner, E.; Fowler, P. W.; Jenneskens, L. W. *Angew. Chem., Int. Ed.* **2001**, *40*, 362–366.

Stone, A. J.; Wales, D. J. *Chem. Phys. Lett.* **1986**, *128*, 501–503.

Sugimoto, K.; Hayashi, R.; Nemoto, H.; Toyooka, N.; Matsuya, Y. *Org. Lett.* **2012**, *14*, 3510–3513.

Suh, M. C.; Jiang, B.; Tilley, T. D. *Angew. Chem. Int. Ed.* **2000**, *39*, 2870–2837.

Sumy, D. P.; Dodge, N. J.; Harrison C. M.; Finke, A. D.; Whalley, A. C. *Chem. Eur. J.* **2016**, *22*, 4709–4712.

Sumy, D. P.; Finke, A. D.; Whalley, A. C. *Chem. Commun.* **2016**, *52*, 12368–12371.

Suzuki, S.; Segawa, Y.; Itami, K.; Yamaguchi, J. *Nature Chemistry.* **2015**, *7*, 227–233.

Sygula, A.; Fronczek, F.; Sygula, R.; Rabideau, P.; Olmstead, M. *J. Am. Chem. Soc.* **2007**, *129*, 3842–3843.

Sygula, A.; Rabideau, P. W. *J. Mol. Struc. (Theochem)* **1995**, *333*, 215–226.

Sygula, A.; Rabideau, P. W. Carbon-Rich Compounds (eds Haley, M. M.; Tykwinski, R. R.) 529–565 Wiley-VCH, **2006**.

Takase, M.; Enkelmann, V.; Sebastiani, D.; Baumgarten, M.; Müllen, K. *Angew. Chem. Int. Ed*. **2007**, *46*, 5524–5527.

Takase, M.; Narita, T.; Fujita, W.; Asano, M. S.; Nishinaga, T.; Benten, H.; Yoza, K.; Müllen, K. *J. Am. Chem. Soc*. **2013**, *135*, 8031–8040.

Thibault, M. E.; Closson, T. L. L.; Manning, S. C.; Dibble, P. W. *J. Org. Chem*. **2003,** *68*, 8373–8378.

Thiemann, C.; Thiemann, T.; Li, Y.; Sawada, T.; Nagano, Y.; Tashiro, M. *Bull. Chem. Soc. Jpn.* **1994**, *67*, 1886–1893.

Thiemann, T,; Ohira, D.; Li, Y.; Sawada, T.; Mataka, S.; Rauch, K.; Noltemeyer, M.; de Meijere, A. *J. Chem. Soc., Perkin Trans. 1.* **2000**, 2968–2976.

Thiemann, T.; Sá e Melo, M. L.; Campos Neves, A. S.; Li, Y.; Mataka, S.; Tashiro, M.; Geißler, U.; Walton, D. *J. Chem. Research (S)* **1998**, 346–347.

Thulin, B.; Wennerström, O. *Acta. Chem. Scand. B.* **1976**, *30b*, 369–371.

Tokoro, Y.; Oishi, A.; Fukuzawa, S. *Chem. Eur. J.* **2016**, *22*, 13908−13915.

Tremblay, N. J.; Gorodetsky, A. A.; Cox, M. P.; Schiros, T.; Kim, B.; Steiner, R.; Bullard, Z.; Sattler, A.; So, W. -Y.; Itoh, Y.; Toney, M. F.; Ogasawara, H.; Ramirez, A. P.; Kymissis, I.; Steigerwald, M. L.; Nuckolls, C. *Chem. Phys. Chem.* **2010**, *11*, 799–803.

Tsefrikas, V. M.; Scott, L. T. *Chem. Rev.* **2006**, *106*, 4868–4884.

Ueda, H.; Yamaguchi, M.; Kameya, H.; Sugimoto, K.; Tokuyama, H. *Org Lett.* **2014**, *16*, 4948–4951.

van der Auweraer, M.; De Schryver, F. C. *Nat. Mater.* **2004**, *3*, 507–508.

Wang, L.; Shevlin, P. B. *Org. Lett.* **2000**, *2*, 3703–3705.

Wang, L.; Shevlin, P. B. *Tetrahedron Lett.* **2000**, *41*, 285–288.

Wang, Z.; Dçtz, F.; Enkelmann, V.; Müllen, K. Angew. Chem. Int. Ed. **2005**, *44*, 1247–1250.

Whalley, A. C.; Plunkett, K. N.; Gorodetsky, A. A.; Schenck, C. L.; Chiu, C. -Y.; Steigerwald, M. L.; Nuckolls, C. *Chem. Sci.* **2011**, *2*, 132–135.

Wong, H. N. C. *Acc. Chem. Res.* **1989**, *22,* 145–152.

Wong, H. N. C.; Garratt, P. J.; Sondheimer, F. J. Am. Chem. Soc. **1974**, *96*, 5604−5605.

Wong, H. N. C.; Man, Y. -M.; Mak, T. C. W. *Tetrahedron Lett.* **1987**, *28,* 6359–6362.
Wu, D.; Zhang, H.; Liang, J.; Ge, H.; Chi, C.; Wu, J.; Liu, S. H.; Yin, J *J. Org. Chem.* **2012**, *77*, 11319–11324.

Wu, J.; Pisula, W.; Müllen, K. *Chem. Rev.* **2007**, *107*, 718–747.

Wu, J.; Tomovic, Z.; Enkelmann, V.; Müllen, K. *J. Am. Chem. Soc.* **2004**, *69*, 5179–5186.

Wu, T. -C.; Chen, M. -K.; Lee, Y. -W.; Kuo, M. -Y.; Wu, Y. -T. *Angew. Chem. Int. Ed.* **2013**, *52*, 1289–1293.

Wu, Y-T.; Siegel, J. S. *Chem. Rev.* **2006**, *106*, 4843–4867.

Wu, Y. -T.; Siegel, J. S. *Chem. Rev.* **2006**, *106*, 4843–4867.

Würthner, F. *Chem. Commun.* **2004**, 1564–1579.

Xiao, S.; Myers, M.; Miao, Q.; Sanaur, S.; Pang, K.; Steigerwald, M. L.; Nuckolls, C. *Angew. Chem. Int. Ed.* **2005**, *44*, 7390–7394.

Xiao, S.; Tang, J.; Beetz, T.; Guo, X.; Tremblay, N.; Siegrist, T.; Zhu, T.; Steigerwald, M.; Nuckolls, C. *J. Am. Chem. Soc.* **2006**, *128*, 10700–10701.

Yamamoto, K.; Harada, T.; Nakazaki, M.; Nakao, T.; Kai, Y.; Harada, S.; Kasai, N. *J. Am. Chem. Soc.* **1983**, *105*, 7171–7172.

Yamamoto, K.; Harada, T.; Okamoto, Y.; Chikamatsu, H.; Nakazaki, M.; Kai, M.; Nakao, T.; Tanaka, M.; Harada, S.; Kasai, N. *J. Am. Chem. Soc.* **1988**, *110*, 3578–3584.

Yamamoto, K.; Sonobe, H.; Matsubara, H.; Sato, M.; Okamoto, S.; Kitaura, K. *Angew. Chem. Int. Ed. Engl.* **1996**, *35*, 69–70.

Yan, Q.; Cai, K. Zhang, C. Zhao, D. *Org. Lett.* **2012**, 4654–4657.

Yan, X; Xi, C. *Acc. Chem. Res.* **2015**, *48*, 935–946.

Yao, P.; Zhang, Y.; Hsung, R.; Zhao, K. *Org. Lett.* **2008**, *10*, 4275–4278.

Zabula, A. V.; Spisak, S. N.; Filatov, A. S.; Grigoryants, V. M.; Petrukhina, M. A. *Chem. Eur. J.* **2012**, *18*, 6476–6484.

Zhai, L.; Shukla, R.; Wadumethrige, S. H.; Rathore, R. *J. Org. Chem.* **2010**, *75*, 4748−4760.

Zhang, B.; Tuan Trinh, M.; Fowler, B.; Ball, M.; Xu, Q.; Ng, F.; Steigerwald, M. L.; Zhu, X. –Y.; Nuckolls, C.; Zhong, Y. *J. Am. Chem. Soc.* **2016**, *138*, 16426–16431.

Zhang, C.; Shi, K.; Cai, K.; Xie, J.; Lei, T.; Yan, Q.; Wang, J.-Y.; Pei, J.; Zhao, D. *Chem. Commun.* **2015**, *51*, 7144–7147.

Zhang, Q.; Peng, H.; Zhang, G.; Lu, Q.; Chang, J.; Dong, Y.; Shi, X.; Wei, J. *J. Am. Chem. Soc.* **2014**, *136,* 5057–5064.

Zhao, D.; Wu, Q.; Cai, Z.; Zheng, T.; Chen, W.; Lu, J.; Yu, L. *Chemistry of Materials* **2016**, *28*, 1139–1146.

Zhong, Y.; Kumar, B.; Oh, S.; Trinh, M. T.; Wu, Y.; Elbert, K.; Li, P.; Zhu, X.; Xiao, S.; Ng, F.; Steigerwald, M. L.; Nuckolls, C. *J. Am. Chem. Soc.* **2014**, *136*, 8122–8130.

Zhou, Z. *J. Phys. Org. Chem.* **1995**, *8*, 103–107.

Zirngast, M; Marschner, C.; Baumgertner, J. *Organometallics* **2008**, *27*, 2570–2583.

Zydziak, N.; Yameen, B.; Barner-Kowollik, C.; *Polym. Chem.* **2013**, *4*, 4072–4086.

APPENDIX I: SPECTROSCOPIC DATA

AI.1 Experimental Data for SYNTHESIS, STRUCTURAL DATA, AND FUNCTIONALIZATION OF TETRABENZO[8[CIRCULENE
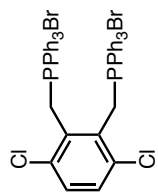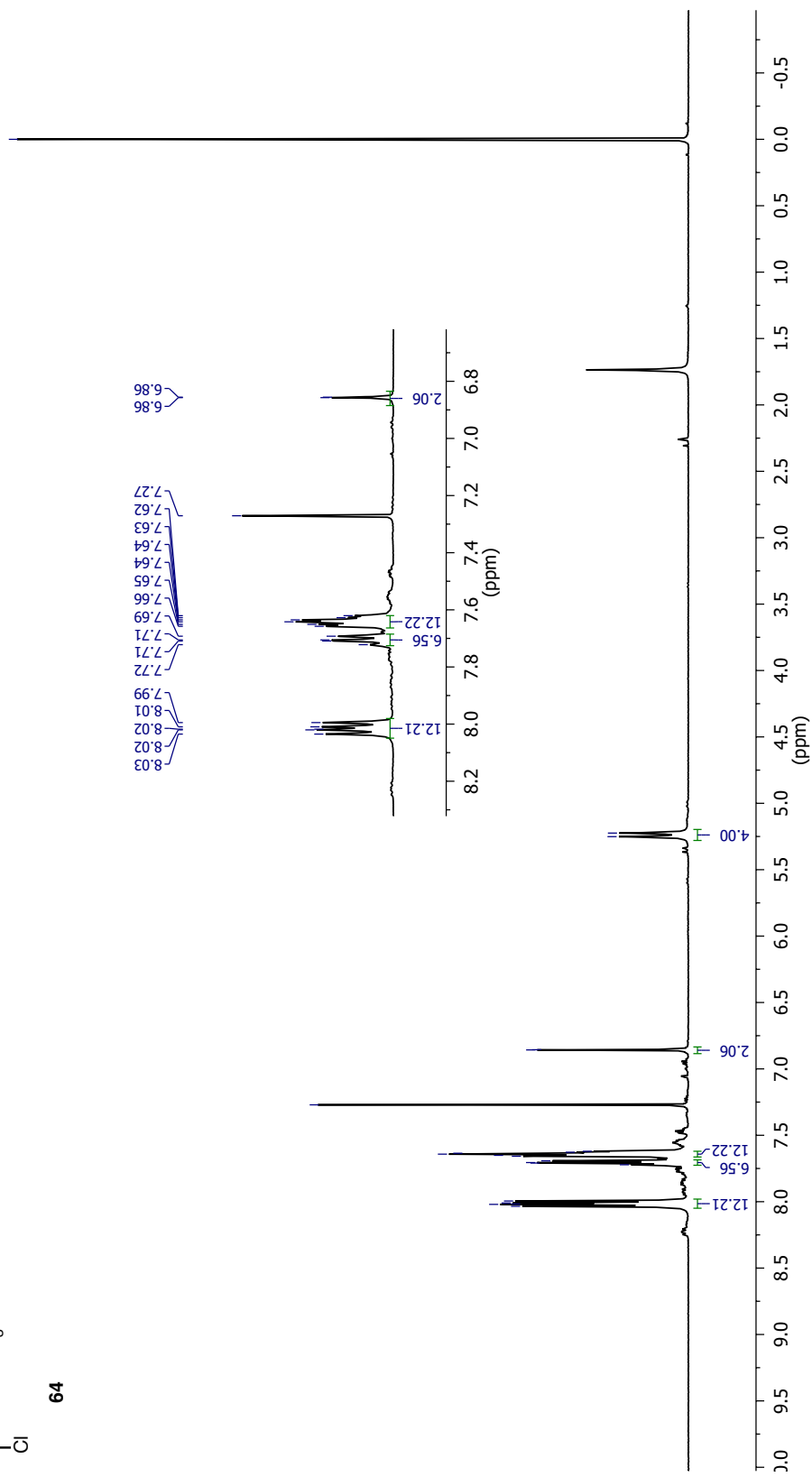
Figure A1.1 ^{1}H NMR Spectrum of **64** in CDCl$_3$
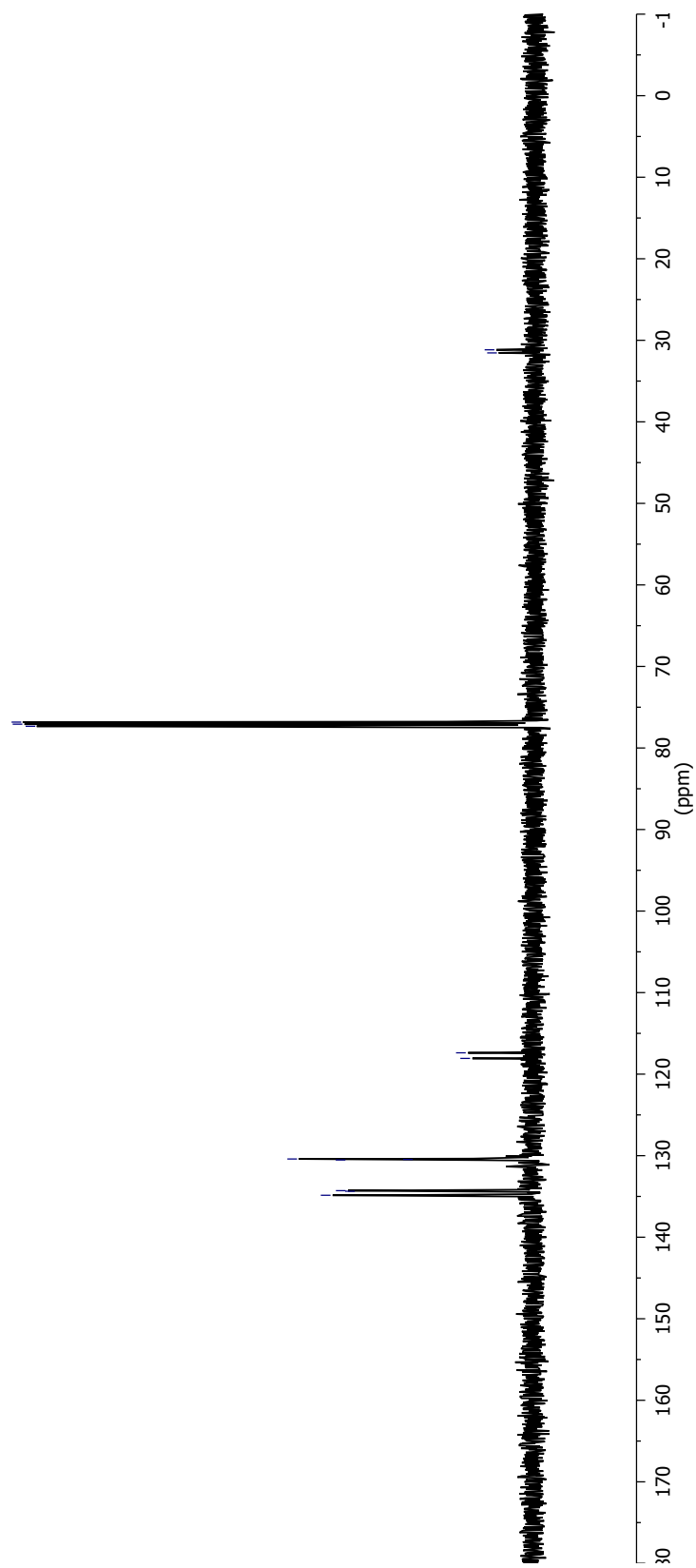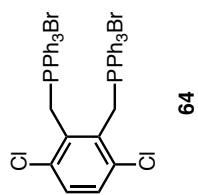
Figure AI.2 ^{13}C NMR Spectrum of **64** in CDCl$_3$
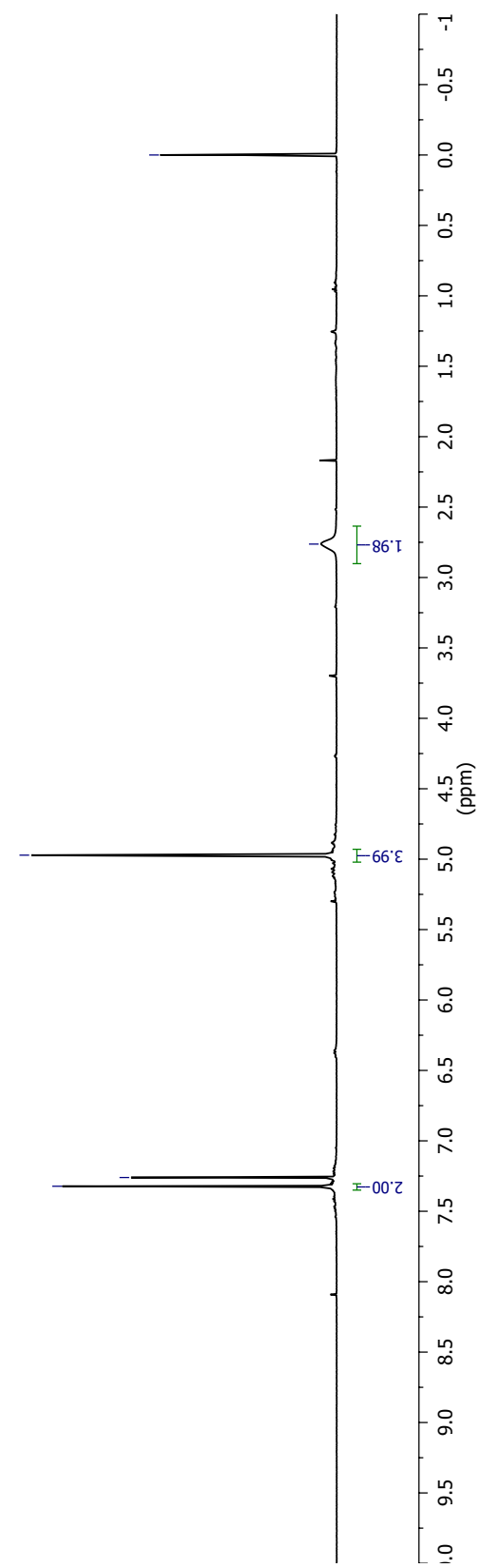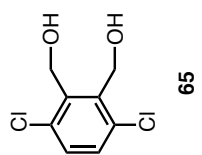
Figure AI.3 ^{1}H NMR Spectrum of **65** in CDCl$_3$

176
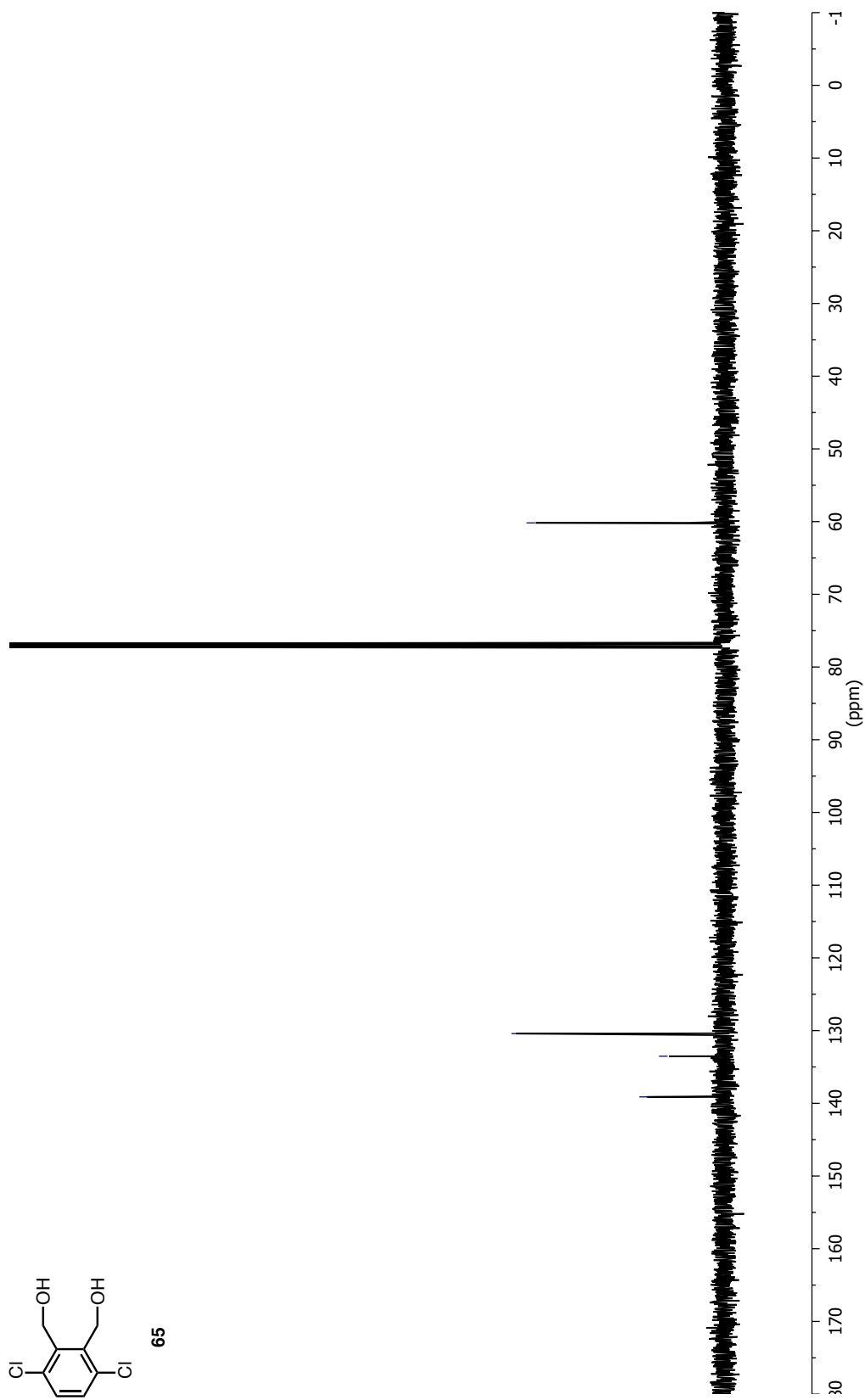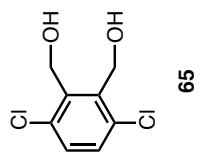
Figure AI.4 ^{13}C NMR Spectrum of **65** in CDCl$_3$

177
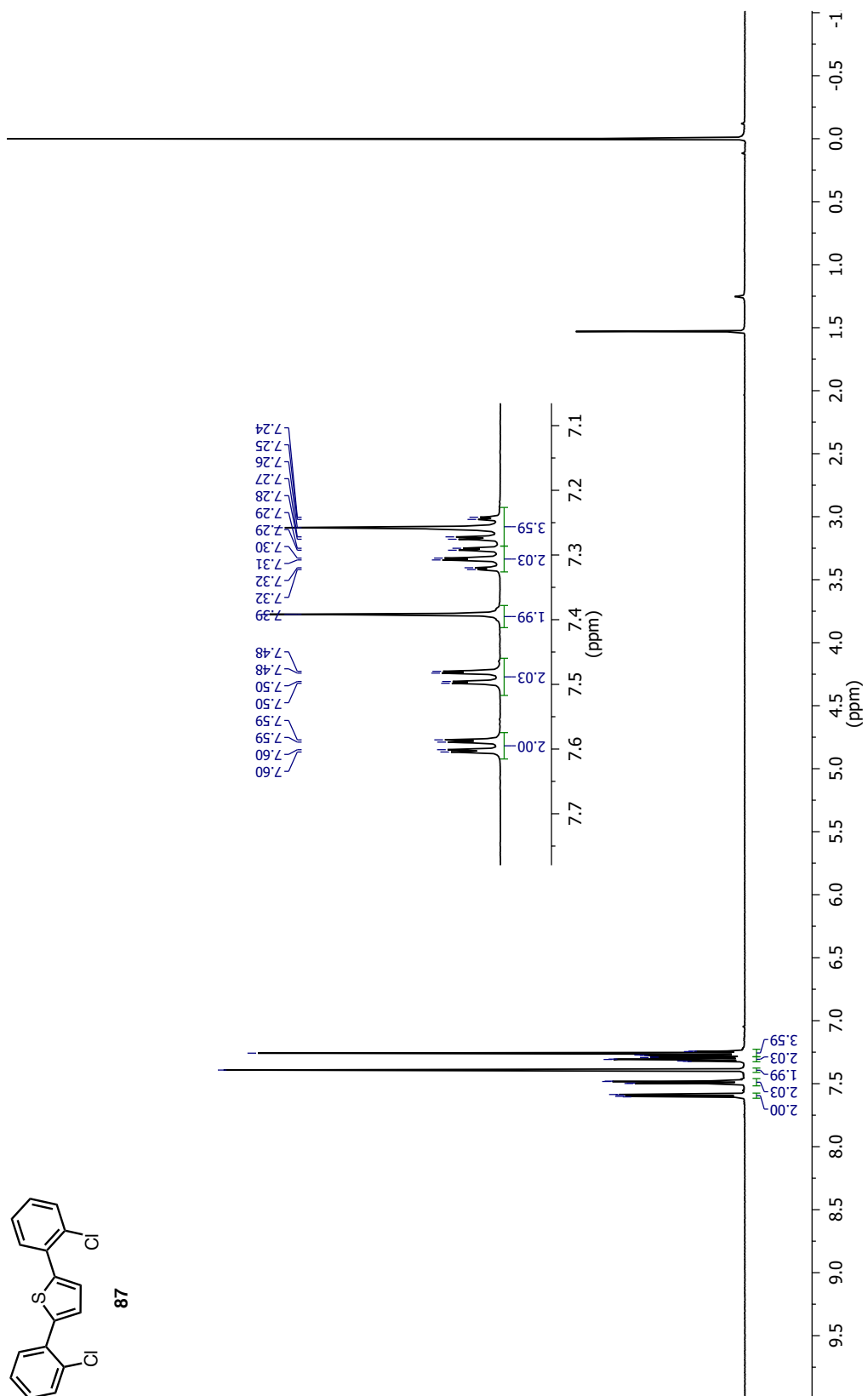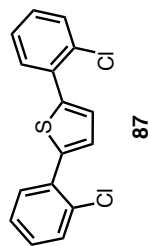
Figure AI.5 ^{1}H NMR Spectrum of **87** in CDCl$_3$

178
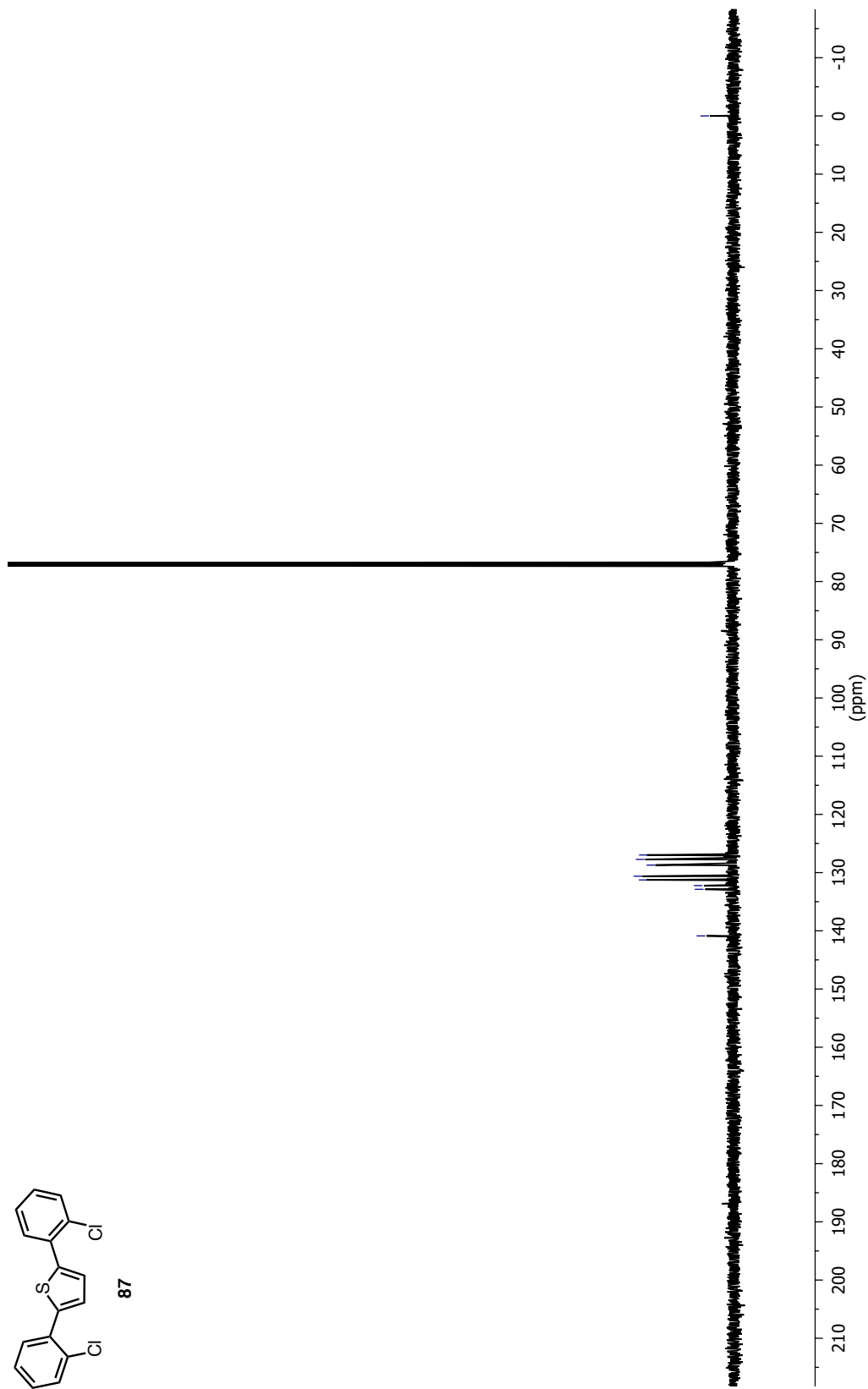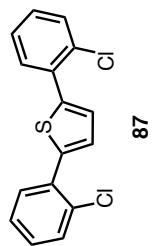
Figure AI.6 ^{13}C NMR Spectrum of **87** in CDCl$_3$

179
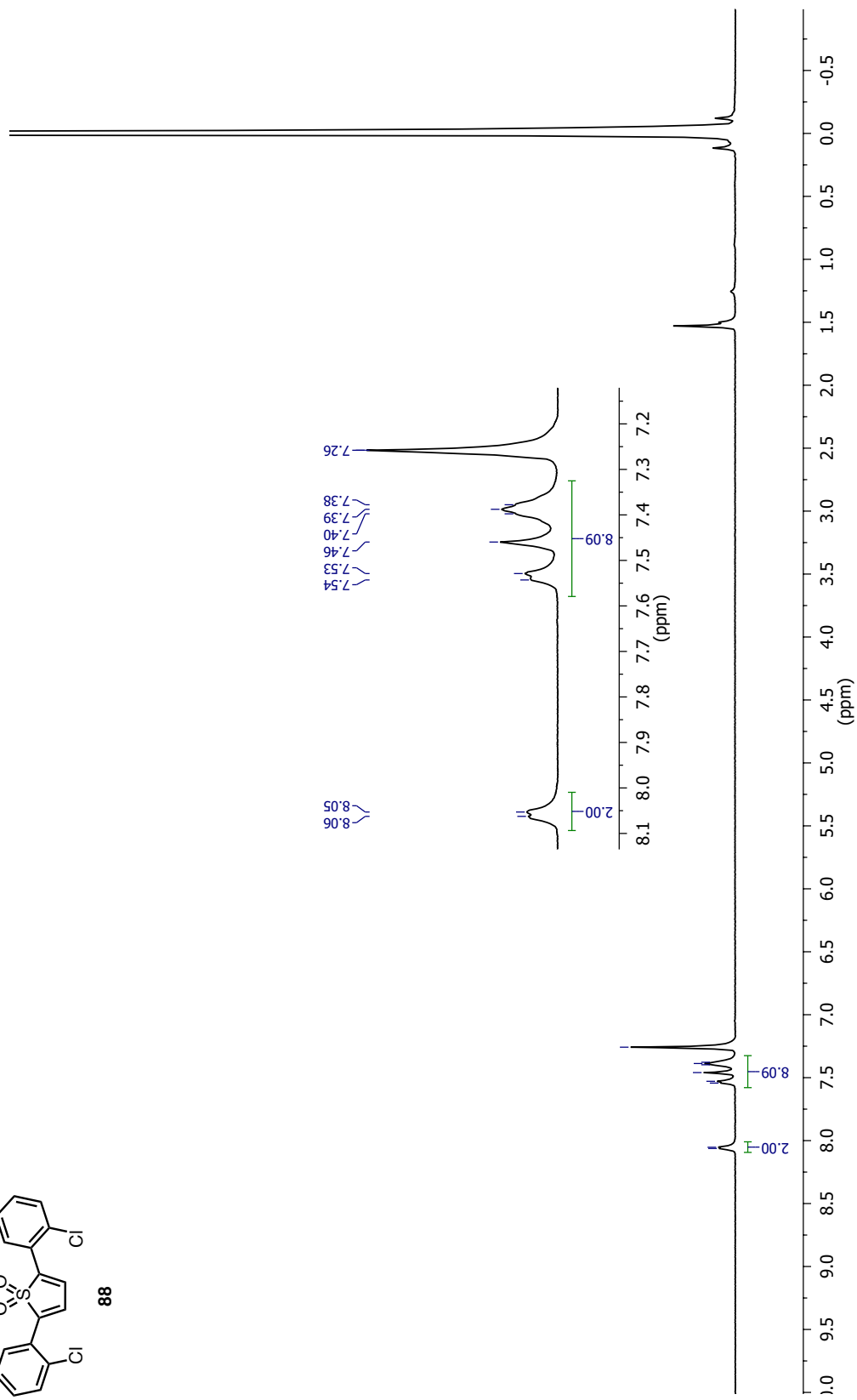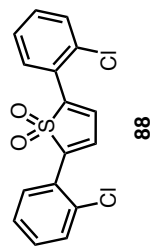
Figure AI.7 ^{1}H NMR Spectrum of **88** in CDCl$_3$
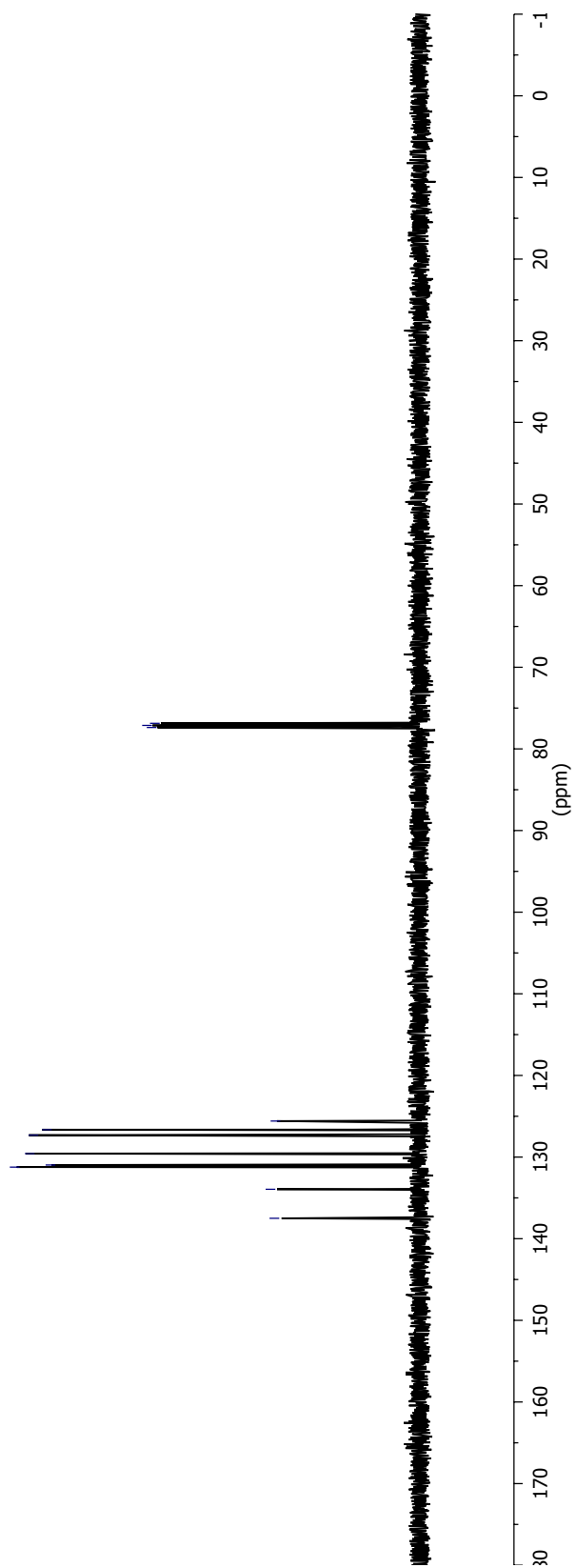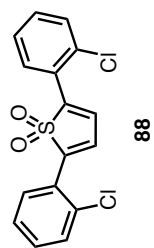
Figure AI.8 ^{13}C NMR Spectrum of **88** in CDCl$_3$

181
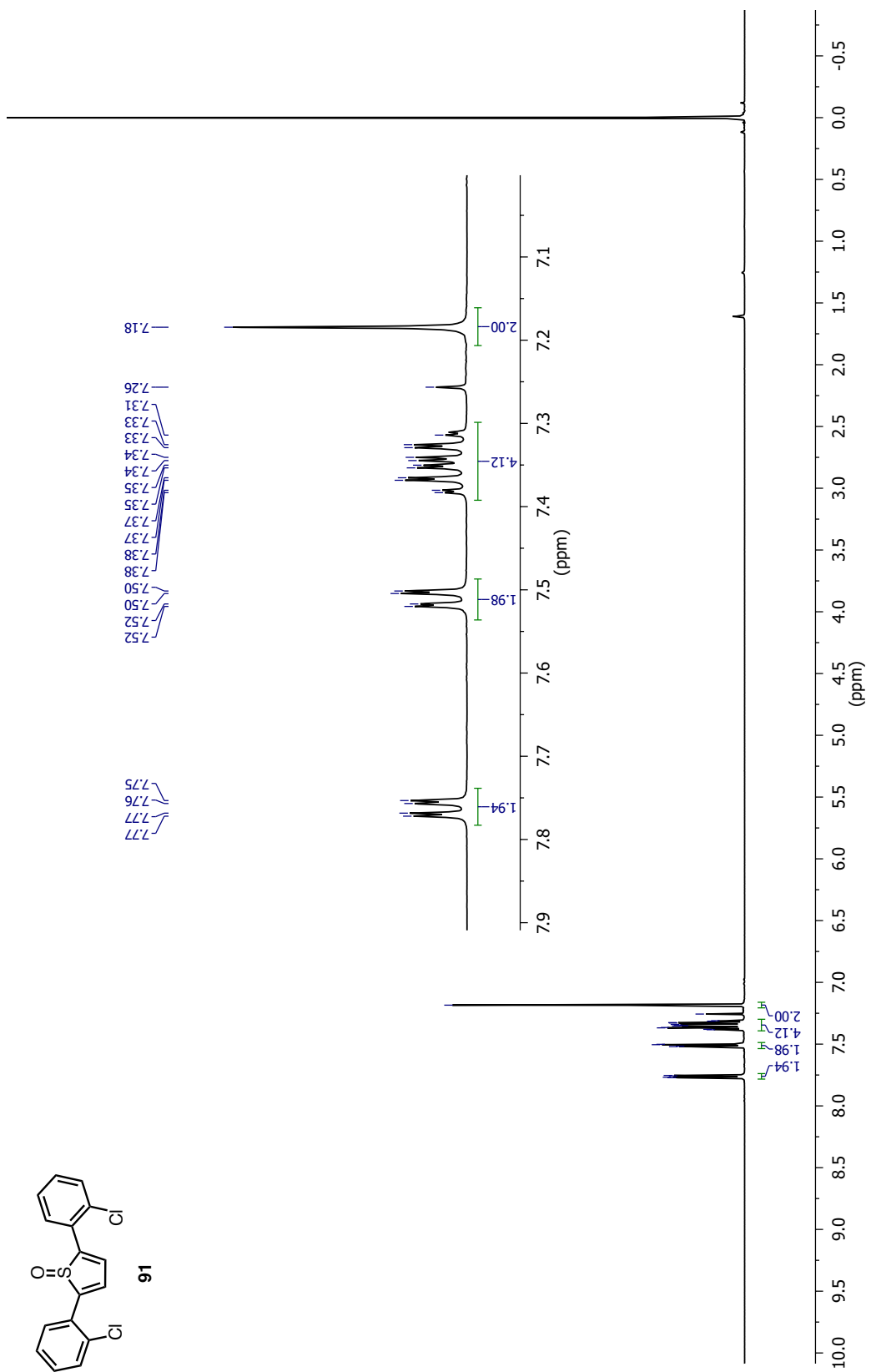
Figure AI.9 ^{1}H NMR Spectrum of **91** in CDCl$_3$

182
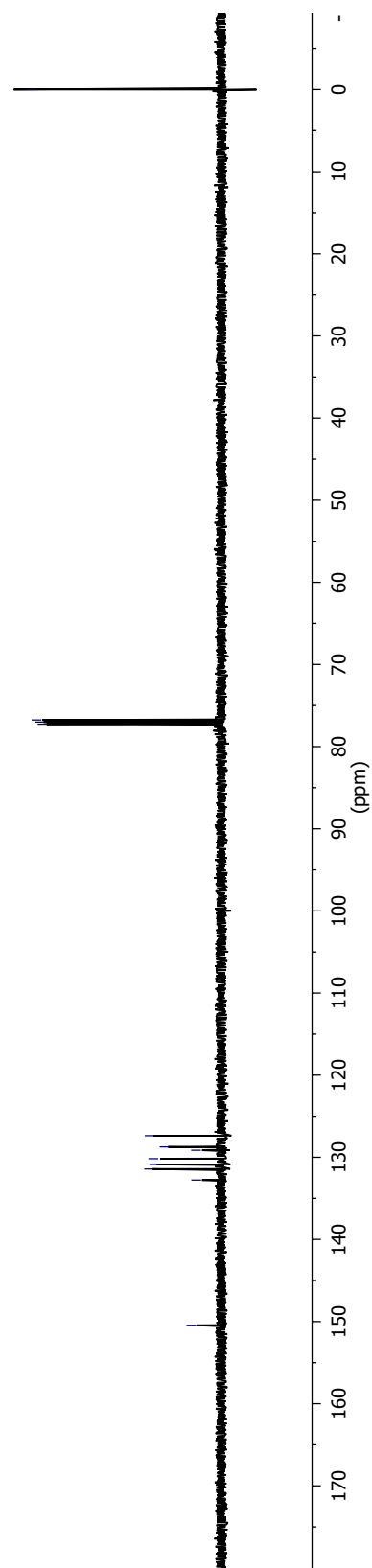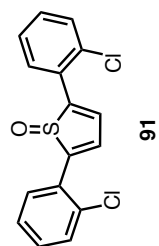
Figure AI.10 ^{13}C NMR Spectrum of **91** in CDCl$_3$

183
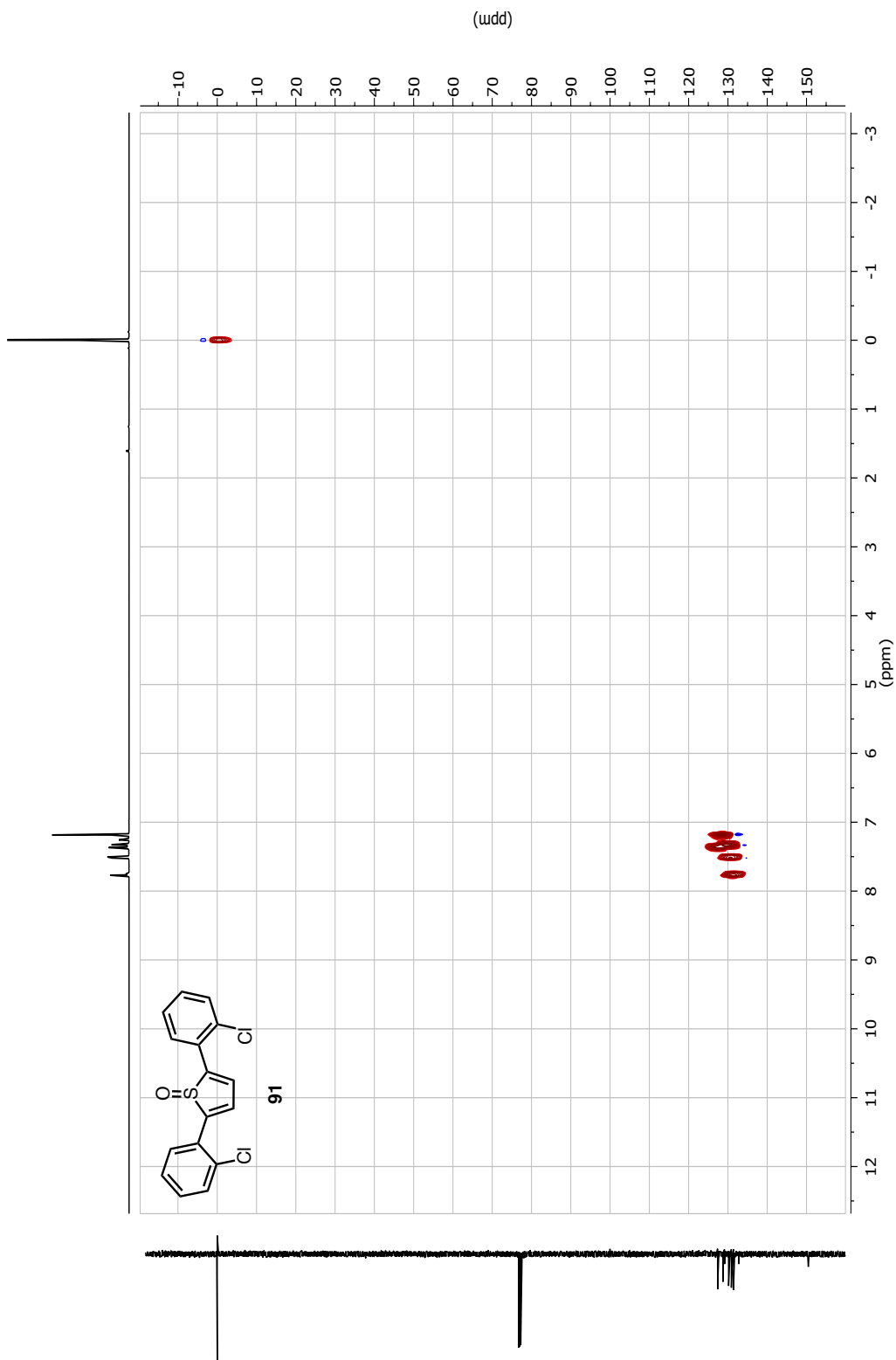
Figure AI.11 2D HSQC NMR Spectrum of **91** in CDCl$_3$
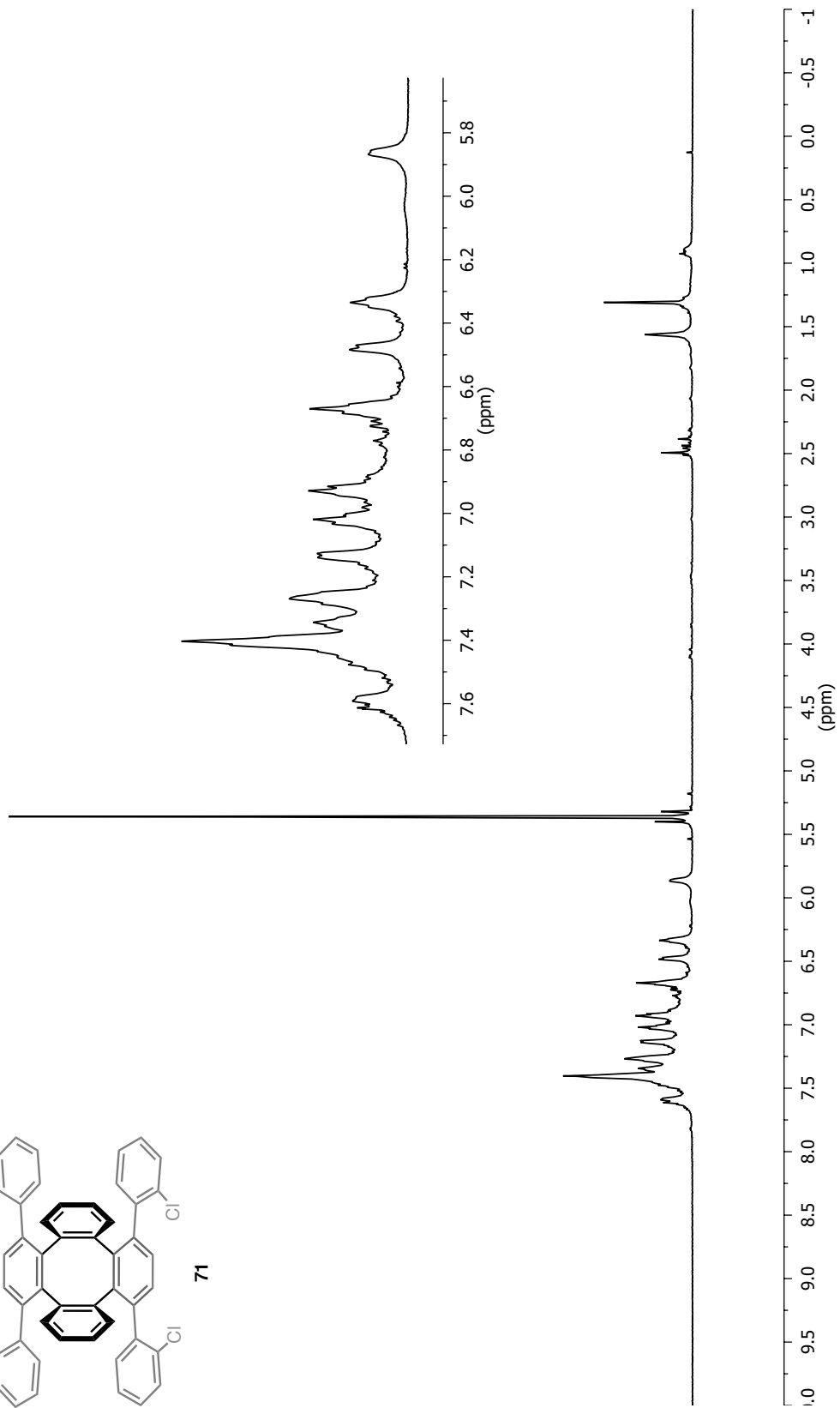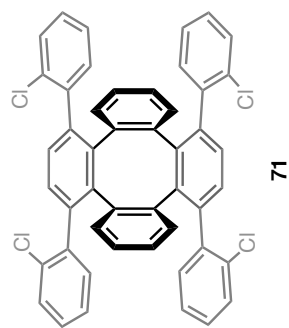
Figure AI.12 ^{1}H NMR Spectrum of **71** in CDCl$_3$

185
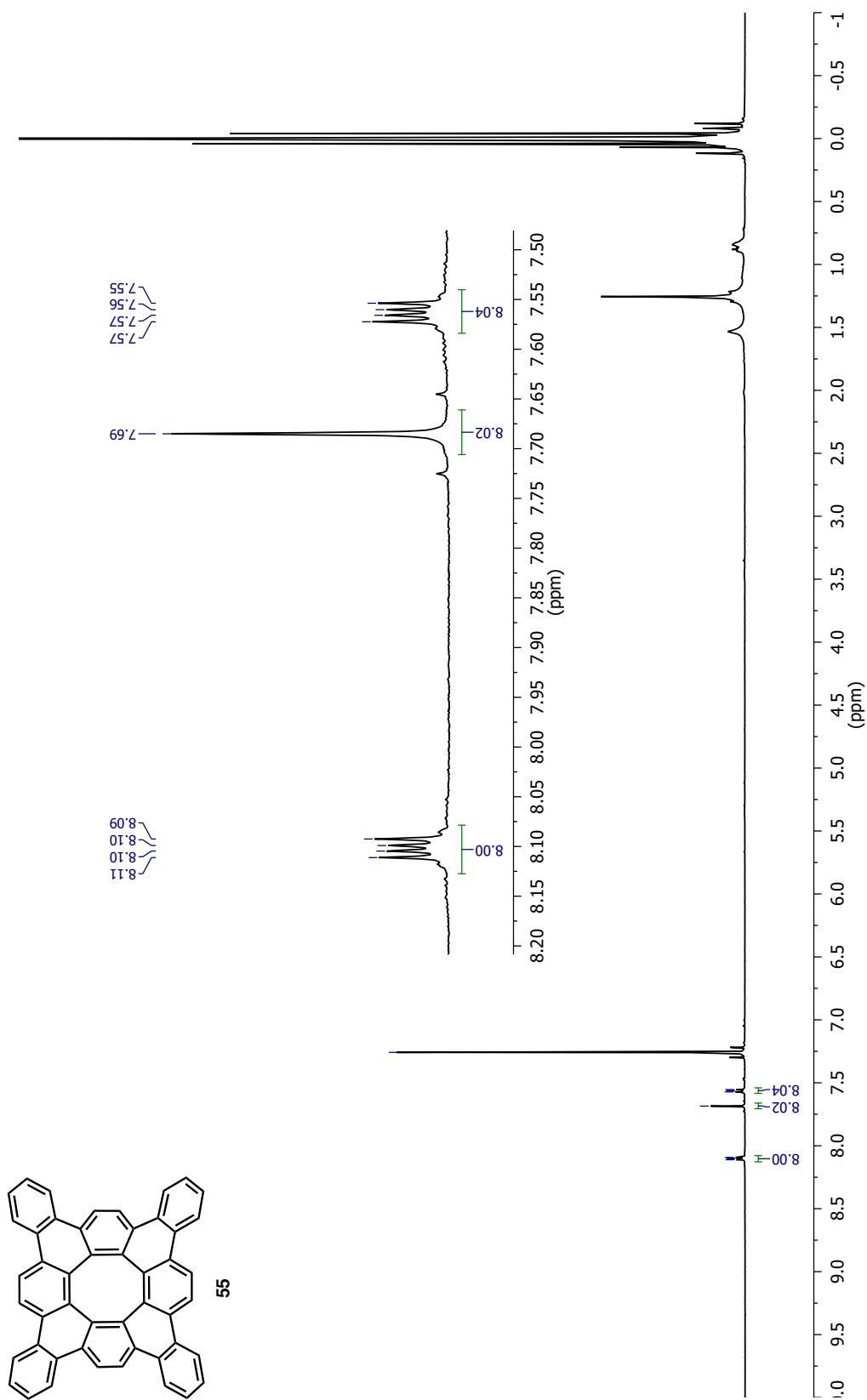
Figure AI.13 ^{1}H NMR Spectrum of **55** in CDCl$_3$
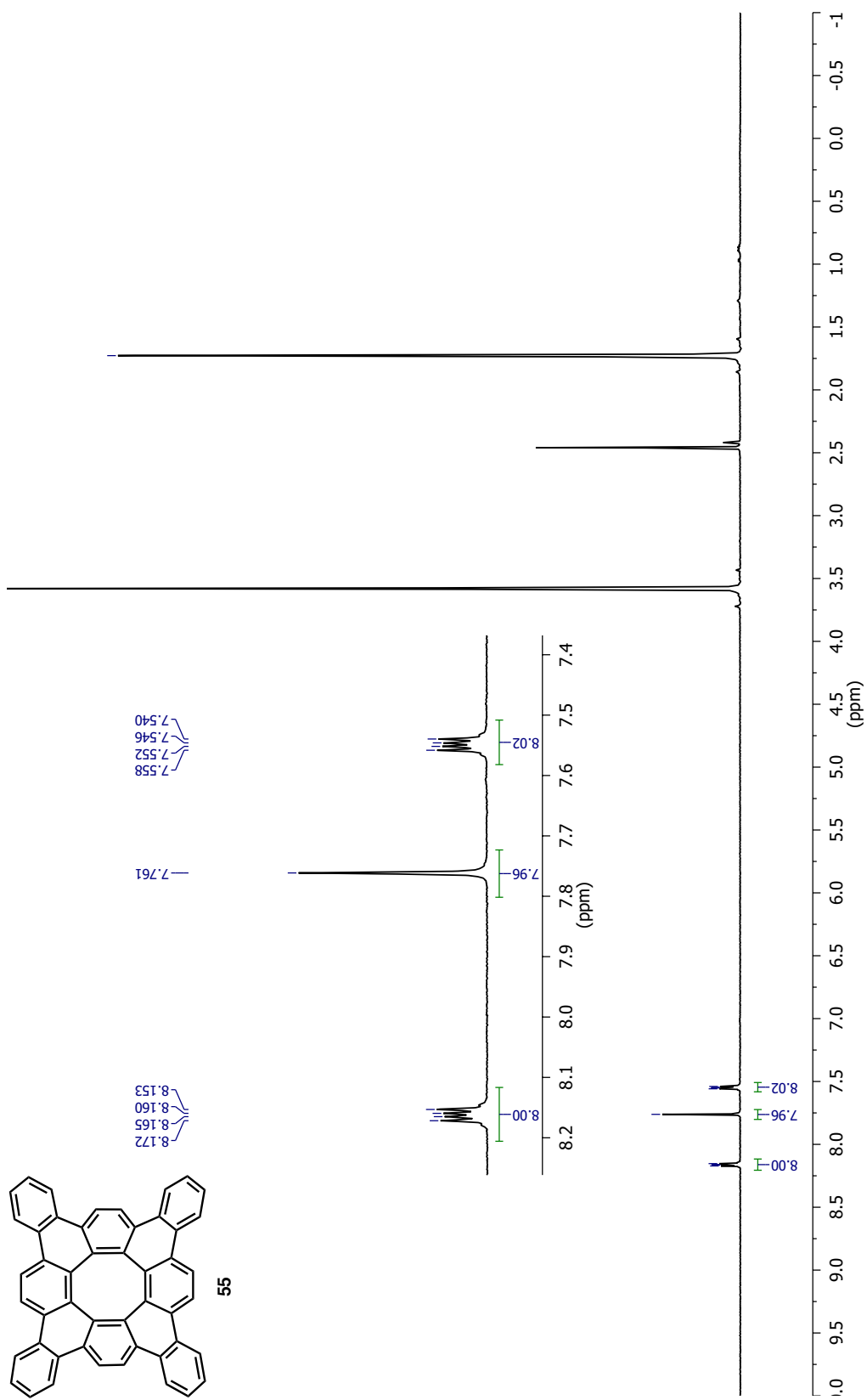
Figure AI.14 ^{1}H NMR Spectrum of **55** in THF-d_8

187
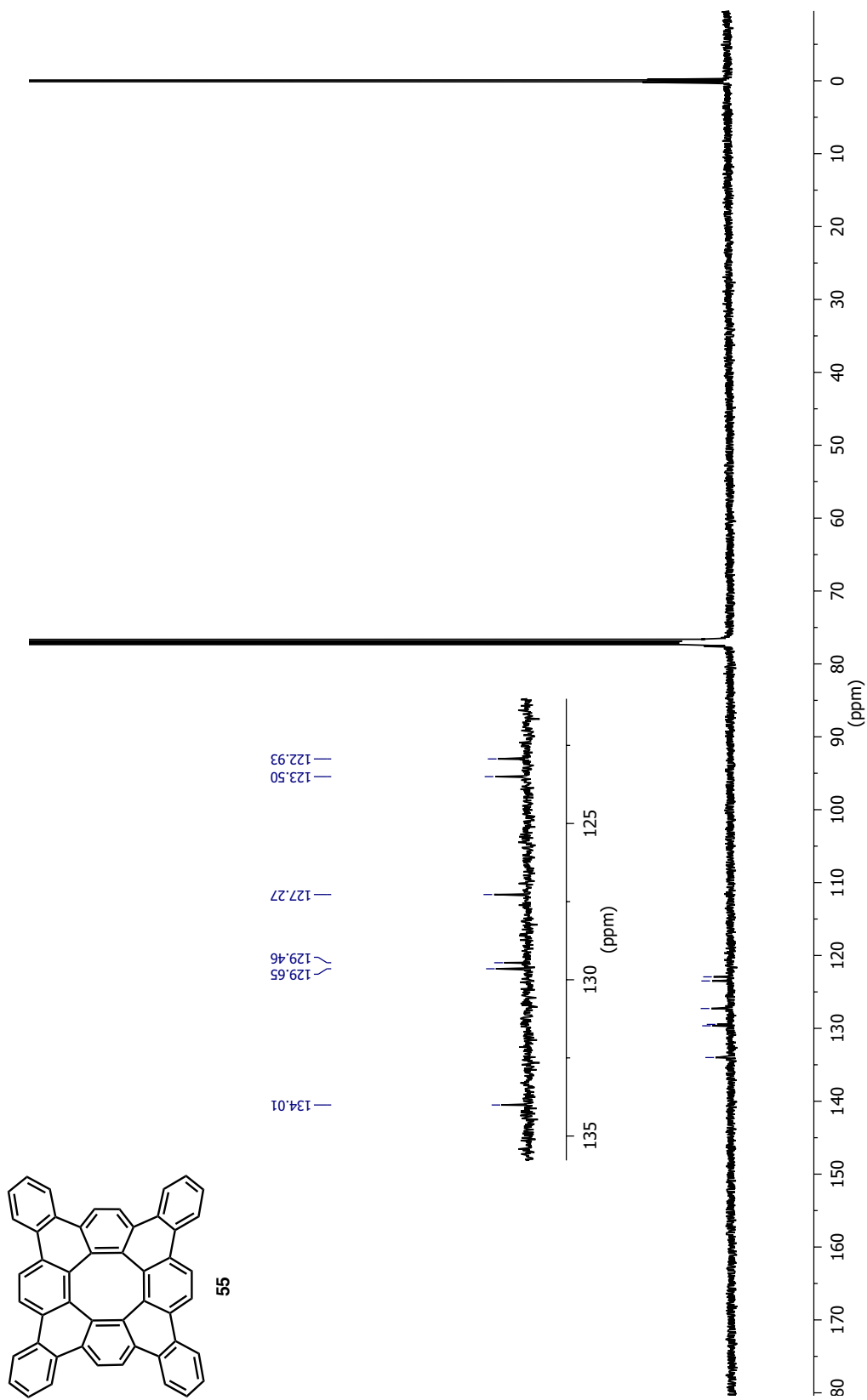
Figure AI.15 ^{13}C NMR Spectrum of **55** in CDCl$_3$

188
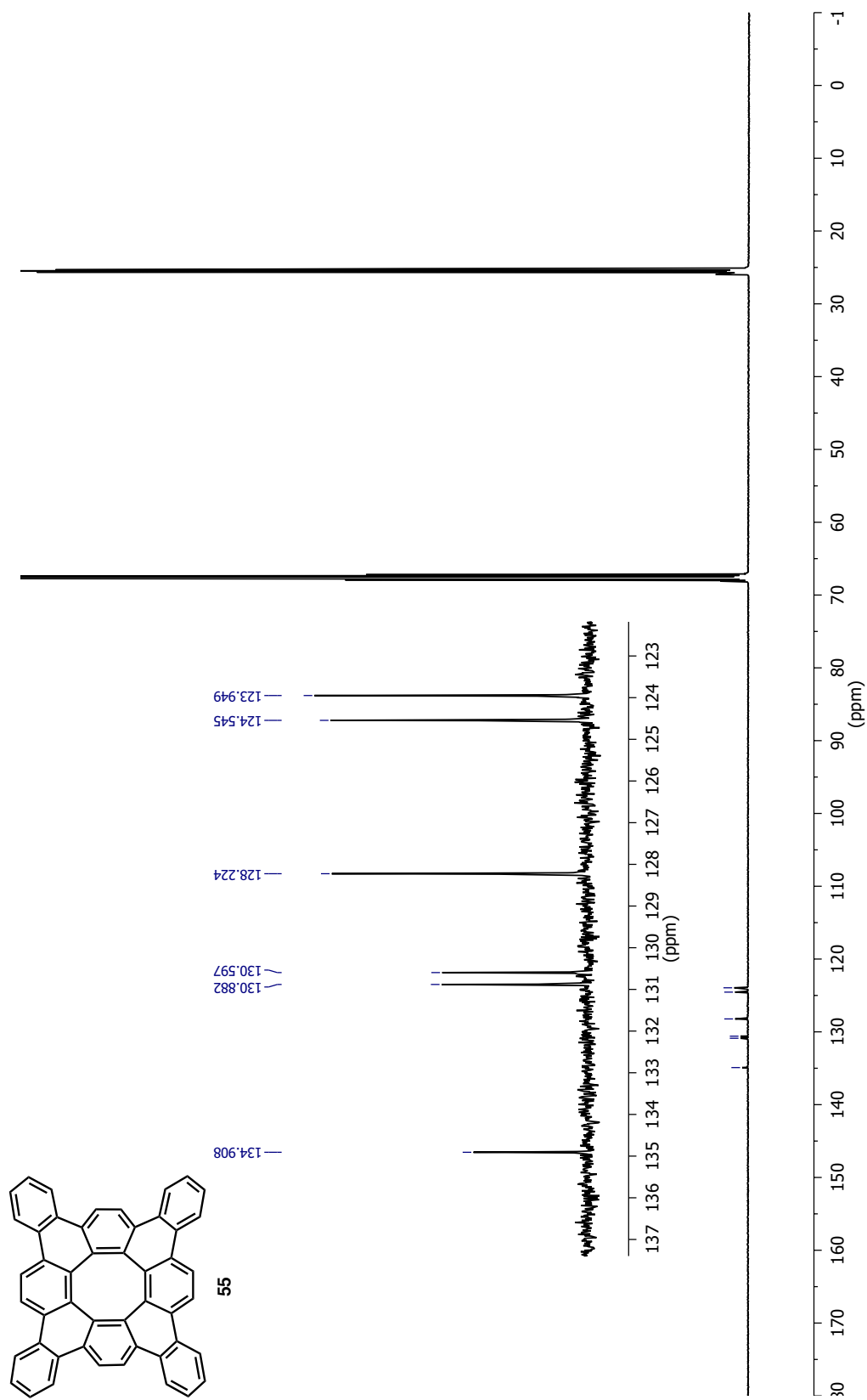
Figure AI.16 ^{13}C NMR Spectrum of **55** in THF-d_8

189

Figure AI.17 2D HSQC NMR Spectrum of **55** in THF-d_8
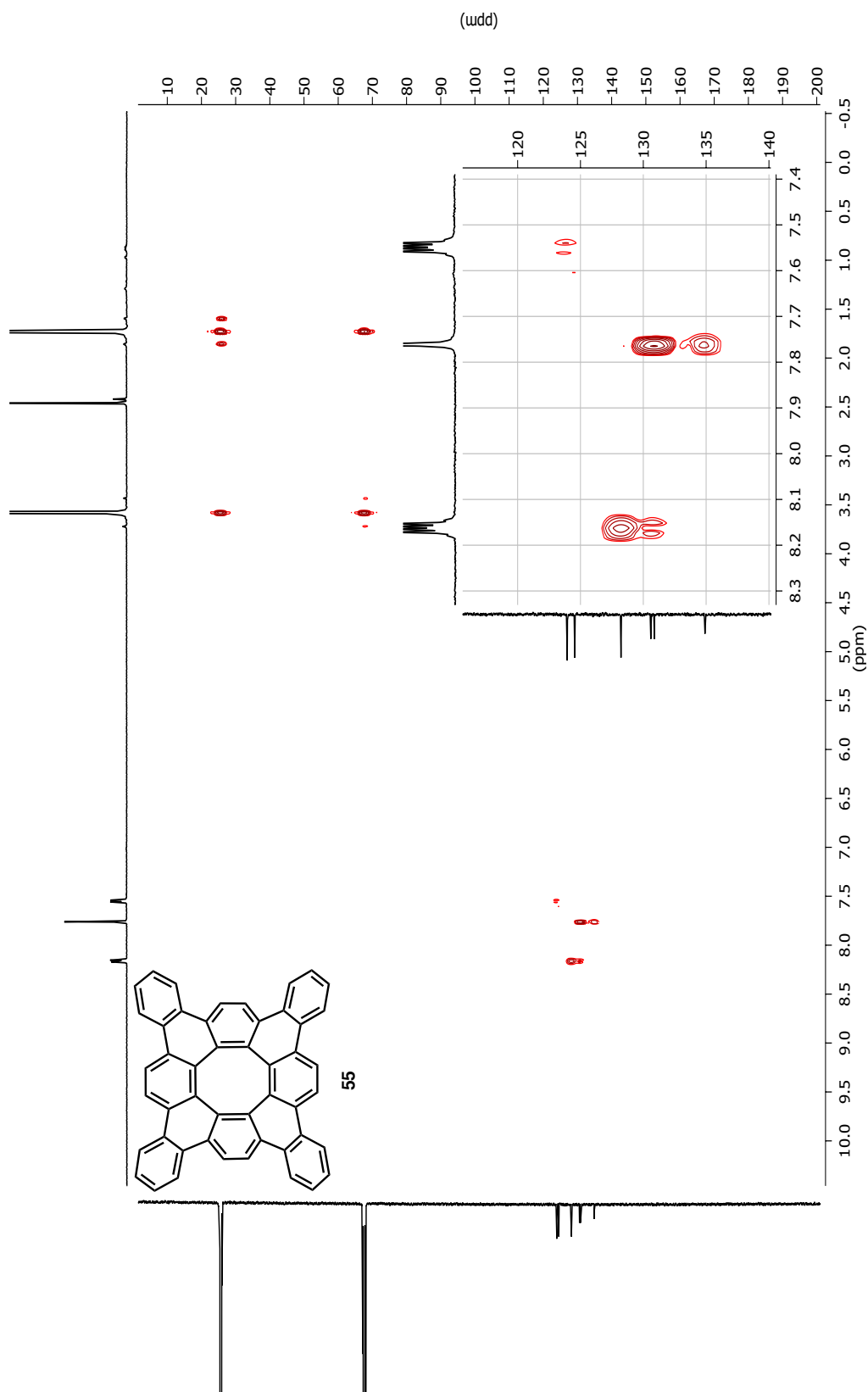
Figure A1.18 2D HMBC NMR Spectrum of **55** in THF-d_8
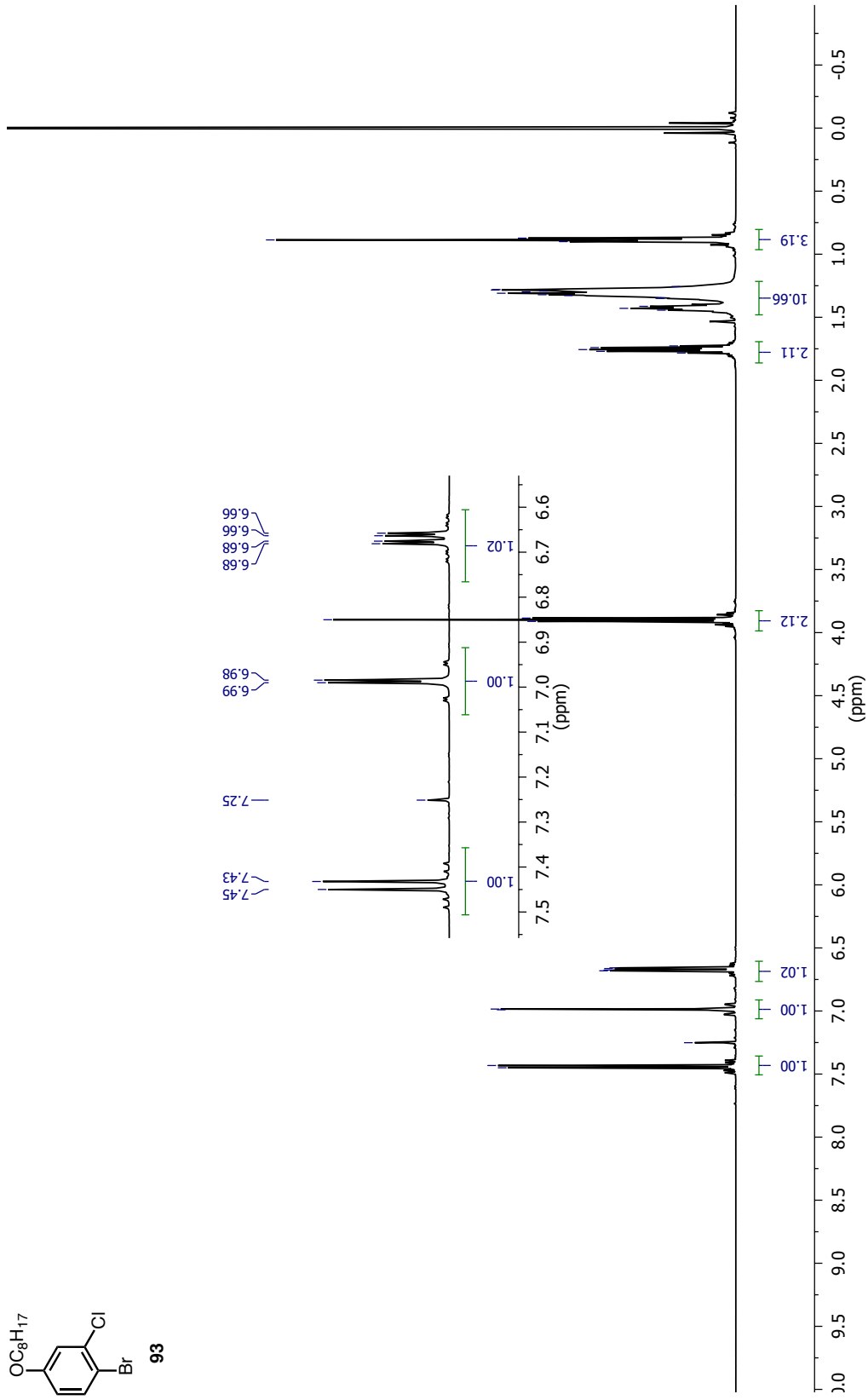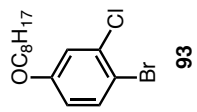
Figure AI.19 ^{1}H NMR Spectrum of **93** in CDCl$_3$
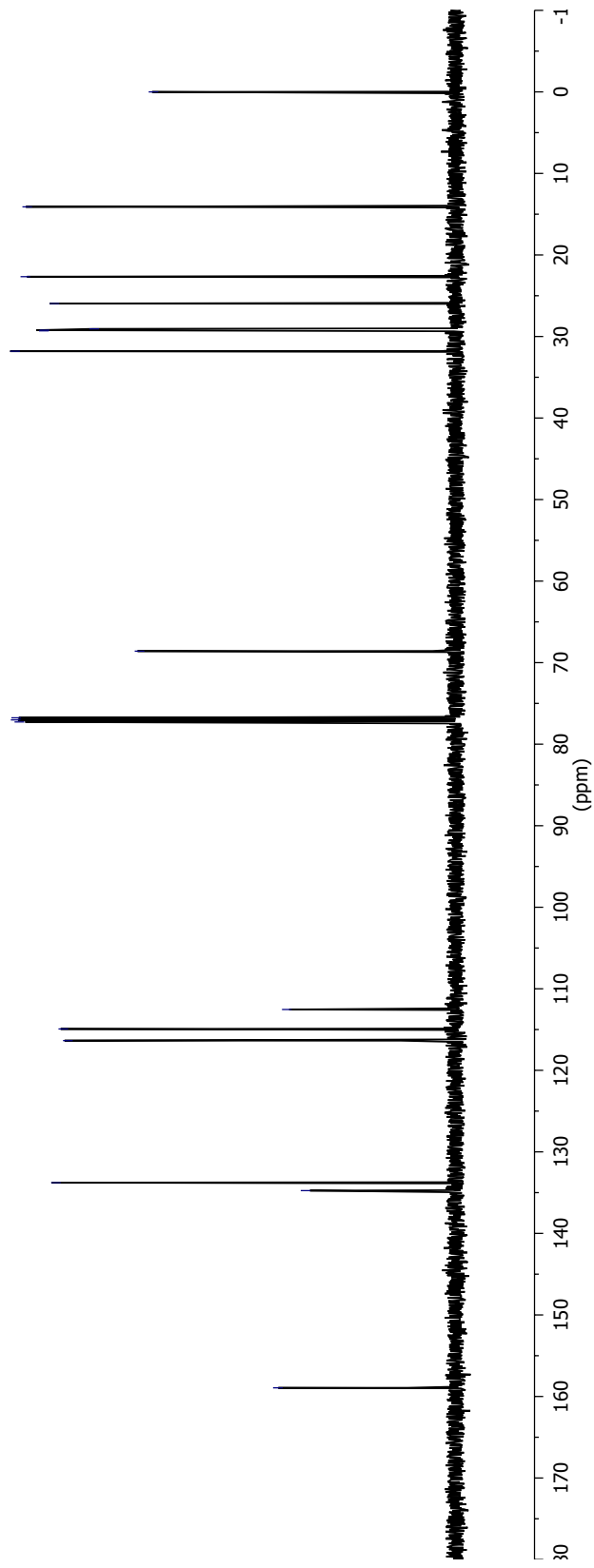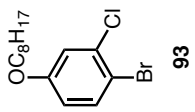
Figure AI.20 ^{13}C NMR Spectrum of **93** in CDCl$_3$

193
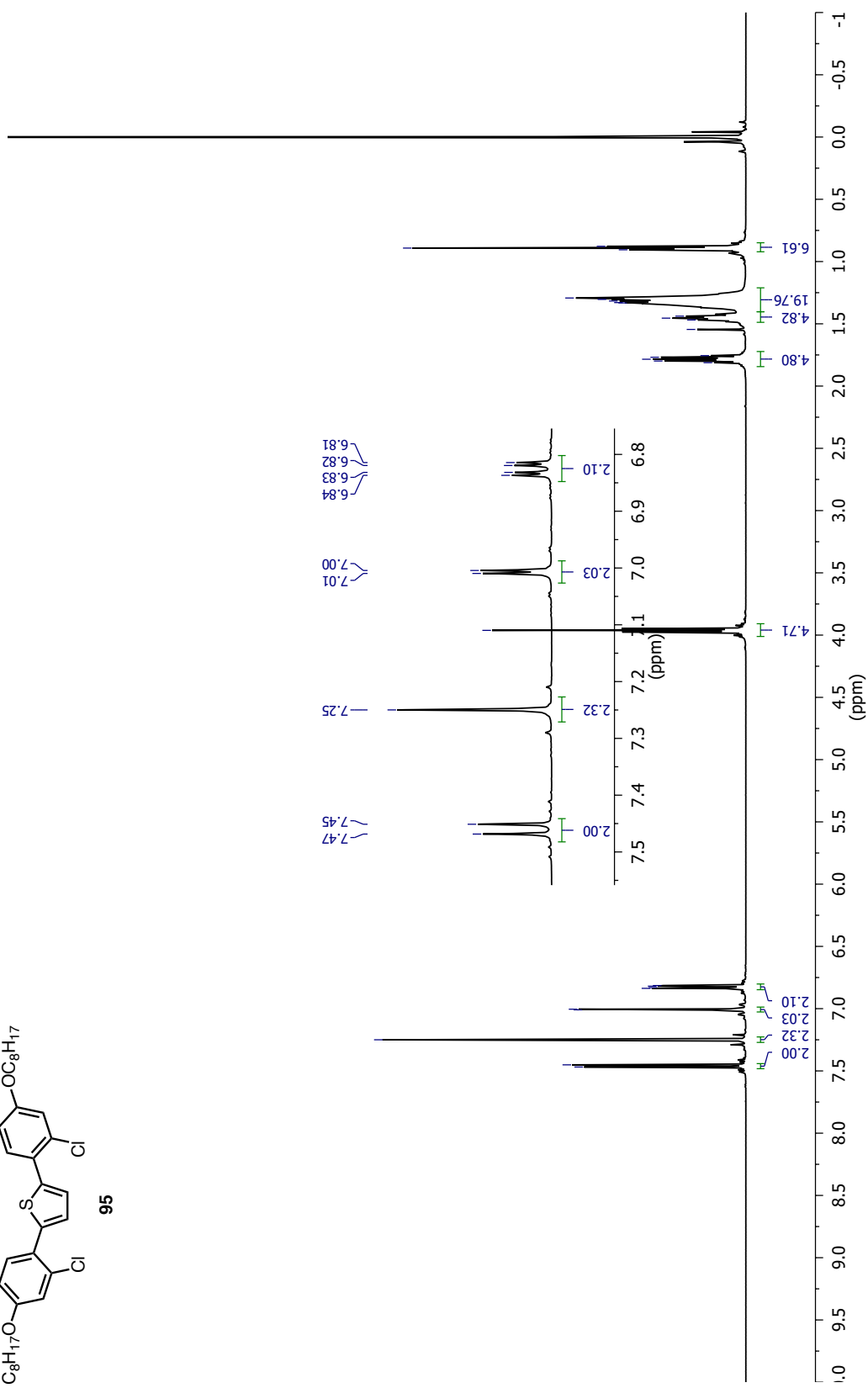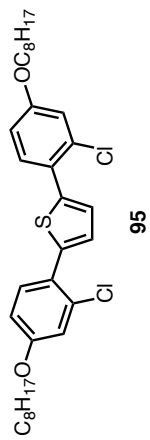
Figure A1.21 ^{1}H NMR Spectrum of **95** in CDCl$_3$

194
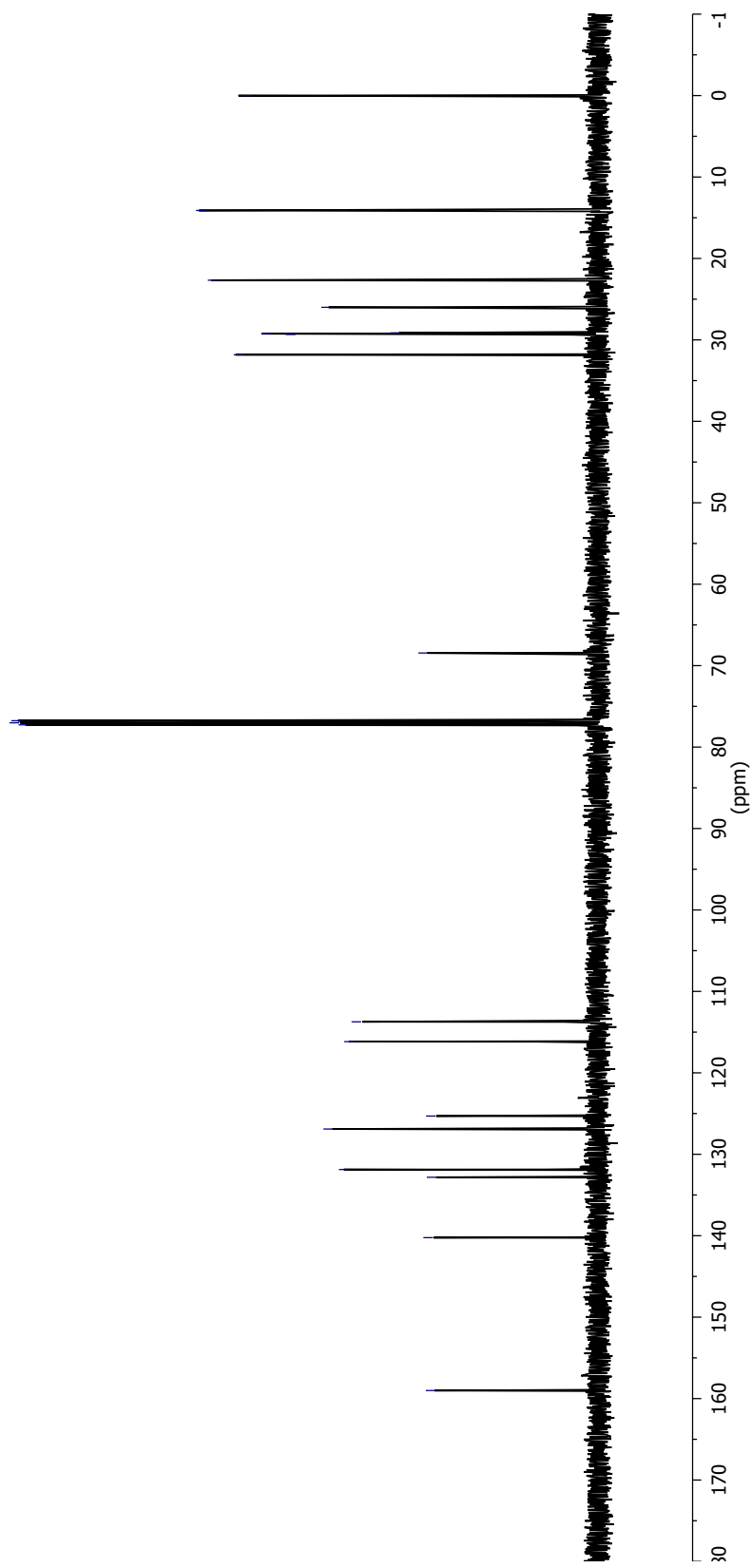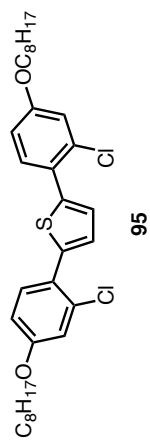
Figure AI.22 ^{13}C NMR Spectrum of **95** in CDCl$_3$

195
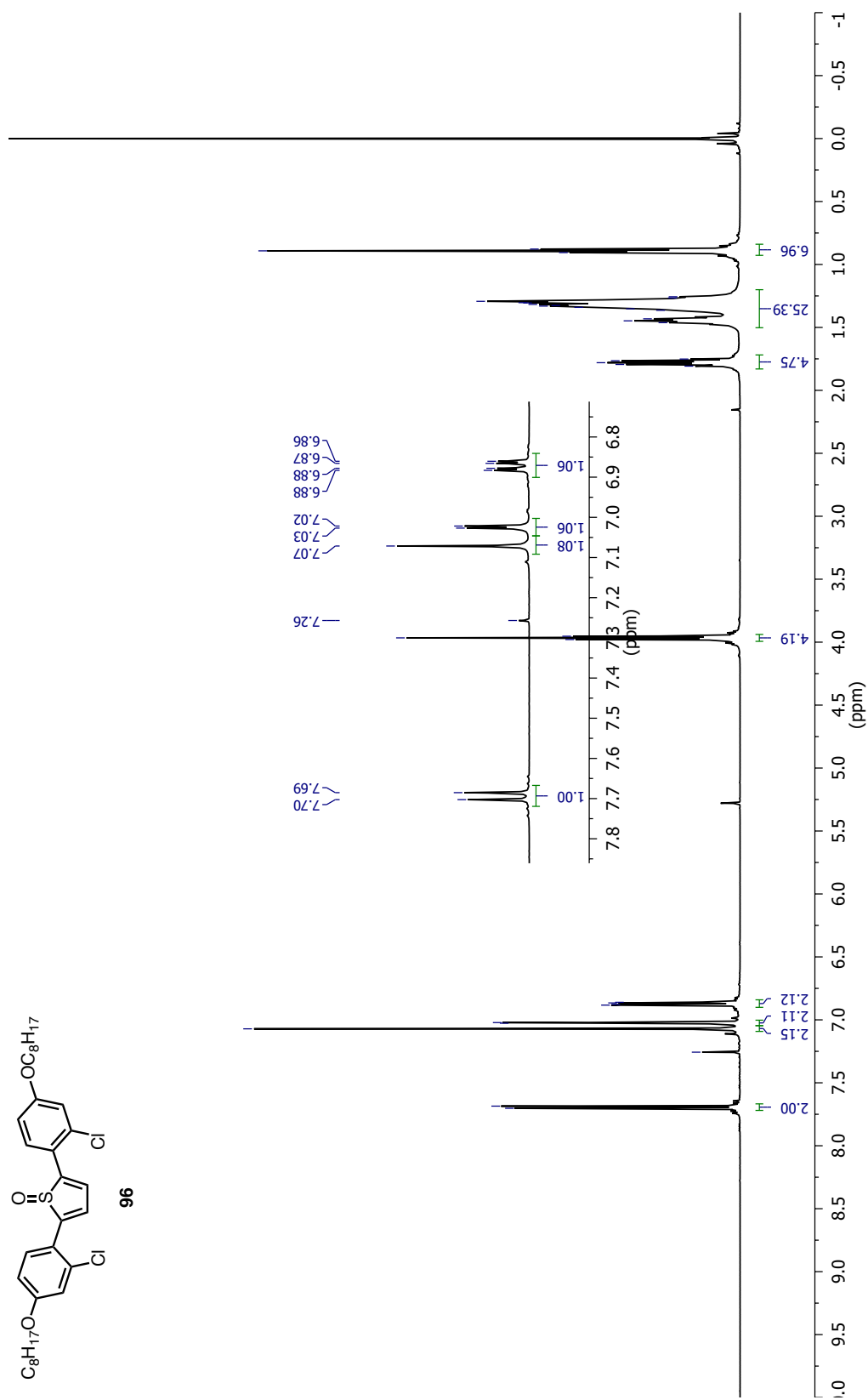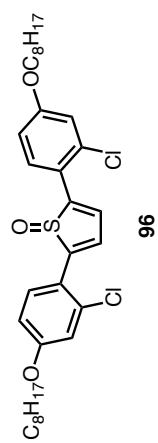
Figure AI.23 ^{1}H NMR Spectrum of **96** in CDCl$_3$
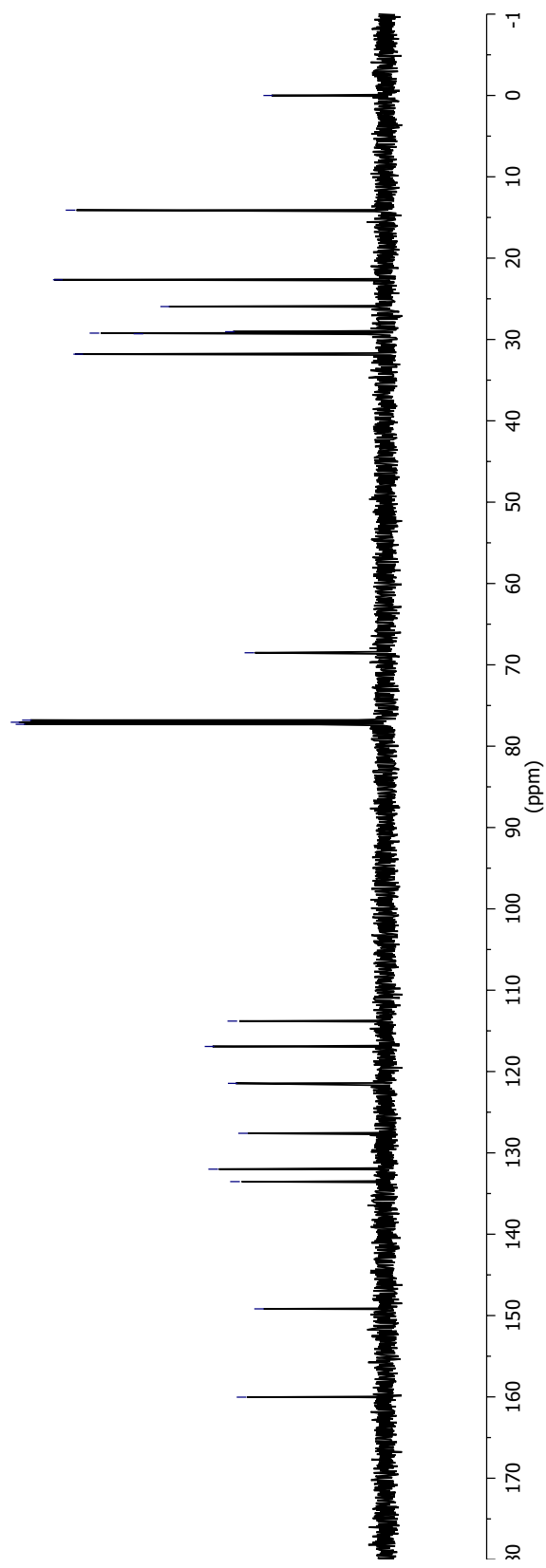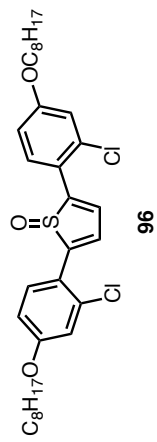
Figure AI.24 ^{13}C NMR Spectrum of **96** in CDCl$_3$

197

Figure AI.25 ^{1}H NMR Spectrum of **98** in CDCl$_3$

Figure A1.26 ^{1}H NMR Spectrum of **98** in CDCl$_3$

Figure AI.27 ^{13}C NMR Spectrum of **98** in CDCl$_3$
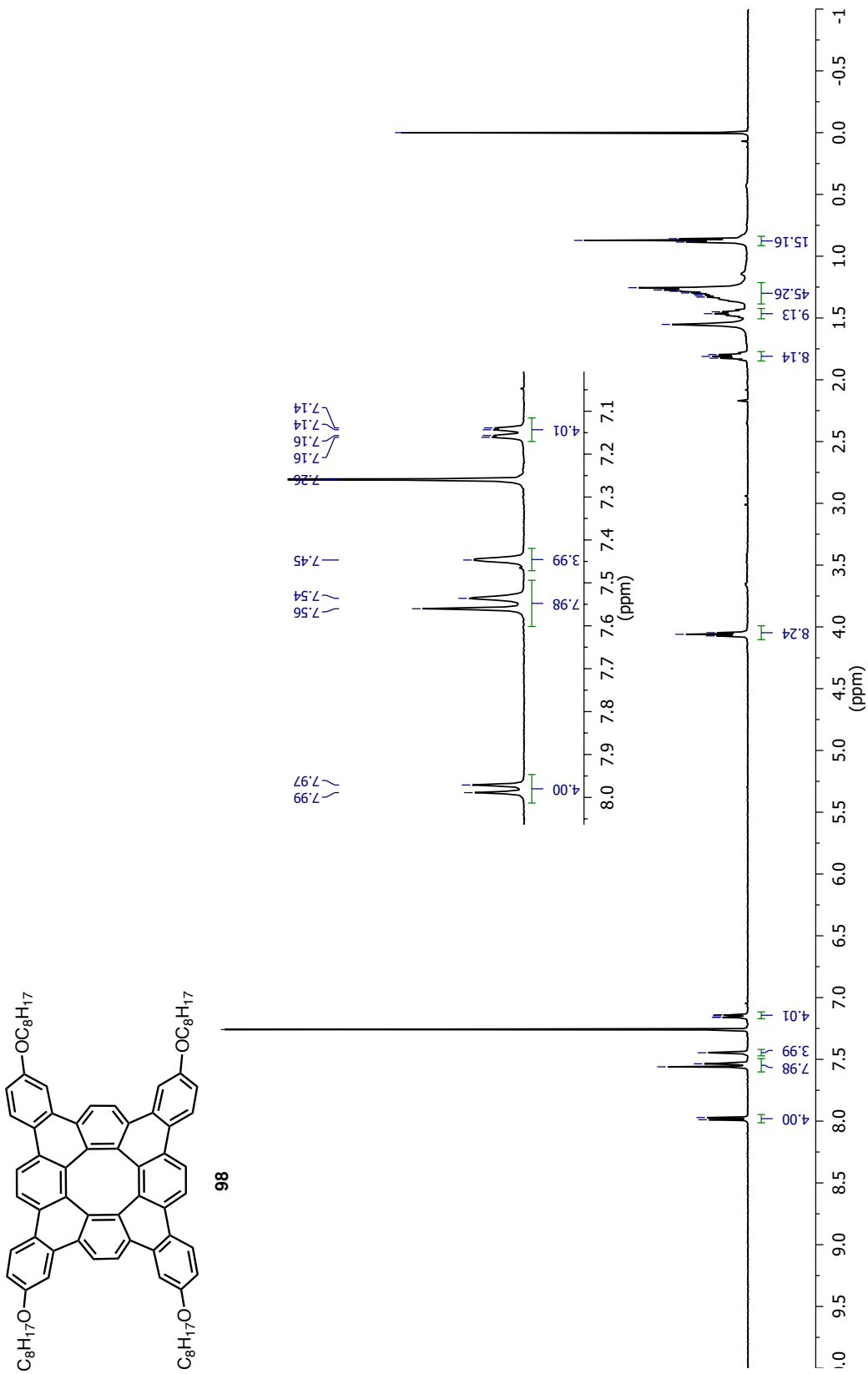
Figure AI.28 ^{1}H NMR Spectrum of **100** in CDCl$_3$
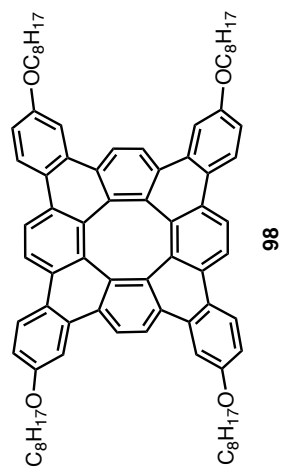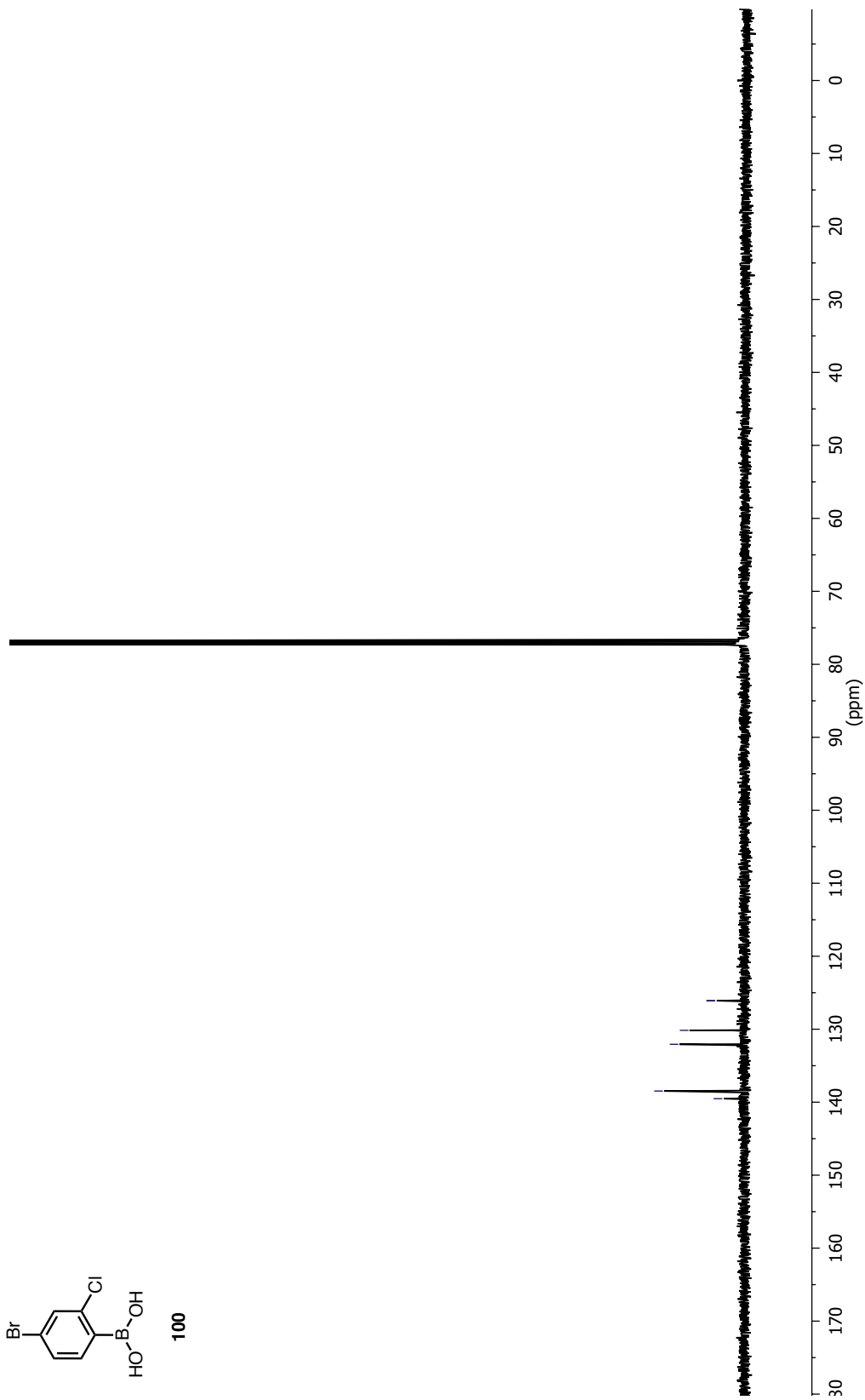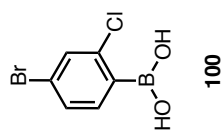
Figure AI.29 ^{13}C NMR Spectrum of **100** in CDCl$_3$

202

Figure AI.30 ^{1}H NMR Spectrum of **101** in CDCl$_3$
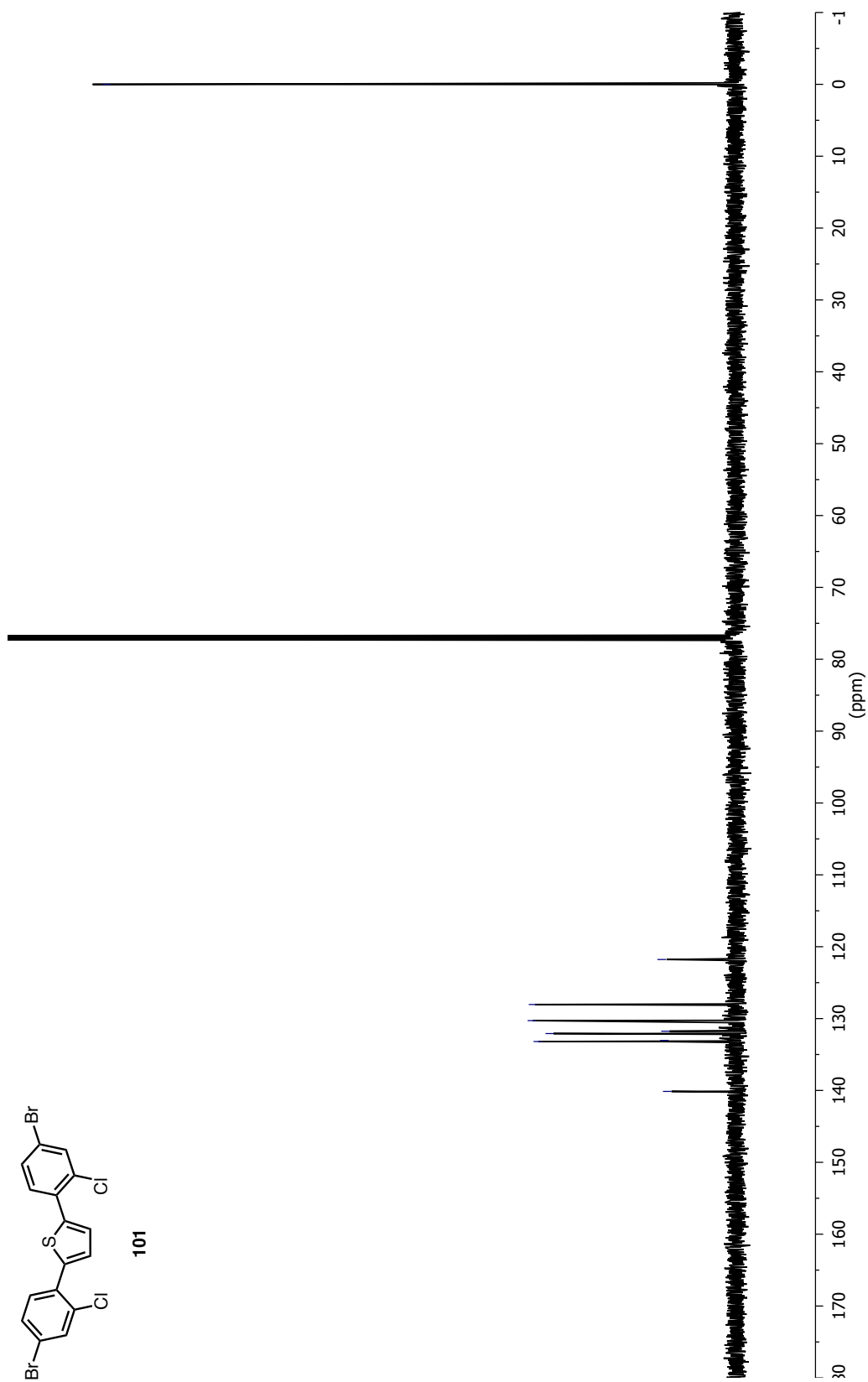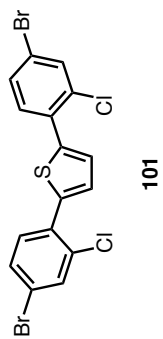
Figure AI.31 ^{13}C NMR Spectrum of **101** in CDCl$_3$

204
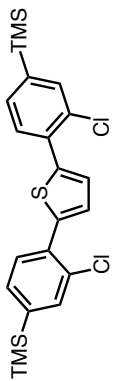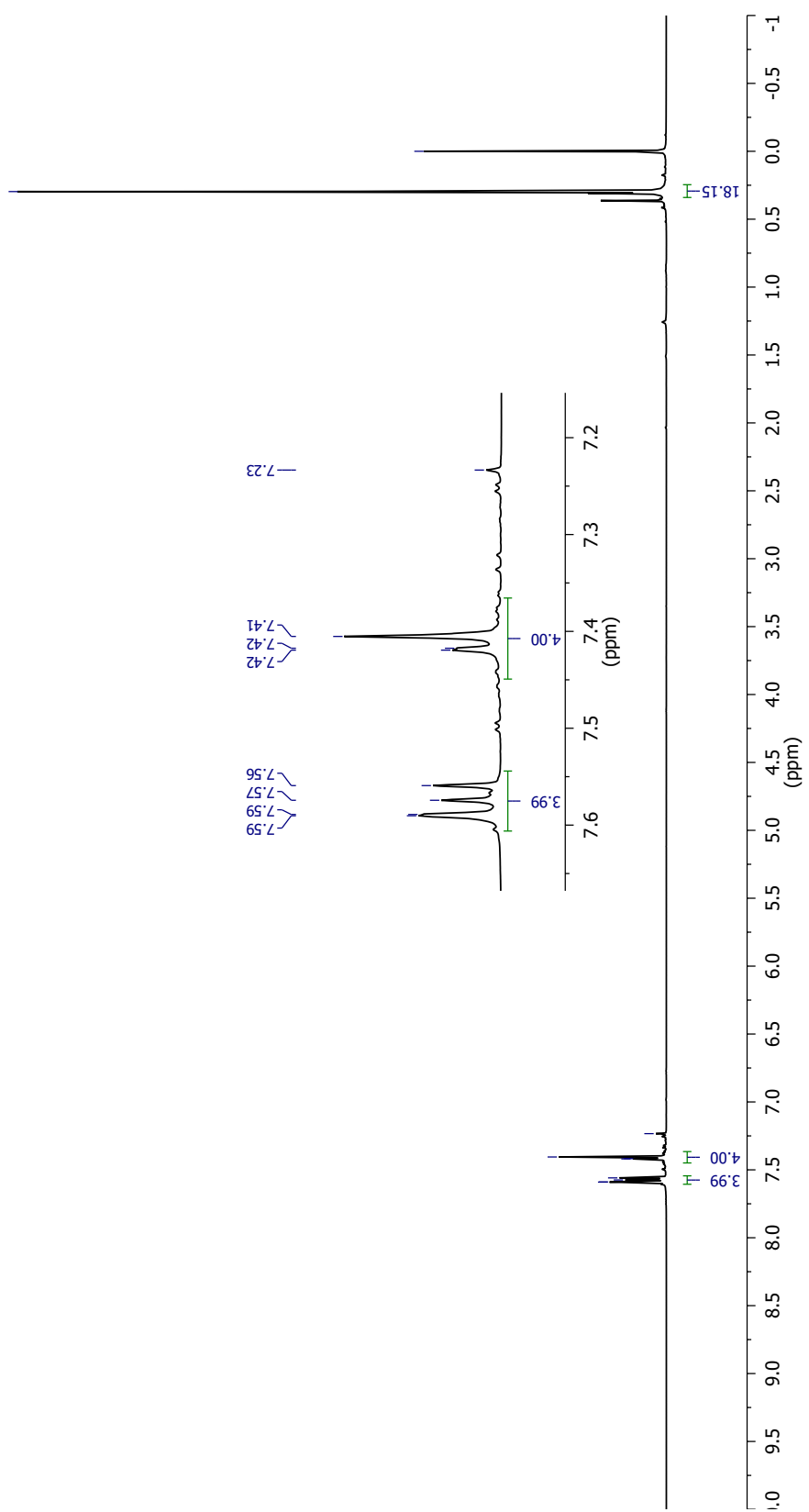
Figure AI.32 ^{1}H NMR Spectrum of **103** in CDCl$_3$
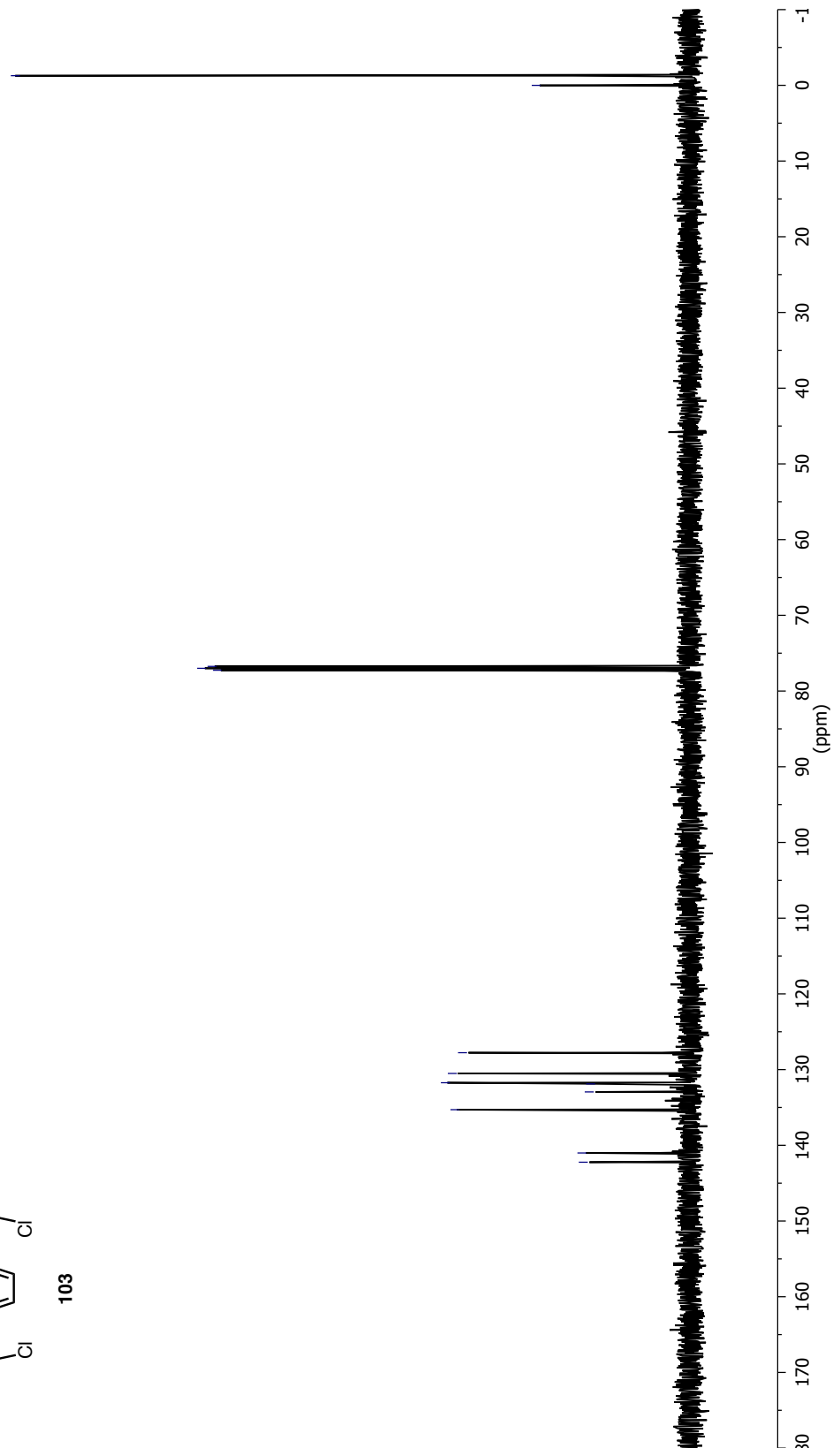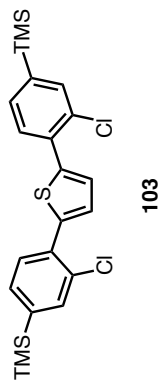
Figure AI.33 ^{13}C NMR Spectrum of **103** in CDCl$_3$

206
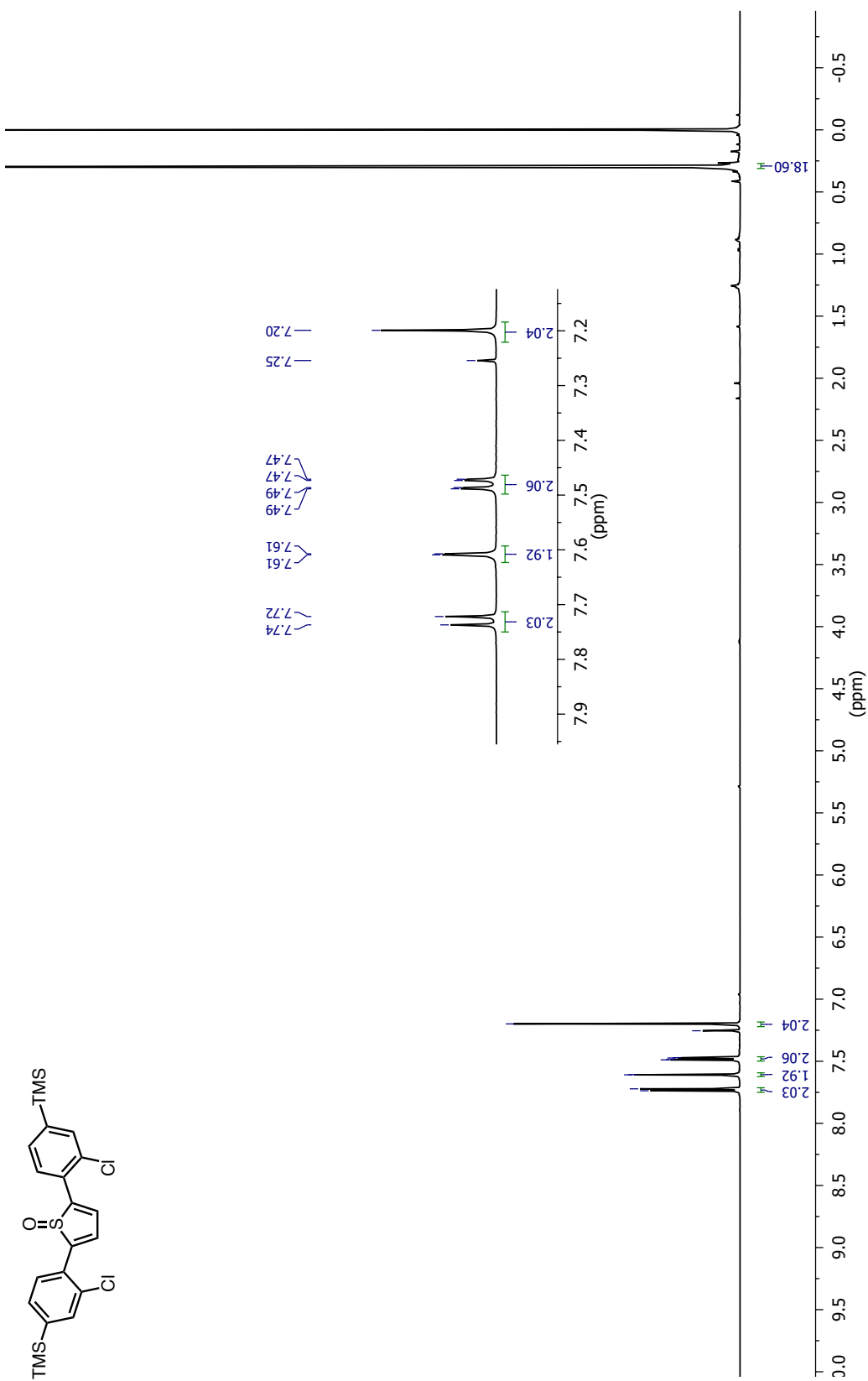
Figure AI.34 ^{1}H NMR Spectrum of **104** in CDCl$_3$
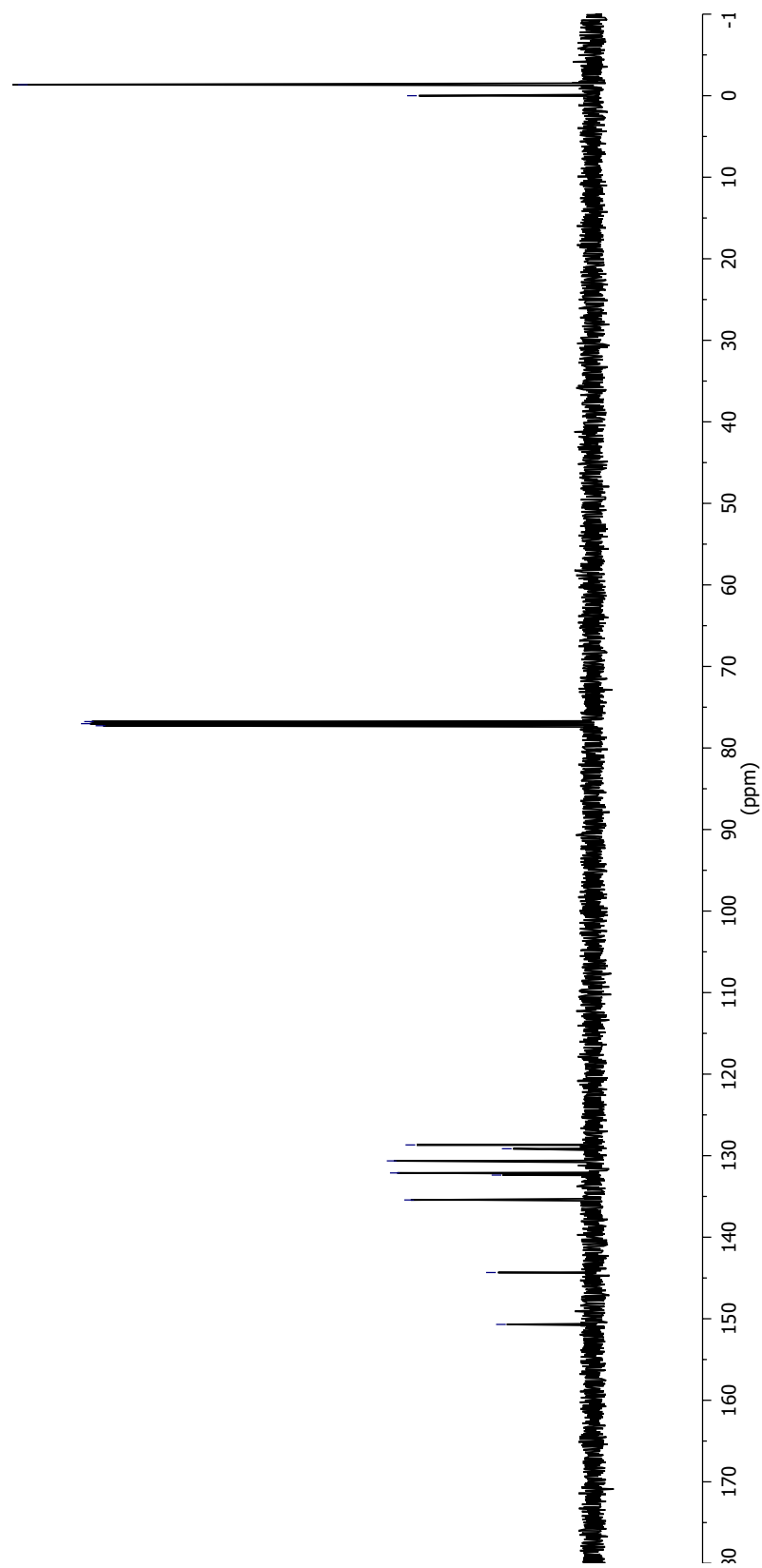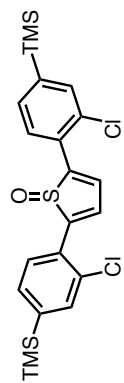
Figure AI.35 ^{13}C NMR Spectrum of **104** in CDCl$_3$

208
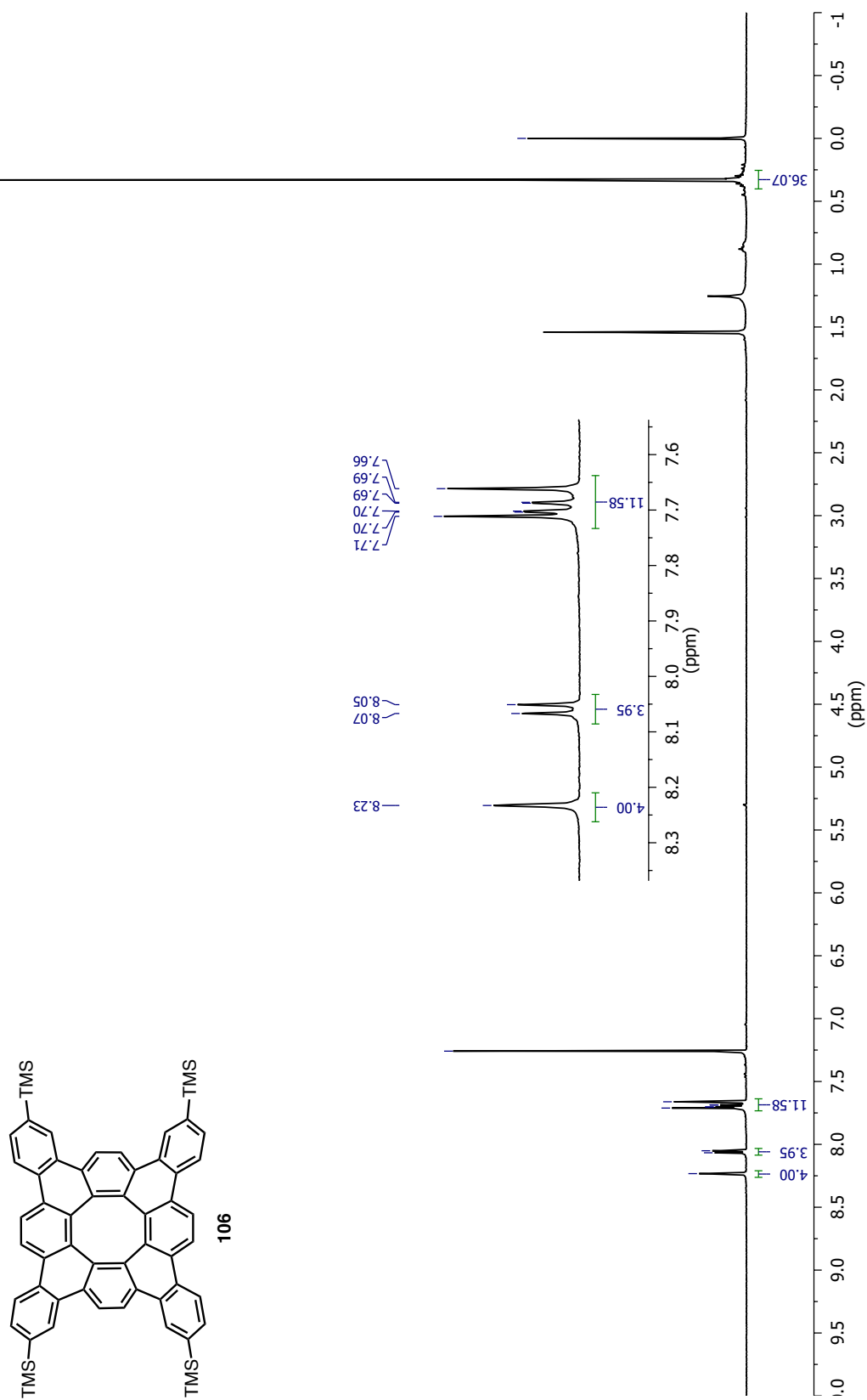
Figure AI.36 ^{1}H NMR Spectrum of **106** in CDCl$_3$
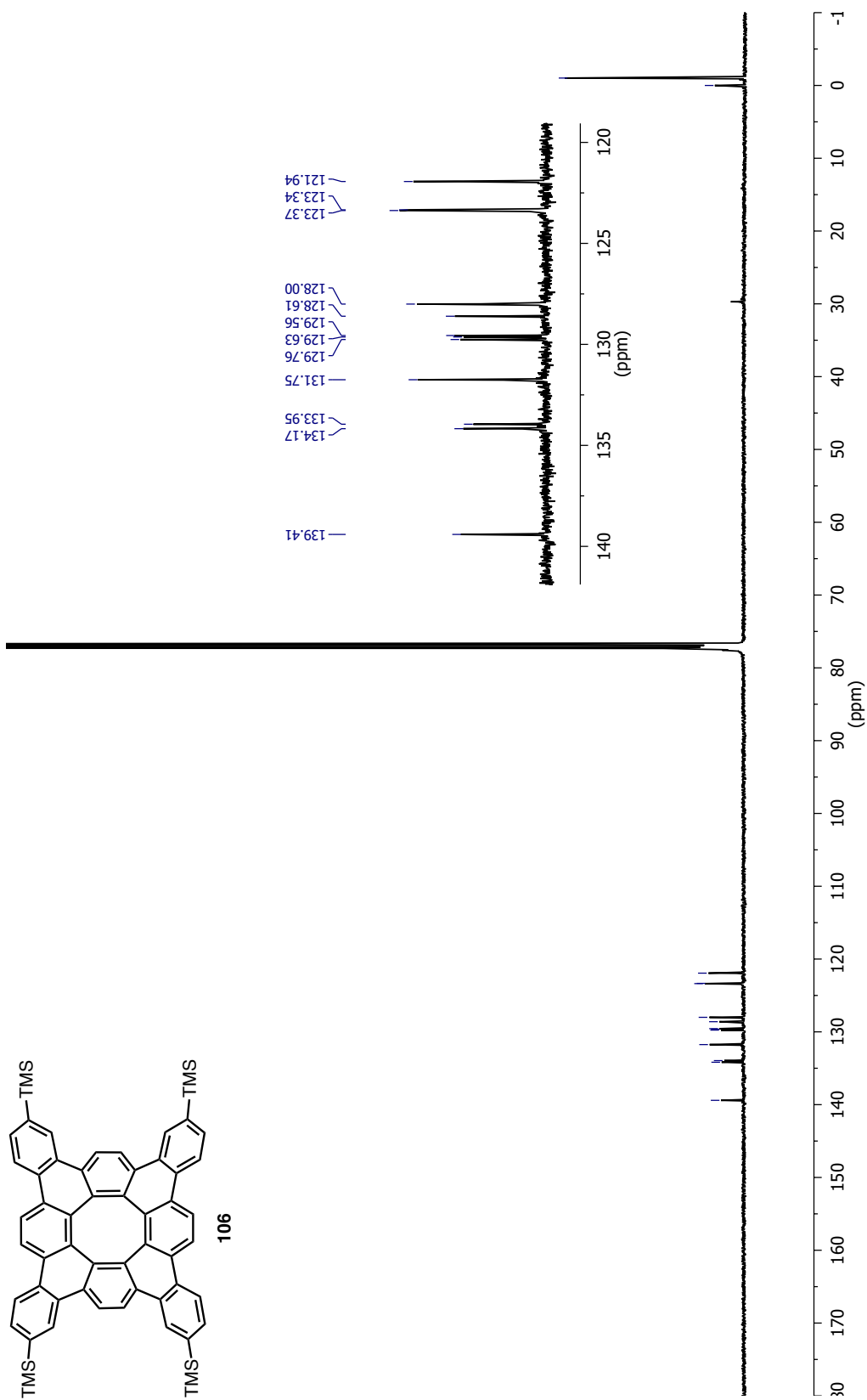
Figure AI.37 ^{13}C NMR Spectrum of **106** in CDCl$_3$

210
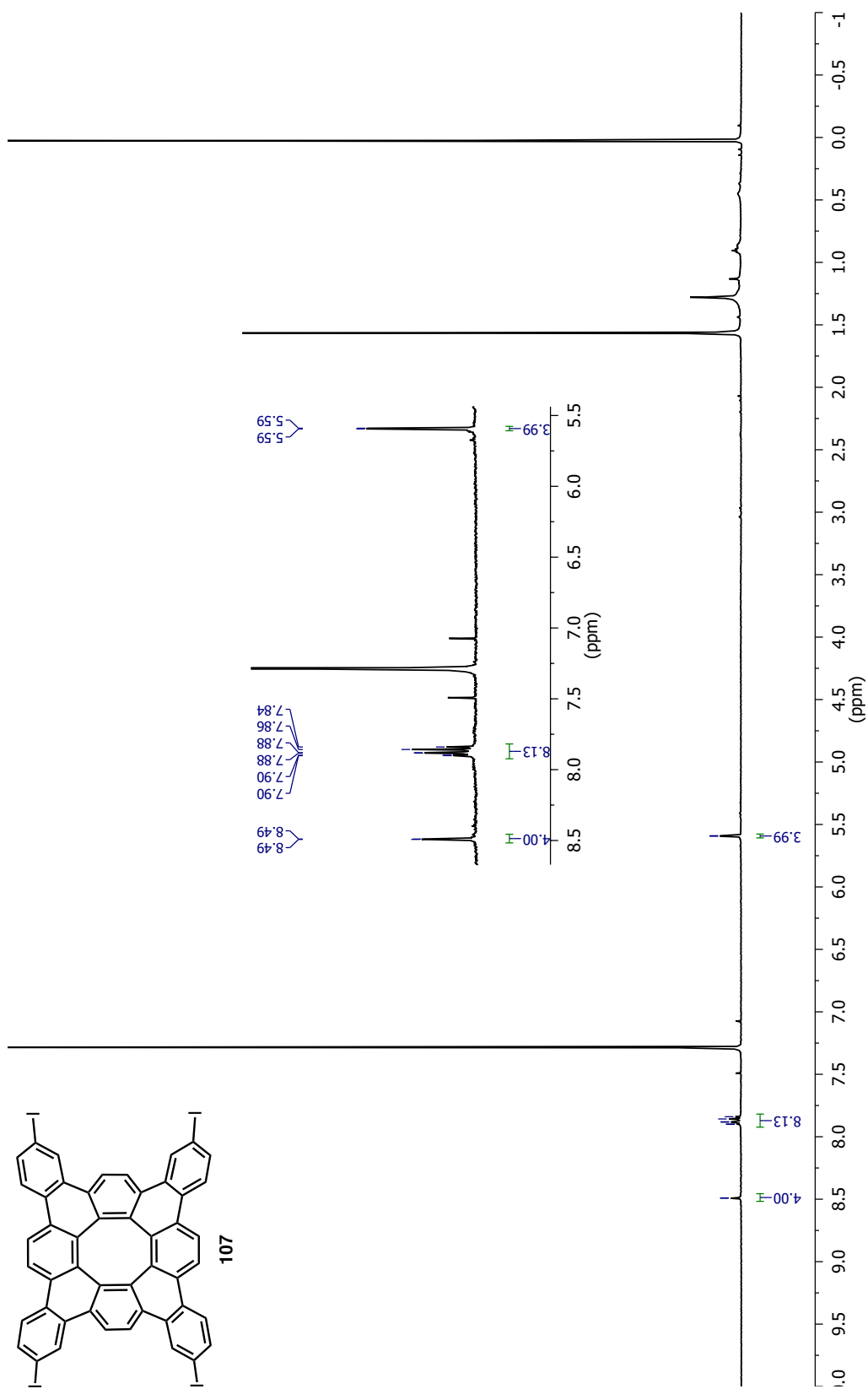
Figure AI.38 ^{1}H NMR Spectrum of **107** in CDCl$_3$
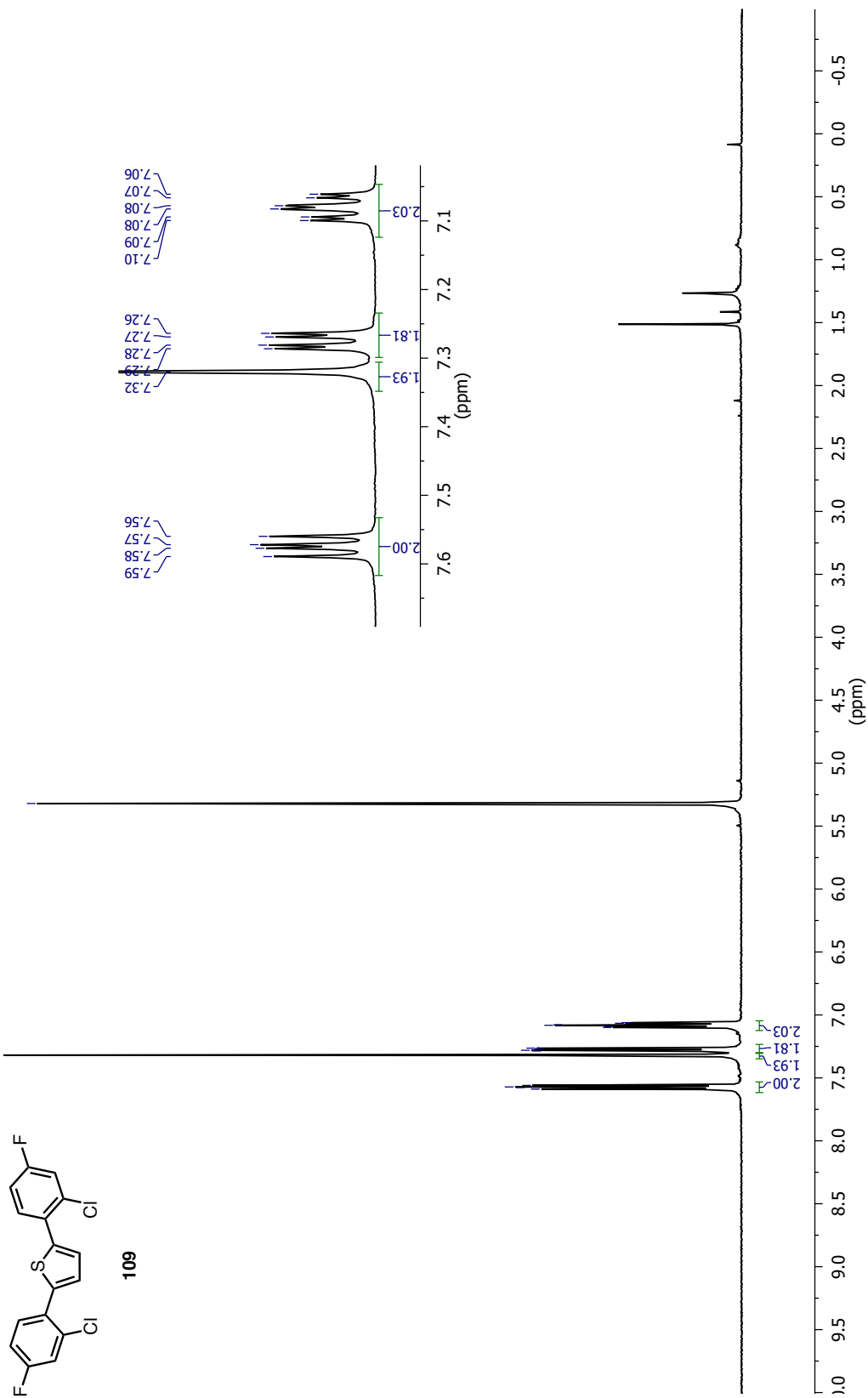
Figure AI.39 ^{1}H NMR Spectrum of **109** in CD$_2$Cl$_2$

212
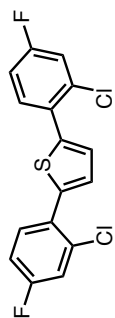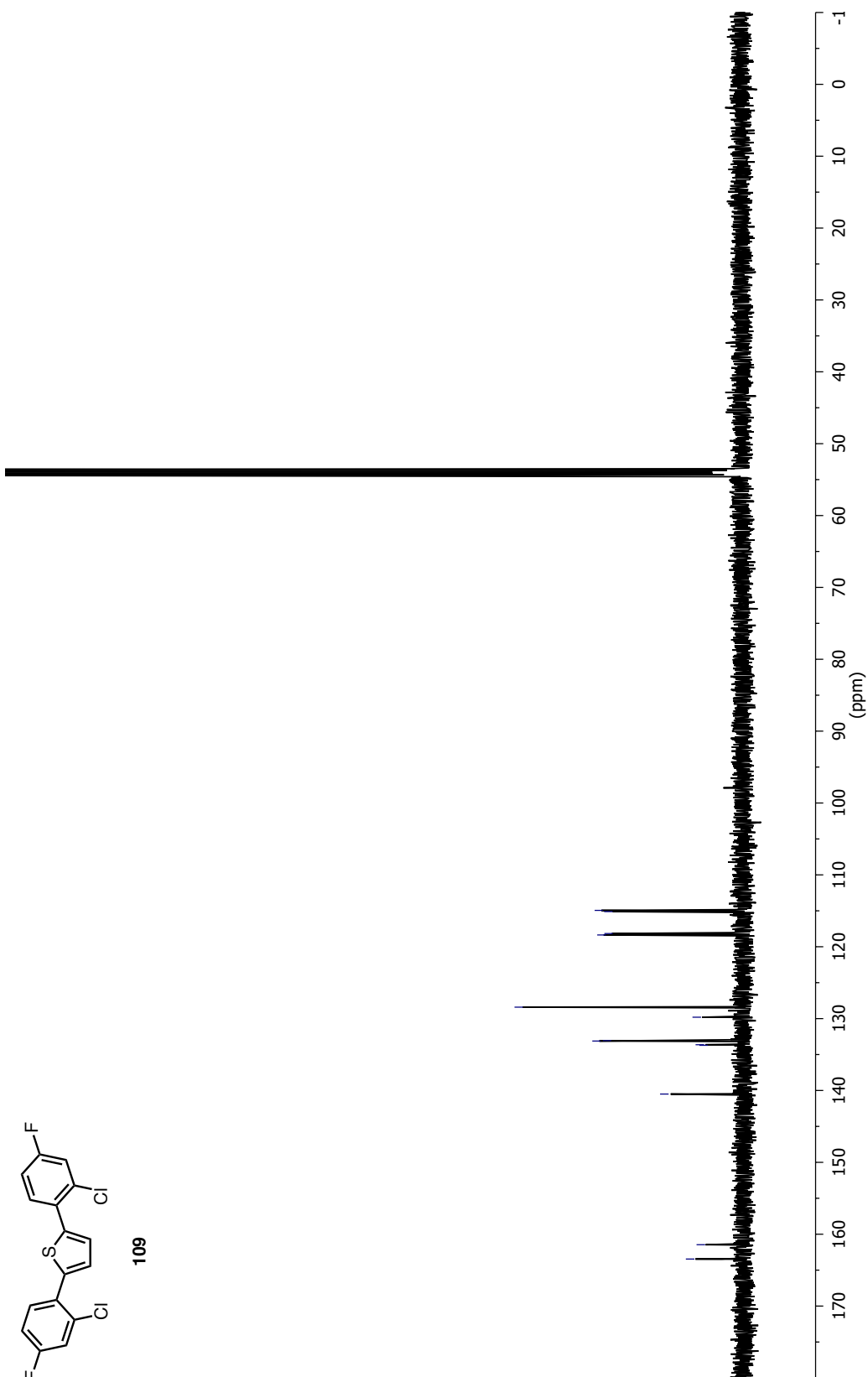
Figure AI.40 ^{13}C NMR Spectrum of **109** in CD$_2$Cl$_2$

213
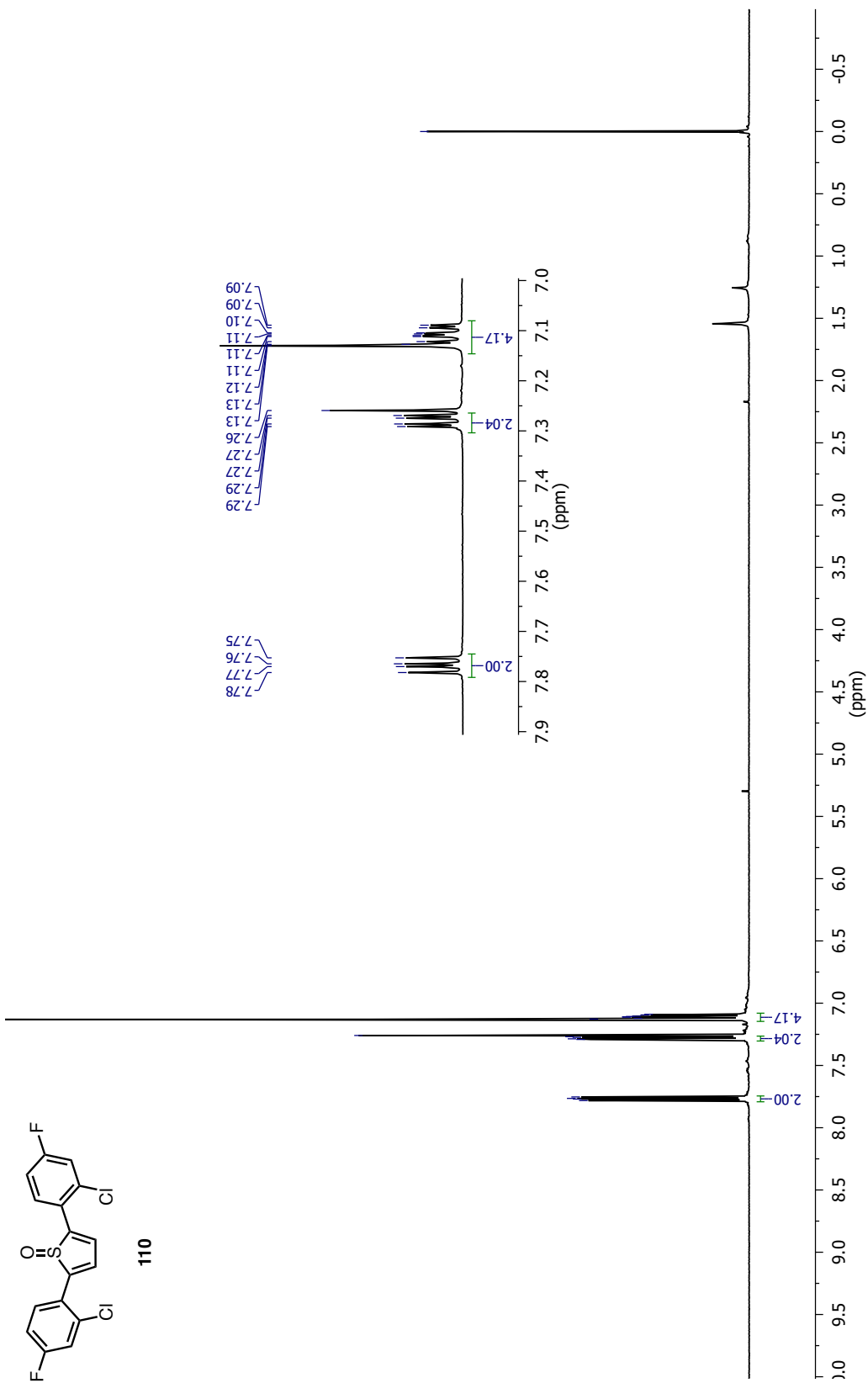
Figure AI.41 ^{1}H NMR Spectrum of **110** in CDCl$_3$
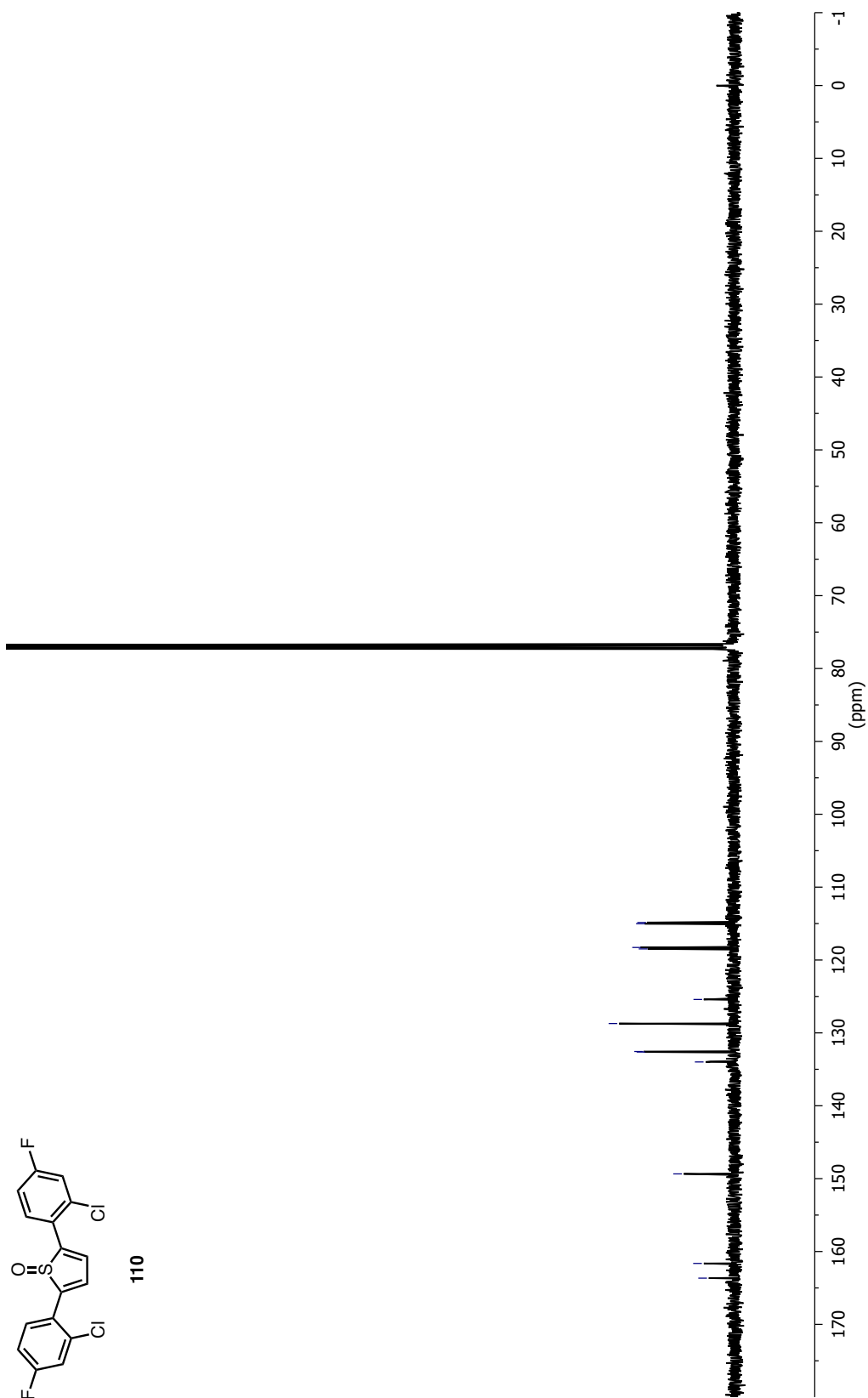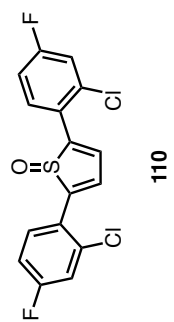
Figure AI.42 ^{13}C NMR Spectrum of **110** in CDCl$_3$

215
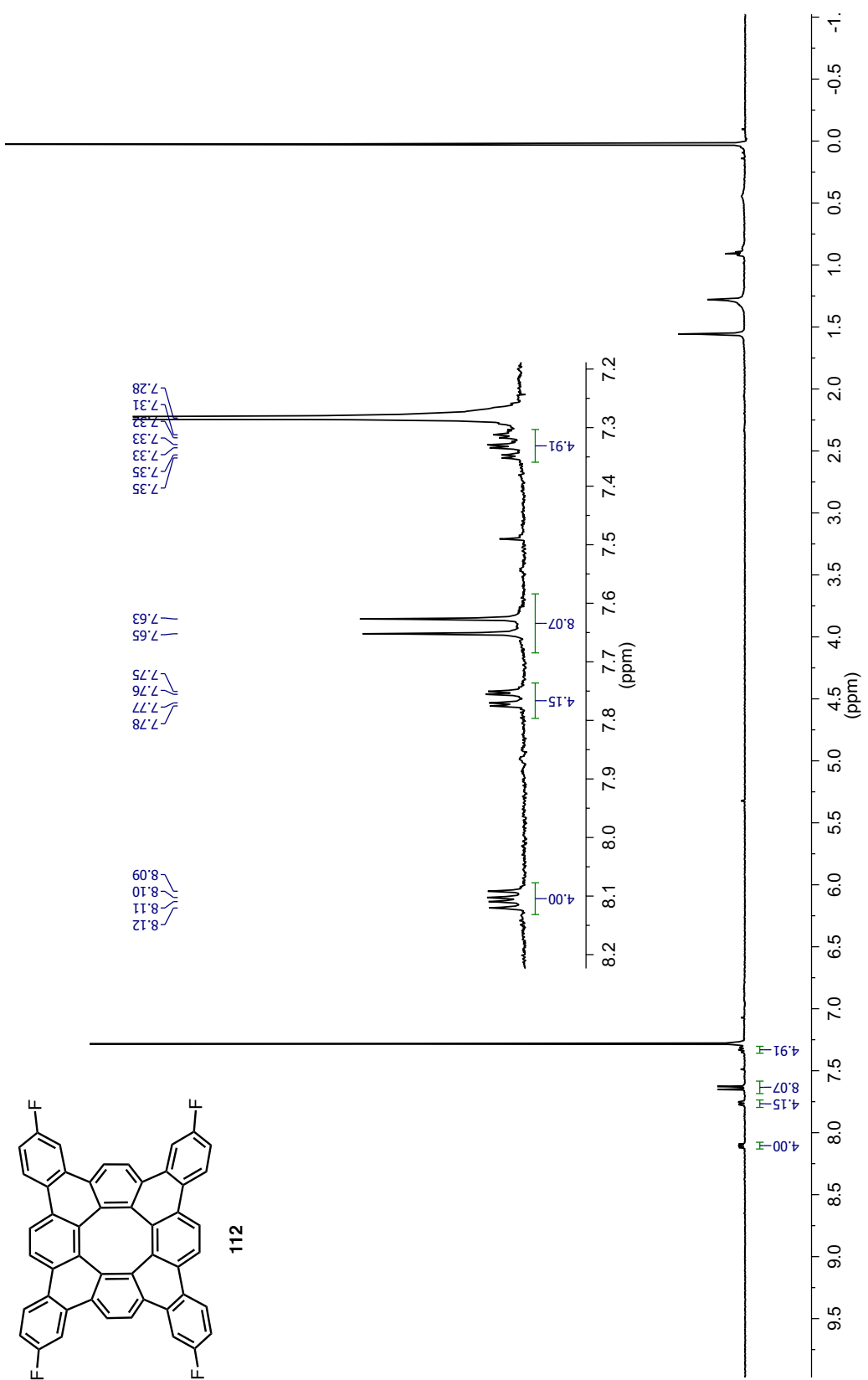
Figure AI.43 ^{1}H NMR Spectrum of **112** in CDCl$_3$
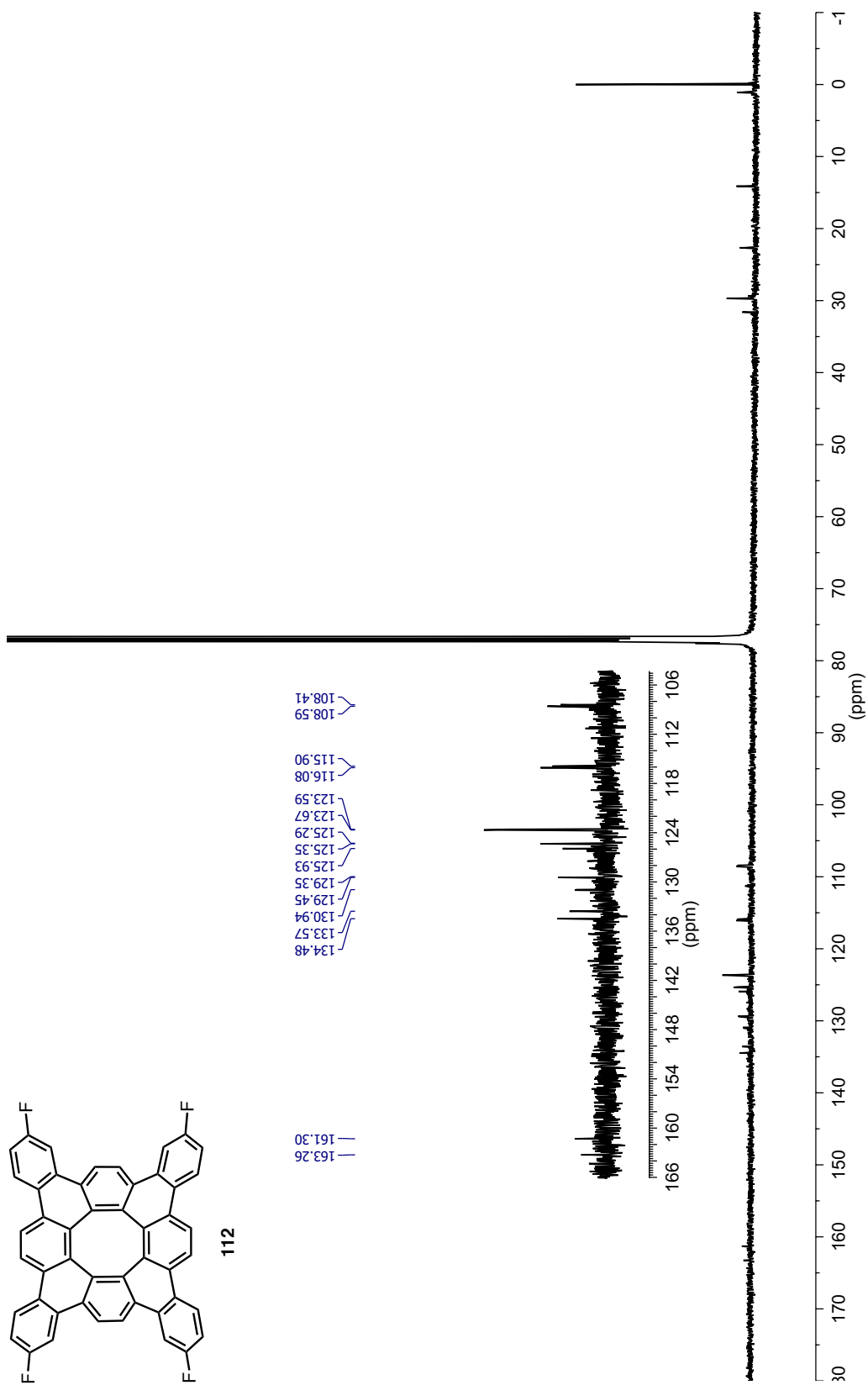
Figure AI.44 ^{13}C NMR Spectrum of **112** in CDCl$_3$

217

AI.2 Experimental Data for A ONE-POT METHOD FOR THE PREPARATION OF 2,5-DIARYLTHIOPHENE-1-OXIDES FROM ARYLACETYLENES
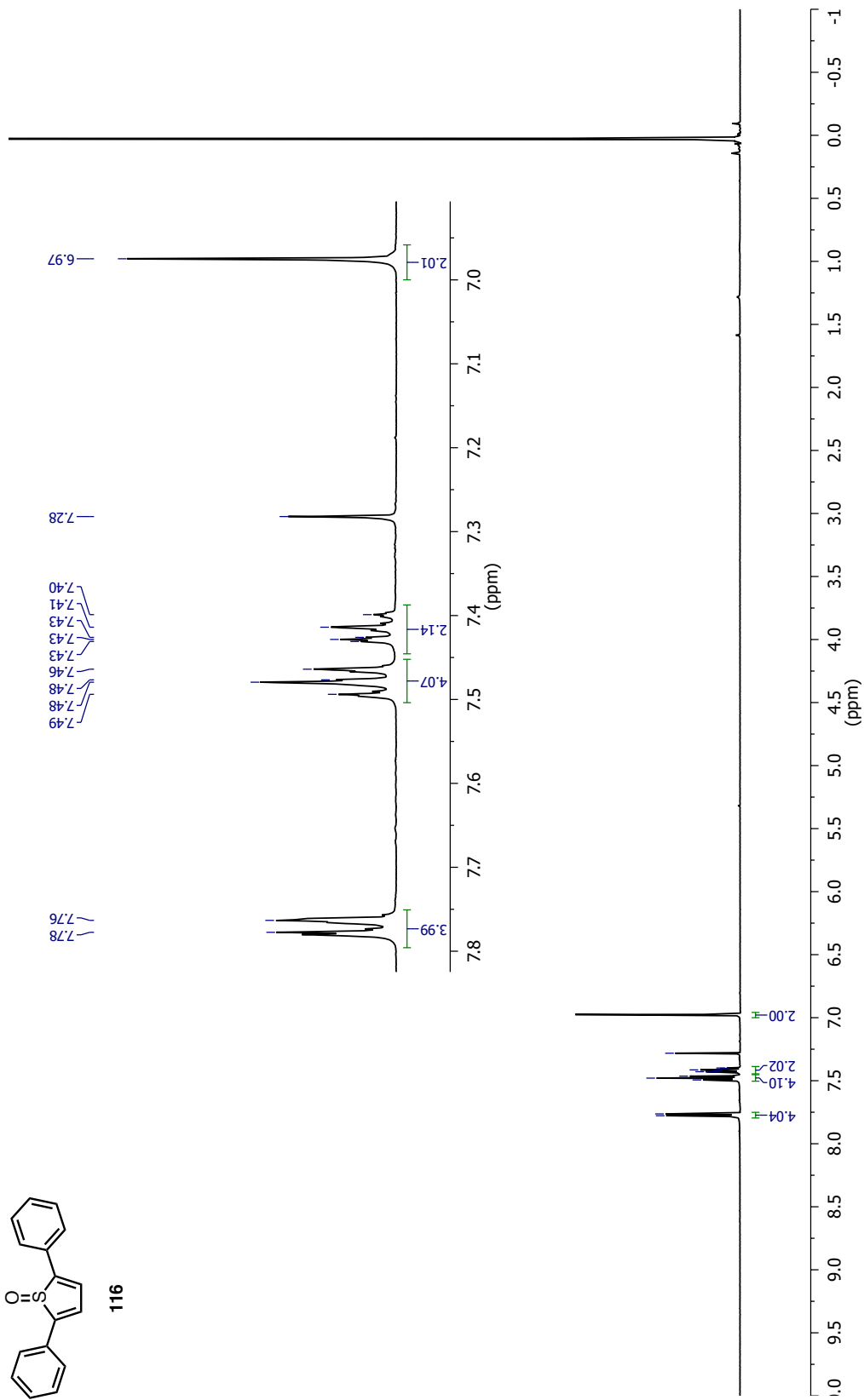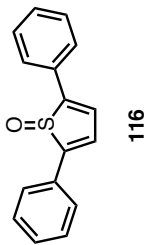
Figure AI.45 ^{1}H NMR Spectrum of **116** in CDCl$_3$
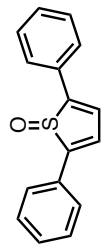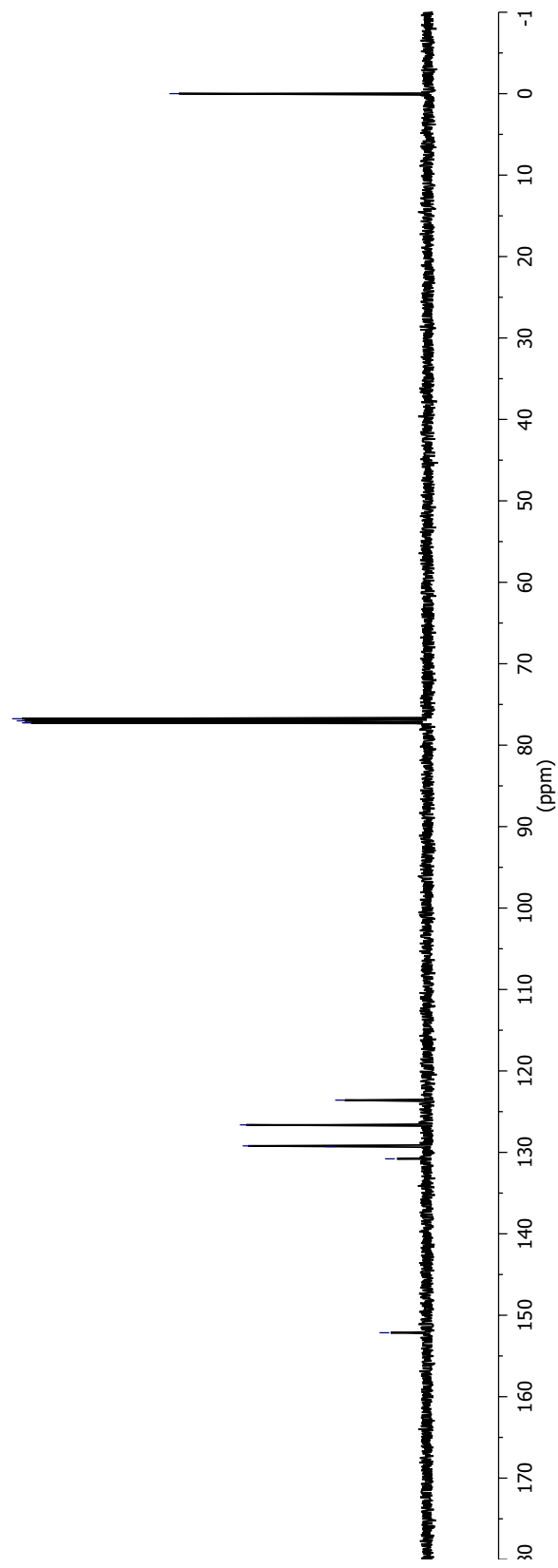
Figure AI.46 ^{13}C NMR Spectrum of **116** in CDCl$_3$
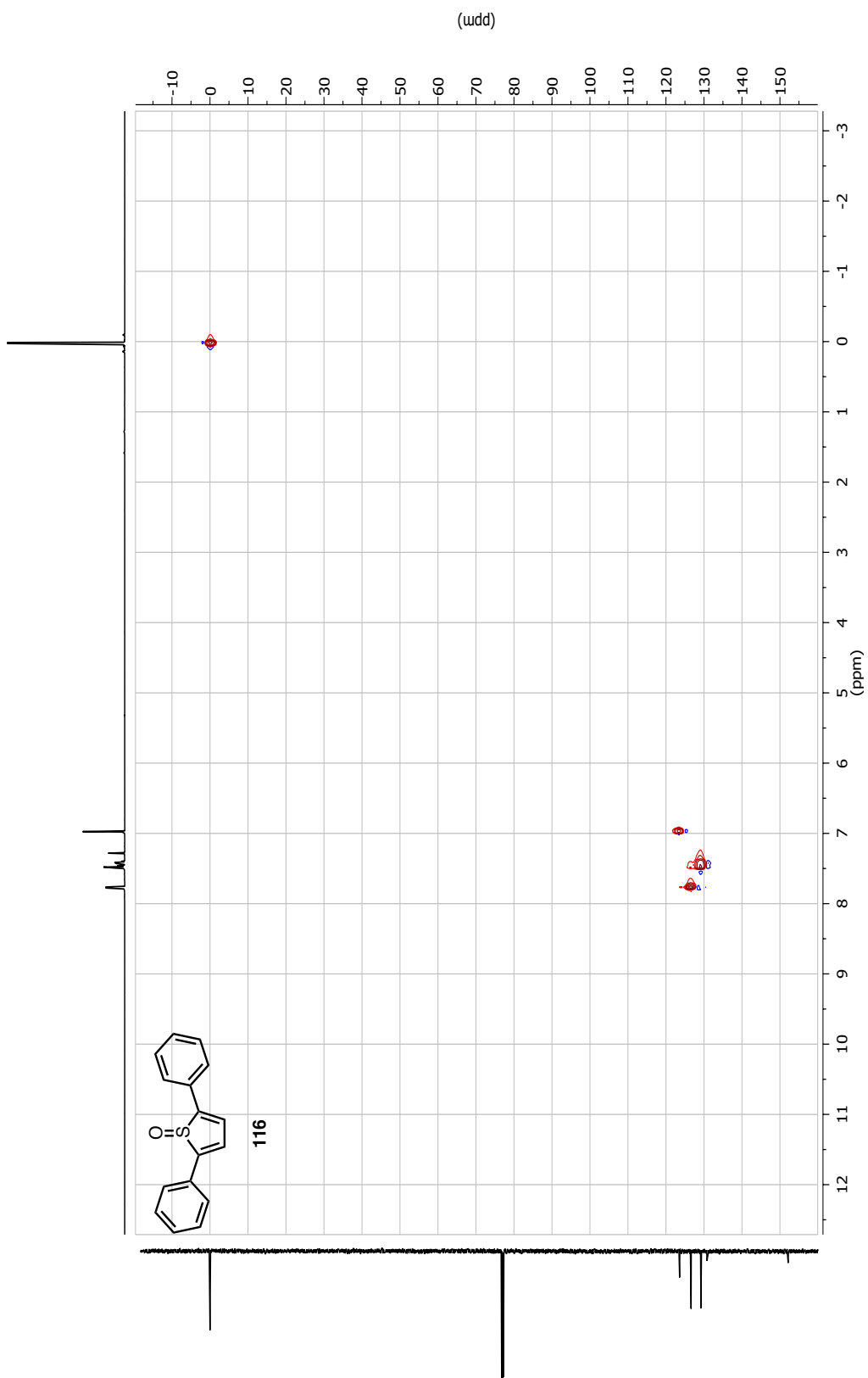
Figure AI.47 2D HSQC NMR Spectrum of **116** in CDCl₃
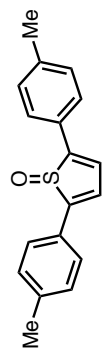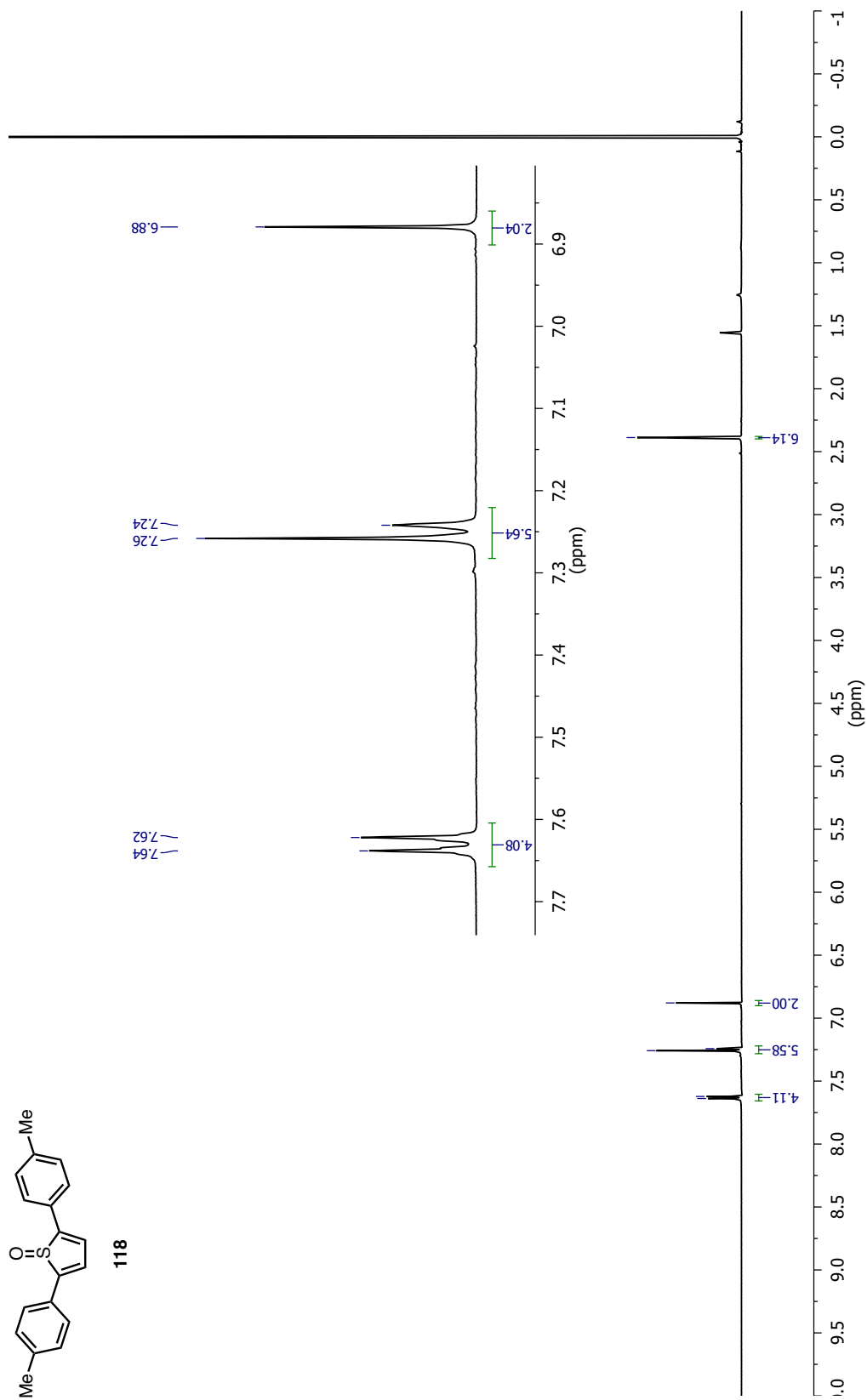
Figure AI.48 ^{1}H NMR Spectrum of **118** in CDCl$_3$
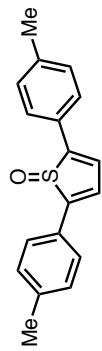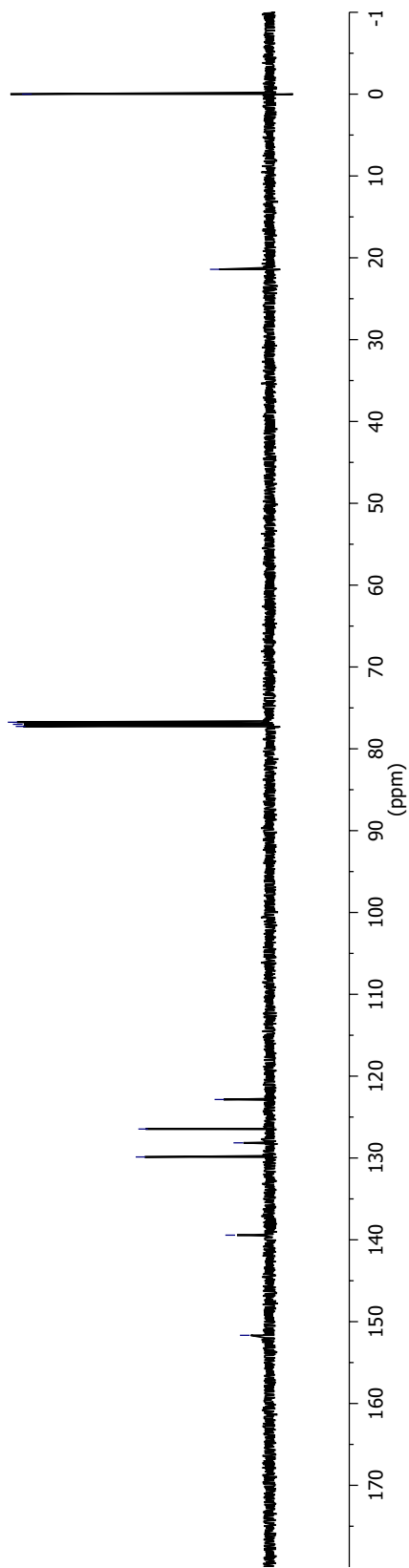
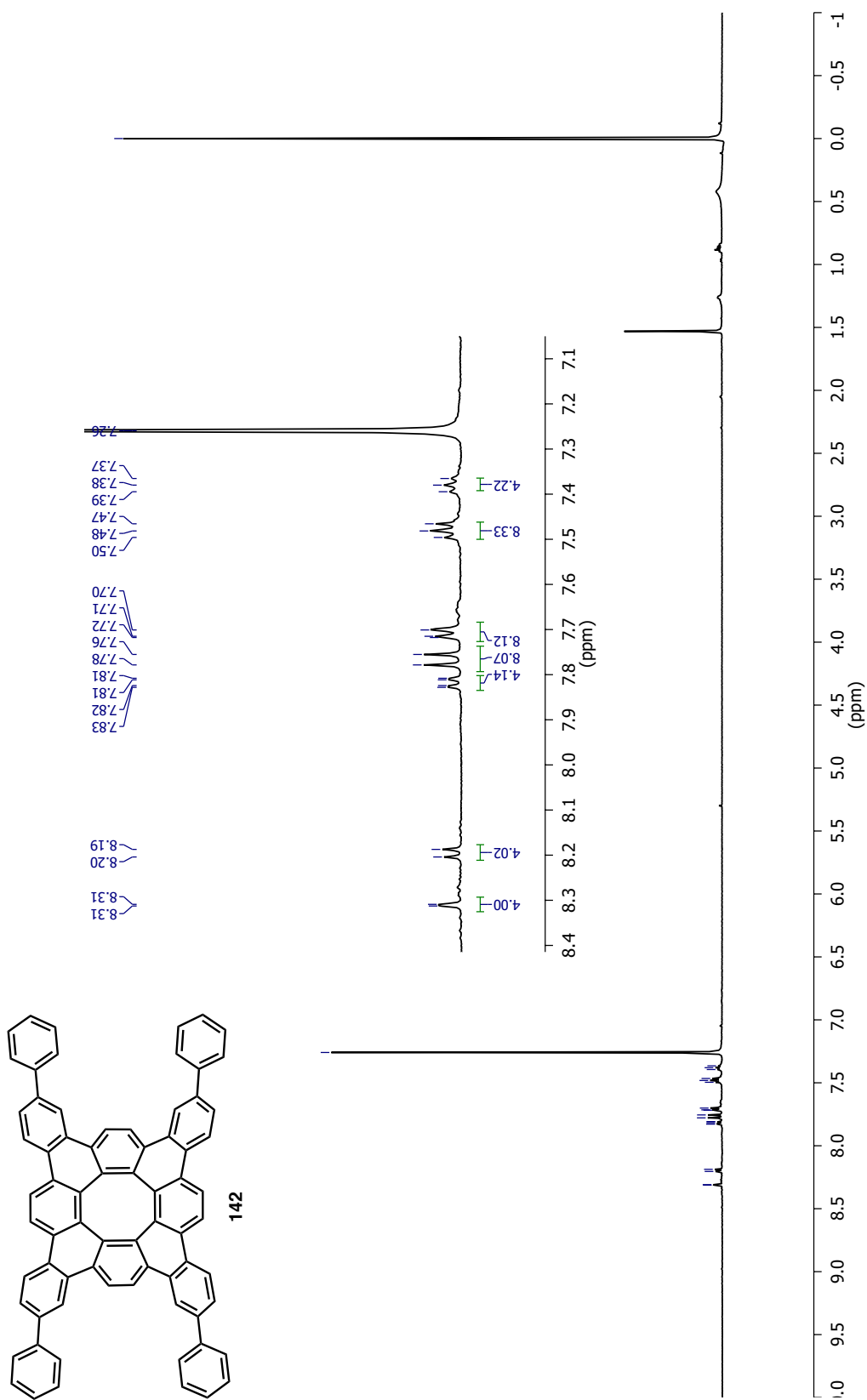**Figure AI.49** ^{13}C NMR Spectrum of **118** in CDCl$_3$

223
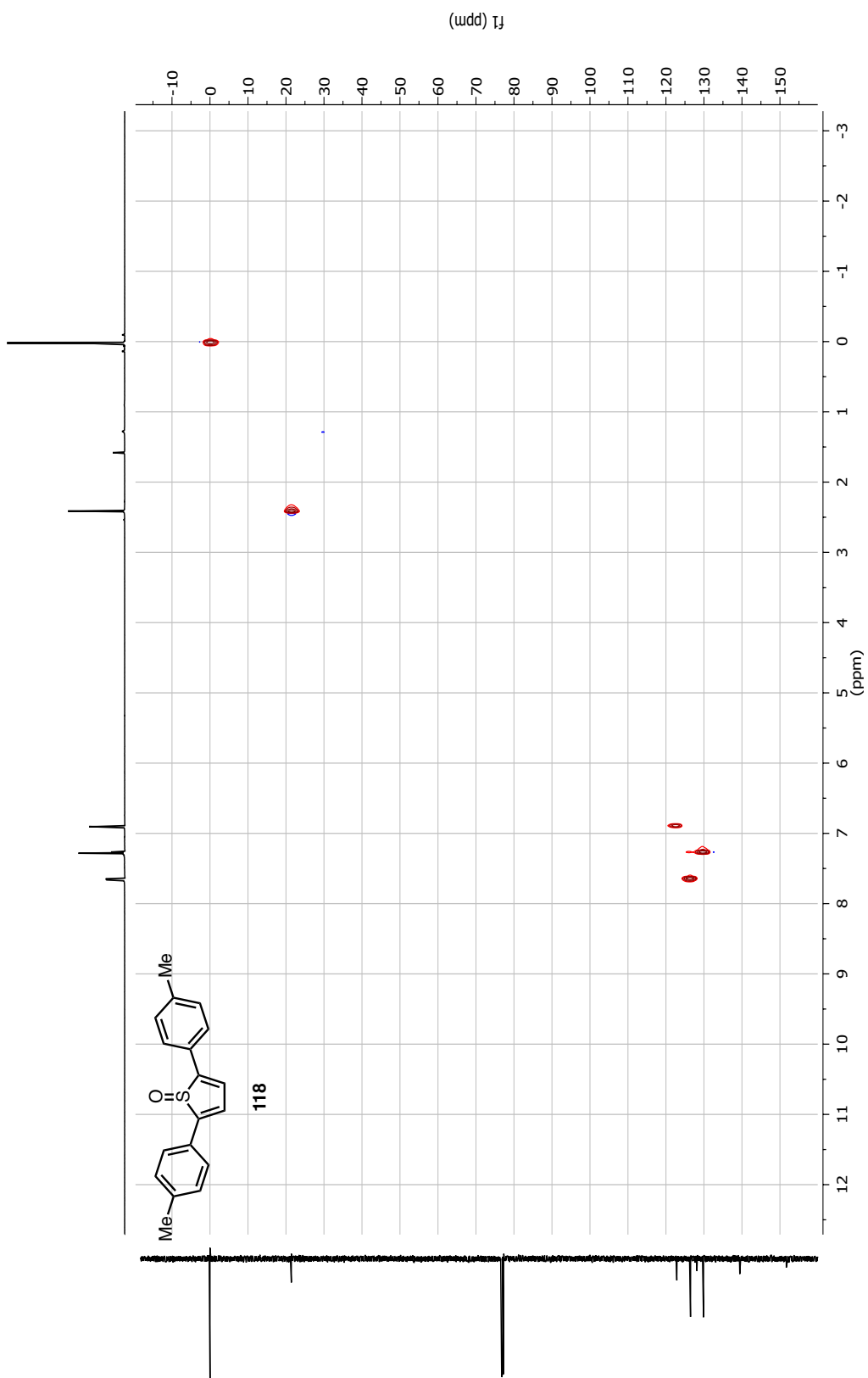
Figure AI.50 2D HSQC NMR Spectrum of **118** in CDCl$_3$
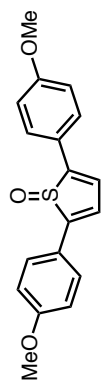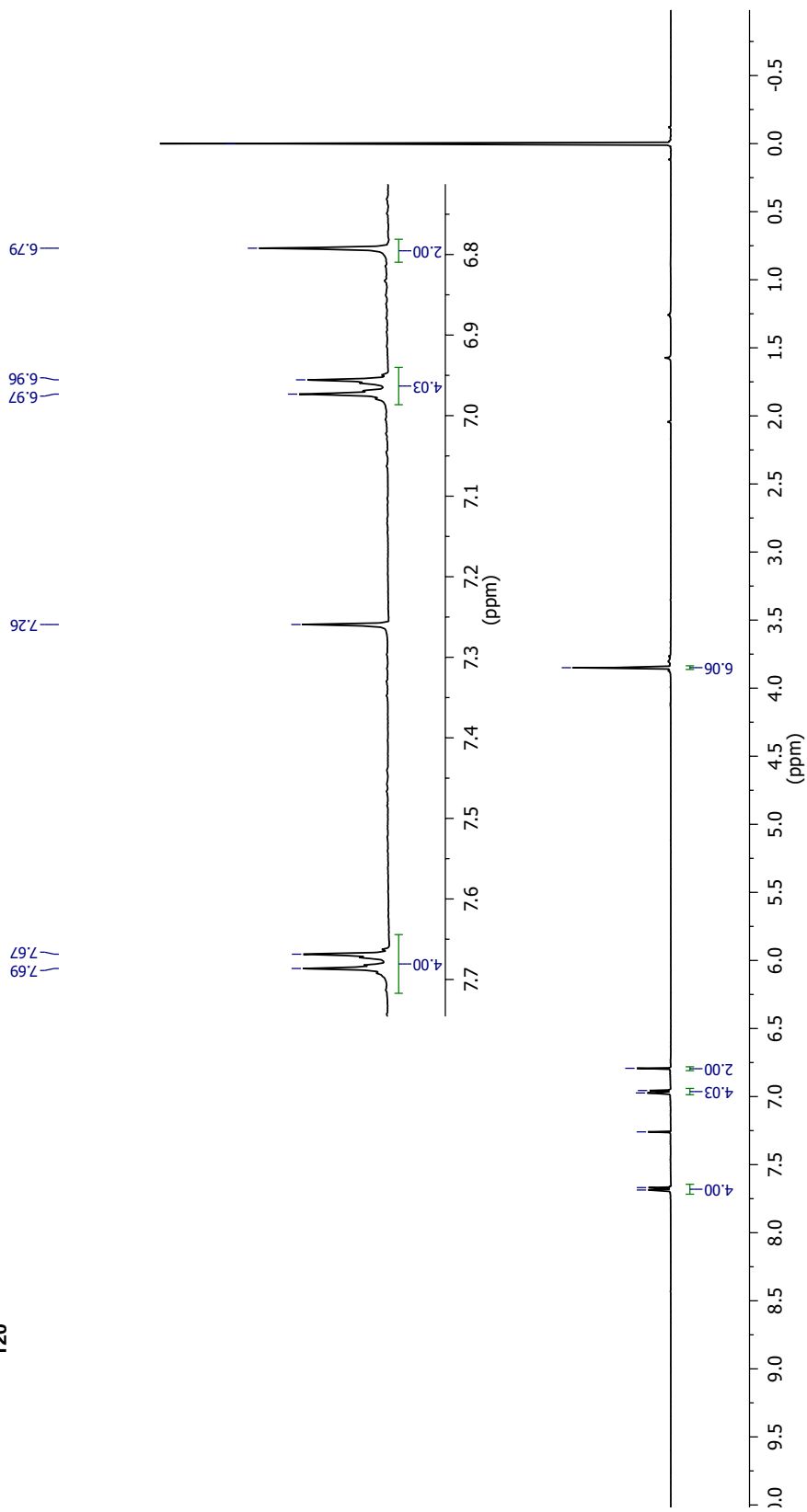
Figure AI.51 ^1H NMR Spectrum of **120** in CDCl$_3$
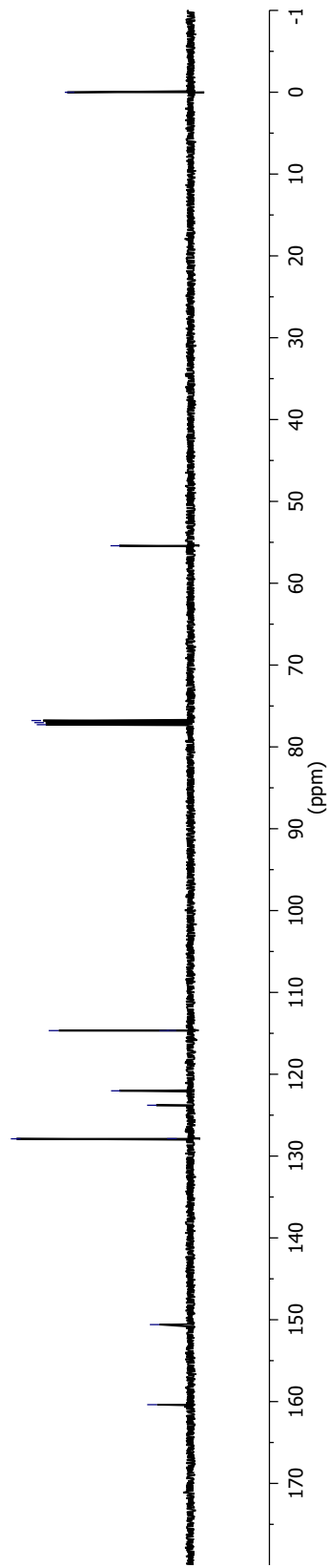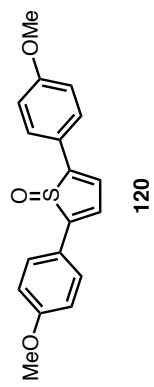
Figure AI.52 ^{13}C NMR Spectrum of **120** in CDCl$_3$

226
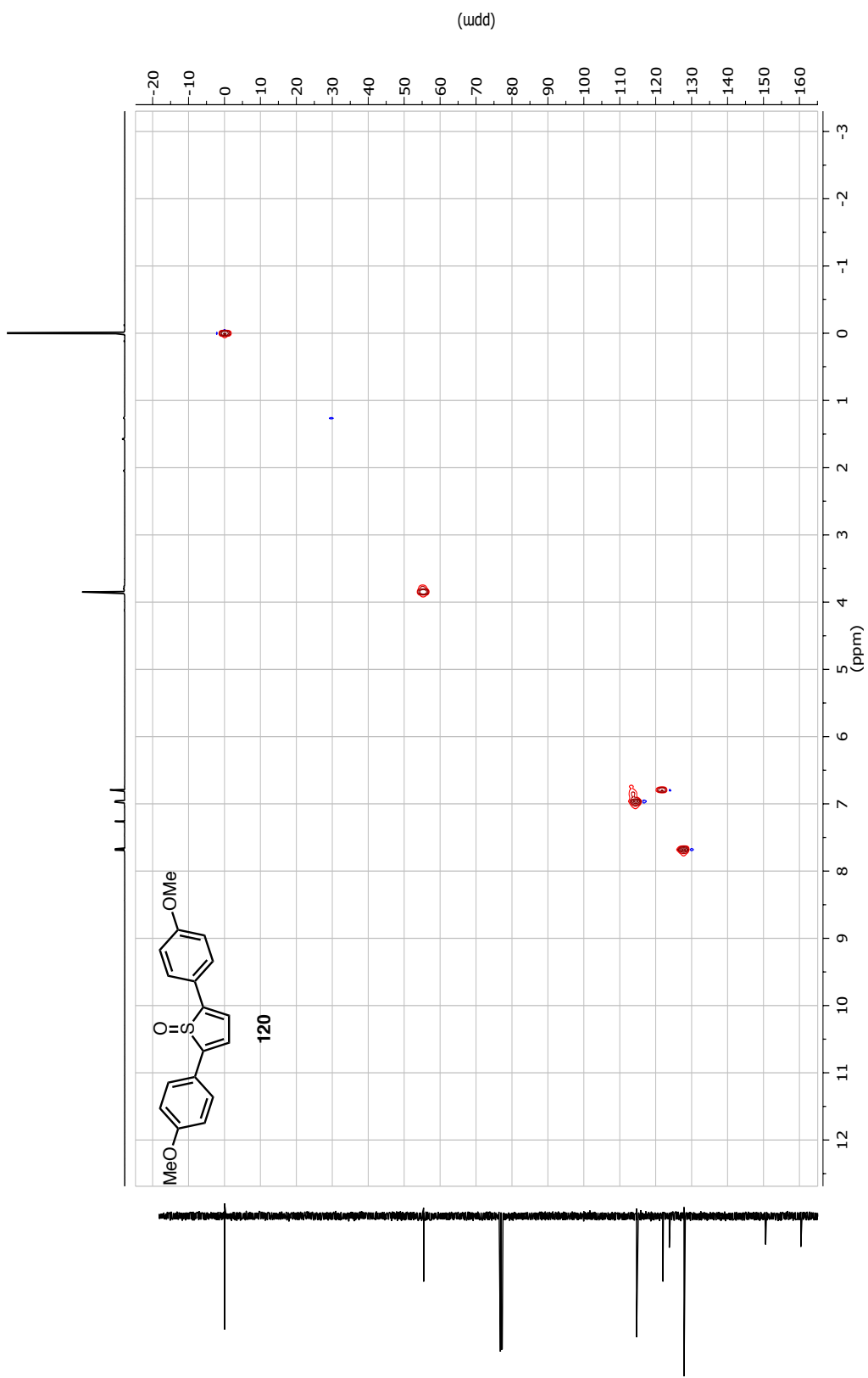
Figure AI.53 2D HSQC NMR Spectrum of **120** in CDCl₃
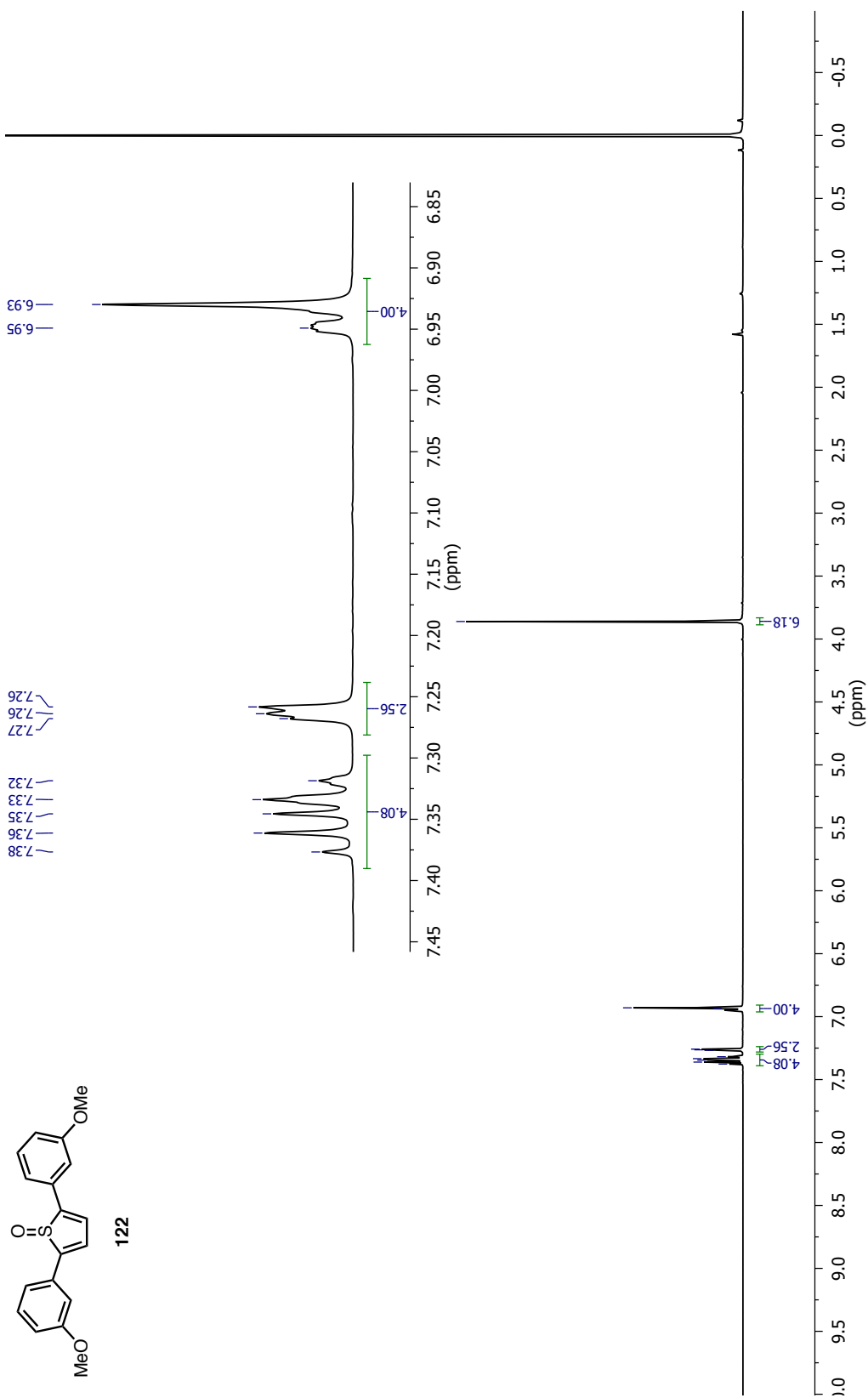
Figure AI.54 ^{1}H NMR Spectrum of **122** in CDCl$_3$
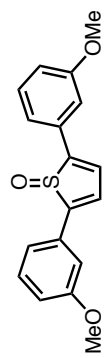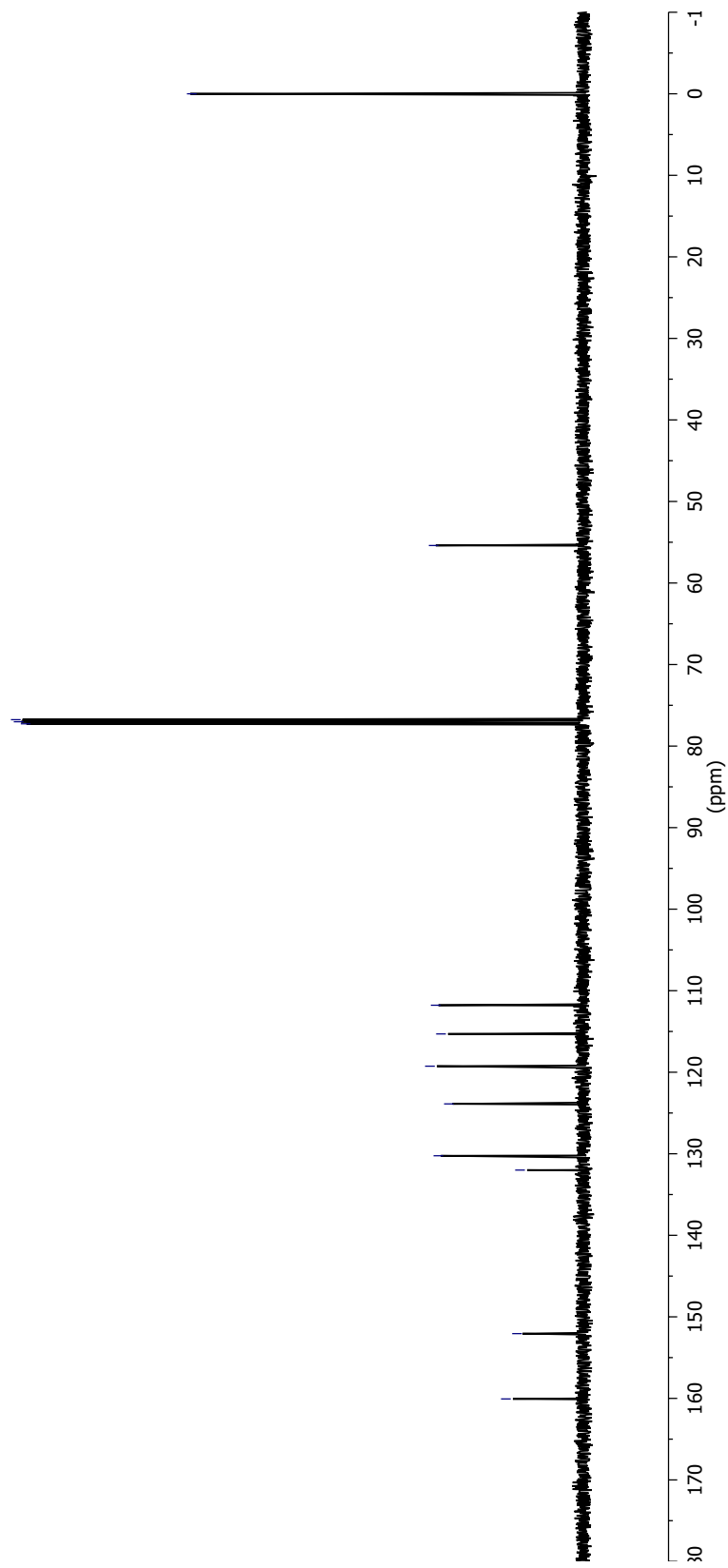
Figure AI.55 ^{13}C NMR Spectrum of **122** in CDCl$_3$

229
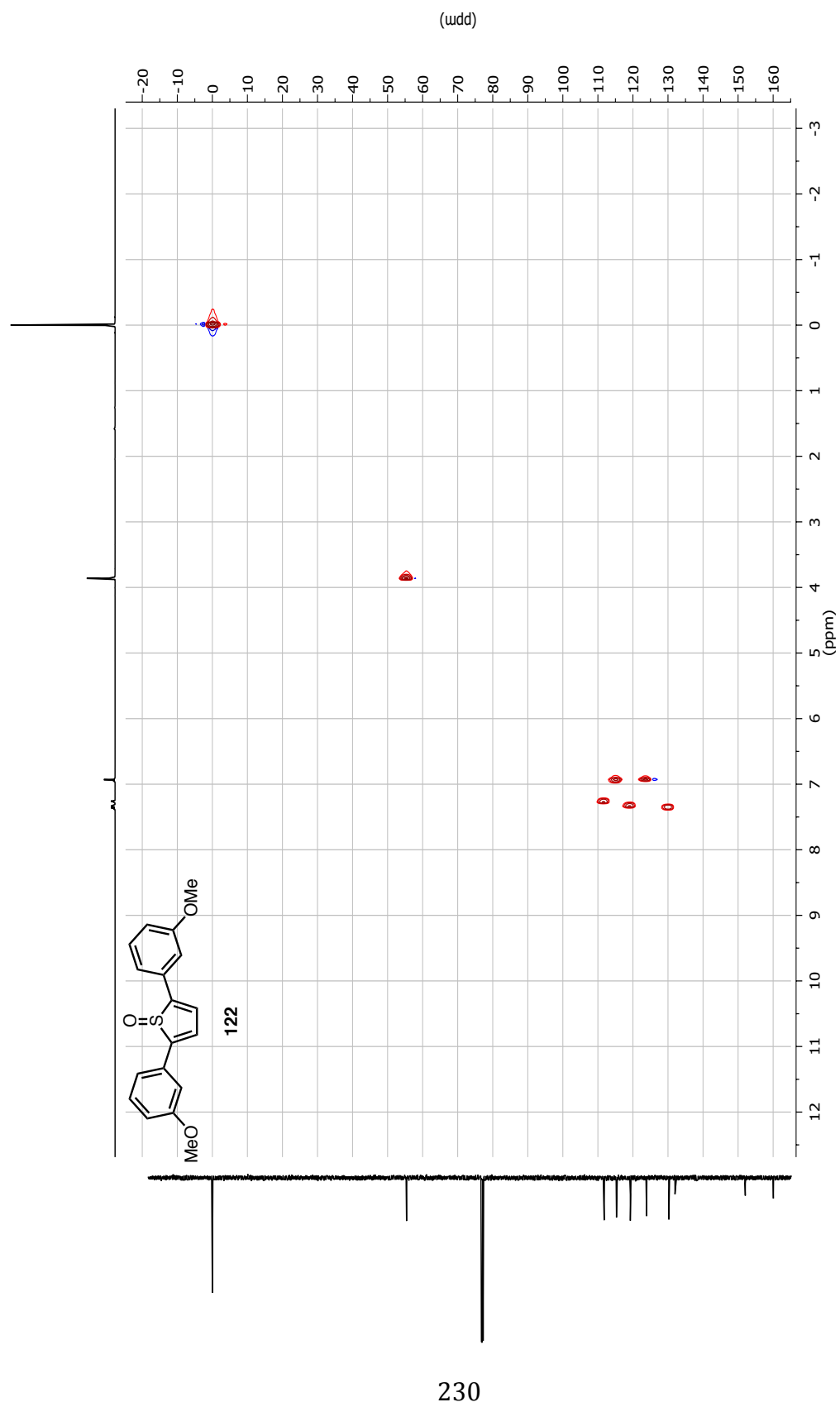
Figure AI.56 2D HSQC NMR Spectrum of **122** in CDCl$_3$

230
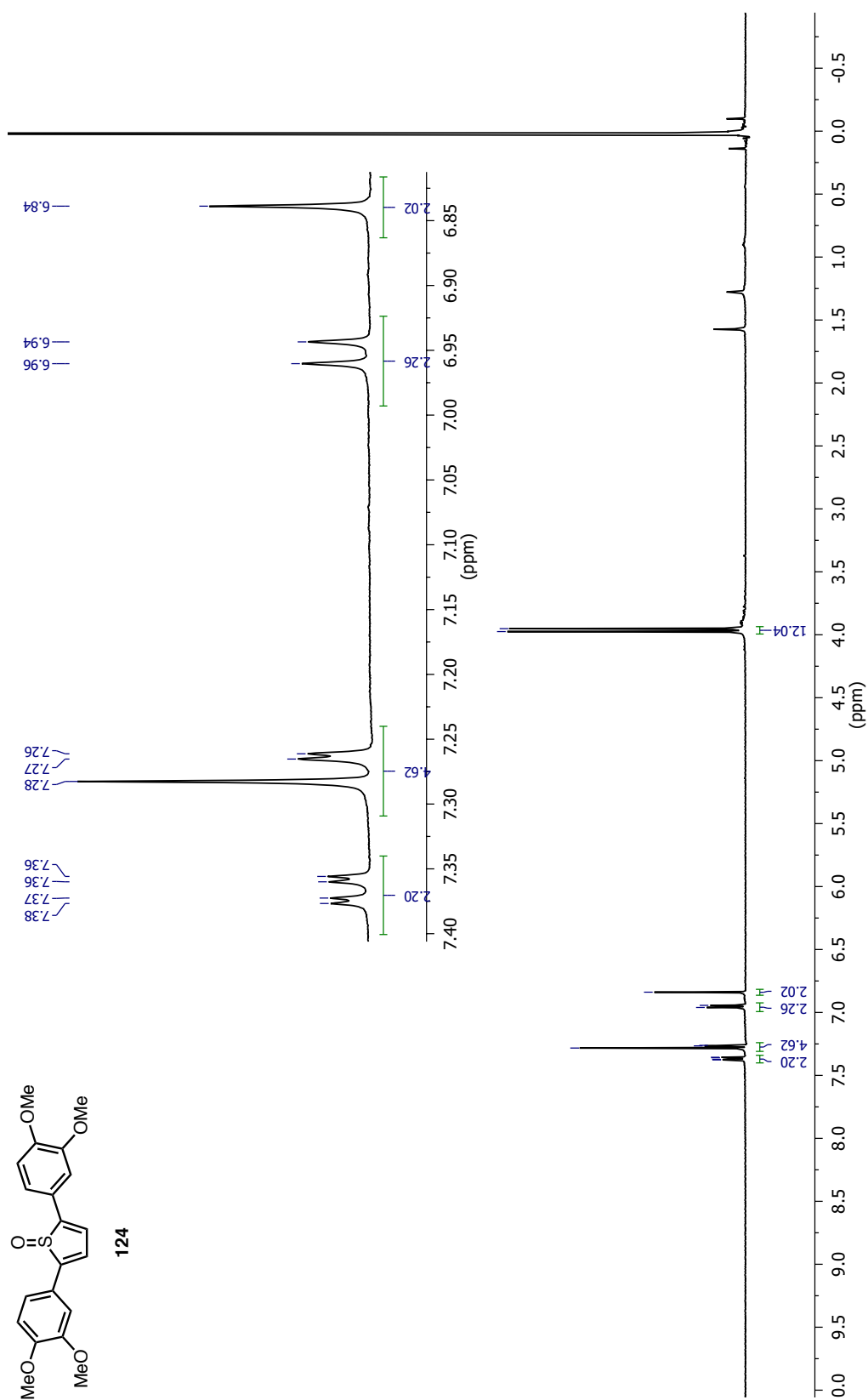
Figure AI.57 ^{1}H NMR Spectrum of **124** in CDCl$_3$
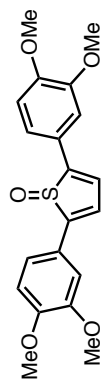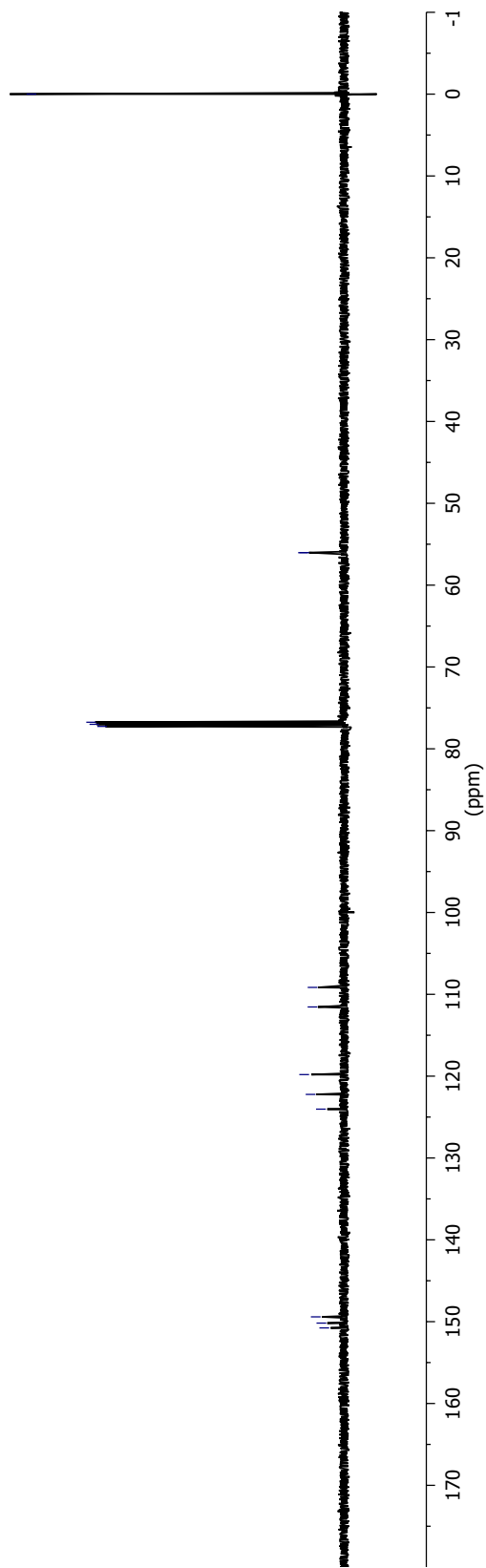
Figure AI.58 ^{13}C NMR Spectrum of **124** in CDCl$_3$

232
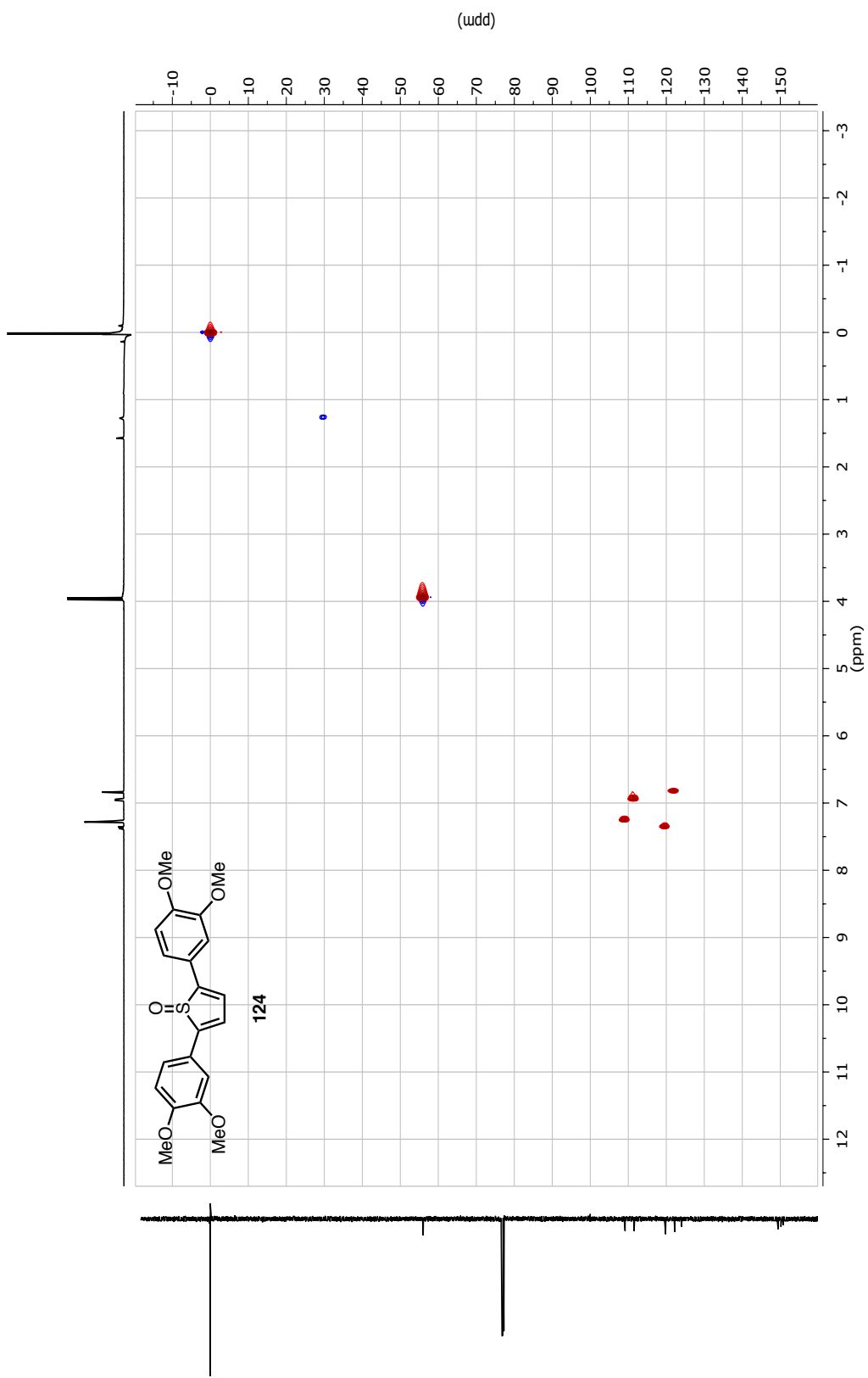
Figure AI.59 2D HSQC NMR Spectrum of **124** in CDCl₃
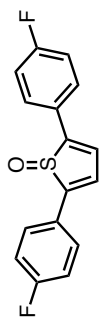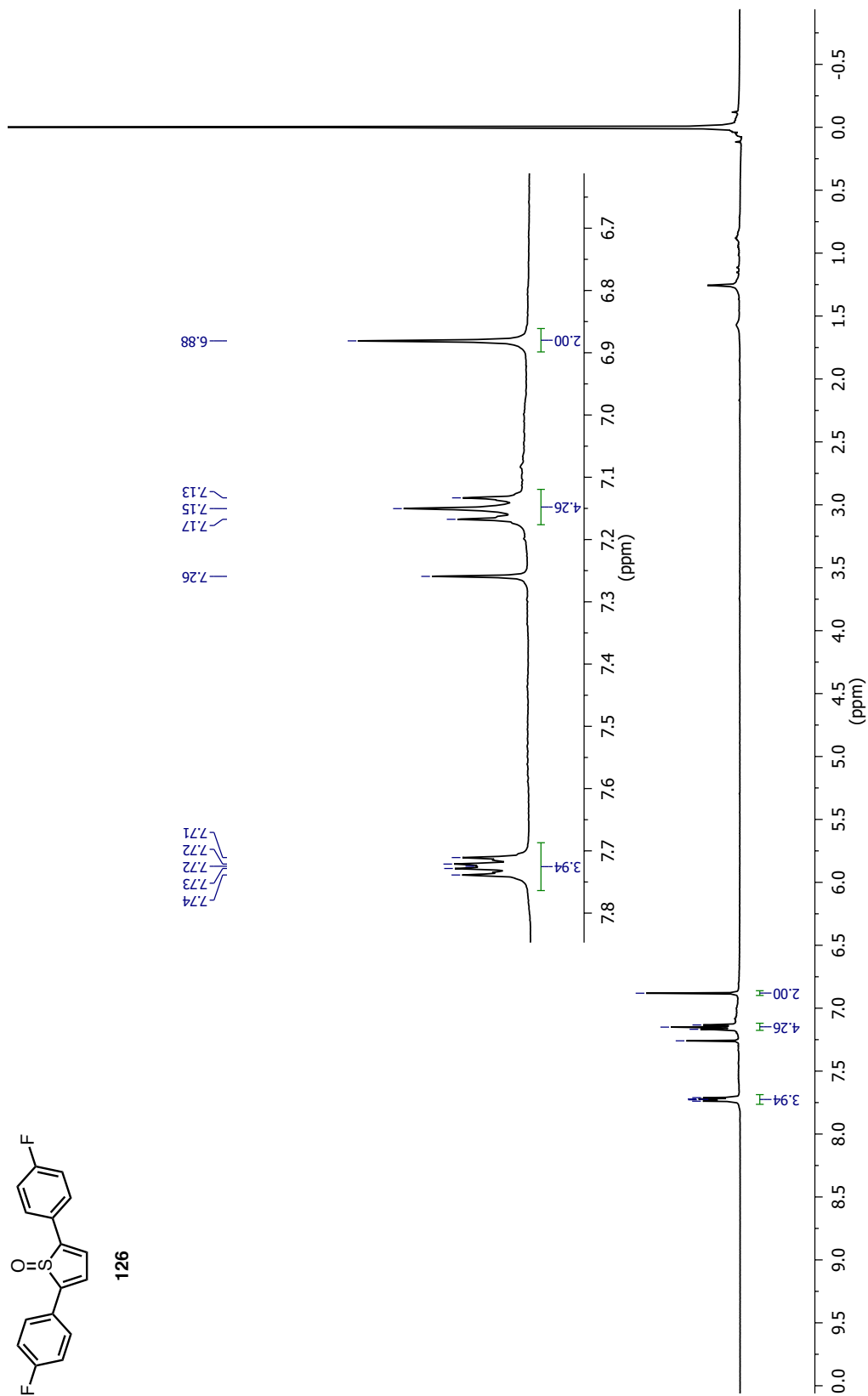
Figure AI.60 ^{1}H NMR Spectrum of **126** in CDCl$_3$
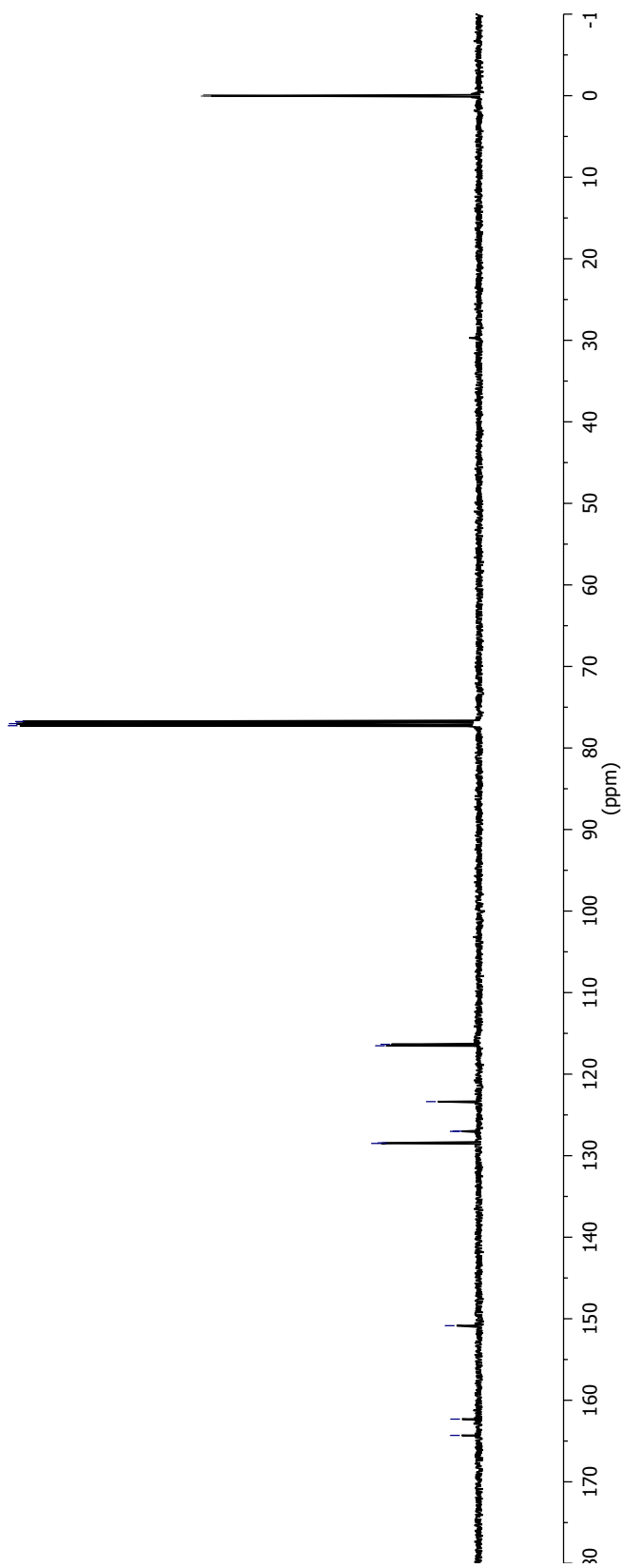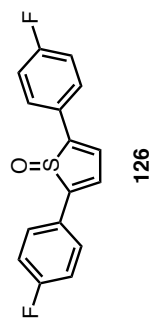
Figure AI.61 ^{13}C NMR Spectrum of **126** in CDCl$_3$

235
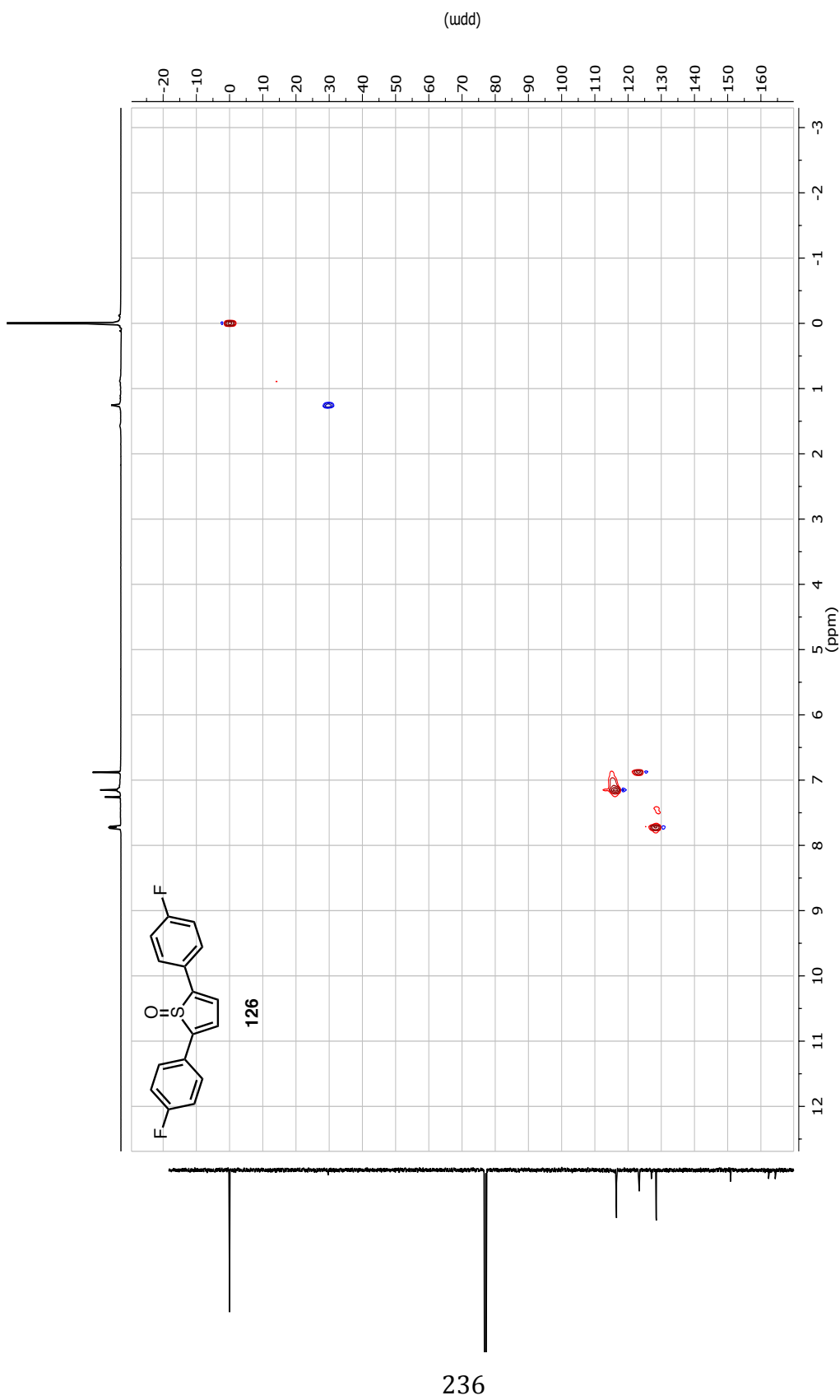
Figure AI.62 2D HSQC NMR Spectrum of **126** in CDCl₃
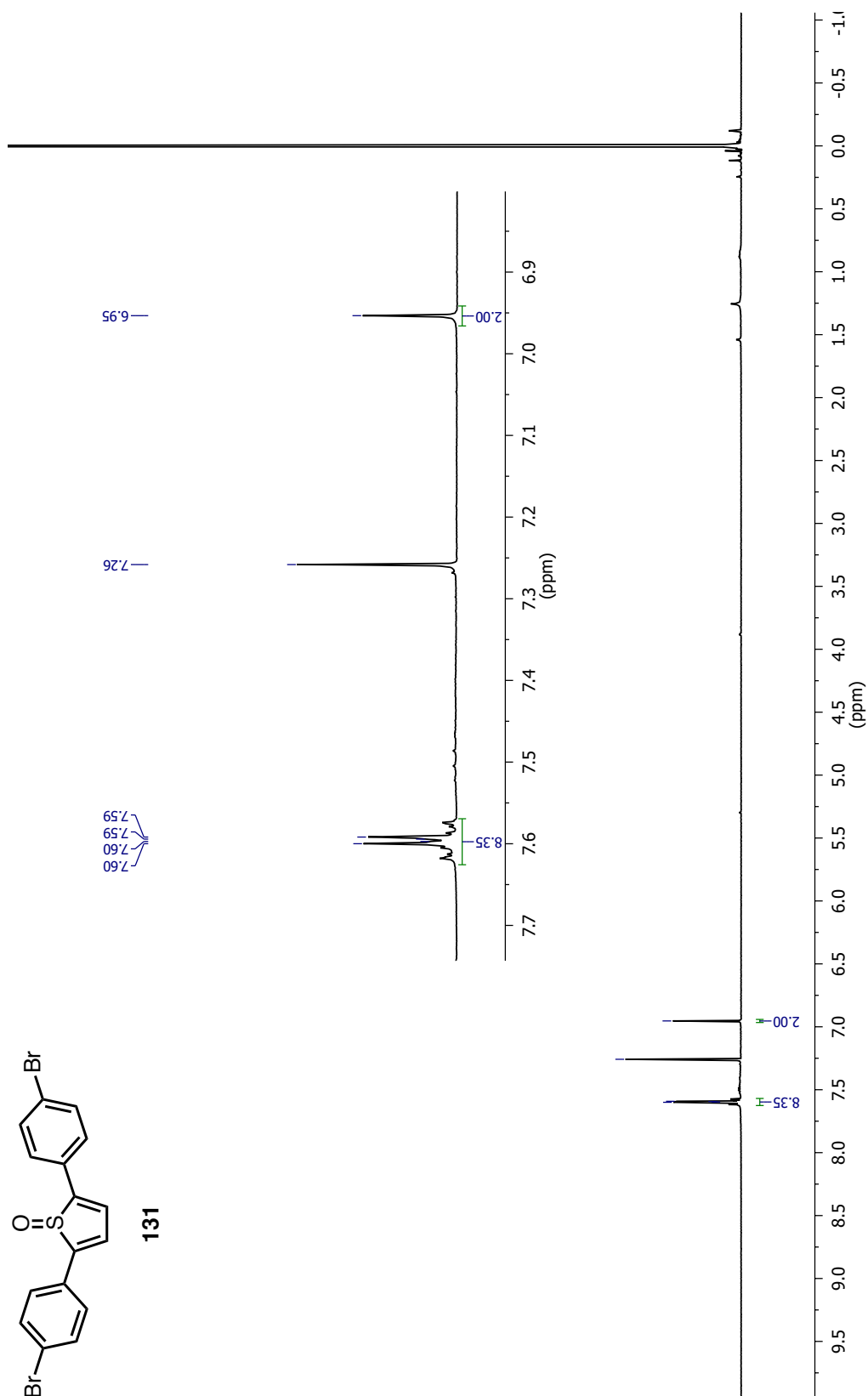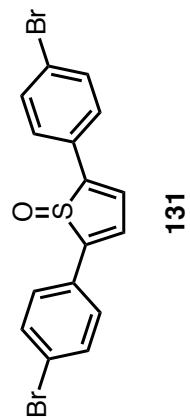
Figure AI.63 ^{1}H NMR Spectrum of **131** in CDCl$_3$

Figure AI.64 ^{13}C NMR Spectrum of **131** in CDCl$_3$

238
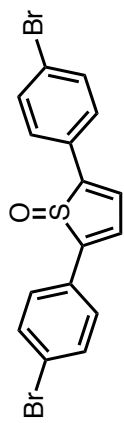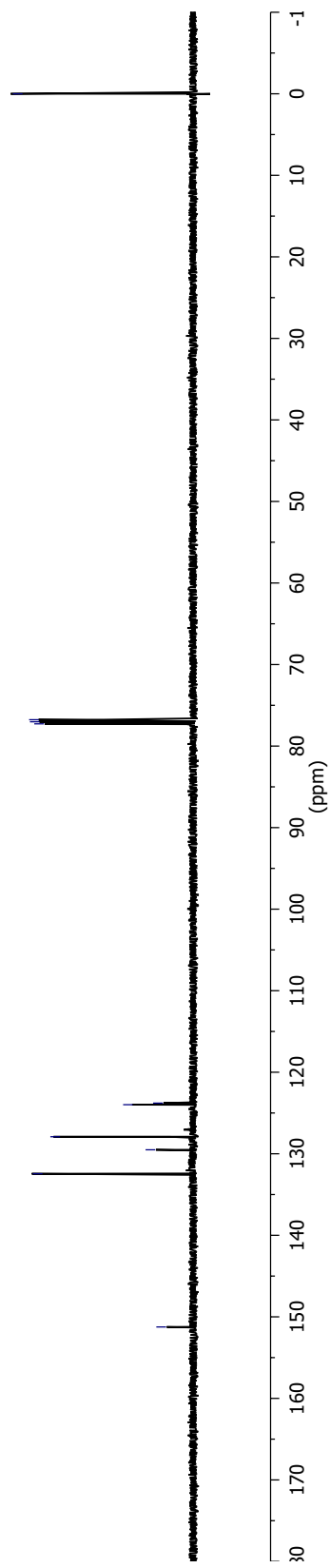
Figure AI.65 2D HSQC NMR Spectrum of **131** in CDCl₃
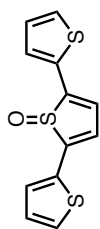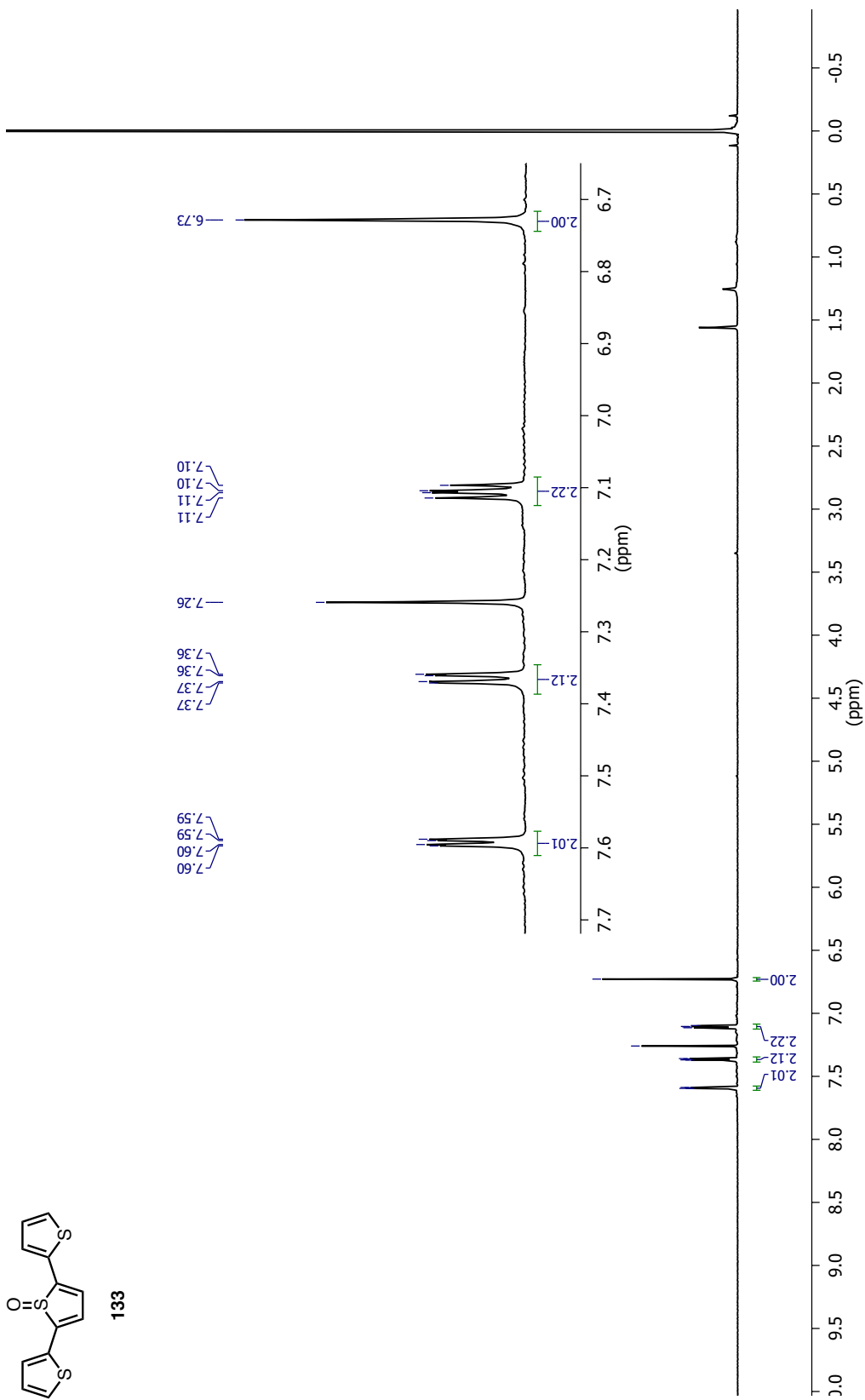
Figure AI.66 ^{1}H NMR Spectrum of **133** in CDCl$_3$
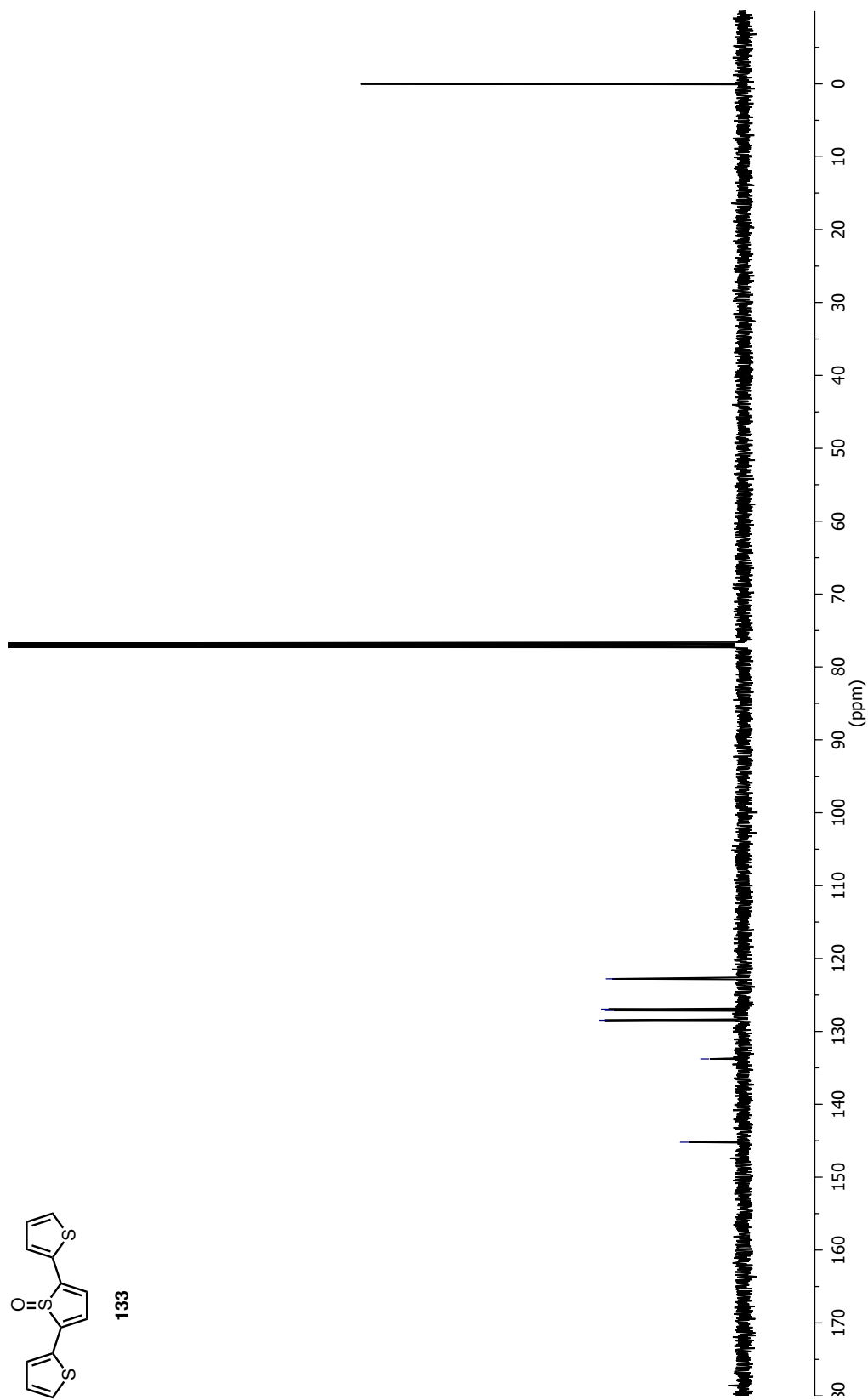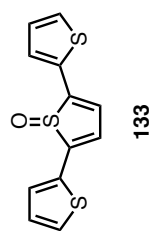
Figure AI.67 ^{13}C NMR Spectrum of **133** in $CDCl_3$
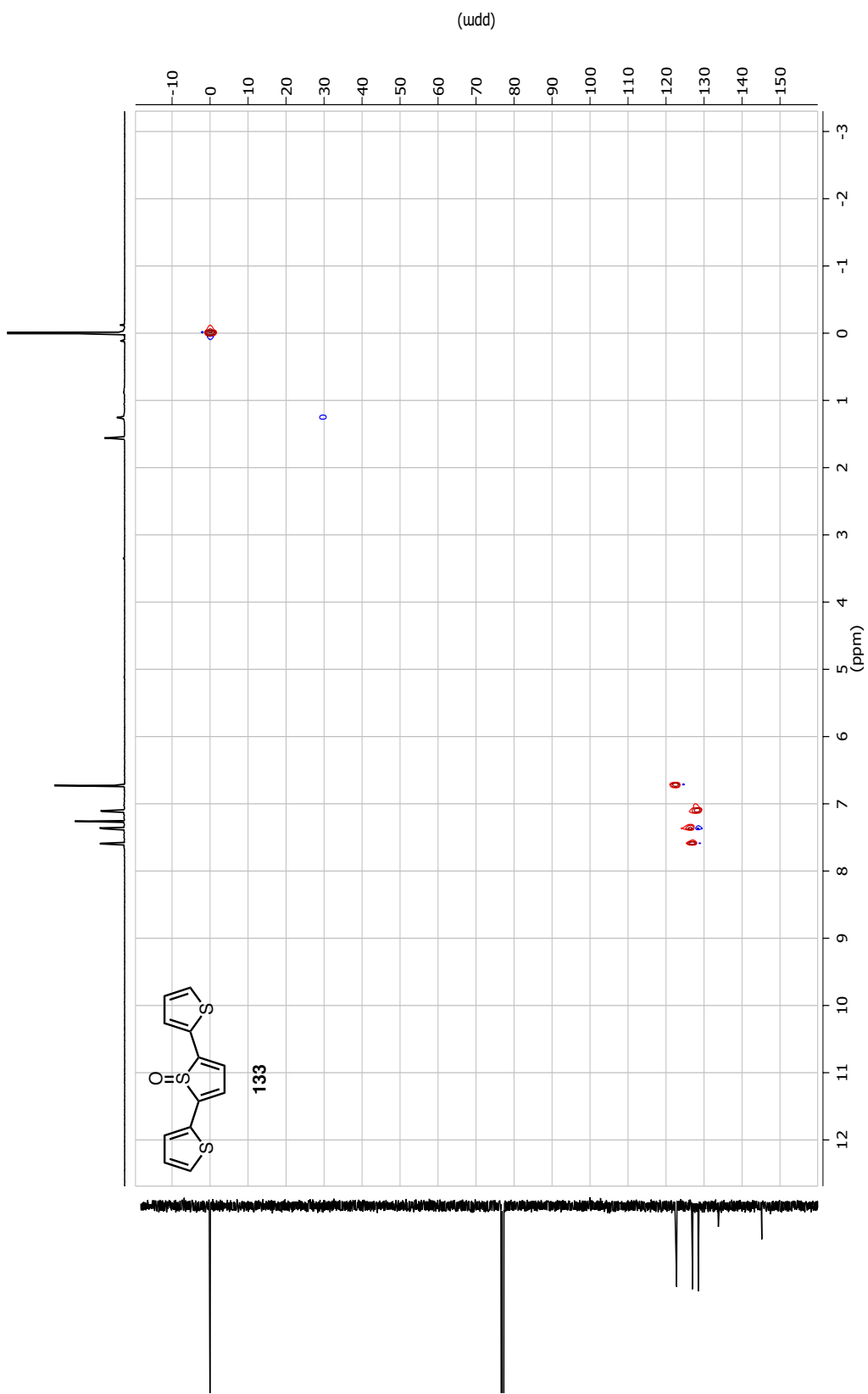
Figure AI.68 2D HSQC NMR Spectrum of **133** in CDCl$_3$

AI.3 Experimental Data for I. GENERAL METHODS FOR THE SYNTHESIS OF

FUNCTIONALIZED TETRABENZO[8]CIRCULENES AND II. STUDIES

TOWARDS EXPANDED [8]CIRCULENE STRUCTURES

Figure AI.69 ^{1}H NMR Spectrum of **134** in CDCl$_3$

125.39
126.35
127.48

129.71
130.76
130.92

139.07
140.14
140.47
141.02

124 126 128 130 132 134 136 138 140 142
(ppm)

134
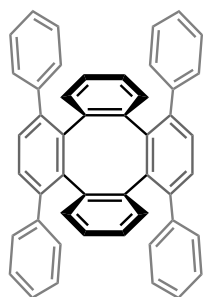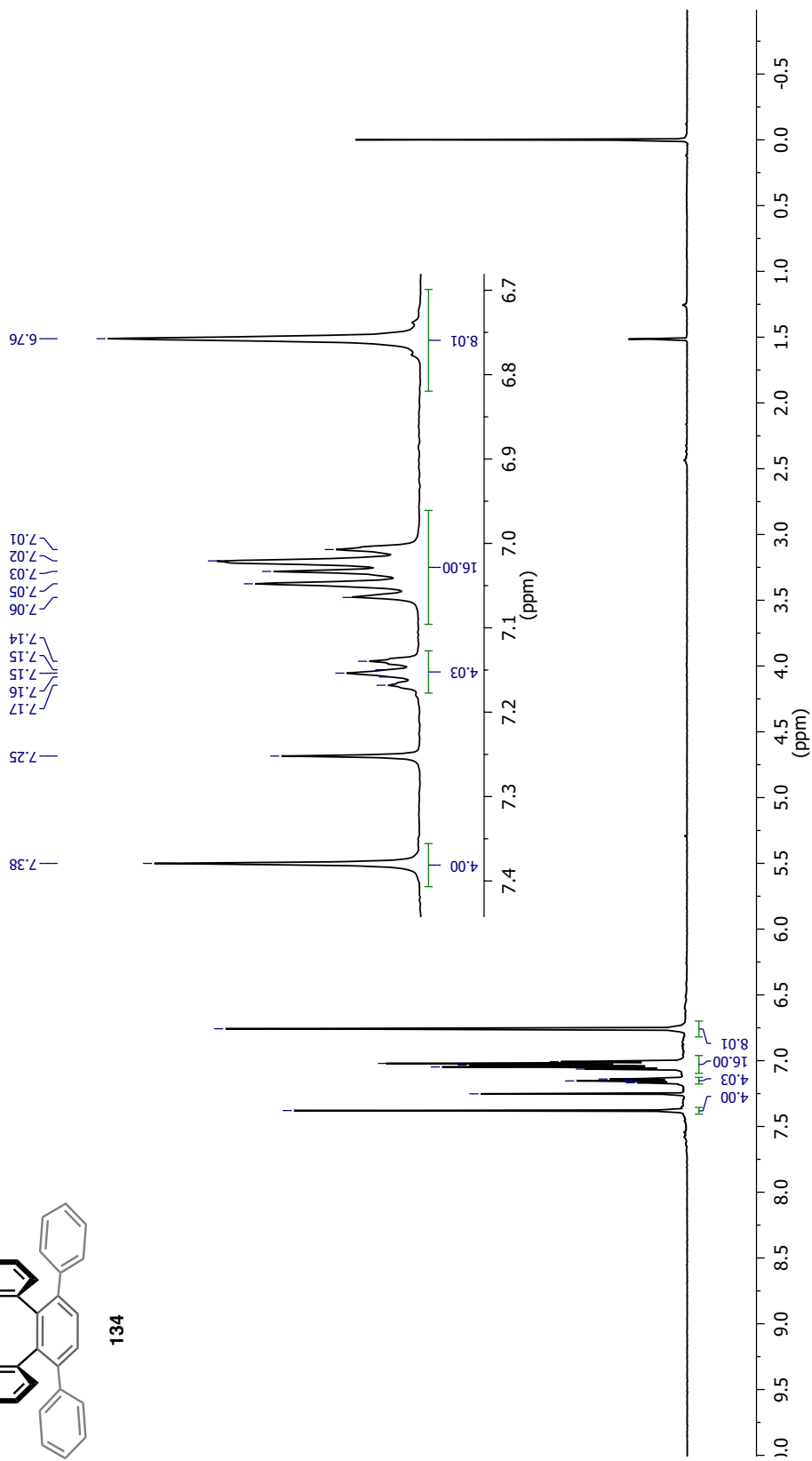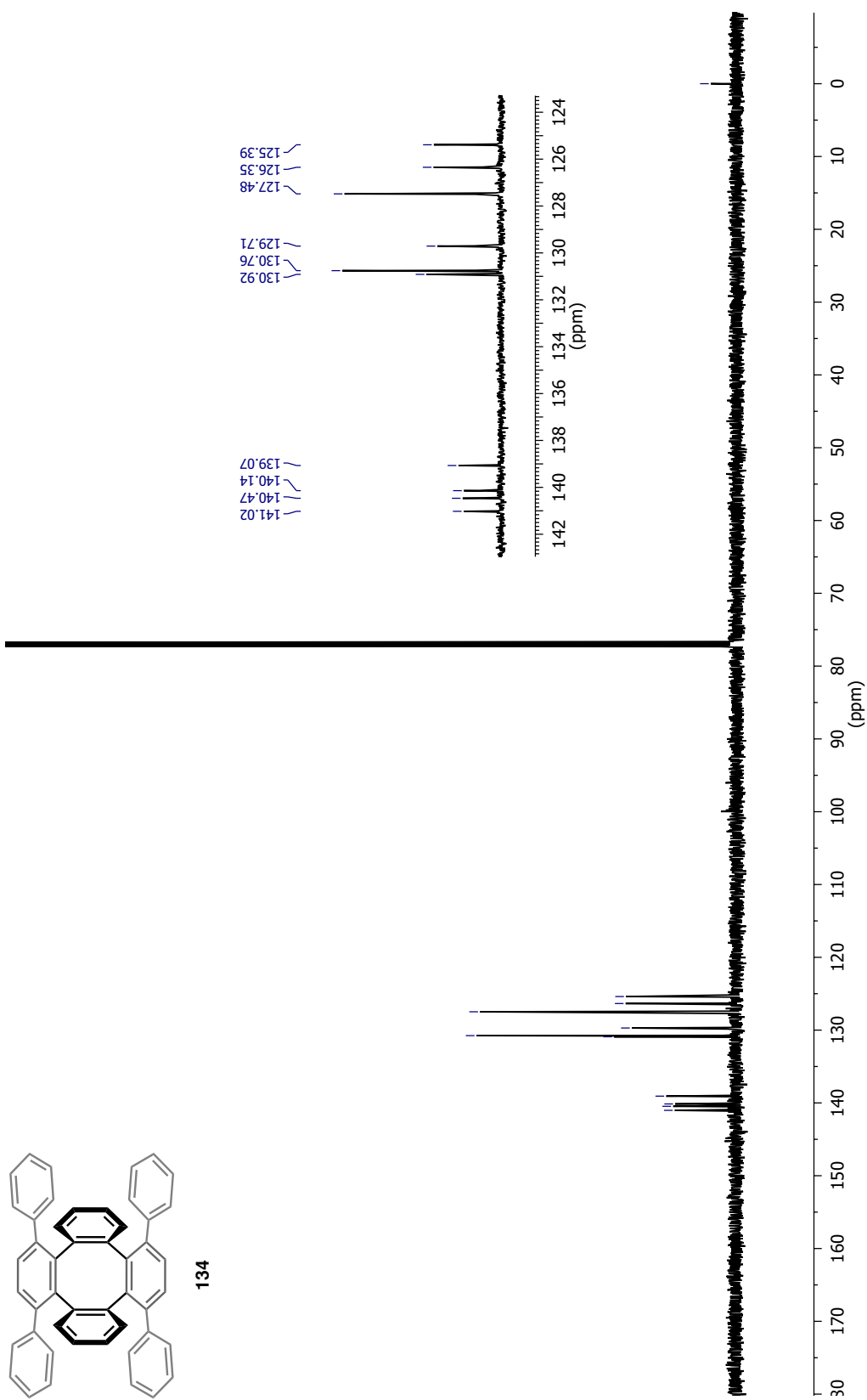
Figure AI.70 ^{13}C NMR Spectrum of **134** in CDCl$_3$

245

Figure AI.71 ^{1}H NMR Spectrum of **135** in CDCl$_3$
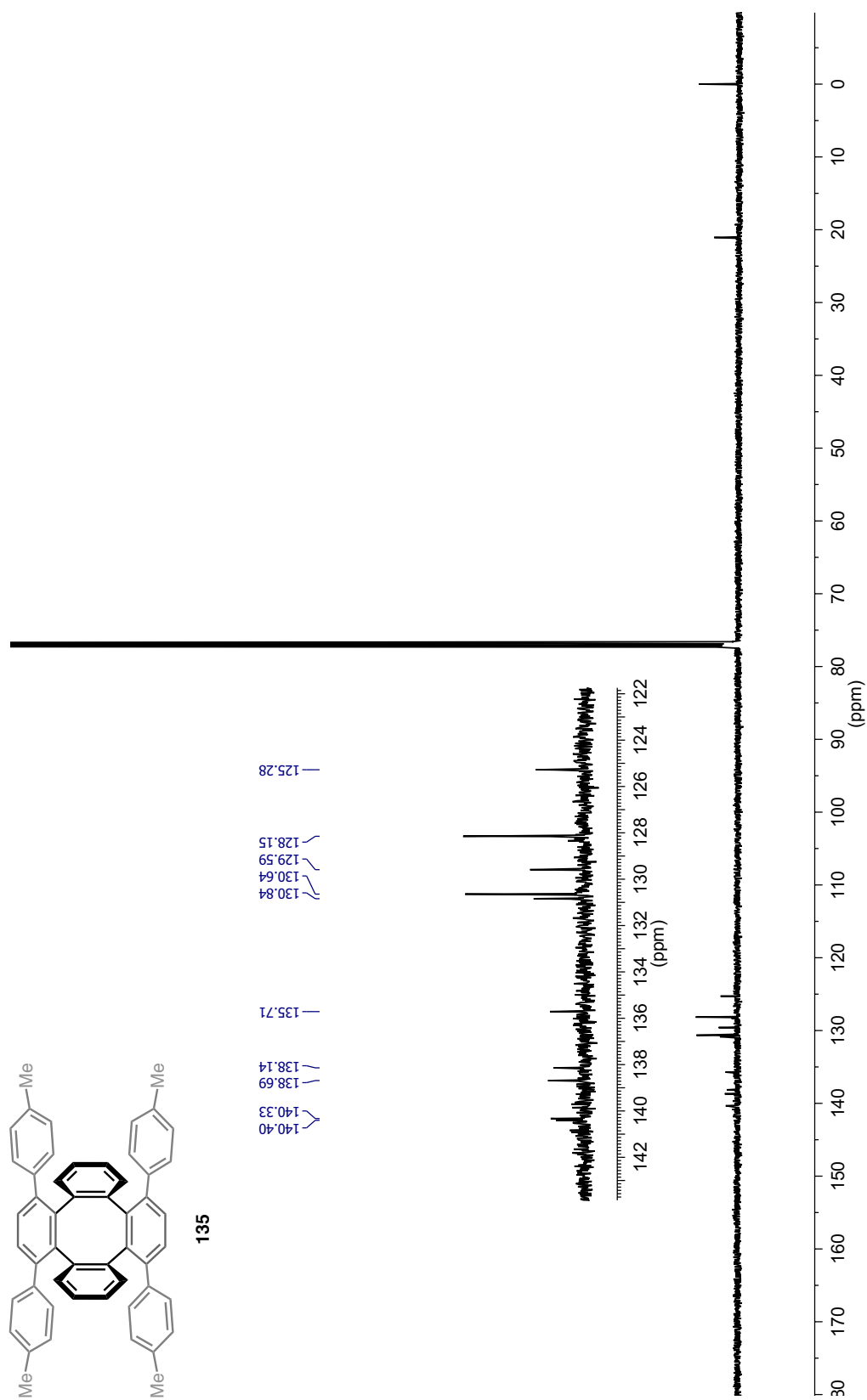
Figure AI.72 ^{13}C NMR Spectrum of **135** in CDCl$_3$
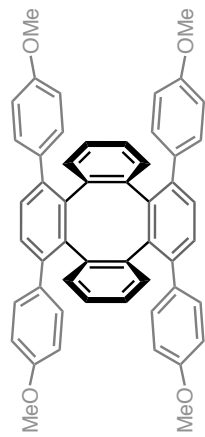
Figure AI.73 ^{1}H NMR Spectrum of **136** in CDCl$_3$

6.57
6.59
6.75
6.75
6.76
6.77
6.77
6.78
6.79
6.79
6.80
6.89
6.90

7.25

7.32

136
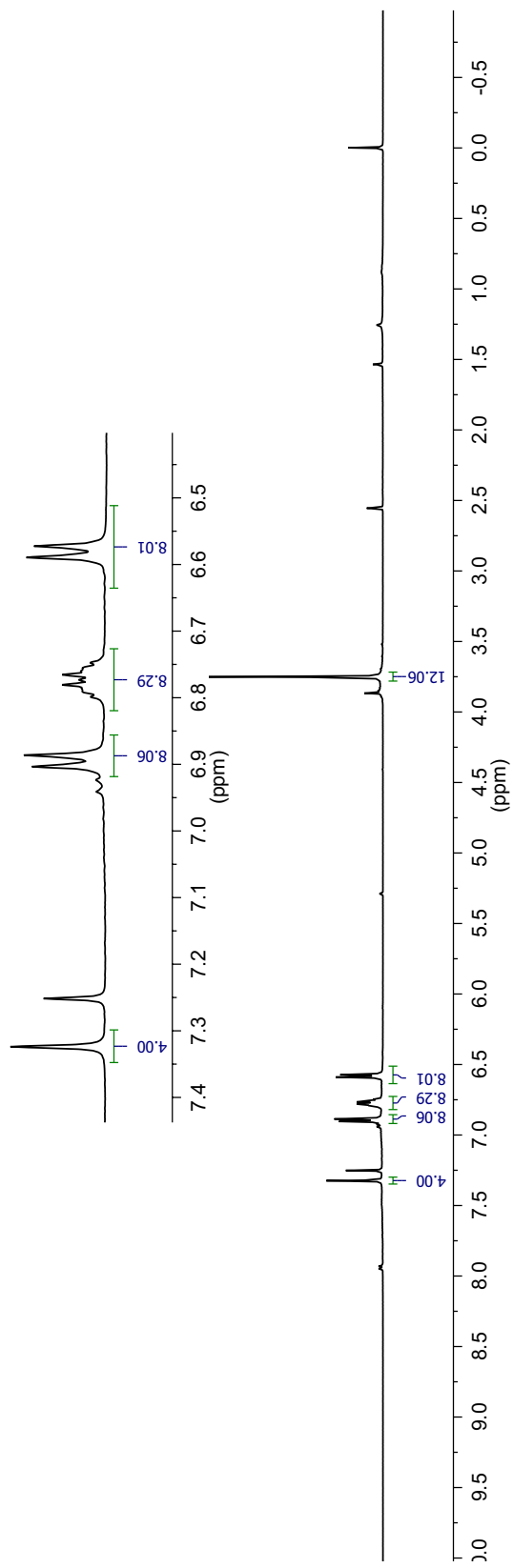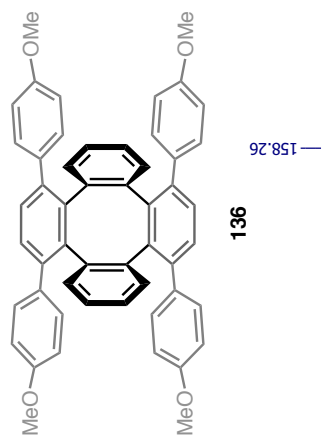
158.26

133.69
132.04
131.06
129.75

125.56

113.05

136

162 158 154 150 146 142 138 134 130 126 122 118 114 110
(ppm)

170 160 150 140 130 120 110 100 90 80 70 60 50 40 30 20 10 0
(ppm)
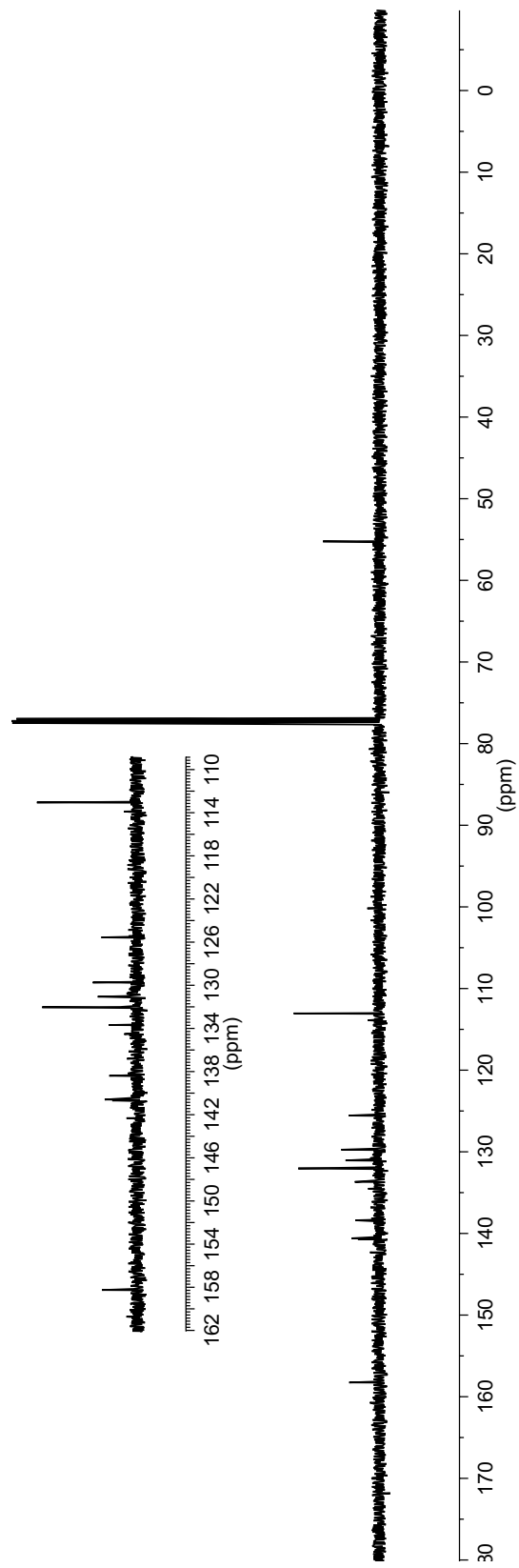
Figure AI.74 ^{13}C NMR Spectrum of **136** in CDCl$_3$
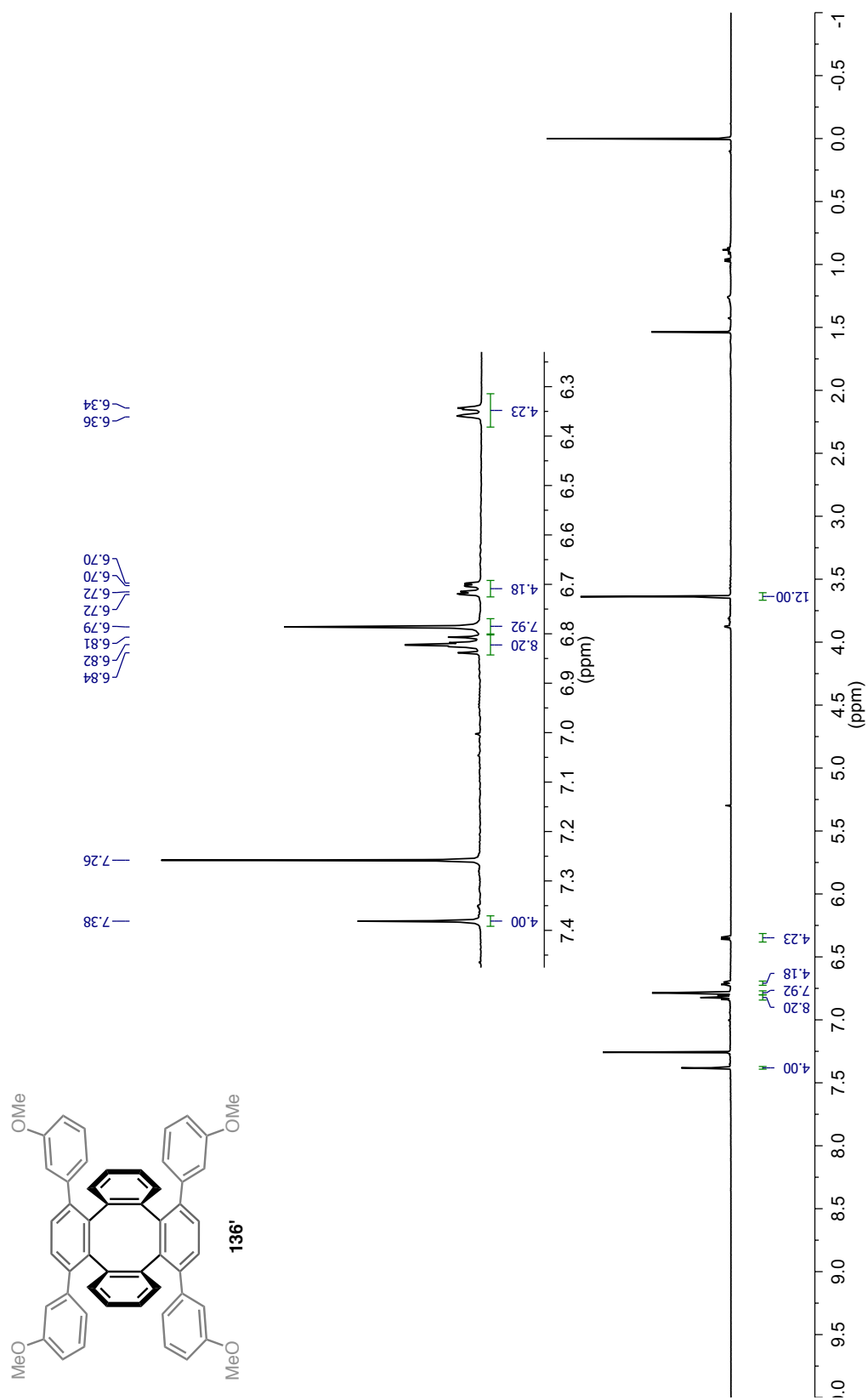
Figure AI.75 ^{1}H NMR Spectrum of **136'** in CDCl$_3$
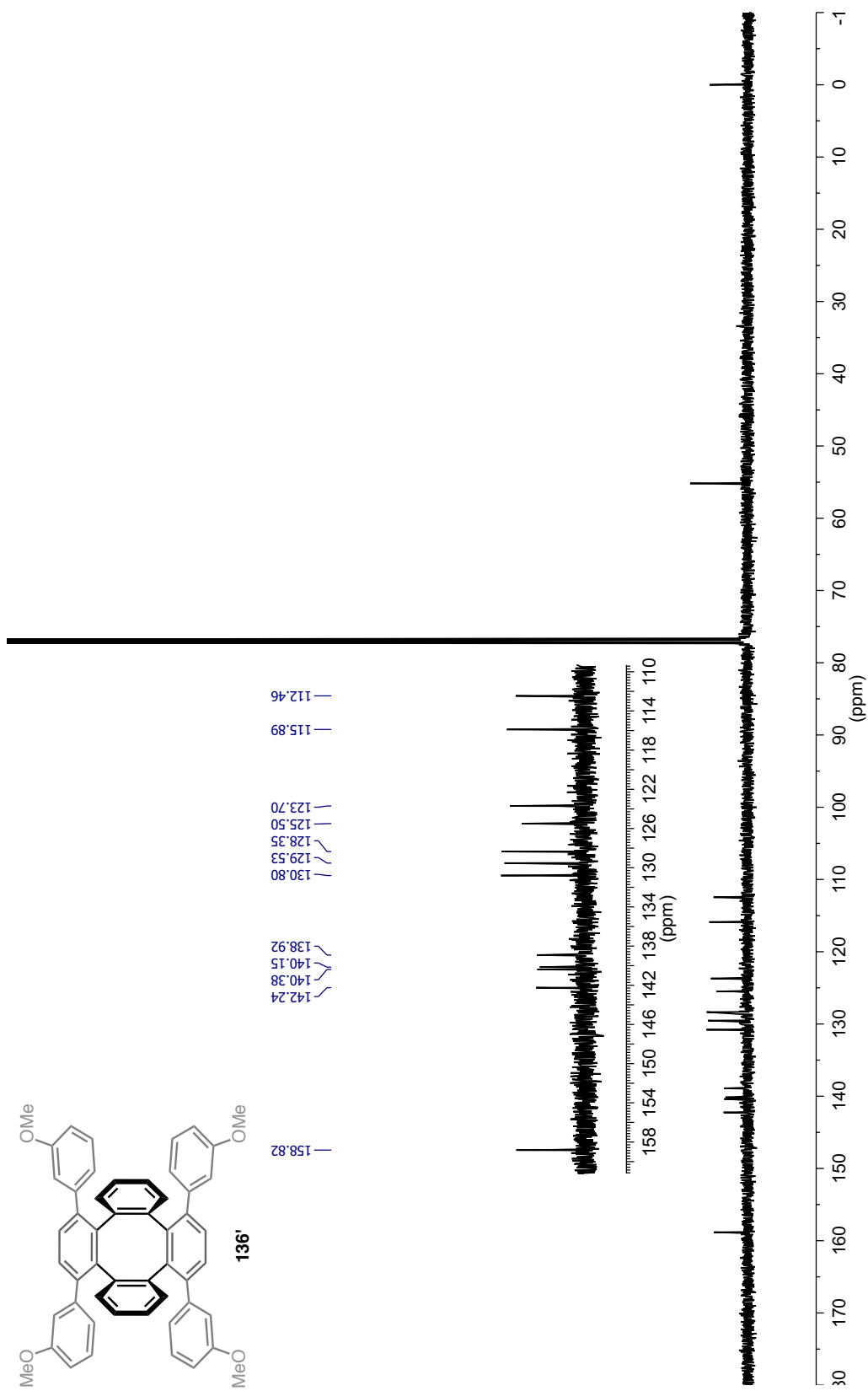
Figure AI.76 ^{13}C NMR Spectrum of **136'** in CDCl$_3$
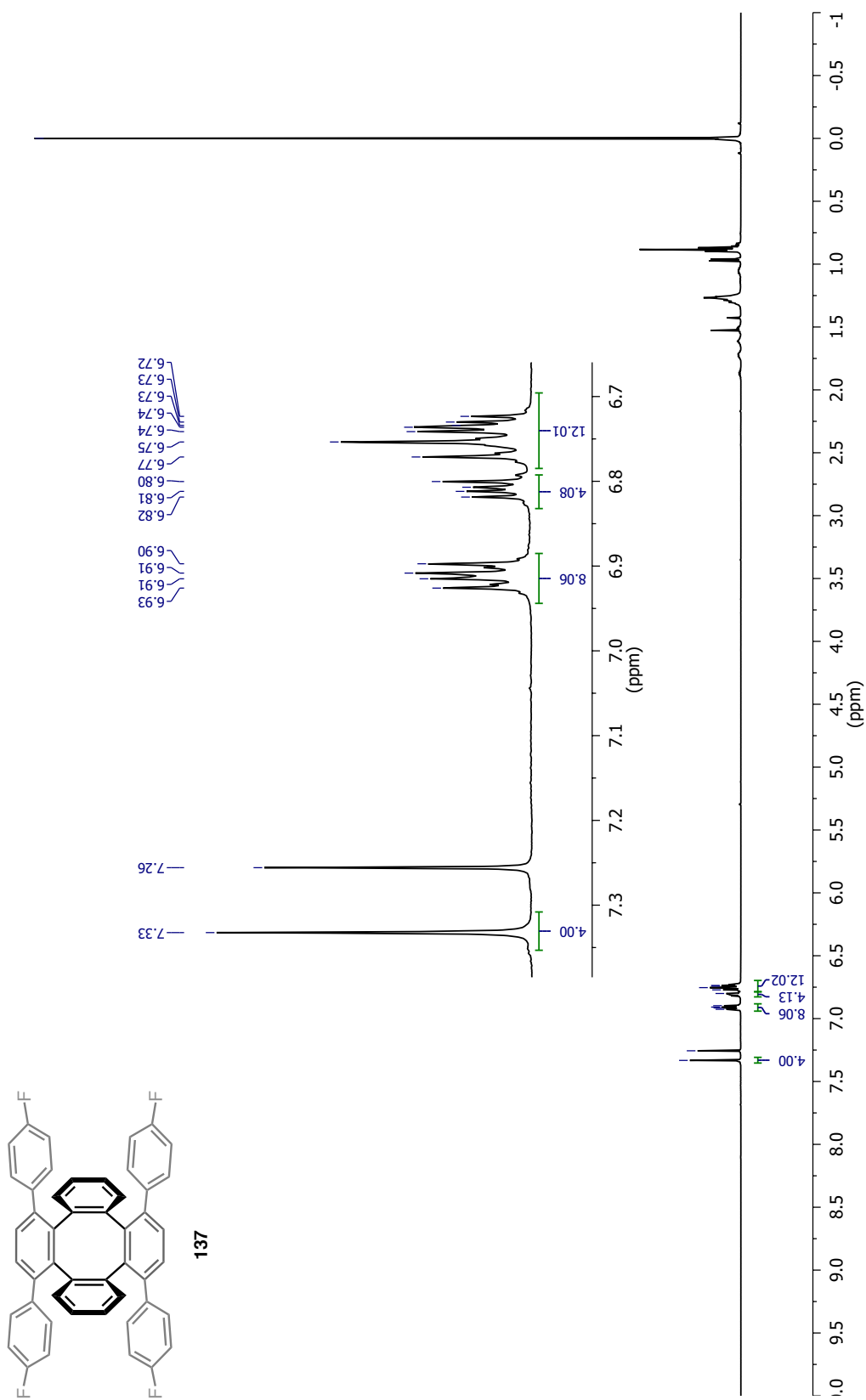
251

Figure AI.77 ^{1}H NMR Spectrum of **137** in CDCl$_3$
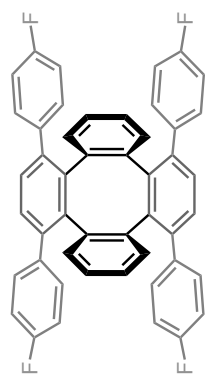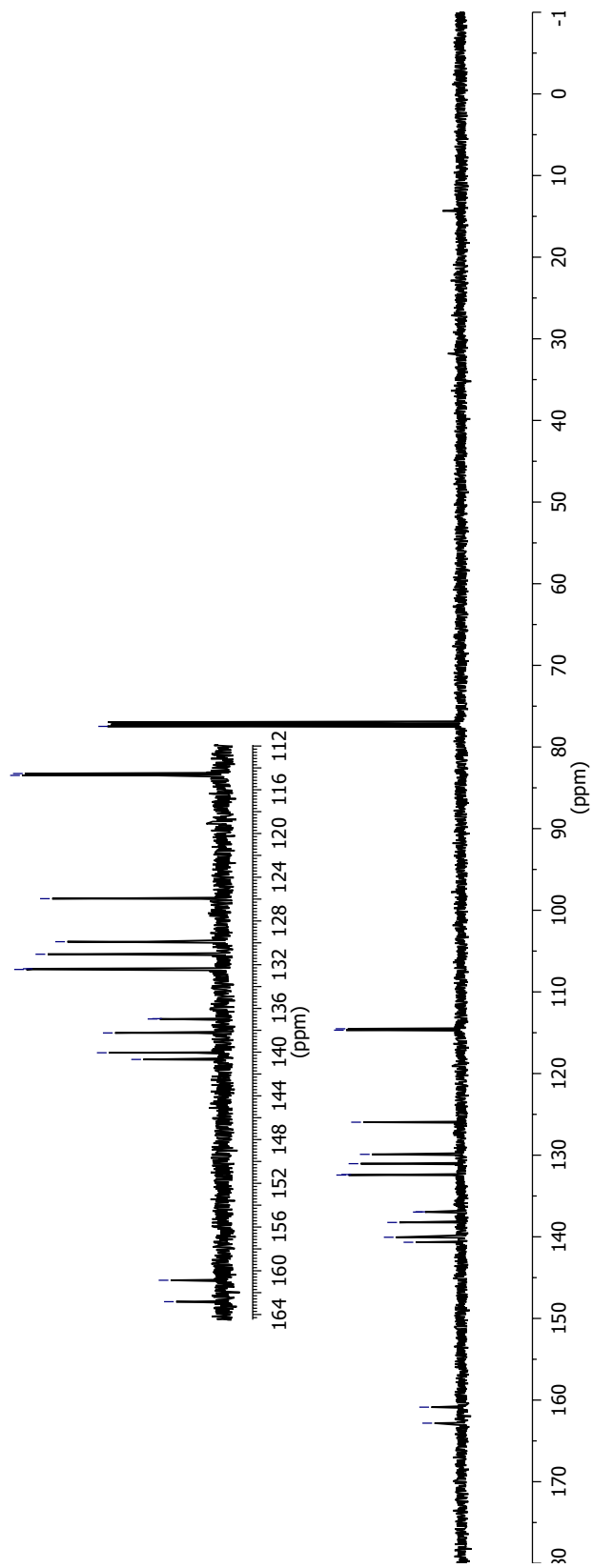
Figure AI.78 ^{13}C NMR Spectrum of **137** in CDCl$_3$
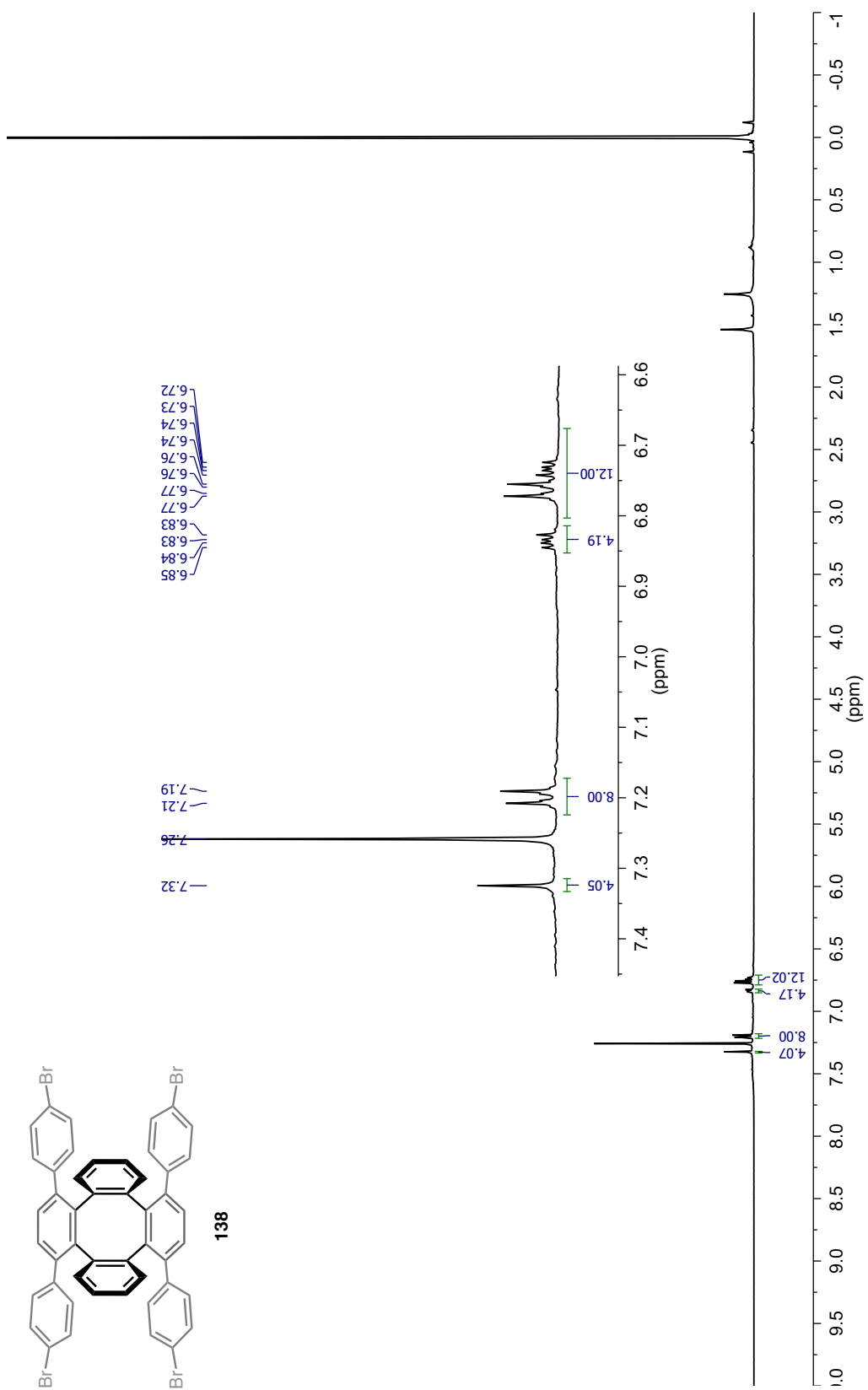
Figure AI.79 ^{1}H NMR Spectrum of **138** in CDCl$_3$

Figure AI.80 ^{13}C NMR Spectrum of **138** in CDCl$_3$
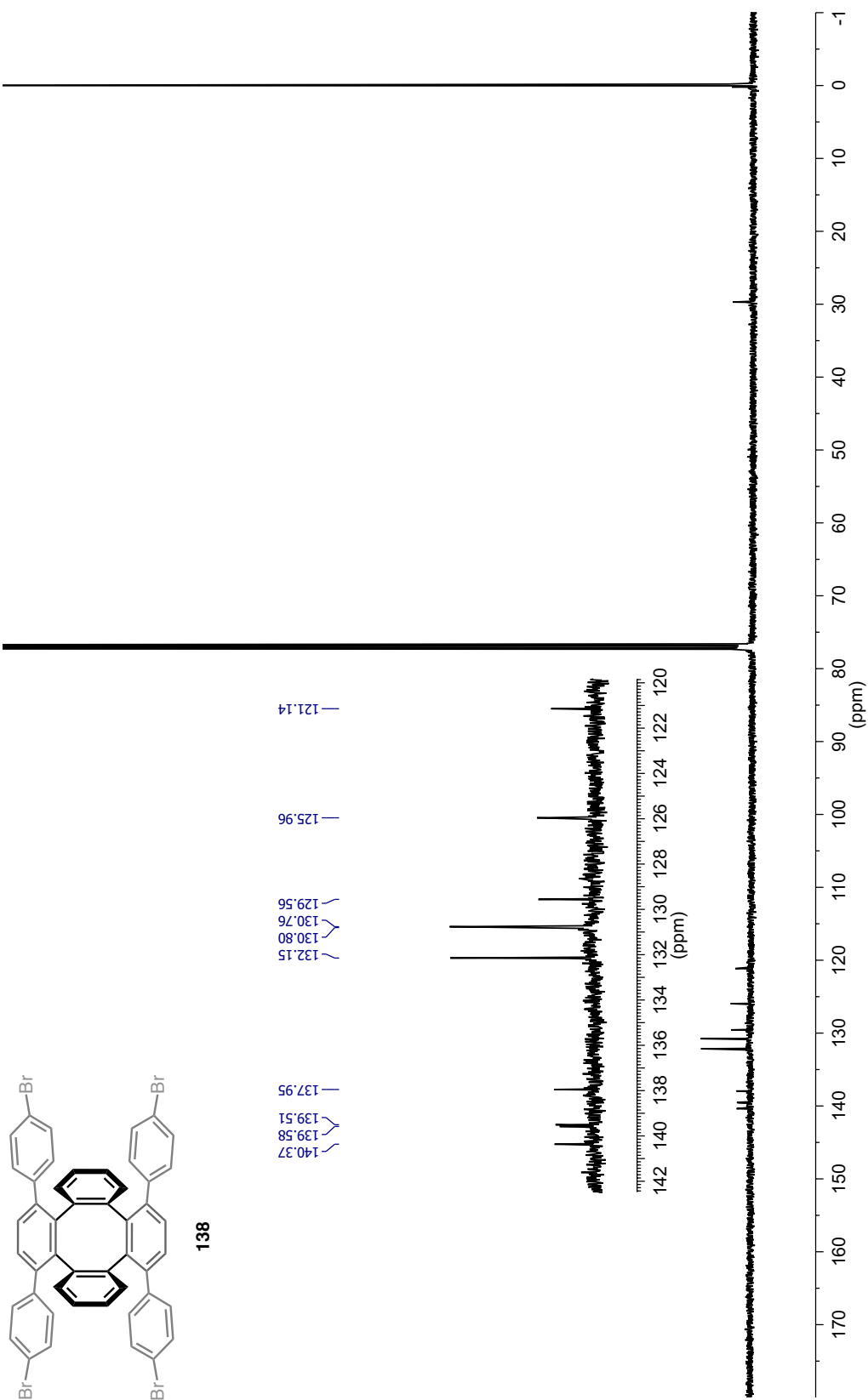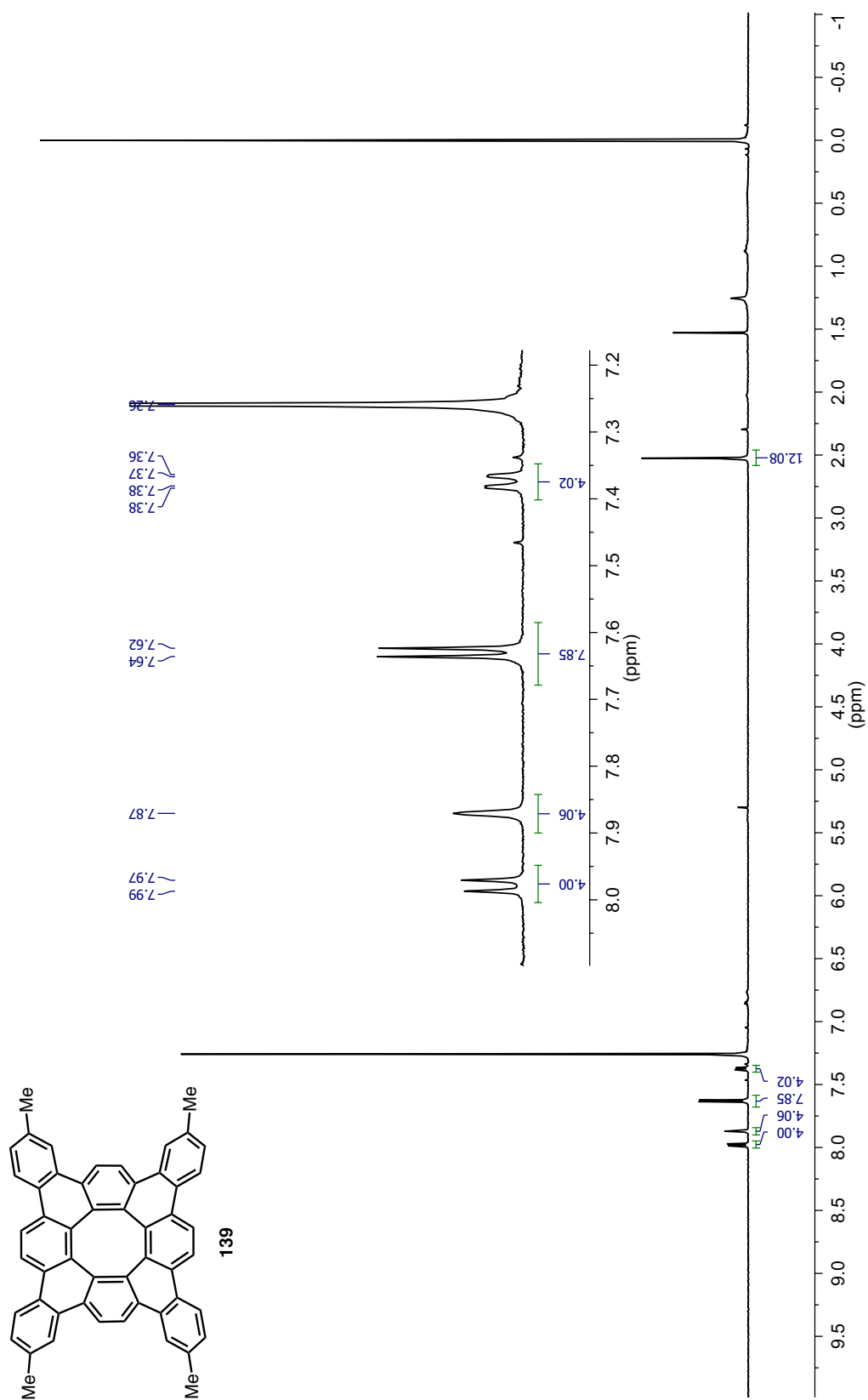
Figure AI.81 ^{1}H NMR Spectrum of **139** in CDCl$_3$
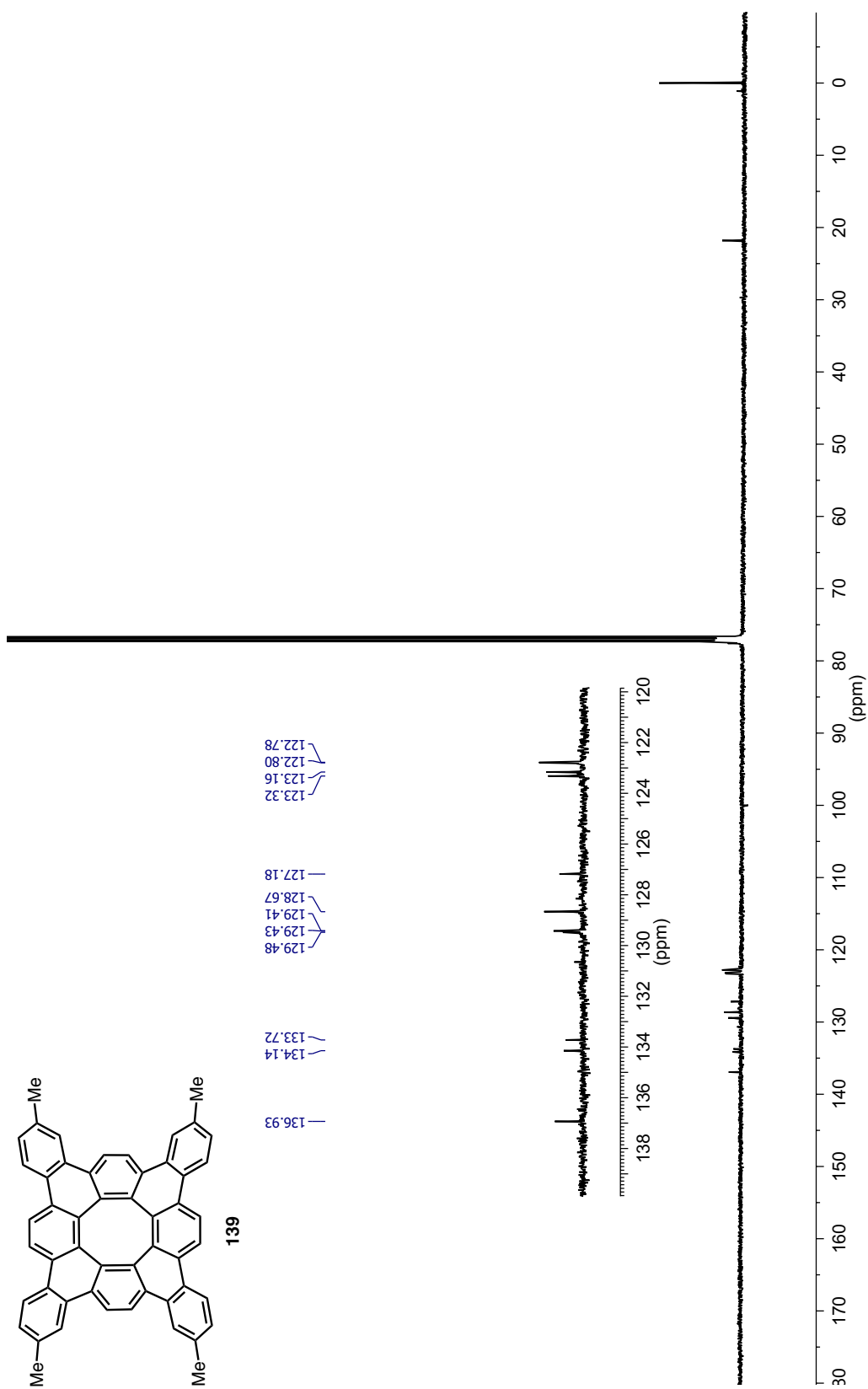
Figure AI.82 ^{13}C NMR Spectrum of **139** in CDCl$_3$
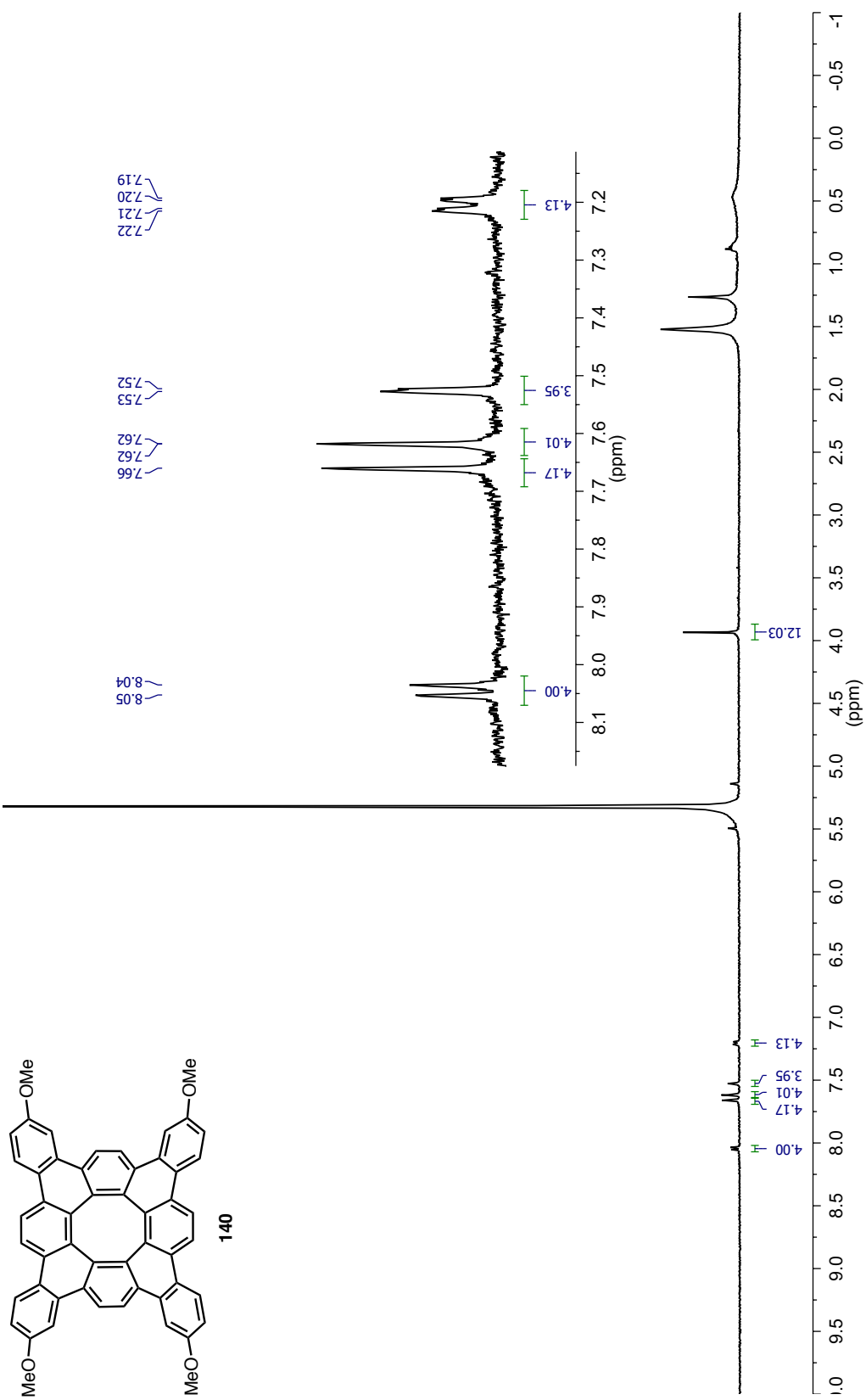
Figure AI.83 ^{1}H NMR Spectrum of **140** in CD$_2$Cl$_2$
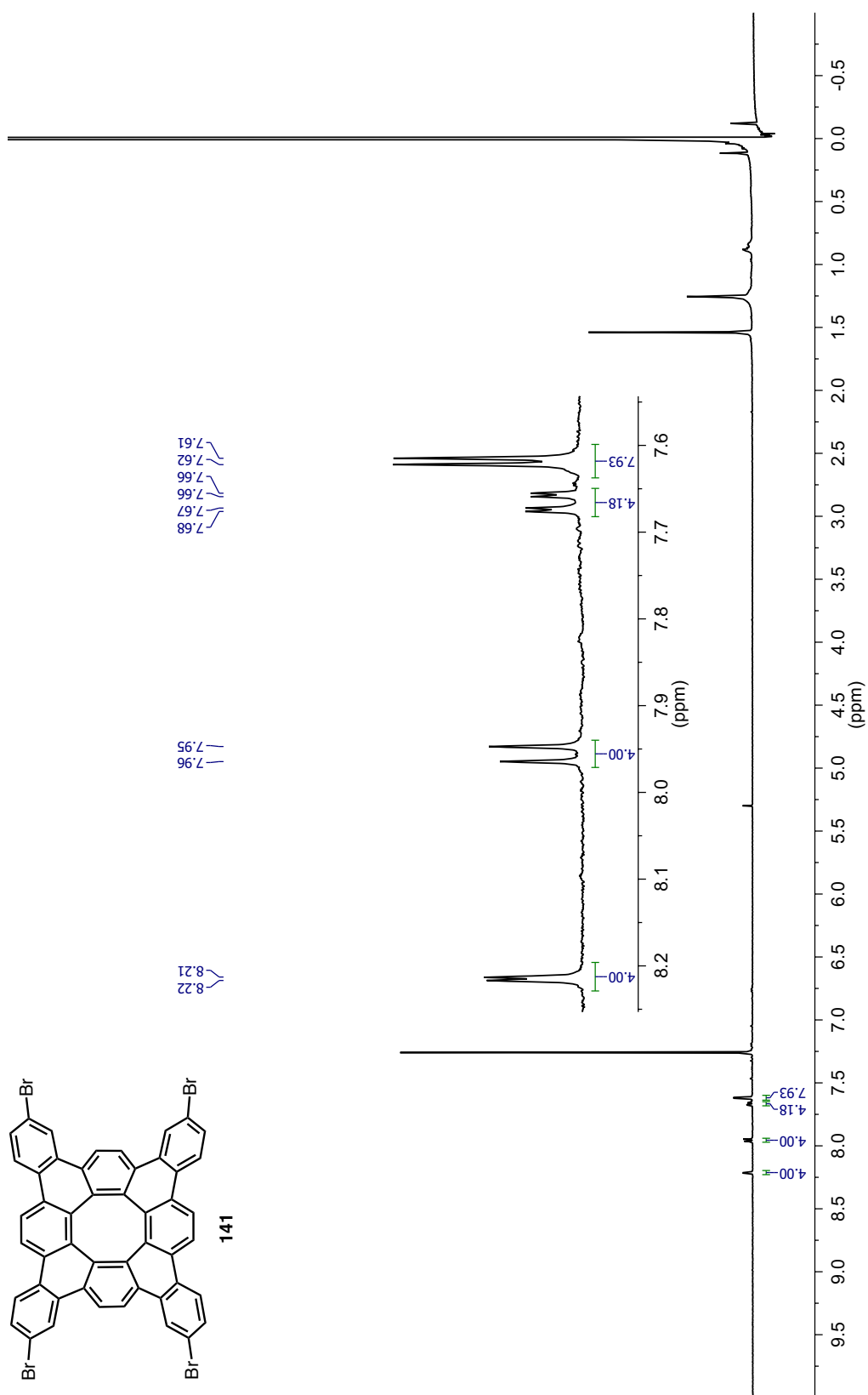
Figure AI.84 ^{1}H NMR Spectrum of **141** in CDCl$_3$
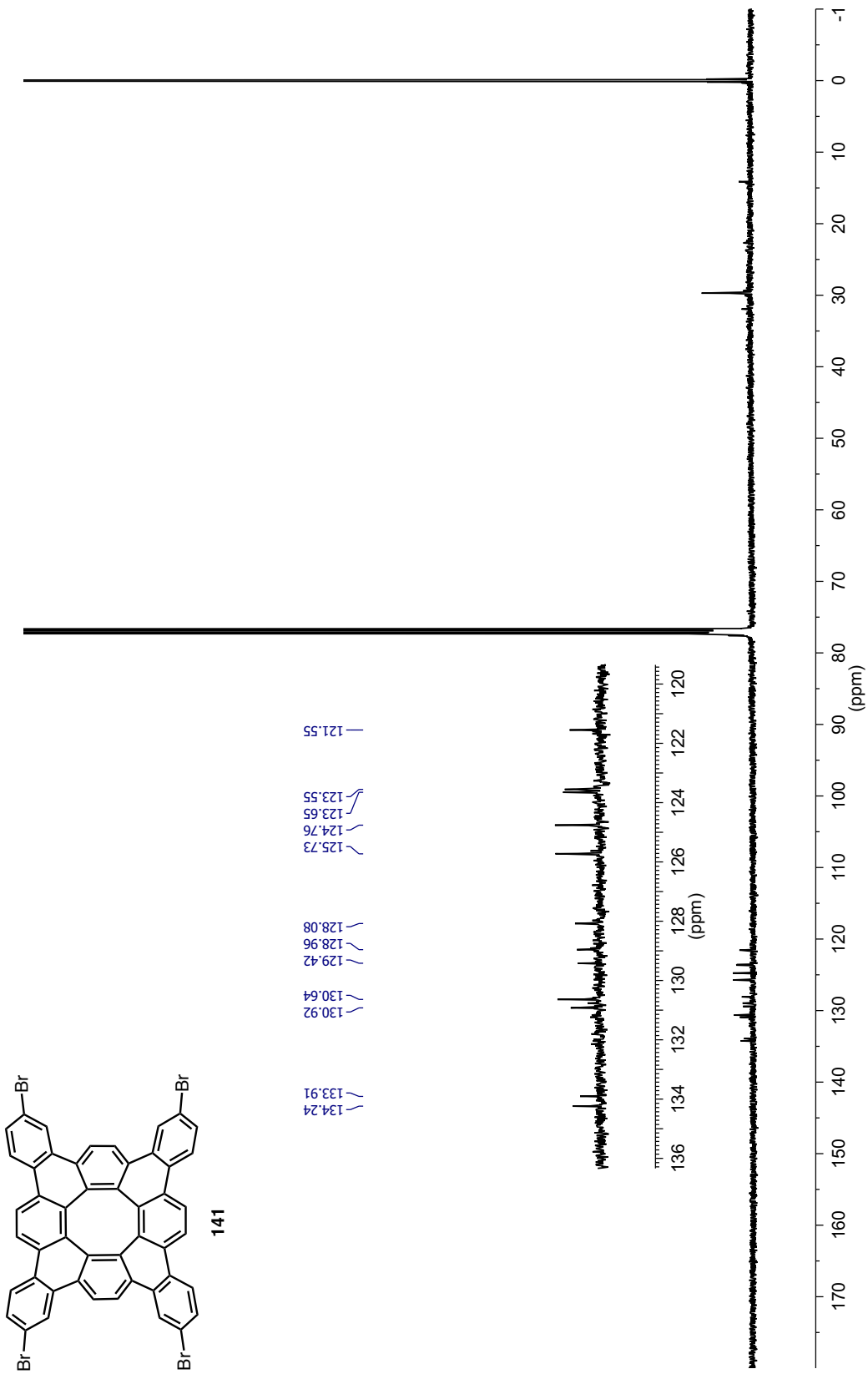
Figure AI.85 ^{13}C NMR Spectrum of **141** in CDCl$_3$

Figure AI.86 ^{1}H NMR Spectrum of **142** in CDCl$_3$
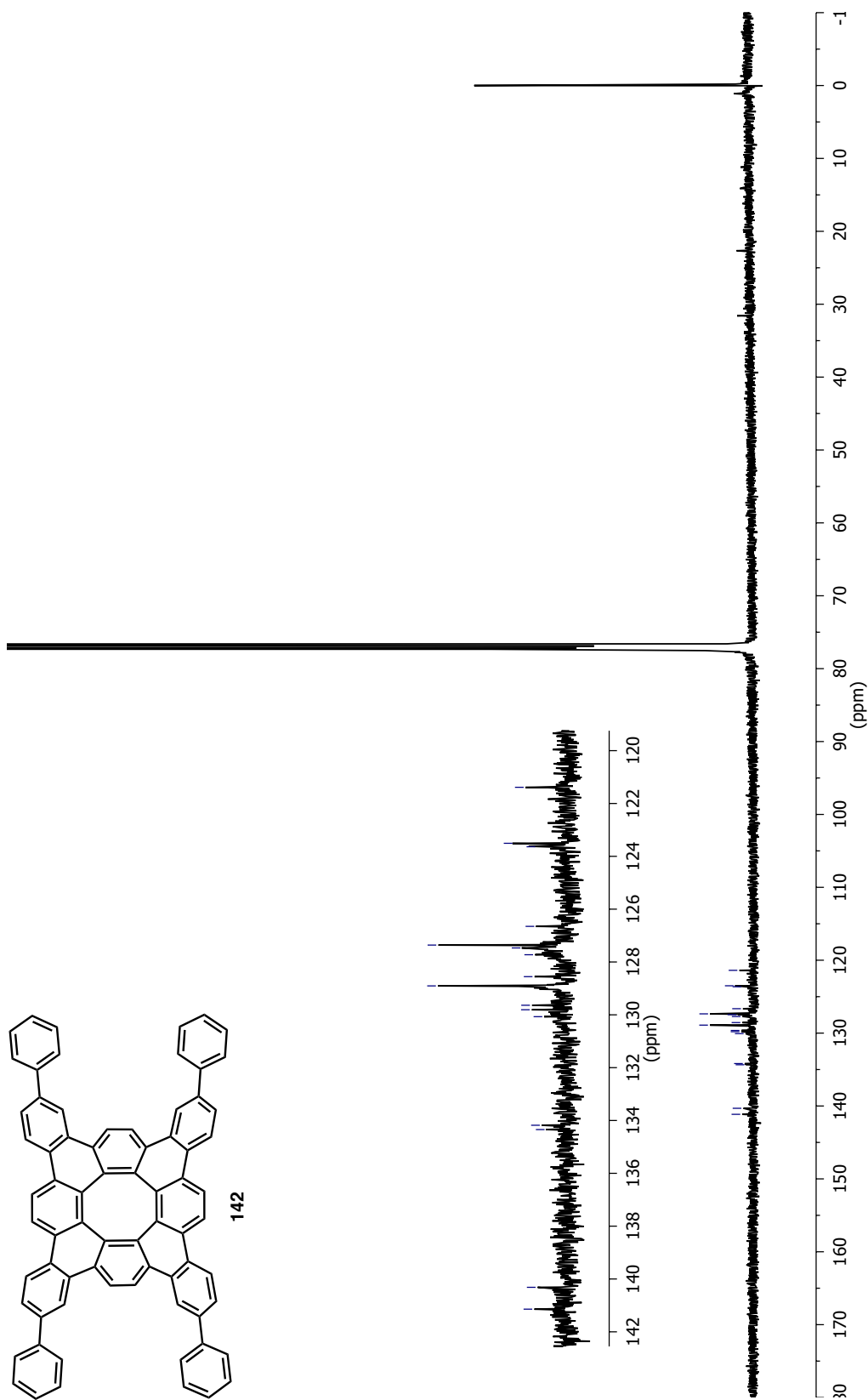
Figure AI.87 ^{13}C NMR Spectrum of **142** in CDCl$_3$

143

Figure AI.88 ^{1}H NMR Spectrum of **143** in THF-d_8

263
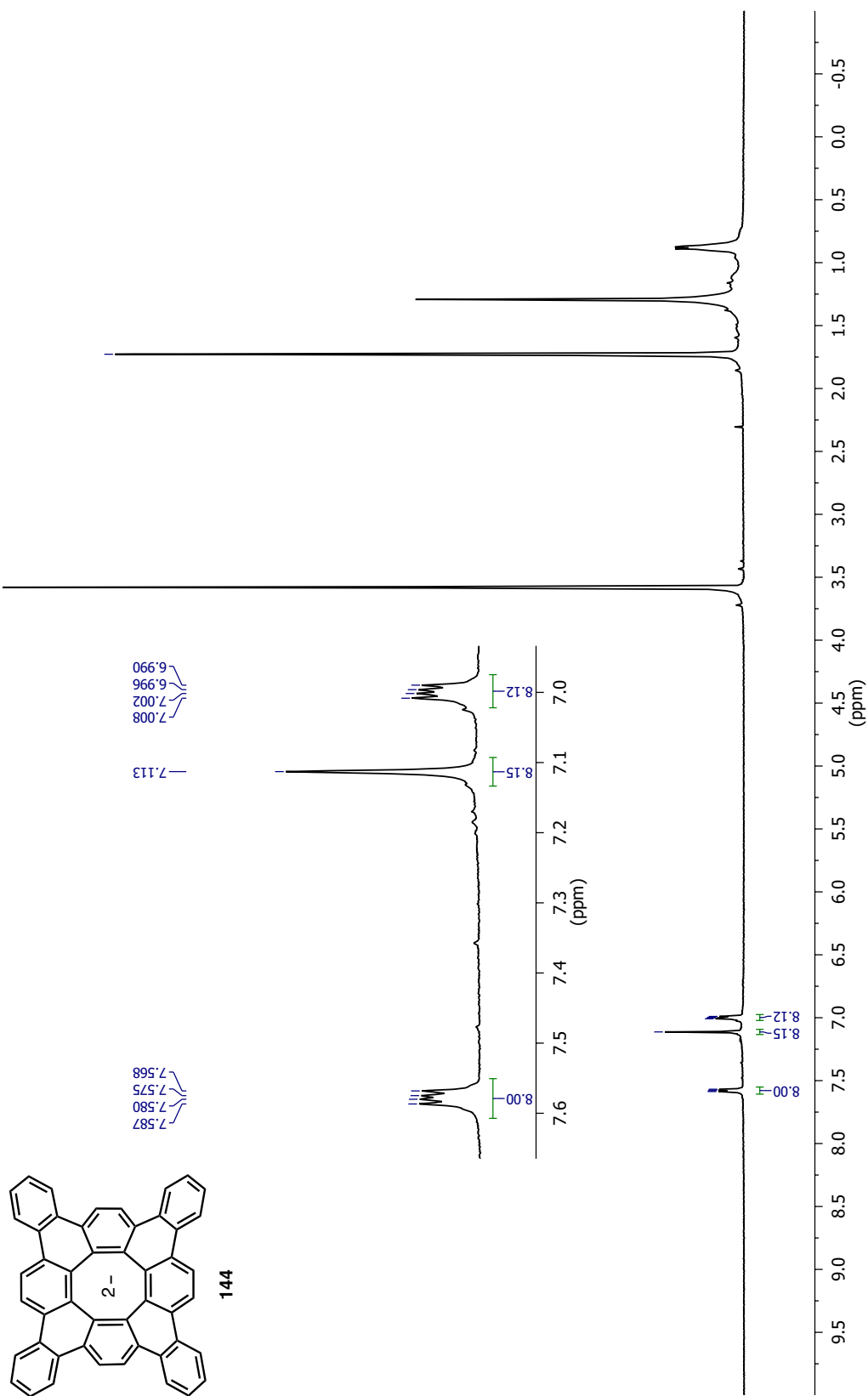
Figure AI.89 ^{1}H NMR Spectrum of **144** in THF-d_8
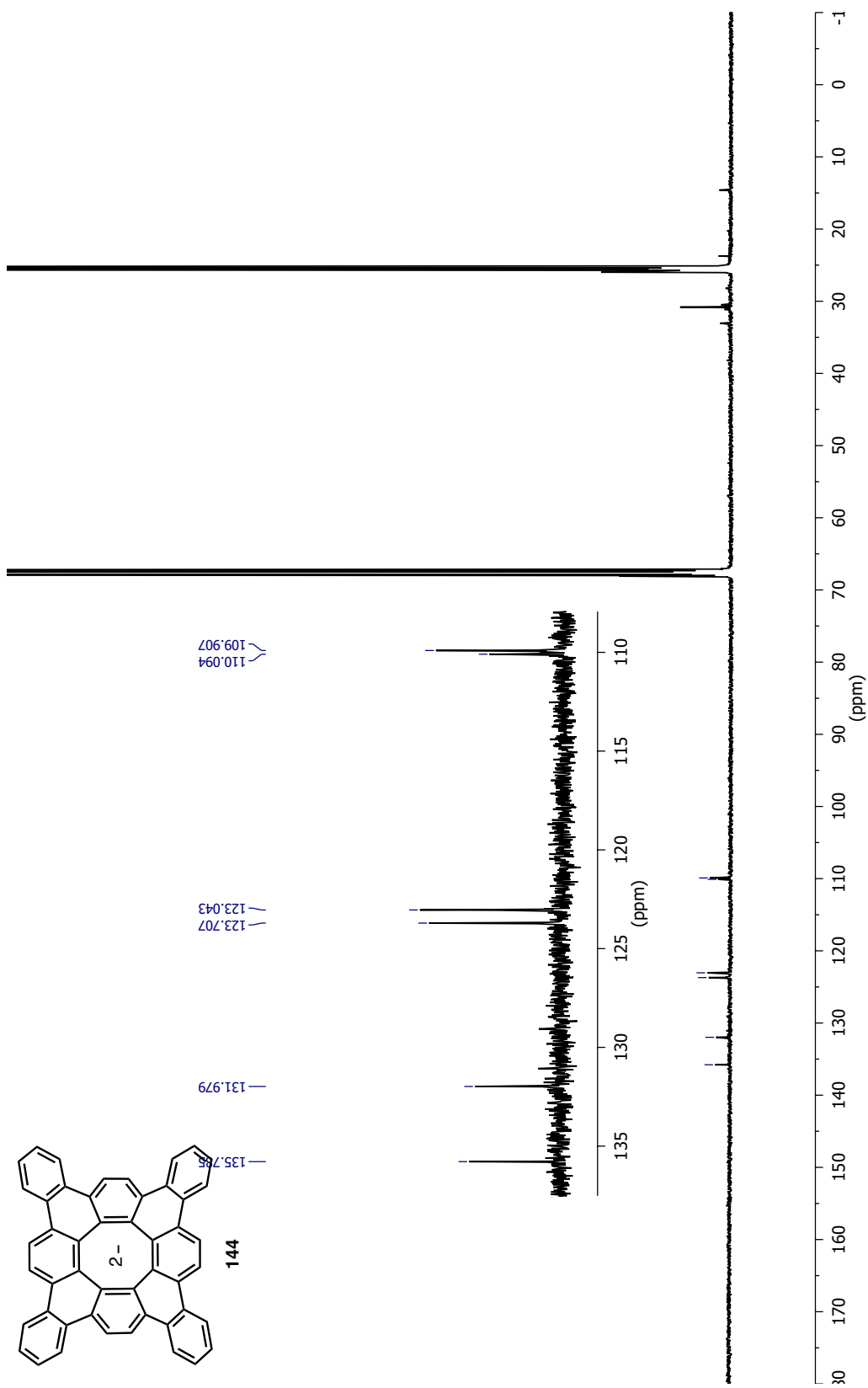
Figure AI.90 ^{13}C NMR Spectrum of **144** in THF-d_8
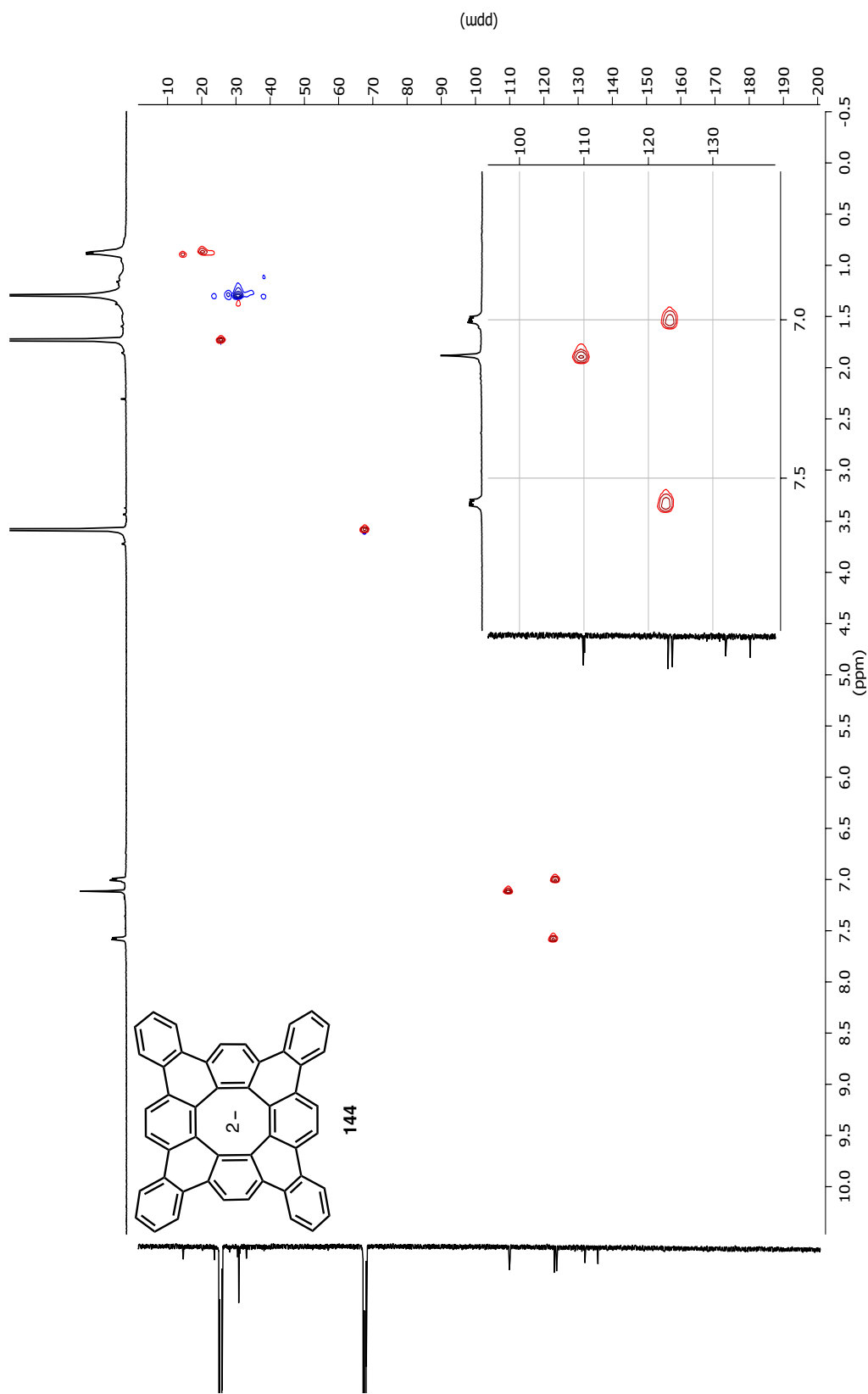
Figure AI.91 2D HSQC NMR Spectrum of **144** in THF-d_8
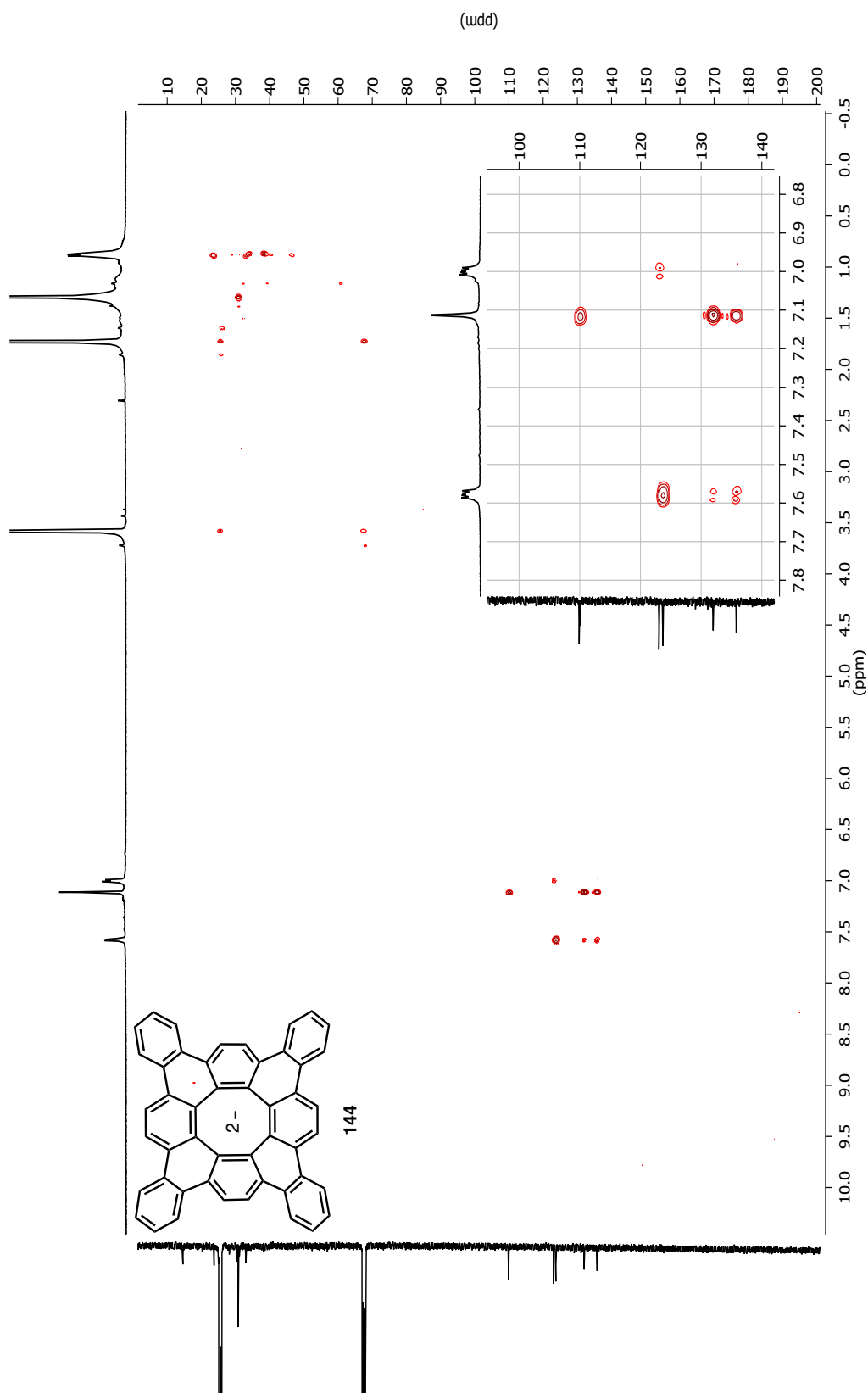
Figure AI.92 2D HMBC NMR Spectrum of **144** in THF-d_8
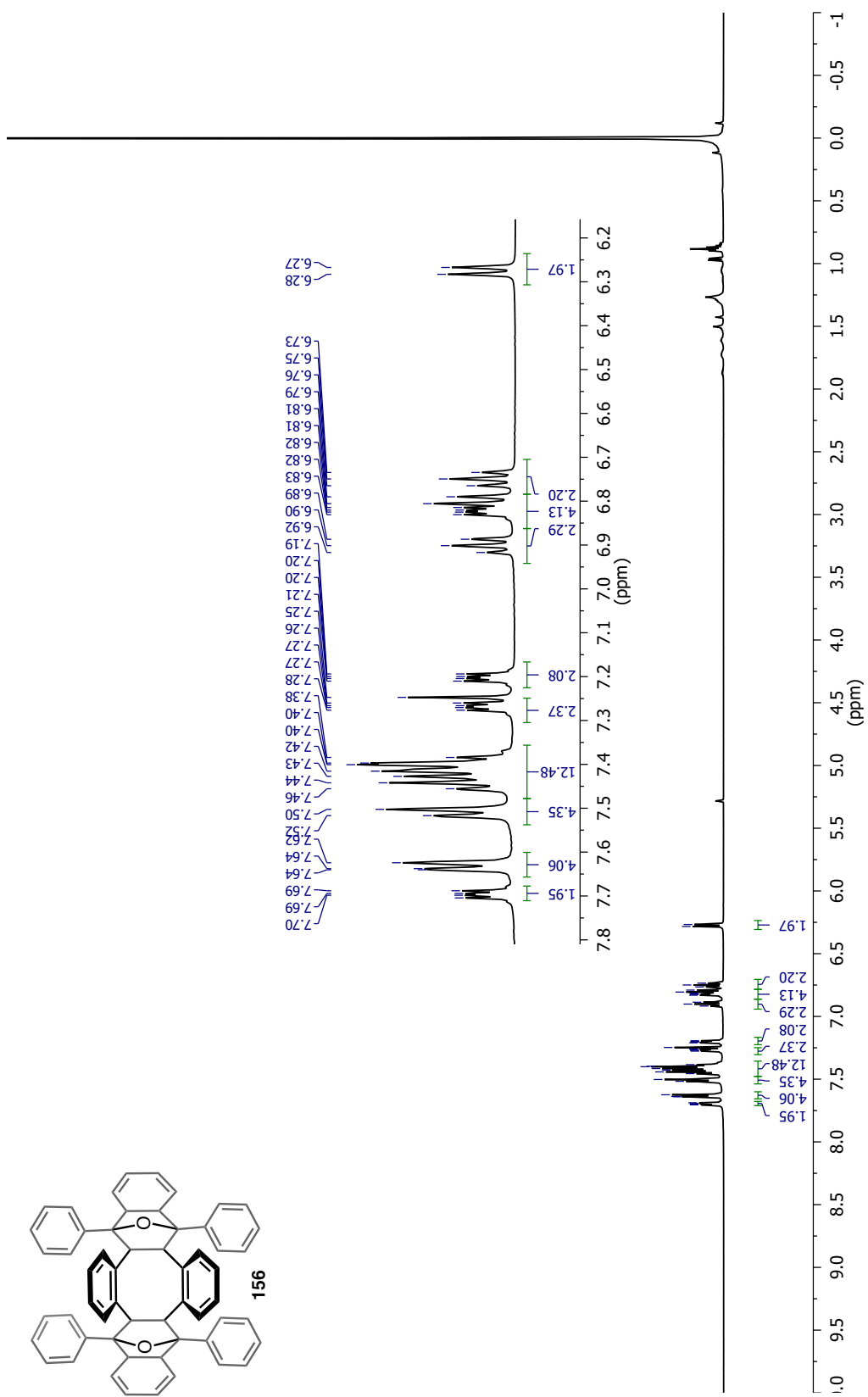
Figure AI.93 ¹H NMR Spectrum of **156** in CDCl₃
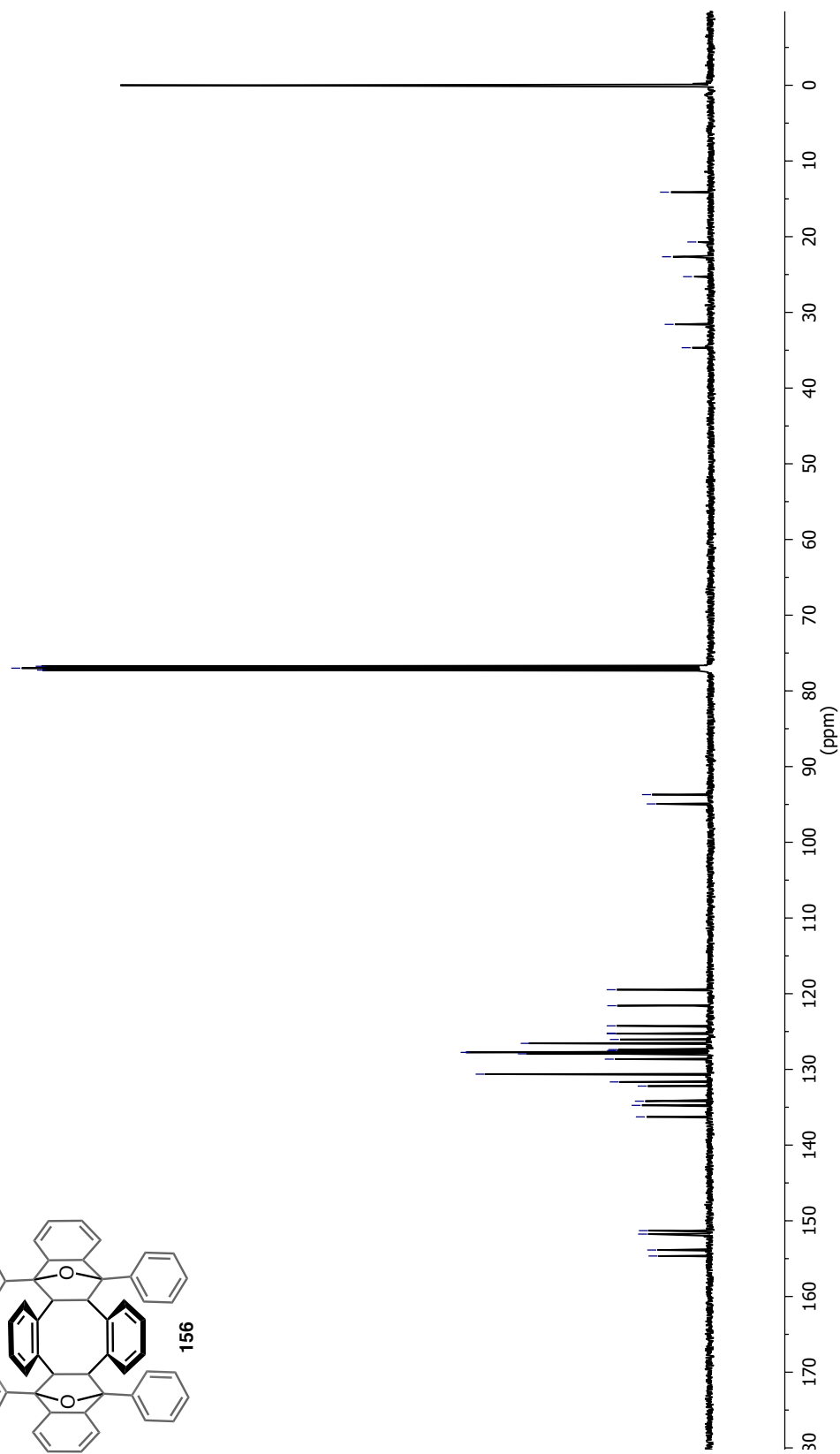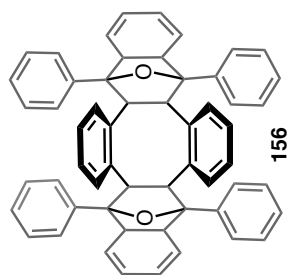
Figure AI.94 ^{13}C NMR Spectrum of **156** in CDCl$_3$

156

269
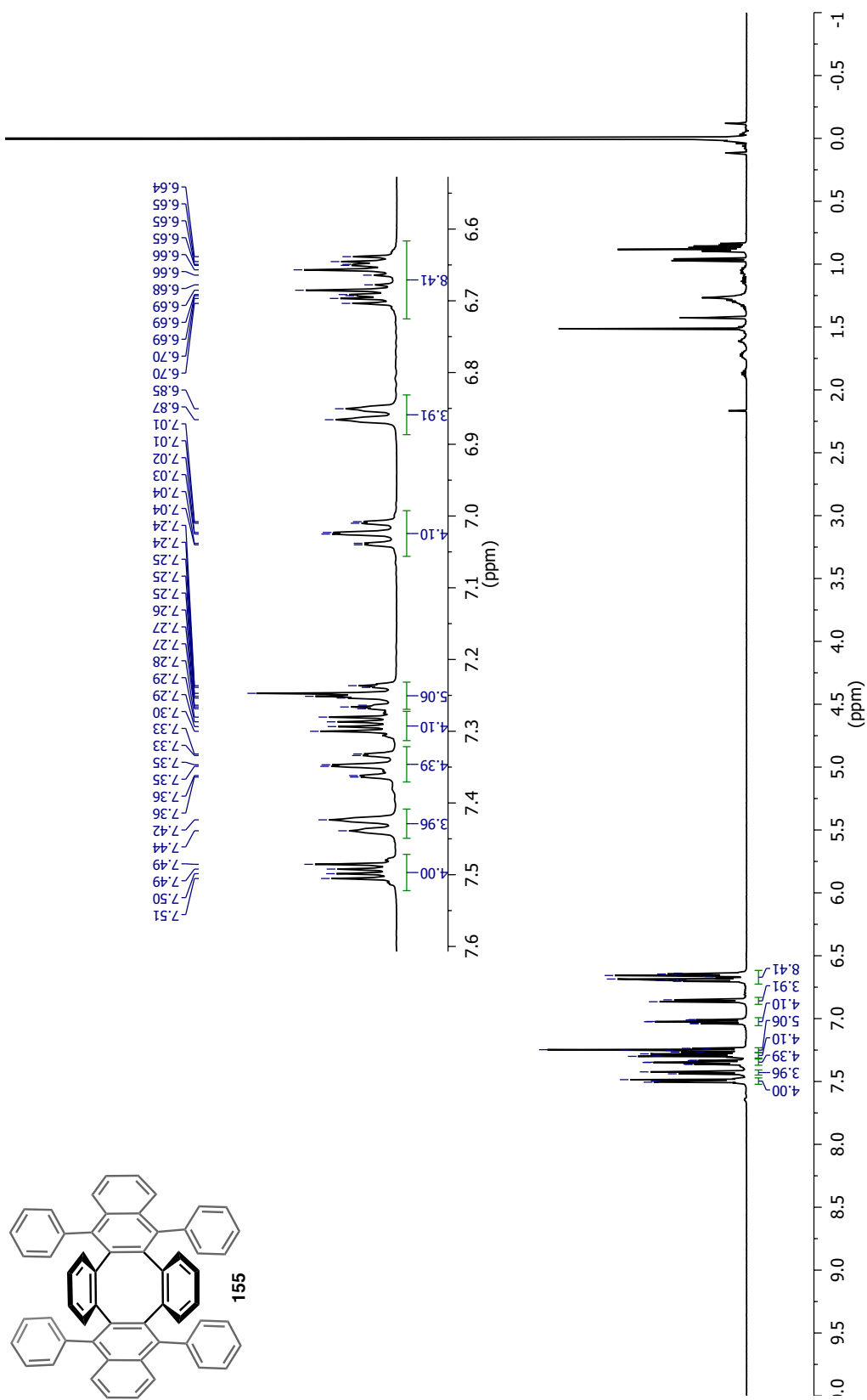
Figure AI.95 ^{1}H NMR Spectrum of **155** in CDCl$_3$
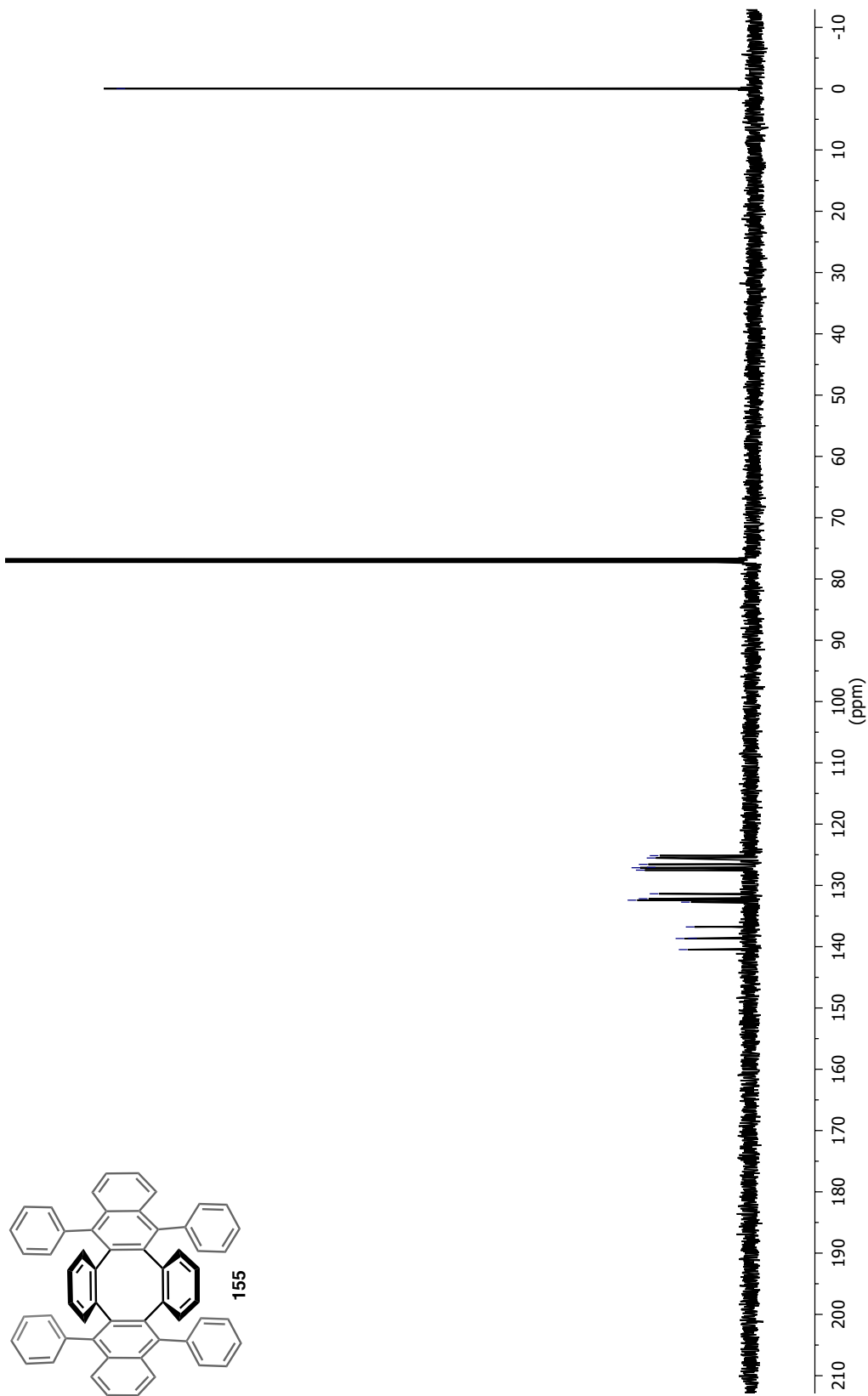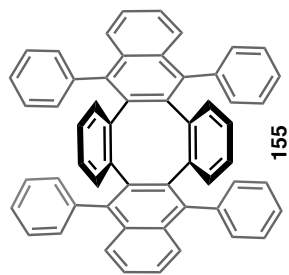
Figure AI.96 ^{13}C NMR Spectrum of **155** in CDCl$_3$
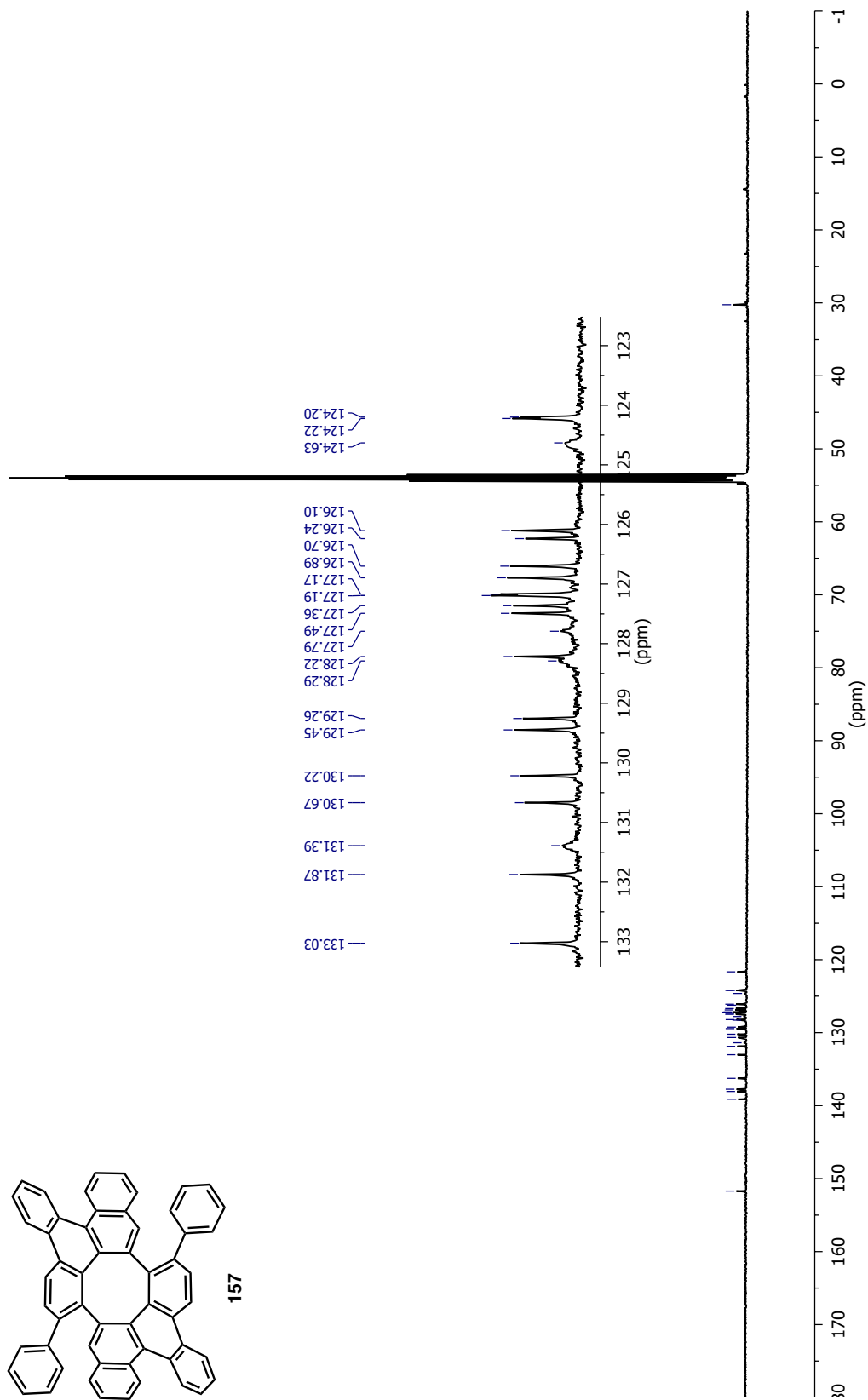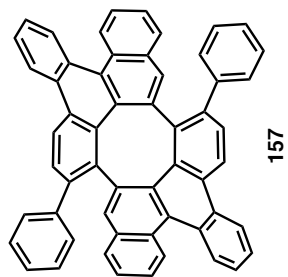
Figure AI.97 ^{1}H NMR Spectrum of **157** in CDCl$_3$

Figure AI.98 ^{13}C NMR Spectrum of **157** in CD$_2$Cl$_2$

Table AII.1 Complete list of bond lengths for the two crystal residues of **55**.
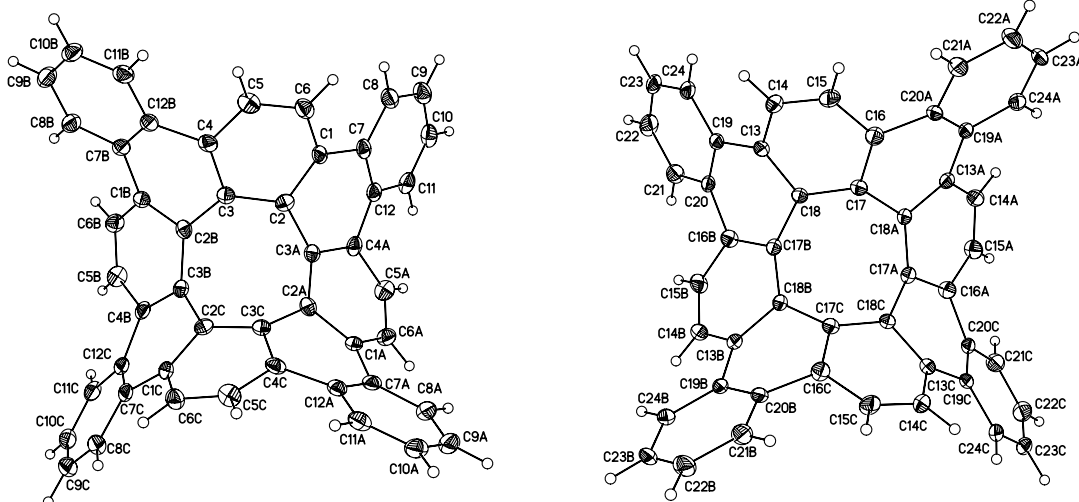
Bond Pair	Length [Å]	Bond Pair	Length [Å]
C(1)-C(6)	1.391(4)	C(13)-C(14)	1.404(4)
C(1)-C(2)	1.408(3)	C(13)-C(18)	1.412(3)
C(1)-C(7)	1.467(3)	C(13)-C(19)	1.470(3)
C(2)-C(3)	1.440(3)	C(14)-C(15)	1.344(4)
C(2)-C(3)#1	1.474(3)	C(15)-C(16)	1.407(3)
C(3)-C(4)	1.401(4)	C(16)-C(17)	1.418(3)
C(3)-C(2)#2	1.474(3)	C(16)-C(20)#3	1.458(3)
C(4)-C(5)	1.408(4)	C(17)-C(18)	1.432(3)
C(4)-C(12)#2	1.468(4)	C(17)-C(18)#3	1.481(3)
C(5)-C(6)	1.361(4)	C(18)-C(17)#4	1.481(3)
C(7)-C(12)	1.403(4)	C(19)-C(20)	1.395(3)
C(7)-C(8)	1.405(4)	C(19)-C(24)	1.405(3)
C(8)-C(9)	1.374(4)	C(20)-C(21)	1.392(4)
C(9)-C(10)	1.378(4)	C(20)-C(16)#4	1.458(3)
C(10)-C(11)	1.351(4)	C(21)-C(22)	1.389(4)
C(11)-C(12)	1.404(4)	C(22)-C(23)	1.377(4)
C(12)-C(4)#1	1.468(4)	C(23)-C(24)	1.370(4)

Symmetry transformations used to generate equivalent atoms: #1 –y+1/2,x-1/2,-z+1/2, #2 y+1/2,-x+1/2,-z+1/2, #3 –y,x,-z, #4 y,-x,-z.

Table AII.2 Complete list of bond lengths for **106**.

Bond Pair	Length [Å]	Bond Pair	Length [Å]
C(1)-C(2)	1.46(2)	C(25)-C(41)	1.40(2)
C(1)-C(8)	1.46(2)	C(26)-C(44)	1.38(2)
C(1)-C(31)	1.42(2)	C(26)-C(27)	1.47(2)
C(2)-C(3)	1.48(2)	C(27)-C(28)	1.41(2)
C(2)-C(28)	1.41(2)	C(28)-C(29)	1.33(2)
C(3)-C(4)	1.45(2)	C(29)-C(30)	1.42(2)
C(3)-C(24)	1.41(2)	C(30)-C(31)	1.44(2)
C(4)-C(5)	1.47(2)	C(31)-C(32)	1.39(2)
C(4)-C(21)	1.40(2)	C(31)-C(45)	1.40(2)
C(5)-C(6)	1.45(2)	C(32)-C(48)	1.39(2)
C(5)-C(18)	1.40(2)	C(33)-C(34)	1.37(2)
C(6)-C(7)	1.45(2)	C(34)-C(35)	1.42(2)
C(6)-C(15)	1.41(2)	C(35)-C(36)	1.36(2)
C(7)-C(8)	1.44(2)	C(37)-C(38)	1.38(2)
C(7)-C(12)	1.42(2)	C(37)-C(39)	1.36(2)
C(8)-C(9)	1.38(2)	C(39)-C(40)	1.40(2)
C(9)-C(10)	1.44(2)	C(41)-C(42)	1.36(2)
C(9)-C(32)	1.44(2)	C(42)-C(43)	1.40(2)
C(10)-C(11)	1.32(2)	C(43)-C(44)	1.36(2)
C(11)-C(12)	1.41(2)	C(45)-C(46)	1.36(2)
C(12)-C(13)	1.44(2)	C(46)-C(47)	1.42(2)
C(13)-C(14)	1.41(2)	C(47)-C(48)	1.40(2)
C(13)-C(33)	1.42(2)	Si(1)-C(34)	1.849(17)
C(14)-C(15)	1.44(2)	Si(1)-C(49)	1.837(17)
C(14)-C(36)	1.38(2)	Si(1)-C(50)	1.856(17)
C(15)-C(16)	1.41(2)	Si(1)-C(51)	1.860(18)
C(16)-C(17)	1.36(2)	Si(2)-C(42)	1.894(18)
C(17)-C(18)	1.41(2)	Si(2)-C(45)	1.86(2)
C(18)-C(19)	1.43(2)	Si(2)-C(56)	1.87(2)
C(19)-C(37)	1.43(2)	Si(2)-C(57)	1.826(18)
C(19)-C(20)	1.39(2)	Si(3)-C(39)	1.891(16)
C(20)-C(21)	1.43(2)	Si(3)-C(52)	1.86(2)
C(20)-C(40)	1.40(2)	Si(3)-C(53)	1.856(19)
C(21)-C(22)	1.41(2)	Si(3)-C(54)	1.822(19)
C(22)-C(23)	1.34(2)	Si(4)-C(47)	1.863(17)
C(23)-C(24)	1.39(2)	Si(4)-C(58)	18.29(18)
C(24)-C(25)	1.47(2)	Si(4)-C(59)	1.859(18)
C(25)-C(27)	1.40(2)	Si(4)-C(60)	1.879(17)

Table AII. 3 Potential versus ferrocene of the various redox processes for TB[8]Cs.

	1 (-H)[a]	2 (-F)[b]	3 (-OMe)[b]	4 (-Ph)[b]	5 (-Me)[b]	6 (-Br)[b]
3rd Oxidation			E_{pa}[c] 1.19 V			
2nd Oxidation	$E_{1/2}$ 0.82 V	$E_{1/2}$ 0.91 V	$E_{1/2}$ 0.72 V	$E_{1/2}$ 0.85 V	E_{pa}[c] 0.74 V	
1st Oxidation	$E_{1/2}$ 0.44 V	$E_{1/2}$ 0.54 V	$E_{1/2}$ 0.38 V	$E_{1/2}$ 0.45 V	$E_{1/2}$ 0.39 V	$E_{1/2}$ 0.39 V
1st Reduction	$E_{1/2}$ -1.79 V	$E_{1/2}$ -1.75 V	$E_{1/2}$ -1.83 V	$E_{1/2}$ -1.77 V	$E_{1/2}$ -1.83 V	$E_{1/2}$ -1.83 V
2nd Reduction		$E_{1/2}$ -1.89 V	$E_{1/2}$ -2.02 V	$E_{1/2}$ -1.92 V		
1st Reduction[d]	$E_{1/2}$ -1.92 V				$E_{1/2}$ -1.95 V	
2nd Reduction[d]	$E_{1/2}$ -2.09 V				$E_{1/2}$ -2.12 V	
HOMO-LUMO Gap	2.23 V	2.29 V	2.21 V	2.22 V	2.22 V	2.22 V

The potential versus ferrocene of the various redox processes for each compound. Unless otherwise noted, the measurements were made in CH_2Cl_2/ 0.05 M [NBu$_4$][TFAB]. [a]CV measurement, scan rate 0.2 V s^{-1}. [b]SWV measurement 5 Hz frequency. [c]Anodic peak potential by CV, 0.2 V s^{-1}. [d]Measurement in THF/ 0.05 M [NBu$_4$][TFAB].

Table AII. 4 Determination of Charge-Distribution for **144**.

Carbon	Charged	Neutral	Difference	# of Carbons	% electron density
C1	123.707	128.224	4.517	36.136	2.926
C2	123.043	123.949	0.906	7.248	0.587
C3	109.907	124.545	14.638	117.104	9.483
C4	135.785	130.597	-5.188	-41.504	-3.361
C5	131.979	130.882	-1.097	-8.776	-0.711
C6	110.094	134.908	24.814	198.512	16.075

Charge density on the carbon π-framework is calculated using the equation: $\rho_\pi = \Delta\delta_c / K_c$ where K_c is a calculated proportionality constant (with a normal value of ca. 160.0 ppm/electron), and ρ_π is the change in the π-charge on the carbon, and $\Delta\delta_c$ is the chemical shift change of the associated carbon from the anionic to the neutral state.

INDEX